Journal of Advanced Transportation

The Role of Emerging Technologies in Road Safety and Driving Behavior

Lead Guest Editor: Milad Haghani
Guest Editors: Bilal Farooq, Inhi Kim, Zhibin Li, Cheol Oh, and Zahra Shahhoseini

The Role of Emerging Technologies in Road Safety and Driving Behavior

Journal of Advanced Transportation

The Role of Emerging Technologies in Road Safety and Driving Behavior

Lead Guest Editor: Milad Haghani
Guest Editors: Bilal Farooq, Inhi Kim, Zhibin Li, Cheol Oh, and Zahra Shahhoseini

Contents

Hindawi
Journal of Advanced Transportation
Volume 2020, Article ID 2023093, 12 pages
https://doi.org/10.1155/2020/2023093

Research Article

Analysis of Driver Decisions at the Onset of Yellow at Signalized Intersections

Juan Li,[1,2] **Boyu Jiang**,[1,2] **Chunjiao Dong**,[1,2] **Jue Wang**,[3] **and Xuan Zhang**[4]

[1]*School of Traffic and Transportation, Beijing Jiaotong University, Beijing, China*
[2]*Key Laboratory of Transport Industry of Big Data Application Technologies for Comprehensive Transport, Beijing Jiaotong University, Beijing, China*
[3]*Center for Forecasting Science, Academy of Mathematics and Systems Science, Chinese Academy of Sciences, Beijing, China*
[4]*Sam's Club Technology, Austin, TX, USA*

Correspondence should be addressed to Juan Li; juanli@bjtu.edu.cn

Received 11 October 2019; Revised 15 January 2020; Accepted 13 February 2020; Published 5 August 2020

Guest Editor: Inhi Kim

Drivers' decisions to either slow and stop or go at the onset of yellow signal impact on intersection safety. This novel study contributes to the new classification scheme for drivers. Two driving style indexes (i.e., the driving reliability index and dangerous driving index) are adopted, along with other known factors to analyze stop/go decision-making. Initially, the driving reliability index is extracted using a Hidden Markov Model (HMM). The dangerous driving index is calculated based on statistics extracted from dangerous driving records. A latent class logit model is then proposed to explore the factors which influence drivers' decisions. Drivers are classified for analytical purposes into "low-risk" and "high-risk" categories according to driving styles and age. Results indicate that those considering "low-risk" tend to stop, while drivers considering "high-risk" are inclined to pass intersections. Furthermore, distractions from cell phones have different influences on each group of drivers. These findings help to determine driver preferences and may be used to formulate strategies to reduce unsafe driving occurring at signalized intersections.

1. Introduction

Signalized intersections are areas where traffic accidents occur frequently. In 2017, there were 34,247 fatal traffic accidents in the United States, involving 52,274 drivers and 37,133 deaths [1]. Over 50 percent of all injuries and fatalities occur at or near signalized intersections [2] and driver errors are the leading cause of intersection-related crashes [3]. At the onset of yellow signal, it is a challenge for drivers to make immediate decisions, especially in yellow light dilemma zones, which are where drivers may neither stop safely nor pass through intersections [4, 5]. Unfortunately, the decision to either stop or go may increase the number of angle crashes and rear-end collisions, as well as injuries and fatalities, which necessitates research into stop/go decision-making at the onset of yellow at signalized intersections.

In order to understand drivers' stop/go decision-making completely, researchers have tried to find demographic attributes besides age and gender. For example, Elhenawy et al. proposed a variable to measure drivers' aggressiveness level at the onset of yellow signal [6]. In this study, we adopt two new variables, i.e., the driving reliability index and dangerous driving index to develop this further. It is hoped that implementing these two new variables will provide a more comprehensive understanding of driving styles. We also conduct sophisticated analysis of heterogeneity, which is necessary considering diversity within any sample involving human participants.

In the past, researchers have used various statistical approaches to gain insight into driving heterogeneity. For example, Savolainen [7] adopted the latent class logit model instead of the fixed logit model. Constant terms were used to formulate classification probabilities. In this study, we

adopted a latent class model with newly proposed variables which contributes in three aspects: (1) involving heterogeneity into drivers' decisions; (2) evaluating the impact of factors on different-class drivers; (3) analyzing the relationship between decision property and driving styles.

The contribution of this study is twofold. Firstly, to uncover class features of drivers' behavior, two novel indexes associated with driving styles (i.e., the driving reliability index and dangerous driving index) are proposed. Unlike previously considered factors (i.e., drivers' demographic attributes, speed, accelerate, and distant to stop line), these two factors are extracted from historic driving records and able to reflect driving styles. Secondly, the latent class logit model categorizes drivers into two groups according to driving style indexes. Compared with traditional logit models, this model considers the group heterogeneity of drivers and thus can distinguish their choice-preference differences.

The remainder part of this paper is organized as follows: Section 2 presents relevant research around factors which influence stop/go decision-making and driving heterogeneity. Section 3 introduces experimental data and provides a description of the analytical dataset. Section 4 provides a detailed description of the methodologies adopted in this study. Section 5 presents model results and the quantified impact of variables. Section 6 discusses the driving risks, distracted driving behavior among different driver classes, and comparative results. The final section, Section 7, provides our conclusions based upon the findings.

2. Literature Review

2.1. Indicators Influencing Driver Decisions. Previous researches focusing on driver decisions at the onset of yellow signal have adopted various data-gathering methods, such as field studies [8, 9], driving simulator studies [6, 10], and video-capture studies [11–14]. Researchers have identified a number of factors that influence driver decisions, such as age, gender, and time to the stop line. The dilemma zone is one of the most important factors involved in stop/go decisions in this scenario.

Type I dilemma zone describes the region where drivers can neither stop safely nor pass through intersections. It has been postulated that this occurs due to insufficient yellow light time caused through high approaching speeds [15]. Type I dilemma zone is therefore formulated using vehicular information and intersection data, such as approach speed, acceleration, and yellow interval [4, 16].

Type II dilemma zone is defined as the zone in which drivers may have trouble making stop/go decisions at the onset of yellow signal [17]. This area can be thought of as a corridor of uncertainty, which is the area ahead of the stop line between the point where 90 percent of drivers will stop and the point where 90 percent of drivers will continue [18]. The existence of what has been described as Types I and II of dilemma zones which occur as drivers approach intersections adds to the complexity of driver's decision-making. However, Types I and II of dilemma zones are not the only situations that increase cognitive load, clouding decision-making.

Distractions are another factor that may influence driving behaviors at the onset of yellow signals. In 2017 in the United States, 3,166 lives were claimed related to driving distractions. Of this total number, 434 people died in fatal crashes involving cell phone use or other cell phone related behaviors [1]. By splitting visual, manual, and cognitive attention, speaking on the phone distracts drivers from the road and therefore increases the likelihood of having an accident and risk of injury to drivers, passengers, and pedestrians [19, 20]. Interestingly, drivers appear more likely to stop when using handheld and hands-free devices, but less likely to stop when using headsets [7].

Several studies have examined other factors associated with drivers' decisions at the onset of yellow, including demographic characteristics such as age and gender, and vehicular conditions such as speed, distance to the stop line, and time to the intersection [6, 12, 21, 22]. Savolainen [7] found that driver decisions are mainly determined by the estimated time to the stop line.

2.2. Driving Heterogeneity. Previous researches have used the binary logit model to analyze drivers' behaviors at signalized intersections. Köll et al. [12], for example, adopted a binary logit model to examine the effect of speed, distance, and potential time at the point at which drivers decide to either stop or proceed. They found that both high speeds and short distances to the stop line decreased the probability of stopping. Papaioannou [23] extended the binary logit model intercalating gender, and evidence suggests that female drivers were less aggressive and more likely to stop when encountering yellow signals. Gates et al. [24] discovered that heavy vehicles were more likely to pass the intersection than passenger vehicles.

Further research has also looked to analyze the influence of the traffic environment, such as pavements and traffic control devices. For example, Yan et al. [25] examined the impact of pavement markings and found that they appear to reduce the probability of both conservative-stop and risky-go decisions. Long et al. [26] employed a binary logit model to identify the influence of countdown devices, which increased the probability of passing the stop line after the onset of yellow signal. Importantly, in the conventional binary logit model, utilities of indicators remain constant across individuals, which means the logit model is incapable of accommodating unobserved heterogeneity between individuals. Therefore, alternative analytical methods which are capable of intercalating individual heterogeneity should be considered.

Latent class analysis was proposed to overcome the limitations of the fixed model [27–29]. The latent class logit model is a semiparametric extension of the logit model which accommodates heterogeneity across individuals with a set of classes and without parametric distribution definition [30]. Various fields of study have adopted this model to evaluate human preferences [31–33]. In the field of transportation, Hess et al. [34] employed the latent class

model to analyze rail and bus travel behavior. Shen [35] used the latent class logit model to predict transport mode choices.

In this study, we make an initial attempt to introduce driving style indexes (i.e., the driving reliability index and dangerous driving index) to examine drivers' stop/go decision-making. A latent class logit model with these new indicators is developed to investigate the influence of each factor on driver subgroups. Also, each class is labeled with a unique driving style, which is necessary for analyzing the relationship between decision preference and driving styles.

3. Data and Analysis

The dataset was collected through the National Advanced Driving Simulator (NADS) at the University of Iowa [10]. In driving simulations, each driver partook in three "drives," where each "drive" consisted of three "segments." Each "segment" contained one rural zone and one urban zone. Each driver encountered five signal-controlled intersections in each "segment," only two of which triggered yellow signals when the driver was approaching. Each driver therefore encountered 18 points which required stop/go decisions. In each "segment," every driver accomplished one of the following three tasks: baseline (no phone call), outgoing (making calls), or incoming (answering calls). These tasks were randomly arranged within each driving "segment" and began prior to the arrival at each segment. This simulation experiment focused on identifying differences in driver decisions at the onset of yellow signal with and without cell phone distractions.

Data were recorded from 49 participants and contained 1157 trials across 17 variables. After deleting the missing and invalid data which were beyond predefined ranges, the final dataset included 829 complete runs. Deleted trials were consistent across age, gender, drive number, and phone status due to the simulator settings. The description of variables in the final dataset is presented in Tables 1 and 2.

According to the data in Table 1, most drivers decided to stop in the simulation experiment. The number of trials in the old age group was the least among all the ages with 304 occurring in the young age group, 295 in the middle-aged group, and 230 in the old age group. Trials with male drivers ($n = 432$) slightly outnumbered those of female drivers ($n = 397$). Also, the 829 trials were roughly balanced in the drive number and phone status. Stop times increased as the number of trials increased with 162 in the first drive, 176 in the second drive, and 194 in the third drive. In addition, the number of stop times under incoming ($n = 181$) or outgoing calls ($n = 178$) was slightly larger than under baseline conditions ($n = 173$).

In Table 2, speeds at the onset of yellow ranged from 11 m/s to 24.12 m/s. The distance to the stop line also ranged from 33.49 m to 86.76 m. Under experimental settings, the duration of the yellow light was triggered at either 3 seconds or 3.75 seconds from the stop line [36]. Given variations in the simulator algorithm, the yellow time varied from 2.78 seconds to 4.38 seconds.

Table 1: Distribution of category variables by drivers' decisions in the dataset.

Variables		Go	Stop	Total
Age	Young group (18–25 years)	100	204	304
	Middle group (30–45 years)	98	197	295
	Old group (50–60 years)	99	131	230
Gender	Male	142	290	432
	Female	155	242	397
Drive number	First drive	114	162	276
	Second drive	98	176	274
	Third drive	85	194	279
Phone status	Baseline	105	173	278
	Incoming	96	181	277
	Outgoing	96	178	274

4. Methodology

A Hidden Markov Model (HMM) and a latent class logit model are devised to analyze drivers' decisions at the onset of yellow at signalized intersections. Initially, the HMM was established to compute a driving reliability index. Then, the dangerous driving index was obtained from the driving records. Finally, a latent class logit model was developed and calibrated based on age and the newly acquired factors of driving styles (i.e., driving reliability index and dangerous driving index). A complete description of model development is provided in Figure 1.

4.1. Hidden Markov Model. During simulations, driver behaviors were continuously tracked to contain a full set of stop/go decisions. Each driver made 18 decisions, where each decision was related to the previous one. The HMM is therefore the rational model to analyze drivers' stop/go decisions because each driver's decision regarding stop and go is unobservable and is therefore a constituent of a hidden state. Obtained vehicular data is denoted as an observable variable.

The HMM is a statistical model, which consists of N hidden states, M observable states, an initial state probability distribution π, a state transition probability matrix A, and an emission matrix B [37]. Model details are described as follows:

$$A = \left[a_{ij}\right]_{N\times N},$$
$$a_{ij} = P\left(i_{t+1} = q_j \,\middle|\, i_t = q_i\right), \quad i = 1, 2, \ldots, N;\ j = 1, 2, \ldots, N, \tag{1}$$

where q represents the individual state, i_t is the state symbol at time t, and a_{ij} represents the transitional probability from state q_i to state q_j:

$$B = \left[b_{jk}\right]_{N\times M},$$
$$b_{jk} = P\left(o_t = v_k \,\middle|\, i_t = q_j\right), \quad j = 1, 2, \ldots, N; k = 1, 2, \ldots, M, \tag{2}$$

Table 2: Descriptive statistics for continuous variables in the dataset.

Variables	Min.	Max.	Mean	Std. dev.
Speed at the stop line (m/s)	0.09	23.17	6.79	7.25
Speed at the onset of red signal (m/s)	0	23.26	8.10	6.71
Speed at the onset of yellow signal (m/s)	11.00	24.12	19.01	2.24
Distance to stop line at the onset of yellow signal (m)	33.49	86.76	62.22	10.20
Time to stop line at the onset of yellow signal (s)	2.48	3.81	3.27	0.38
Yellow signal duration (s)	2.78	4.08	4.00	0.22
Average acceleration rate (m/s^2)	−7.13	3.33	−1.37	1.95

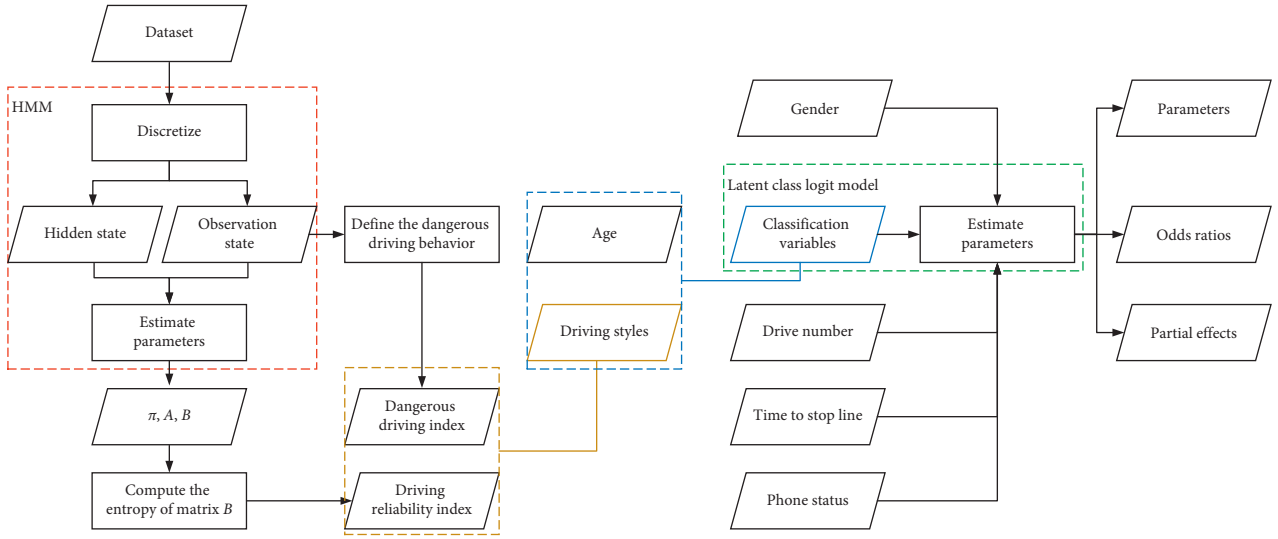

Figure 1: Model development flow chart.

where v is the possible observation state, o_t is the observation symbol at time t, and b_{jk} represents the probability of the state q_j at time t with the observation v_k:

$$\begin{aligned} \pi &= (\pi_i), \\ \pi_i &= P(i_1 = q_i), \quad i = 1, 2, \ldots, N, \end{aligned} \tag{3}$$

where π_i is the probability of q_i being the state at time $t = 1$. π and A produce the state sequence, and B derives the observation sequence. HMM can be described as π, A, and B. Although in an HMM, the hidden state cannot be observed directly, the output, derived from the state, can be observed. State estimation is therefore derived through a probability distribution across the full range of possible outputs. In HMM, the sequence of outputs provides essential information for model estimations [38]. There are two kinds of methods to estimate π, A, and B: the supervised learning algorithm and the unsupervised learning algorithm. In this study, the parameters (π, A, and B) were estimated using an unsupervised approach, known as the expectation maximization (EM) algorithm.

4.2. Indicators Associated with Driving Styles

4.2.1. Driving Reliability Index. In order to account for the level of driving reliability, we use driving reliability index to characterize driving styles. When encountering yellow signals, driver's manipulation (e.g., acceleration and deceleration) appears similar, which means that his or her behavior is relatively stable and predictable.

An HMM was employed to calculate the driving reliability index. Each row of the estimated emission probability matrix B represents the probabilities of each observation state under one hidden state. Therefore, if a single driver presented many driving states in the same traffic scene, this would mean that his/her behavior was unstable, and the corresponding B would become a dense matrix. The denser a matrix B is, the larger the driver's driving reliability index would be. Information *entropy* within each row of a matrix was used to describe the sparsity of matrix B. The normalized entropy of the matrix B was calculated as follows:

$$\begin{aligned} H_j &= -(\log_2 M)^{-1} \sum_{k=1}^{M} \left(b'_{jk} \times \log_2\left(b'_{jk}\right)\right), \\ b'_{jk} &= \begin{cases} b_{jk}, & b_{jk} \neq 0 \\ 1, & b_{jk} = 0 \end{cases}, \\ & j = 1, 2, \ldots, N; k = 1, 2, \ldots, M, \end{aligned} \tag{4}$$

where H_j is the entropy of row j in matrix B and b_{jk} stands for the probability of the observation state k under the hidden state j in B. Although each driver had more than one hidden

state (i.e., a decision), the driving reliability index was defined according to arithmetic means of the entropy of each row in matrix B:

$$\text{driving reliability index} = \frac{1}{N}\sum_{j=1}^{N} H_j. \tag{5}$$

4.2.2. Dangerous Driving Index. Dangerous driving index is proposed to represent the level of driving risk, which is also an indicator of driving style. Traffic records imply that drivers' accident proneness exists, and the proneness appears to be sustainable under various traffic circumstances [39]. Therefore, the risk of drivers' behavior can be identified by examining driving records. According to Farmer and Chambers [39], one drive trial can be categorized as either dangerous or safe. Dangerous driving behavior is more likely to result in traffic accidents, and therefore driver behavior can be evaluated by the probability of dangerous driving using driving histories found within records, which creates the dangerous driving index.

In this study, the dangerous driving index was defined as the probability of their dangerous behavior during the experiment, which was computed as follows:

$$\text{dangerous driving index} = \frac{1}{h}\sum_{d=1}^{h} x_d', \tag{6}$$

where h represents the number of trials for each driver and x_d equals 1 when the driver's behavior in the dth trial is considered dangerous and 0 when the behavior is relatively safe.

4.3. Latent Class Logit Model. The binary logit model is a classical method used to study drivers stop/go decisions. While in the conventional binary logit model, there is a potential problem with the estimation of parameters. The impact of heterogeneity makes drivers more likely to either stop or go at the onset of yellow signal. Also, this hidden heterogeneity can lead to biased parameter estimations. Hence, the latent class logit model was proposed to intercalate heterogeneity across individuals.

The latent class logit model is an improved model of the conventional logit model. The utility function of the logit model is written as

$$S_{ij} = \beta' x_{ij}' + \varepsilon_{ij}, \tag{7}$$

where S_{ij} is the utility function that determines the probability of decision outcome j for individual i; β' is a vector of parameters; x_{ij}' is a vector of observed variables; and ε_{ij} is the error term, which is independent and follows Gumbel distribution. The probability (P_{ij}) of one alternative j (stop/go) for individual i is defined as

$$P_{ij} = \frac{\exp\left(\beta' x_{ij}'\right)}{1 + \exp\left(\beta' x_{ij}'\right)}. \tag{8}$$

The logit model was estimated with maximum likelihood estimation (MLE) procedures.

In the latent class model, heterogeneity is modeled using a set of groups, otherwise known as classes. Specifically, each individual is distributed to a "latent" class. It is assumed that parameters within each class contain the same effects, but there are different effects across classes. Model estimations are split into parameters related to each class, and a set of class probabilities [40]. Within the class, choice probabilities are calculated using the multinomial logit model:

$$P_{j|q} = \frac{\exp\left(\beta_q' x_{ij}'\right)}{\sum_{j=1}^{J}\exp\left(\beta_q' x_{ij}'\right)}, \quad q = 1, 2, \ldots, Q, \tag{9}$$

where Q is the number of latent classes, J represents the alternatives, x_{ij}' is the vector of all variables in the utility function, and β_q' is the class-specific parameter vector. The class for a specific individual is unobservable. Class probabilities are therefore generated using the multinomial logit form, as follows:

$$C_{iq} = \frac{\exp\left(\theta_q' z_i'\right)}{\sum_{q=1}^{Q}\exp\left(\theta_q' z_i'\right)}, \quad \theta_Q' = 0, \tag{10}$$

where z_i is an optional set of personal invariant characteristics. In this study, z_i denotes demographic and driving styles. For estimation, the last of parameter θ_Q was fixed as zero. For an individual, the estimation of the probability of a specific choice is the expected value (over classes) of the class-specific probabilities:

$$P_{ij} = \sum_{q=1}^{Q} C_{iq} P_{j|q}. \tag{11}$$

The number of classes, Q, is fixed, which is generally determined by setting an initial value and adjusting it. However, extended classes may not yield the best estimations and can sometimes create model instability and divergence [30]. In this study, the latent class logit model provides the best fit when Q was set to 2.

4.4. Model Development

4.4.1. HMM Estimates. HMM was established to extract the driving reliability index, one of driving style indexes. To establish the observation sequence, three variables were selected: speed, average acceleration rate, and phone status, which are proven to influence drivers' decision-making behaviors [41–44]. As illustrated in Table 3, the data of observed variables were discretized into three categories. Discretization thresholds for speed and average acceleration rate were the 50$^{\text{th}}$ and 85$^{\text{th}}$ percentiles. The observable state in HMM was the combination of the discrete data including 27 values, signed by a number from 1 to 27, respectively. Table 4 shows part of the ordered sequence of this observed data combination. Each trial was denoted with a corresponding figure which created a sequence. After coding the input sequence, the HMM for each driver was estimated using the EM algorithm.

Table 3: Rules of data discretization.

Speed		Average acceleration rate		Phone status	
Before (m/s)	After	Before (m/s^2)	After	Before	After
[11, 19.49)	1	(−2.24, 1.34]	1	Baseline	1
[19.49, 21.14)	2	(−4.02, −2.24], (1.34, 2.24]	2	Incoming	2
[21.14, 24.12]	3	[−7.13, −4.02], (2.24, 3.33]	3	Outgoing	3

Table 4: Rules of the observed combination sequence (partial).

Sequence number	Speed	Average acceleration rate	Phone status
1	1	1	1
2	1	1	2
3	1	1	3
4	1	2	1
5	1	2	2
6	1	2	3
7	1	3	1
8	1	3	2
9	1	3	3

4.4.2. Calculate Indicators Associated with Driving Styles. After estimating HMM, it becomes possible to calculate the driving reliability index. Before calculating the dangerous driving index, the dangerous drive needs to be identified. Telephone conversations (i.e., incoming calls or outgoing calls) and sudden braking/accelerating (i.e., average acceleration rate greater than $1.34\,m/s^2$ or less than $-2.24\,m/s^2$) were distinguished as dangerous behaviors. There were 12 dangerous states described with the observation combination sequence as shown in Table 4: (1, 2, 2), (1, 2, 3), (1, 3, 2), (1, 3, 3), (2, 2, 2), (2, 2, 3), (2, 3, 2), (2, 3, 3), (3, 2, 2), (3, 2, 3), (3, 3, 2), and (3, 3, 3). Corresponding sequence numbers were 5, 6, 8, 9, 14, 15, 17, 18, 23, 24, 26, and 27. Therefore each trial which involved dangerous behavior was identified. This key analytical step is the basis of calculating the dangerous driving index.

4.4.3. Estimation of the Latent Class Logit Model. Table 5 presents variables in the latent class logit model, including drivers' decisions, basic demographics (i.e., gender and age), driving styles (i.e., driving reliability index and dangerous driving index), and experimental variables such as drive number, phone status, and predicted time to stop line. It should be noted that the "predicted time to the stop line" was calculated by dividing the current distance from the stop line with the instant speed at the onset of yellow signal. According to the definition of the latent class logit model, variables for latent classification need to present demographics and driving characteristics. In this study, three variables were selected for latent classification–age, driving reliability index, and dangerous driving index.

5. Results

Table 6 provides estimates for the two new indicators of driving styles. The driving reliability index ranged from 0.465 to 0.692, while the dangerous driving index fluctuated from 0 to 0.611. For instance, the driving reliability index for Driver #2 had a maximum value of 0.692 which means that his/her driving decision was relatively unpredictable. Driver #2's dangerous driving index was 0.222 which was lower than the average. This means the probability of dangerous driving behavior was only 22.2%; therefore it can be understood that this driver's behavior in these trials was comparatively safe. Given that each indicator was different across drivers, these two indicators can be regarded as driver identifiers and further used for latent classification.

Estimation results are provided in Table 7, including a binary logit model without new indicators, a binary logit model with new indicators, and a latent class logit model with new indicators. When investigating fitting criterion indicators, the latent class model got 0.105 for the McFadden R-squared and 996.3 for the Akaike information criterion (AIC). These suggest that the latent class model provides the best fit and additionally explained attributes for each of the members within the class. Also, the McFadden R-squared of the binary logit model without the new predictors was 0.02, while this figure rose to 0.028 after adding the new indicators. The AIC of the binary logit model without new indicators is 1076.1, and it drops to 1071 after adding the new indicators. This suggests the derived estimations validate the precision of two indicators.

5.1. Direction and Magnitude of Parameters. When considering the results in Table 7, one might conclude that directions of parameters in both binary logit models and the latent class logit model are generally consistent. However, there are significant differences in the magnitude of these effects. Parameter estimations for the latent class model highlight the differences between drivers. Statistically significant parameters of the latent classification variables (i.e., age and dangerous driving index) indicate that these indicators influenced class probabilities. Also, the indicator, "DrR_Index," derived using HMM is statistically significant ($\alpha = 0.01$) in the binary logit model, which indicates that this is an additional attribute to affect the decision-making process of the participants.

The directions of most parameter estimation in two classes are opposing, which highlights the differences between groups. Class I accounts for 53.3% of all participants. Visually, the parameter of the indicator "Time" is negative. The parameter of "Time_Baseline" (−2.395) is less than that of "Time_Income" (−2.468) or "Time_Outgo" (−2.493). This may have occurred because nonsignificant parameters for the second/third driving experiment had no apparent inclination of stopping or going as the experiment commenced.

Class II accounted for 46.7% of the participants. The parameter of indicator "Time" is positive and the parameters for "Time" under different conditions are almost the same

Table 5: Descriptions for selected variables.

Variables	Description	Values
Dependent variables		
Drivers' decisions	Stop Go	0 = stop 1 = go
Independent variables		
Gender	Male Female	0 = male 1 = female
Age	Young group (18–25 years) Middle-aged group (30–45 years) Old group (50–60 years)	0 = young and middle-aged groups 1 = old group
2nd_drive	Driver's second "drive" experiment	0 = others 1 = the second "drive" experiment
3rd_drive	Driver's third "drive" experiment	0 = others 1 = the third "drive" experiment
Time_Baseline	Expected time to stop line without phone calls	Continuous
Time_Income	Expected time to stop line with incoming phone calls	Continuous
Time_Outgo	Expected time to stop line with outgoing phone calls	Continuous
DrR_Index	Driving reliability index	Continuous
Ddr_Index	Dangerous driving index	Continuous

Table 6: Indicators associated with driving styles (partial).

	Min.	Max.	Mean	Driver ID									
				1	2	3	4	5	6	7	8	9	10
Driving reliability index	0.465	0.692	0.601	0.558	0.692	0.619	0.533	0.560	0.649	0.603	0.686	0.465	0.587
Dangerous driving index	0	0.611	0.233	0.167	0.222	0.154	0.056	0.111	0.529	0.167	0.471	0	0.118

Table 7: Parameter estimation results for models.

Parameter	Binary logit model without new indicators	Binary logit model with new indicators	Latent class logit model	
			Class I	Class II
Constant	0.460 (0.651)	**−2.504 (1.214)****	1.498 (2.419)	2.695 (2.755)
Gender	**0.306 (0.147)****	**0.388 (0.151)****	**2.038 (0.551)*****	**−1.303 (0.325)*****
2nd_drive	−0.233 (0.177)	−0.252 (0.178)	0.002 (0.355)	**−0.709 (0.334)****
3rd_drive	**−0.465 (0.180)*****	**−0.474 (0.181)*****	−0.142 (0.362)	**−0.996 (0.349)*****
Time_Baseline	−0.316 (0.196)	**−0.328 (0.198)***	**−2.395 (0.688)*****	**1.578 (0.424)*****
Time_Income	**−0.353 (0.198)***	**-0.367 (0.199)***	**−2.493 (0.719)*****	**1.560 (0.430)*****
Time_Outgo	**−0.340 (0.198)***	**−0.353 (0.199)***	**−2.468 (0.705)*****	**1.594 (0.433)*****
Age	**0.460 (0.161)*****	**0.553 (0.165)*****	**−3.889 (1.480)*****	0
DrR_Index	—	**5.144 (1.837)*****	−10.479 (8.695)	0
Ddr_Index	—	−0.630 (0.597)	**−11.513 (3.486)*****	0
Constant_Class	—	—	**10.186 (6.019)***	0
Class probabilities	—	—	0.533 (0.403)	0.467 (0.403)
Log likelihood	−530.06	−525.50	−478.17	
McFadden *R*-squared	0.020	0.028	0.105	
AIC	1076.1	1071.0	996.3	

Tabular values indicate parameter estimates (standard errors) for each model. The symbols ***, **, and * mean statistical significance at $\alpha = 0.01$, 0.05, 0.1, respectively.

(1.578, 1.560, and 1.594). Drivers in Class II were perhaps influenced by the simulator environment because "2nd_drive" and "3rd_drive" indicators were significant at $\alpha = 0.05$ and 0.01, respectively.

5.2. Quantified Impact of Variables. To quantify the impact of these variables, partial effects were calculated as follows:

$$\frac{\partial E[y \mid x]}{\partial x} = \frac{\partial F(\beta\prime x)}{\partial x} = \frac{\mathrm{d}F(\beta\prime x)}{\mathrm{d}\beta\prime x}\beta = f(\beta\prime x)\beta, \quad (12)$$

where $f(\beta\prime x)$ is the density function of x. When the variable in x is a dummy variable, the alternative method is

$$\begin{aligned}\Delta F_{x_k} &= \text{Prob}[y = 1 \mid x_k = 1] - \text{Prob}[y = 1 \mid x_k = 0] \\ &= F\left(\beta\prime x + \alpha x_k \mid x_k = 1\right) - F\left(\beta\prime x + \alpha x_k \mid x_k = 0\right) \\ &= F(\beta\prime x + \alpha) - F(\beta\prime x).\end{aligned} \tag{13}$$

Partial effects were calculated by averaging the function over the sample observations. Findings suggest an average change in the probability of going for a 1-unit change in scale factor, or the change in the probability of going compared with the baseline category in dummy factor. Table 8 presents partial effects and odds ratios for each model.

From Table 8, the effects of indicators on different classes can be identified. In Class I, the odds ratios of "Time" indicators which ranged from 0.08 to 0.09, are all less than 1. This means that these drivers were more likely to stop, as the time to the stop line increases. Odds ratios of women in Class I making the "go" decision were 7.68 times those of men in the same class.

In Class II, odds ratios of "Time" indicators ranged from 4.76 to 4.92 and were larger than 1. This suggests that these drivers tend to pass the intersection as the time to stop line increases. Odds ratios for "go" during the 2nd experimental phase were 0.49 times those during the first one, and this figure decreased to 0.37 in the 3rd experiment. This suggests that drivers in Class II generally prefer to stop as experiment proceeds. Odds ratios for women in Class II making the "go" decision were 0.27 times those of men in the same class.

In terms of partial effects of three models, several conclusions can be made. Female drivers are 6.9%–10.1% more likely to choose to go compared to male drivers. Old drivers are 10.6%–12.6% more likely to choose to go than young and middle-aged drivers. Compared with 1st "drive," drivers were 5.2%–7.0% and 10.2%–11.5% less likely to choose to go in their 2nd and 3rd "drive" experience. There was also a 114% increase in the probability of going which was estimated with every 1-unit increase in the driving reliability index. Each 1-second increase in the time to stop line manifested in a 7.1%–12.7% decreased probability of going.

Considering the phone as a distraction related to stop/go behavior in these circumstances, there was relative conformity with empirical judgment. Partial effects of the three models suggest that compared with uninterrupted driving, incoming/outgoing calls increase the probability of stopping slightly. When investigating the effect on drivers in a specific class, the odds ratios of "Time" under different calling tasks were almost equivalent. Further details about the effect of phone distractions will be critically discussed in the following section.

6. Discussion

6.1. Driving Risk of Different Classes. Analysis using the latent class model indicates that two classes of drivers with different driving styles exist. The negative parameters of latent classification variables (−3.889 for "Age" and −11.513 for "Ddr_Index," significant at $\alpha = 0.01$) in Table 7 suggest that increasing these values contributes to a higher probability of Class II categorization. Additionally, the data provided in Figure 2 validates that as drivers' age or the value of drivers' dangerous driving index increases, the probability of Class II increases. Ultimately, this means that those who were categorized as Class II were old and more likely to display risky behaviors, such as sudden acceleration and braking.

Before discussing drivers' decision properties, experimental settings of triggering yellow signals need to be specified. As drivers approached simulated intersections, traffic signal began to change to yellow at one of the two preset intervals (i.e., 3 seconds or about 3.75 seconds). From the designers' perspective, the first interval of 3 seconds was intended to elicit a "go" response from the participant, whereas the second interval of 3.75 seconds was intended to elicit a "stop" response. In other words, the probability of going at around 3 seconds was expected to be larger than that at 3.75 seconds. This enabled us to determine what was considered *safe* decisions.

Drivers' decision properties can be identified and evaluated using data provided in Figure 3. The distribution of dots for Class I individuals shows that these drivers are more likely to go through the intersection when the time to stop line is less than 3 seconds. Although the same drivers are also more likely to halt further when the time to stop line is 3.75 seconds, this decision appears identical to the expected safe decision probably because these drivers appear to prefer the low-risk choice. Decisions of Class II drivers are comparatively inconsistent. The probability of going under the 3.75 seconds interval is equal or larger than that observed in the 3-second interval. This result may be interpreted according to their respective high-risk driving characteristics.

Considering driving styles and stop/go decision property discussed above, drivers in Class I can be confirmed as "low-risk drivers," while drivers in Class II are defined as "high-risk drivers."

6.2. Distraction Effects on Different Classes. The effects of cell phone distractions on stop/go decisions were evaluated using changes in probability. For instance, when drivers were near the intersection with a time to the stop line of fewer than 3 seconds, the probability of going with an incoming call decreased compared with no call scenarios. This would suggest that drivers receiving a call are more likely to slow and stop even though passing the intersection was actually the safer choice.

Figure 4 demonstrates the effects of calling distraction on drivers' decisions. "Low-risk" drivers, categorized as Class I, were disturbed only when the time to stop line was less than 3 seconds. Compared with uninterrupted driving, drivers in Class I with phone calls appeared to prefer to stop, which may actually be improper because passing the intersection was the safer choice at this point. This effect was the same under both incoming and outgoing calls. The influence of

Table 8: Quantified impact of variables.

Variables	Binary logit model without new indicators		Binary logit model with new indicators		Latent class logit model		
	Partial effect (%)	Odds ratio	Partial effect (%)	Odds ratio	Partial effect (%)	Odds ratio	
						Class I	Class II
Gender	+6.9	1.36	+8.6	1.47	+10.1	7.68	0.27
2^{nd}_drive	−5.2	0.79	−5.5	0.78	−7.0	1.00	0.49
3^{rd}_drive	−10.2	0.63	−10.3	0.62	−11.5	0.87	0.37
Time_Baseline	−7.1	0.73	−7.3	0.72	−11.4	0.09	4.85
Time_Income	−7.9	0.70	−8.1	0.69	−12.7	0.08	4.76
Time_Outgo	−7.6	0.71	−7.8	0.70	−12.1	0.08	4.92
Age	+10.6	1.58	+12.6	1.74	—	—	—
DrR_Index	—	—	+114.0	171.40	—	—	—
Ddr_Index	—	—	−14.0	0.53	—	—	—

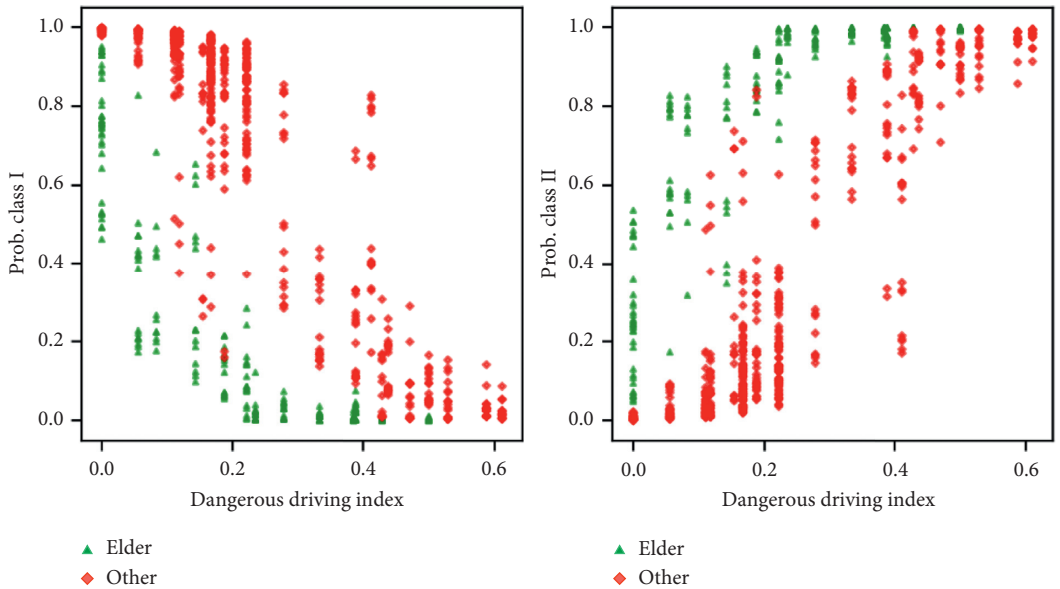

Figure 2: Effect of driving styles on the probability of Classes I and II.

phone calls on "high-risk" drivers in Class II changed under different circumstances. When they were close to the stop line with less than 2.95 seconds, both incoming and outgoing calls increased the likelihood probability of slowing and stopping, compared with uninterrupted driving. Although when the time to stop line was 3 seconds, incoming calls resulted in a greater decrease in the probability of going, compared to outgoing calls. While drivers were still at a distance from the stop line, with times longer than 3.6 seconds, both incoming and outgoing calls increase the probability of deciding to go, compared with uninterrupted driving.

It could be concluded that taking a phone call can initiate unsafe decisions in both Classes I and II. This could be in terms of both slowing unnecessarily and deciding to go when the time does not permit. Results show that Class II is more sensitive to this distraction having a greater change in the probability of deciding to go. This analysis suggests therefore that higher-risk drivers are more likely to respond frivolously to distractions such as an incoming or outgoing phone call.

6.3. Results Comparison with Previous Research. The findings of this study add to the growing evidence base. For example, we find age and gender influence drivers' stop/go decision-making, which agrees with previous studies [7, 45–47]. The results also suggest that most female drivers are more likely to run the yellow signal, compared with their male counterparts. Additionally, compared with adolescent and middle-aged drivers, old drivers (over 50 years old) are more likely to make unsafe decisions, which may be due to the long perception-reaction time.

The results agree with the research which suggests that drivers' decisions are influenced by their familiarity with the traffic environment [7]. We further find that most drivers have no apparent inclination of stopping or going as the simulation experiment carries on, while a small portion of

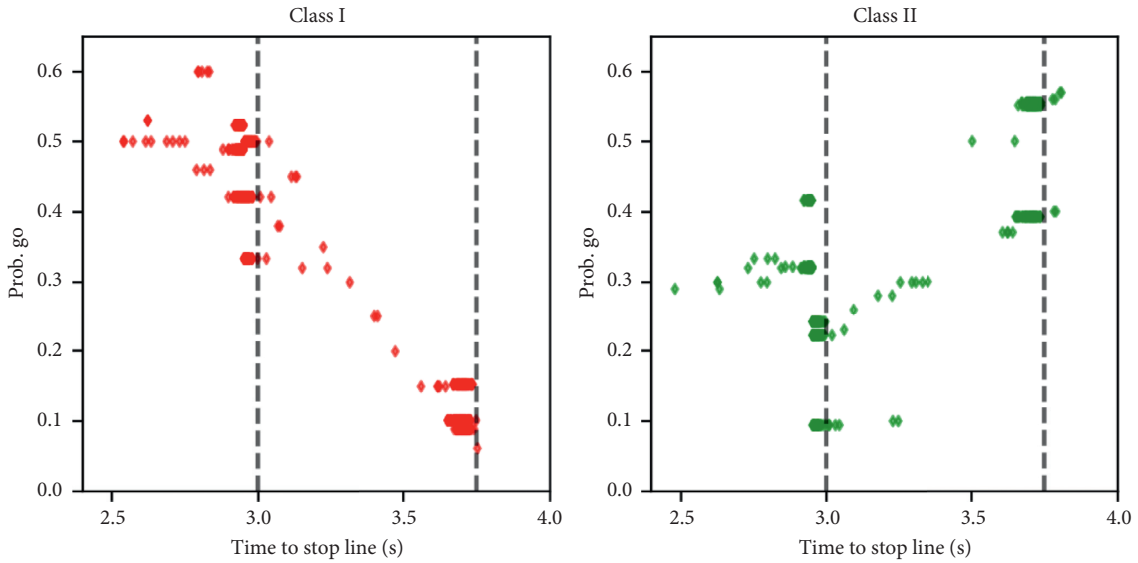

Figure 3: Decision properties for Classes I and II of drivers.

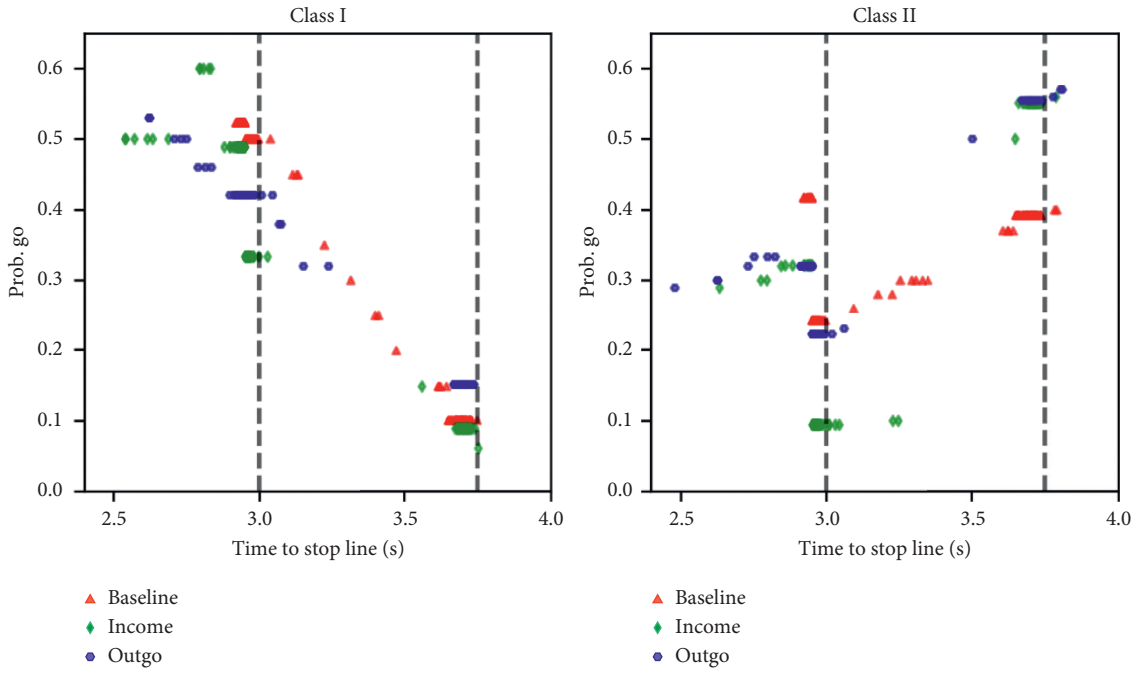

Figure 4: Effect of distraction on decisions in Classes I and II of drivers.

drivers tend to stop as the experiment proceeds. This may reflect that part drivers are more accustomed to the simulation environment and anticipate signal changes as the experiment commences.

The findings confirm that cell phone talk can induce drivers to make unsafe decisions [7, 10, 47]. Furthermore, we find drivers' behavioral differences in decision-making under distractions. Only close to the stop line are most drivers disturbed to make unsafe decisions. A small portion of drivers in distractions will make unsafe decisions wherever they were, which may be due to their oldness and high-risk driving style.

7. Conclusions

Drivers' improper stop/go decisions at the onset of yellow signals may cause numerous problems at intersections. Improper decisions may lead to rear-end collisions or red-light running violations. To address the decision issues and accommodate group heterogeneity, a latent class logit model

was used to analyze drivers' decision-making processes in this study.

We explored two new variables associated with driving styles (i.e., the driving reliability index and dangerous driving index), which further calibrated the class probabilities in the latent class model. Indicators for the goodness of fit demonstrate that our model with driving styles is superior to binary logit models. Therefore, the latent class model considering driving styles can accurately evaluate drivers' decisions at the onset of yellow signal.

Drivers are classified into "low-risk" and "high-risk" categories according to driving styles. The driving reliability index appears to influence drivers' stop/go decision-making whereas the dangerous driving index influences the proportion of two categories. Results indicate that "low-risk" drivers are less likely to make risky decisions, while "high-risk" drivers are more likely to make improper decisions.

Similar with previous research, we found that driving while talking on the phone may cause drivers' inappropriate decisions at the onset of yellow signal. The effects of cell phone distractions were inconsistent within our sample of drivers. For "low-risk" drivers, it seemed that they were only slightly disturbed by the phone calls and more prone to stop when close to the stop line. However, there was little difference in the effect of incoming or outgoing calls. "High-risk" drivers presented obvious differences in the decision when using cell phones. This group appeared to behave completely differently to "low-risk" drivers meaning that our classification was meaningful.

Drivers in different groups have different preferences in stop/go decision-making. To improve safety at signalized intersections, policy-makers need to pay more attention to "high-risk" drivers, although critically speaking risking driving may be an impulse rather than a consistent factor. Nevertheless, "high-risk" drivers might be more intensively observed to ensure there are fewer risky behaviors. Imposing higher fines, reeducation, and higher charge rates of insurance may incentivize changes. Once the "high-risk" drivers develop stable and safe driving habits, the intensity of observation might be reduced.

Data Availability

The data used for this study are from experiments conducted at the University of Iowa-National Advanced Driving Simulator (NADS), which can be accessed from the following website: http://depts.washington.edu/hfsm/upload.php.

Conflicts of Interest

The authors declare that there are no conflicts of interest regarding the publication of this paper.

Acknowledgments

This research was supported by the Fundamental Research Funds for the Central Universities (no. 2019JBM036).

References

[1] National Center for Statistics and Analysis, "Distracted driving in fatal crashes, 2017," Report No. DOT HS 812 700, National Highway Traffic Safety Administration, Washington, DC, USA, 2019.

[2] The Federal Highway Administration (FHWA), *Intersection Safety: Background and Objectives*, The Federal Highway Administration (FHWA), Washington, DC, USA, 2018, https://highways.dot.gov/research-programs/safety/intersection-safety.

[3] E.-H. Choi, "Crash factors in intersection-related crashes: An on-scene perspective (No. HS-811366)," National Center for Statistics and Analysis, National Highway Traffic Safety Administration, US Department of Transportation, Washington, DC, USA, 2010, https://crashstats.nhtsa.dot.gov/Api/Public/ViewPublication/811366.

[4] D. Gazis, R. Herman, and A. Maradudin, "The problem of the amber signal light in traffic flow," *Operations Research*, vol. 8, no. 1, pp. 112–132, 1960.

[5] C. Liu, R. Herman, and D. C. Gazis, "A review of the yellow interval dilemma," *Transportation Research Part A: Policy and Practice*, vol. 30, no. 5, pp. 333–348, 1996.

[6] M. Elhenawy, A. Jahangiri, H. A. Rakha, and I. El-Shawarby, "Modeling driver stop/run behavior at the onset of a yellow indication considering driver run tendency and roadway surface conditions," *Accident Analysis and Prevention*, vol. 83, pp. 90–100, 2015.

[7] P. T. Savolainen, "Examining driver behavior at the onset of yellow in a traffic simulator environment: comparisons between random parameters and latent class logit models," *Accident Analysis and Prevention*, vol. 96, pp. 300–307, 2016.

[8] K. L. Young, P. M. Salmon, and M. Cornelissen, "Distraction-induced driving error: an on-road examination of the errors made by distracted and undistracted drivers," *Accident Analysis and Prevention*, vol. 58, pp. 218–225, 2013.

[9] S. G. Klauer, F. Guo, B. G. Simons-Morton, M. C. Ouimet, S. E. Lee, and T. A. Dingus, "Distracted driving and risk of road crashes among novice and experienced drivers," *The New England Journal of Medicine*, vol. 370, no. 1, pp. 54–59, 2014.

[10] A. D. Ohlhauser, L. N. Boyle, D. Marshall, and O. Ahmad, "Drivers' behavior through a yellow light: effects of distraction and age," *Proceedings of the Human Factors and Ergonomics Society Annual Meeting*, vol. 55, no. 1, pp. 1919–1923, 2011.

[11] B. E. Porter and K. J. England, "Predicting red-light running behavior: a traffic safety study in three urban settings," *Journal of Safety Research*, vol. 31, no. 1, pp. 1–8, 2000.

[12] H. Köll, M. Bader, and K. W. Axhausen, "Driver behaviour during flashing green before amber: a comparative study," *Accident Analysis and Prevention*, vol. 36, no. 2, pp. 273–280, 2004.

[13] Y. Liu, G.-L. Chang, R. Tao, T. Hicks, and E. Tabacek, "Empirical observations of dynamic dilemma zones at signalized intersections," *Transportation Research Record: Journal of the Transportation Research Board*, vol. 2035, no. 1, pp. 122–133, 2007.

[14] N. Elmitiny, X. Yan, E. Radwan, C. Russo, and D. Nashar, "Classification analysis of driver's stop/go decision and red-light running violation," *Accident Analysis and Prevention*, vol. 42, no. 1, pp. 101–111, 2010.

[15] Y. Wu, M. Abdel-Aty, Y. Ding, B. Jia, Q. Shi, and X. Yan, "Comparison of proposed countermeasures for dilemma zone at signalized intersections based on cellular automata simulations," *Accident Analysis and Prevention*, vol. 116, pp. 69–78, 2018.

[16] Urbanik T., Koonce P., The dilemma with dilemma zones, 2007, http://redlightrobber.com/red/links_pdf/The-Dilemma-with-Dilemma-Zones.pdf.

[17] C. V. Zegeer and R. C. Deen, "Green-extension systems at high-speed intersections," *Ite Journal-Institute of Transportation Engineers*, vol. 48, no. 11, pp. 19–24, 1978.

[18] L. A. Klein, M. K. Mills, and D. R. P. Gibson, *Traffic Detector Handbook*, US. Department of Transportation, Federal Highway Administration, Washington, DC, USA, 3rd edition, 2006.

[19] N. K. Chaudhary, T. D. Casanovapowell, L. Cosgrove, I. Reagan, and A. Williams, "Evaluation of NHTSA distracted driving demonstration projects in connecticut and New York," 2014, http://www.nhtsa.gov/staticfiles/nti/pdf/811635_Eval_NHTSA_Distracted_Driving_Demo_Proj_Comm_CT_and_NY.pdf.

[20] B. J. Russo, J. J. Kay, P. T. Savolainen, and T. J. Gates, "Assessing characteristics related to the use of seatbelts and cell phones by drivers: application of a bivariate probit model," *Journal of Safety Research*, vol. 49, pp. 137.e1–142, 2014.

[21] I. El-Shawarby, H. A. Rakha, V. Inman, and G. Davis, "Effect of yellow-phase trigger on driver behavior at high-speed signalized intersections," in *Proceedings of the IEEE Intelligent Transportation Systems Conference*, pp. 683–688, Toronto, Canada, September 2006.

[22] H. Rakha, I. El-Shawarby, and J. R. Setti, "Characterizing driver behavior on signalized intersection approaches at the onset of a yellow-phase trigger," *IEEE Transactions on Intelligent Transportation Systems*, vol. 8, no. 4, pp. 630–640, 2007.

[23] P. Papaioannou, "Driver behaviour, dilemma zone and safety effects at urban signalized intersections in Greece," *Accident Analysis and Prevention*, vol. 39, no. 1, pp. 147–158, 2007.

[24] T. J. Gates, D. A. Noyce, L. Laracuente, and E. V. Nordheim, "Analysis of driver behavior in dilemma zones at signalized intersections," *Transportation Research Record*, vol. 2030, no. 1, pp. 29–39, 2007.

[25] X. Yan, E. Radwan, D. Guo, and S. Richards, "Impact of "signal ahead" pavement marking on driver behavior at signalized intersections," *Transportation Research Part F: Traffic Psychology and Behaviour*, vol. 12, no. 1, pp. 50–67, 2009.

[26] K. Long, Y. Liu, and L. D. Han, "Impact of countdown timer on driving maneuvers after the yellow onset at signalized intersections: an empirical study in Changsha, China," *Safety Science*, vol. 54, pp. 8–16, 2013.

[27] C. R. Bhat, "An endogenous segmentation mode choice model with an application to intercity travel," *Transportation Science*, vol. 31, no. 1, pp. 34–48, 1997.

[28] K. Roeder, K. G. Lynch, and D. S. Nagin, "Modeling uncertainty in latent class membership: a case study in criminology," *Journal of the American Statistical Association*, vol. 94, no. 447, pp. 766–776, 1999.

[29] J. S. Uebersax, "Probit latent class analysis with dichotomous or ordered category measures: conditional independence/dependence models," *Applied Psychological Measurement*, vol. 23, no. 4, pp. 283–297, 1999.

[30] W. H. Greene and D. A. Hensher, "A latent class model for discrete choice analysis: contrasts with mixed logit," *Transportation Research Part B: Methodological*, vol. 37, no. 8, pp. 681–698, 2003.

[31] J. W. Milon and D. Scrogin, "Latent preferences and valuation of wetland ecosystem restoration," *Ecological Economics*, vol. 56, no. 2, pp. 162–175, 2006.

[32] J. L. Walker and J. Li, "Latent lifestyle preferences and household location decisions," *Journal of Geographical Systems*, vol. 9, no. 1, pp. 77–101, 2007.

[33] A. R. Hole, "Modelling heterogeneity in patients' preferences for the attributes of a general practitioner appointment," *Journal of Health Economics*, vol. 27, no. 4, pp. 1078–1094, 2008.

[34] S. Hess, A. Stathopoulos, and A. Daly, "Allowing for heterogeneous decision rules in discrete choice models: an approach and four case studies," *Transportation*, vol. 39, no. 3, pp. 565–591, 2012.

[35] J. Shen, "Latent class model or mixed logit model? A comparison by transport mode choice data," *Applied Economics*, vol. 41, no. 22, pp. 2915–2924, 2009.

[36] TRB Statistics Committee (ABJ80), "Questions and answers for 2014 TRB contest," 2013, http://trbstats.weebly.com/uploads/6/6/6/4/6664035/q_a_for_2014_trb_contest_nov_18_2013.pdf.

[37] L. E. Baum and T. Petrie, "Statistical inference for probabilistic functions of finite state Markov chains," *The Annals of Mathematical Statistics*, vol. 37, no. 6, pp. 1554–1563, 1966.

[38] L. R. Rabiner, "A tutorial on hidden markov models and selected applications in speech recognition," *Proceedings of the IEEE*, vol. 77, no. 2, pp. 267–296, 1989.

[39] E. Farmer and E. G. Chambers, "A study of accident proneness among motor drivers," *Journal of the Royal Statistical Society*, vol. 103, no. 2, p. 254, 1940.

[40] Greene W. H., NLOGIT 5, Version 5.0, 2012, http://www.limdep.com.

[41] A. Sharma, "Integrated behavioral and economic framework for improving dilemma zone protection systems," Purdue University, West Lafayette, IN, USA, Doctoral Dissertation, 2008.

[42] A. Amer, H. Rakha, and I. El-Shawarby, "Agent-based behavioral modeling framework of driver behavior at the onset of yellow indication at signalized intersections," in *Proceedings of the 2011 14th International IEEE Conference on Intelligent Transportation Systems*, pp. 1809–1814, Washington, DC, USA, October 2011.

[43] A. Sharma, D. Bullock, and S. Peeta, "Estimating dilemma zone hazard function at high speed isolated intersection," *Transportation Research Part C: Emerging Technologies*, vol. 19, no. 3, pp. 400–412, 2011.

[44] J. Li, Q. He, H. Zhou, Y. Guan, and D. Wei, "Modeling driver behavior near intersections in hidden markov model," *International Journal of Environmental Research and Public Health*, vol. 13, no. 12, p. 1265, 2016.

[45] S. M. Lavrenz, V. D. Pyrialakou, and K. Gkritza, "Modeling driver behavior in dilemma zones: a discrete/continuous formulation with selectivity bias corrections," *Analytic Methods in Accident Research*, vol. 3-4, pp. 44–55, 2014.

[46] H. Xiong, P. Narayanaswamy, S. Bao, C. Flannagan, and J. Sayer, "How do drivers behave during indecision zone maneuvers?" *Accident Analysis & Prevention*, vol. 96, pp. 274–279, 2016.

[47] M. M. Haque, A. D. Ohlhauser, S. Washington, and L. N. Boyle, "Decisions and actions of distracted drivers at the onset of yellow lights," *Accident Analysis & Prevention*, vol. 96, pp. 290–299, 2016.

Hindawi
Journal of Advanced Transportation
Volume 2020, Article ID 5898762, 11 pages
https://doi.org/10.1155/2020/5898762

Research Article

Driving Performance Evaluation Correlated to Age and Visual Acuities Based on VR Technologies

Sooncheon Hwang,[1] Sunhoon Kim,[1] and Dongmin Lee [2]

[1]*Department of Transportation Engineering, The University of Seoul, 163 Slsiripdae-Ro, Dongdaemun-Gu, Seoul 02504, Republic of Korea*
[2]*Department of Transportation Engineering & Department of Smart City, The University of Seoul, 163 Seoulsiripdae-Ro, Dongdaemun-Gu, Seoul 02504, Republic of Korea*

Correspondence should be addressed to Dongmin Lee; dmlee@uos.ac.kr

Received 19 December 2019; Accepted 21 April 2020; Published 1 July 2020

Academic Editor: Inhi Kim

There is currently much debate regarding the effectiveness of the driver license system in South Korea, due to the numerous traffic crashes caused by drivers who are suspected of having insufficient physical and mental abilities. Through the present system, it is quite difficult to identify such drivers indirectly through physical tests, such as visual acuity tests, since the correlation of such results with driving performance remains unclear. The objective of this study was to investigate the relationship between driving performance and visual acuities for improving the South Korean driver license system. In this study, two investigations were conducted: static and dynamic visual acuity examinations and driving performance tests based on a virtual reality (VR) system. The driving performance was evaluated with a driving simulator, based on driving behaviors in different experimental scenarios, including daytime and nighttime driving on a rural highway, and unexpected incident situations. Here, we produce statistically significant evidence that reduced visual acuity impairs driving performance, and driving behaviors differ significantly among groups with different vision capabilities, especially dynamic vision. Visual acuities, typically dynamic visual acuity, greatly influenced driving behavior, as measured by the standard deviation of speeds and vehicle LPs, and this was especially notable in curved road segments in daytime experiment. These experimental results revealed that the driving performance of participants with impaired dynamic visual acuity was deficient and unsafe. This confirmed that dynamic visual acuity levels are significant determinants of driving behavior, and they well explain driver performance levels. These findings suggest that the South Korean driver license system should include a test of dynamic visual acuity to create better and safer driving.

1. Introduction

There are many ways to improve transportation safety, including improving geometric conditions, increasing education, publicizing campaigns, and taking other approaches to improve traffic safety. However, in the context of traffic safety, one of the most important steps is to evaluate whether drivers have adequate capabilities for driving. Driver performance evaluations are critical for identifying individuals who are not qualified to drive because such drivers can seriously affect safety on the road.

Generally, the driver license system is the first stage of preventing traffic crashes, as it evaluates driver performance to identify drivers with inadequate physical abilities. However, there have recently been many arguments regarding the effectiveness of the driver license system in South Korea, due to the many traffic crashes caused by drivers with insufficient physical and mental abilities. The current system in South Korea does not identify such drivers because some of the tests are rather cursory, such as vision and hearing tests. In contrast, many other countries, including Germany, France, Japan, the US, and the UK, have implemented a variety of tests to regularly identify unqualified drivers, including high-level standards for vision tests, viewing angle tests, cognitive ability tests, and other standard medical tests. However, driving performance tests

cannot be conducted on real roads. It is also quite difficult to evaluate driving performance indirectly through physical tests, such as visual acuity and muscle performance tests, since the correlation of their results with driving performance is unclear. Thus, to improve traffic safety, a new method of accurately evaluating driving performance must be developed.

In this study, driving performance was evaluated through virtual reality (VR) technology to identify unqualified drivers. Recently, VR technology has been used in many areas of transportation engineering, such as driver education, primary driving testing, and driver behavior studies. Such technology has also been used to evaluate driver performance in many studies, due to the difficulty of performing real-time road tests.

The objectives of this study were to determine the relationships between driving performance and physical abilities based on driving simulator experiments and to develop an appropriate method of evaluating driver performance. Physical abilities that are easily measurable and closely related to driver performance were used to develop the evaluation method. Among various physical abilities, the visual acuity levels in different age groups were used to evaluate driving performance, since drivers generally obtain the information needed to safely operate their vehicles through vision, for example, road alignments, road signs, and other driving environments. After visual acuity was examined and driving simulator experiments were conducted, driving behaviors and performance characteristics were analyzed by a statistical modeling process to determine those influencing factors on reaction time which significantly affect traffic crashes.

2. Literature Review

It is generally known that drivers get most of the information they need to drive through vision [1], making vision the most important ability for driving. Visual acuity is a measure of the spatial resolution of the visual processing system, and a visual acuity test is an eye exam that checks how well a person sees the details of an object from a specific distance [2, 3]. There are different types of visual acuities related to driving such as static and dynamic visual acuity.

Visual acuity normally declines with age, as shown in several studies that investigated the relationship between age and visual acuities [4–7]. Another study of vision tests for drivers found that the number of drivers with visual acuity loss was four times greater among those aged 65 years or older than in younger drivers [8]. Those researchers conducted an automated visual inspection on 10,000 drivers and found that only 3% to 3.5% of those who were aged 16 to 60 years had impaired vision, whereas 13% of those who were aged 65 years and over had vision problems.

Insufficient visual acuity may cause poor driving performance, as evidenced by driving violations and traffic crashes [8–12]. Burg investigated the relationship between visual acuity, driving violations, and traffic crashes in California, USA, and found a slight correlation among them [9], and a similar analysis [10] indicated that measures of visual performance, such as static and dynamic visual acuity, correlated significantly with the crash rate of drivers over the age of 54. In another related study of the visual acuity levels (static and dynamic) of 12,400 drivers and their traffic crashes and law violations, it was found that drivers over the age of 66 had a higher risk of crashes [11]. However, those previous studies indirectly analyzed the relationship between a visual acuity and driving performance by tracking the number of violations and traffic crashes. In this study, the influence factors on driving violations and traffic crashes were driving distance, age, gender, and visual acuity (static and dynamic).

Among the various types of visual acuities, dynamic visual acuity is known to significantly affect recognition of traffic ahead and road conditions [13–19]. Hofstetter [14] found a meaningful relationship between dynamic visual acuity and recognition of moving objects, and Long and Kearns [15] also revealed similar results regarding the relationship between traffic sign recognition and dynamic visual acuity. Higgins and Wood [17] tested the effects of visual acuity against measures for driving performance, including gap perception, total driving time, and sign recognition, using a lens designed with different visual acuity levels (ranging from 0.1 to 1.5). They observed poor driving performance based on those measures in participants with lower dynamic visual acuity. These results also revealed that vision tests for only static vision acuity (not for dynamic vision acuity) are of limited usefulness in this context. Because the relationship between such tests and driving performance was not really proven statistically, there is still needed to develop effective and reliable methods that can precisely correlate visual acuity and driver performance [12, 20].

Several previous studies used a driving simulator to investigate driver behaviors and performance, due to real-time road test limitations such as safety hazards and difficulty in preparing designed situations for experiments [16, 21–24, 25–27]. Only a few studies have used a driving simulator to directly investigate the relationship between visual acuity and driving performance. Wilkins [16] conducted a driving simulator test to measure brake response rates in hazardous situations and found that drivers with better dynamic visual acuity had better risk detection records. In another study on the effects of visual acuity on the driving ability of multiple sclerosis patients, a driving simulator was used to evaluate the subjects' driving performance [28].

There have also been studies recommending the improvement of driver license systems [29, 30]. For example, Owsley and McGwin [21] suggested that it is necessary to measure visual acuity more precisely in the driver licensing system of England, but they failed to find clear evidence that an improved driver licensing system would reduce traffic crashes.

Our reviews of the relevant literature found the following meaningful issues. First, visual acuity, which is highly important for safe driving, normally weakens with age, and this deterioration of vision may cause driving violations and traffic crashes. Thus, declining visual acuity is a critical safety

problem. Second, dynamic visual acuity is known to significantly affect driving performance, but it is hard to measure it and to prove a statistically relevant relationship between dynamic visual acuity and driving performance. Therefore, more precise methods to measure visual acuities should be developed, and studies to investigate the relationship between visual acuity and driving performance need to be conducted.

3. Methodology

In this study, two different investigations were conducted: a visual acuity test and a driving performance test utilizing a VR system. The relationship between driving performance and physical abilities was determined using that VR driving simulator in a series of experiments. Figure 1 illustrates the detailed study flows.

3.1. Visual Acuity Evaluation. For visual acuity evaluations, different types of visual acuities were examined, including static and dynamic visual acuity, because dynamic visual acuity are known to have greater effects on driving performance than static visual acuity [1]. Our visual acuity evaluations were conducted with the Multifunctional Vision Test System developed and verified by the Korea Road Traffic Authority. First, we reanalyzed the visual acuity evaluations results examined by this test system in a previous study [31]. This study was conducted only to evaluate the performance of the vision test system; the data used for verification in that study were used in this study to investigate the reduction in visual acuity performance with aging. Second, the same test system was used to evaluate the visual acuity of the participants in this study, so that subject driving performance could be compared according to visual acuity level. The purpose of this visual acuity test was to evaluate subjects' ability to identify fixed and moving objects. The test results were scored from 0.1 to 1.5, and subjects with scores greater than 0.5 were judged as having passed the vision test, while the rest were judged as having failed. These criteria were based on the standards of the driving aptitude test used by driving license institutes in South Korea. These thresholds were applied for evaluation of static and dynamic visual acuity.

3.2. Driving Simulator Experiments. We conducted driving simulator experiments to measure various driving behaviors under many different driving conditions. In total, 65 participants (35 younger drivers and 30 older drivers, 49 male and 16 female drivers) who drove at least three or four times in every week with an active driver's license were involved in the experiments. Among the younger drivers, there were 11 participants in their twenties, 9 participants in their thirties, 8 participants in their forties, and 7 participants in their fifties; the older drivers were those older than 65 years.

The experiments to evaluate driving performance were conducted in two designed scenarios based on rural highway driving: daytime (scenario 1) and nighttime (scenario 2). Unexpected incident situations, as shown in Figure 2, were created in a driving simulator based on VR technology. The unexpected incident #1 was a dog that suddenly ran into the driving lane, and the driver had to stop to avoid hitting it. In incident #2, a vehicle in the adjacent lane suddenly cut into the driving lane. In the last incident, a heavy vehicle was approaching from a cross road to an unsignalized intersection.

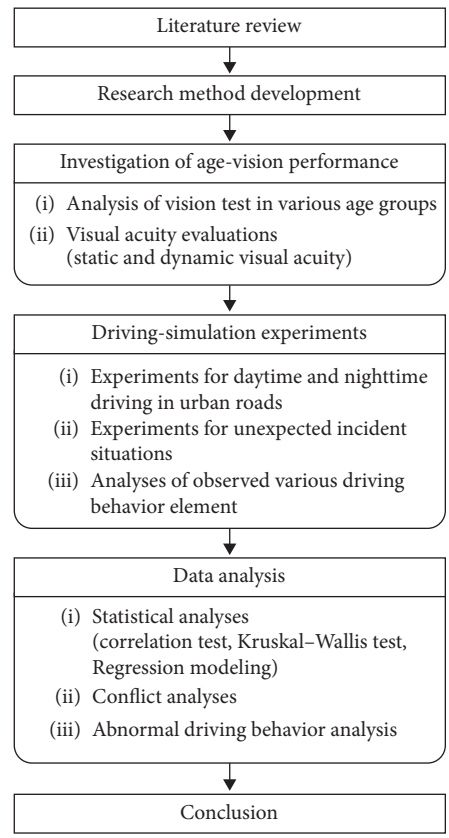

Figure 1: Flowchart of this study.

The visual acuity of each participant was first tested by the vision test system, and then, the driving simulator experiments were conducted. The two different scenarios were presented in random order to each participant to prevent any learning or familiarity effects in the experiments. The VR images in the driving simulator were implemented by the UC-WinRoad program (ver. 12.0) by Forum8 Corp which is in Anyang city, South Korea. Prior to the main test, a predriving test was administered so that participants would become familiar with the driving simulator.

3.3. Statistical Analysis. Correlation analysis is a method to investigate the degree and direction of a relationship between two variables [32], and we conducted it to determine whether visual acuity level influenced driving behavior and performance measures, including variations of speed, braking force, and lateral placement during driving. The Kruskal–Wallis test is a rank-based nonparametric test that can be used to determine whether there is a statistically significant difference between continuous or ordinal dependent variables in two or more groups [33]. We used this

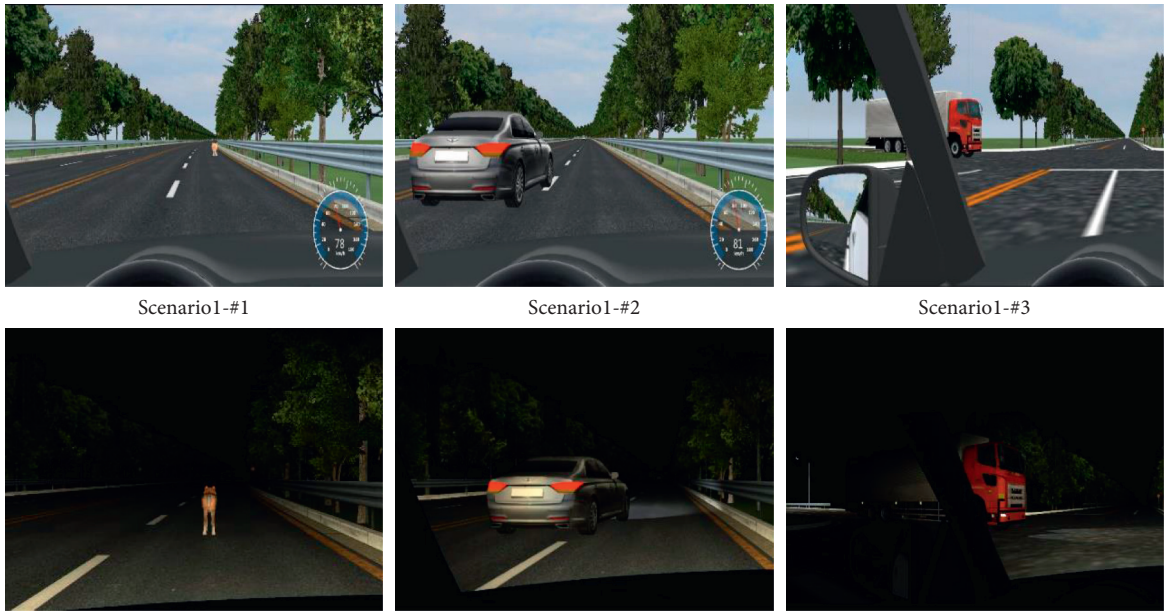

Figure 2: Images of experimental scenarios.

test to determine whether the occurrence of traffic conflicts in each scenario differed significantly among the groups classified according to visual acuity level. A traffic conflict is an observable event which would result in a crash if drivers do not act appropriately, such as by slowing down, changing lanes, or accelerating to avoid a collision. In this study, conflicts were measured as near-collisions with incident objects, such as a dog, a lane-changing vehicle, or an approaching heavy vehicle, by analysis of videos recorded in the experiment. The number of actual collisions was also included in the number of conflicts here for the purpose of the analysis. Finally, we used regression analysis to determine whether visual acuity levels and age had a significant effect on perception reaction time (PRT) in the unexpected incident situations. This analysis was conducted to determine whether lately perceiving and identifying ahead risky events can increase the probability of traffic crashes and whether the driver's age and visual acuity level are the main influencing factors for those unsafe driving behaviors.

4. Results

4.1. Vision Test Results. In agreement with the general knowledge that static visual acuity and dynamic visual acuity decline with aging, our investigation of visual acuity revealed that participants over age 40 had significantly lower visual acuity levels, typically in dynamic visual acuity, than younger participants. In a previous study [31], static and dynamic visual acuities were measured for 276 participants using the same vision measurement device used in this study; we reanalyzed those results to investigate the declination of vision with age. We found large decreases in vision test passing rates among older drivers, especially for dynamic visual acuity, using the Korean standard of static vision acuity in its driver license system, 0.5 points (20/40), as shown in Table 1. Even though the threshold of dynamic visual acuity can be different from that of static visual acuity, we applied the same threshold for dynamic vision.

In our evaluation of these data, 75.4% (56.9% + 18.5%) of the participants had adequate static visual acuity, as shown in Table 2, while 28 participants (12 + 16 participants) failed the dynamic visual acuity test and 16 participants failed both the dynamic and static visual acuity tests. Such individuals should not drive, considering their insufficient physical performance in terms of dynamic visual ability. As demonstrated here, vision performance typically declines much more rapidly after the age of 50; therefore, driving inspections should be improved for those over the age of 50.

4.2. Driving Simulator Experiment Results

4.2.1. Visual Acuities and Driving Behaviors. In the driving simulator experiments, many participants with lower visual acuity levels drove with higher variations in speed, as can be seen in Figure 3. The data in Figure 3 and Tables 3 and 4 are from the experimental highway segments where no unexpected incidents occurred, meaning these results represent general driving conditions without any effects from incidents. As can be seen in Figures 3(a)–3(c), the standard deviation of driving behavior measures the driving performance, including speed, brake force, and vehicle lateral placement (LP), which were all relatively higher in drivers with lower visual acuities. These trends were slightly more obvious in the dynamic visual acuity results.

Tables 3 and 4 display the correlation results for the daytime (scenario 1) and nighttime (scenario 2) experiments, respectively. These results indicate that in the daytime, visual acuities greatly influenced driving behavior, as measured by the standard deviation of speeds and vehicle

Table 1: Results of the vision test in different age groups.

Age	Static visual acuity (people)		Dynamic visual acuity (people)		Total (people)
	Pass (%)	Fail (%)	Pass (%)	Fail (%)	
20–29	4 (100%)	0	4 (100%)	0	4
30–39	57 (98%)	1 (2%)	57 (98%)	1 (2%)	58
40–49	121(97%)	4 (3%)	115(92%)	10 (8%)	125
50–59	24 (71%)	10 (29%)	14 (41%)	20 (59%)	34
65–69	27 (69%)	12 (31%)	11 (28%)	28 (72%)	39
Over 70	11 (69%)	5 (31%)	5 (31%)	11 (69%)	16
Total	244 (88%)	32 (12%)	206 (75%)	70 (25%)	276

Source: these data are from the Korea Agency for Infrastructure Technology Advancement (2017) [25] to determine whether different age groups passed or failed using the Korean standard for static visual acuity in its driver license system for all visual acuities. The original study merely examined those visual acuities to verify the Multifunctional Vision Test System developed by the study.

Table 2: Visual acuity evaluation results.

No.	Groups categorized by visual acuities						No. of participants (%)
	Static			Dynamic			
	Result	Mean	SD	Result	Mean	SD	
1	Pass	0.95	0.36	Pass	0.86	0.29	37 (56.9%)
2	Pass	0.57	0.08	Fail	0.33	0.09	12 (18.5%)
3	Fail	0.26	0.12	Fail	0.21	0.09	16 (24.6%)
			Total				65 (100%)

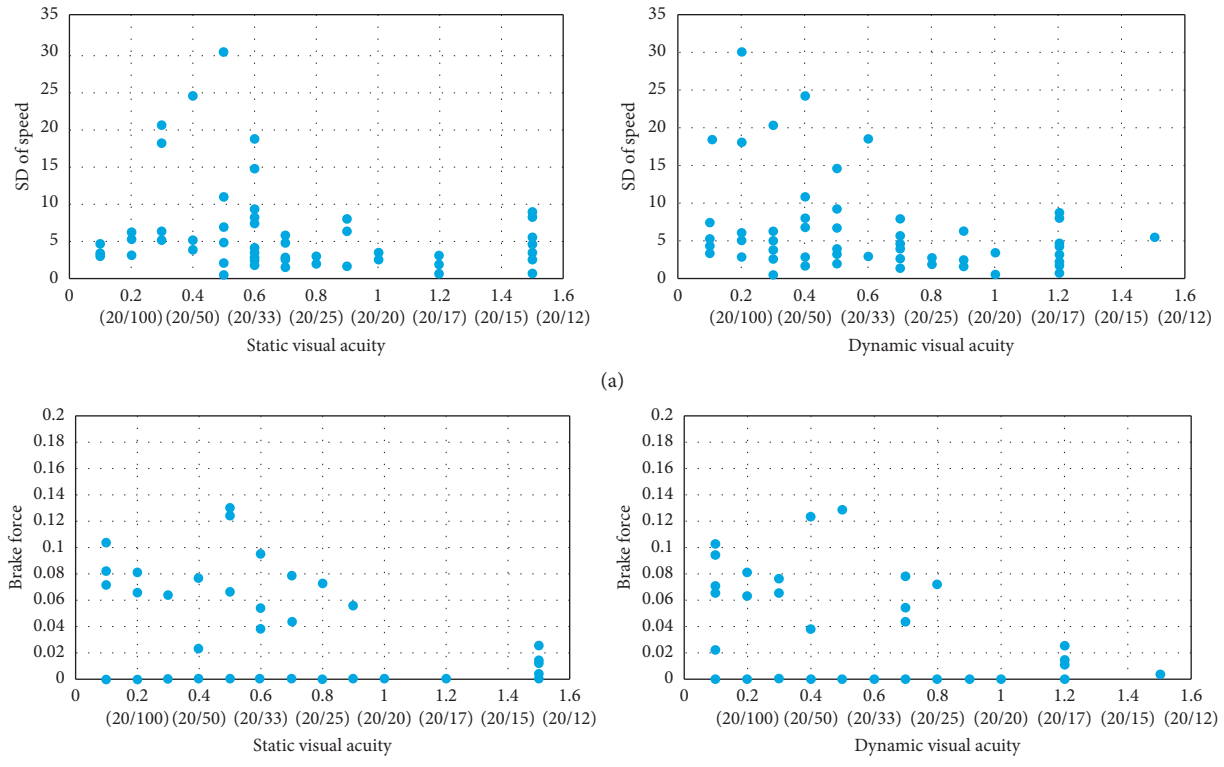

Figure 3: Continued.

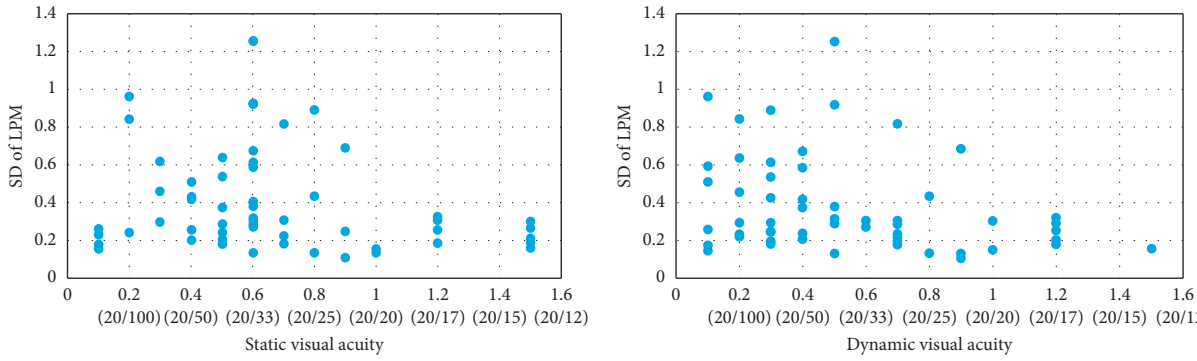

(c)

Figure 3: Comparison of driving behaviors according to visual acuity. Comparison of SD of (a) speed, (b) brake force, and (c) lateral placement according to visual acuity.

Table 3: Correlation analyses and Kruskal–Wallis tests in scenario 1 (daytime).

Categories			SD of running speed	SD of brake force	SD of LP
Correlation test	Tangent road section	Static visual acuity	−0.131 ($p = 0.299$)	−0.180 ($p = 0.150$)	−0.235 ($p = 0.059$)
		Dynamic visual acuity	−0.198 ($p = 0.114$)	−0.183 ($p = 0.145$)	−0.327* ($p = 0.008$)
	Curved road section	Static visual acuity	−0.253* ($p = 0.042$)	−0.127 ($p = 0.312$)	−0.253* ($p = 0.042$)
		Dynamic visual acuity	−0.356* ($p = 0.004$)	−0.183 ($p = 0.145$)	−0.352* ($p = 0.004$)
Kruskal–Wallis test	Tangent road section		$\chi^2 = 2.543$ ($p = 0.280$)	$\chi^2 = 0.156$ ($p = 0.925$)	$\chi^2 = 7.223$* ($p = 0.027$)
	Curved road section		$\chi^2 = 7.586$* ($p = 0.023$)	$\chi^2 = 1.315$ ($p = 0.518$)	$\chi^2 = 6.754$* ($p = 0.034$)

* p value <0.05 (statistically significant).

Table 4: Correlation analyses and Kruskal–Wallis tests in scenario 2 (nighttime).

Categories			SD of running speed	SD of brake force	SD of LP
Correlation test	Tangent road section	A static visual acuity	−0.036 ($p = 0.775$)	0.079 ($p = 0.532$)	−0.065 ($p = 0.606$)
		A dynamic visual acuity	−0.069 ($p = 0.587$)	0.063 ($p = 0.620$)	−0.062 ($p = 0.626$)
	Curved road section	A static visual acuity	−0.210 ($p = 0.093$)	−0.149 ($p = 0.236$)	−0.160 ($p = 0.202$)
		A dynamic visual acuity	−0.241* ($p = 0.050$)	−0.142 ($p = 0.258$)	−0.251* ($p = 0.043$)
Kruskal–Wallis test	Tangent road section		$\chi^2 = 1.533$ ($p = 0.465$)	$\chi^2 = 3.065$ ($p = 0.216$)	$\chi^2 = 0.073$ ($p = 0.964$)
	Curved road section		$\chi^2 = 4.471$ ($p = 0.107$)	$\chi^2 = 0.158$ ($p = 0.924$)	$\chi^2 = 4.049$ ($p = 0.132$)

* p value <0.05 (statistically significant).

LPs, and this was especially notable in curved road segments. Again, these results were more obvious for dynamic visual acuity. Of these driving behavior measures, the standard deviation of vehicle LPs had a stronger correlation with visual acuities, typically dynamic visual acuity. The Kruskal–Wallis test results showed that the differences in the correlations of static and dynamic visual acuities with the standard deviation of vehicle LPs only in the tangent road section, and the standard deviation of speed and vehicle LPs in the curved road section were statistically significant.

Meanwhile, in scenario 2 (nighttime), the correlations between visual acuities and driver behavior measures were less significant than those in the daytime (Table 4). The Kruskal–Wallis test results showed that differences of these correlations of driving behavior measures with static and dynamic visual acuity were not statistically significant in the

nighttime. This indicates that there might be other influencing factors that were not considered in this study, such as nighttime visual acuity.

4.2.2. Visual Acuity and Driving Conflicts. Traffic conflicts while driving in unexpected incident situations in the daytime were used for comparing the groups divided according to the determined visual acuity level. Table 5 displays the average number of conflicts for each group. The largest number of conflicts (3.3) was recorded for those who passed the static acuity test but failed the dynamic acuity test. Fewer conflicts (2.1) were observed for those who passed all the acuity tests than for those who failed all of the tests (2.2). Participants who failed the dynamic vision test had more conflicts during the experiments, as can be seen in Table 5.

These conflict results showed that the drivers with insufficient dynamic visual acuity (even if they had acceptable static visual acuity) were more frequently involved in traffic accidents. This confirms that dynamic visual acuity levels strongly affect driving behavior and help to determine the driving performance level. These findings suggest that the driver license system in South Korea should include tests of dynamic visual acuity to create safer driving conditions.

4.2.3. Analysis of the Effects of Visual Acuities on Reaction Time. When a driver is slow to perceive and identify upcoming dangerous situations, the risk of a collision increases. For this reason, analyzing the effects of visual acuities on the time needed for perceiving and identifying can be meaningful. However, because it is generally quite difficult to measure exact time for perceiving and identifying approaching objects in the VR simulator experiment, we used the entire perception reaction time (PRT) instead of just time to perceive and identify ahead the object. The reaction time used in this study was derived from the following equation:

$$\text{measured PRT} = T_1 - T_2, \tag{1}$$

Measured PRT (T_1 and T_2 were measured using raw data related to driving behaviors that the driving simulator automatically produced.): time difference between time (T_1) when a driver starts to step on the brake and time (T_2) when the hazard obstacle appears ahead.

The results showed a significant correlation between the measured PRT and actual conflicts for incidents 1 and 3 in both the daytime and nighttime experiments, as shown in Table 6. However, results for incident 2 in the daytime and nighttime experiments were not significant. This might be explained that incidents 1 and 3 occurred some distance ahead and were completely unexpected, but incident 2, in which a vehicle in the adjacent lane suddenly cut into the driving lane, occurred in front of participants' very eyes. Therefore, incident 2 might have been relatively less affected by the driver's visual acuity. These results demonstrate that PRT has a significant relationship with conflicts and possibly with traffic accidents.

Table 5: Comparison of driving conflicts according to visual acuity performance.

Groups by determined visual acuities			Average conflicts of groups
Group no.	Static	Dynamic	
1	Pass	Pass	2.1
2	Pass	Fail	3.3
3	Fail	Fail	2.2

A regression analysis was conducted to investigate the significant visual acuities that affected the measured PRT (Table 7). Dynamic visual acuity had statistically significant effects in both daytime and nighttime situations, but static visual acuity was not statistically significant. The PRT decreased as the dynamic visual acuity decreased, as the coefficient of the dynamic visual acuity was negative. There was little difference in the coefficient values between daytime and nighttime conditions. This result confirms that dynamic visual acuity, which measures how accurately a moving object is observed, is an important driver aptitude in both daytime and nighttime conditions.

4.2.4. Ability to Cope with Incidents according to Visual Acuities. Generally, drivers with vision problems do not cope well with sudden incidents, due the association of poor vision with impaired cognitive capacity to respond quickly and accurately. The experiments in this study confirmed this general tendency, as shown in Figure 4. Old drivers and non-old drivers who passed the static and dynamic visual acuity levels (Group 1) had similar speed and brake force patterns (Figure 4(a)), but those who passed the static visual acuity test but failed the dynamic visual acuity test (Group 2) had different speed and brake force patterns. For example, to cope with incident #3, non-old drivers started to brake and reduced speed at the appropriate time, but old drivers started to brake and reduced speed too late (Figure 4(b)). As mentioned previously, about 70% of the old participants and about 30% of the non-old participants in this experiment failed in the dynamic vision test. In sudden incident events, the worst behaviors were observed in participants with insufficient dynamic vision acuity (about 10% of the drivers), including sudden harsh braking due to late identification of the incident. However, this difference was smaller in participants who failed both static and dynamic vision tests (Group 3) as can be seen in Figure 4(c). It might be because drivers with poor static vision performance usually more concentrate on ahead conditions in driving and are ready to cope with them.

Figure 5 shows two examples of those extreme cases. The first case involved a 50-year-old female participant with 20 years of driving experience; she had driven five times per week but failed both the static and dynamic visual acuity tests. The other case was an older male driver with 30 years of driving experience who had driven every day. He failed the dynamic visual acuity tests, although he passed the static visual acuity test. Neither subject identified sudden events fast enough to successfully respond. When the woman

Table 6: Correlation analyses between reaction time and conflicts in three incidents.

Categories		Conflicts	
		Scenario 1 (daytime)	Scenario 2 (nighttime)
Reaction time	Incident #1 (dog runs into road)	0.462* ($p < 0.001$)	0.564* ($p < 0.001$)
	Incident #2 (car in adjacent lane veers)	0.063 ($p = 0.666$)	0.331* ($p = 0.020$)
	Incident #3 (heavy vehicle approaches)	0.653* ($p < 0.001$)	0.632* ($p < 0.001$)

* p value <0.05 (statistically significant).

Table 7: Regression models for conflicts using visual acuities.

Model	Variable	Unstandardized coefficients		t	Sig.
		B	Std. error		
Daytime	Constant	5.827*	0.417	13.986	0.000
	Dynamic visual acuity	−1.560*	0.638	−2.447	0.018
Nighttime	Constant	2.644*	0.421	6.279	0.000
	Dynamic visual acuity	−1.658*	0.645	−2.572	0.013

* p value <0.05 (statistically significant).

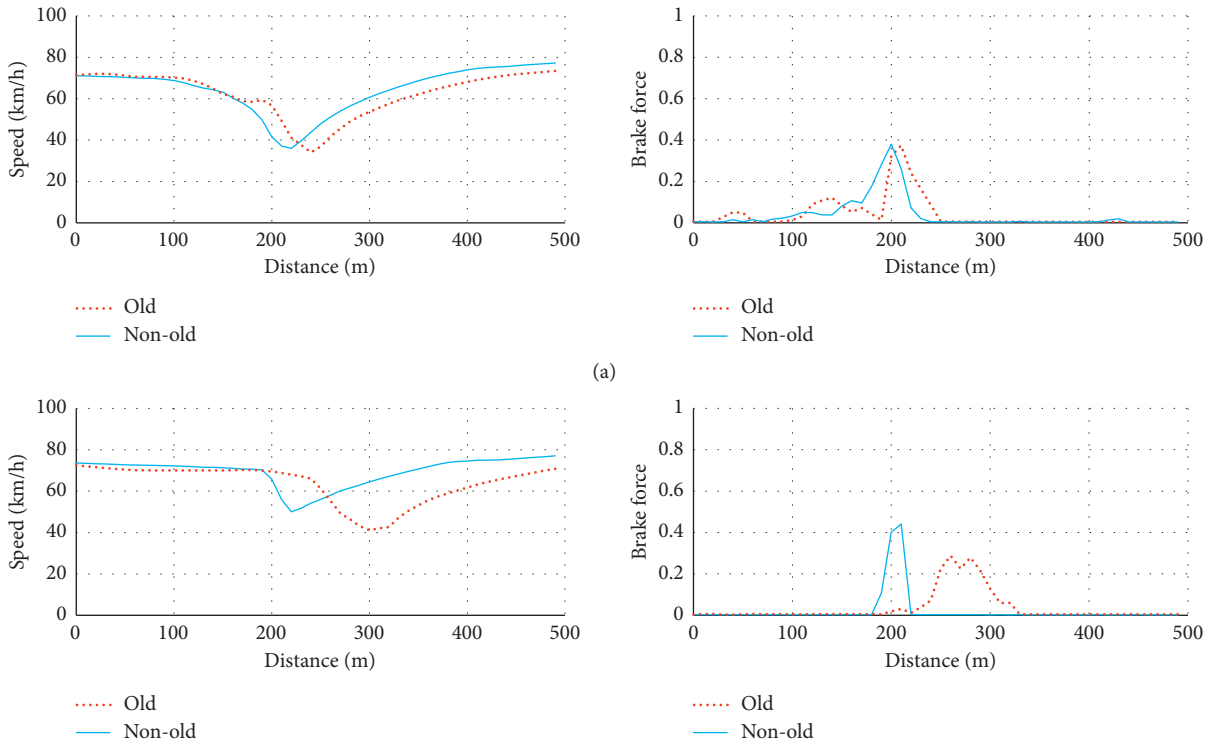

Figure 4: Continued.

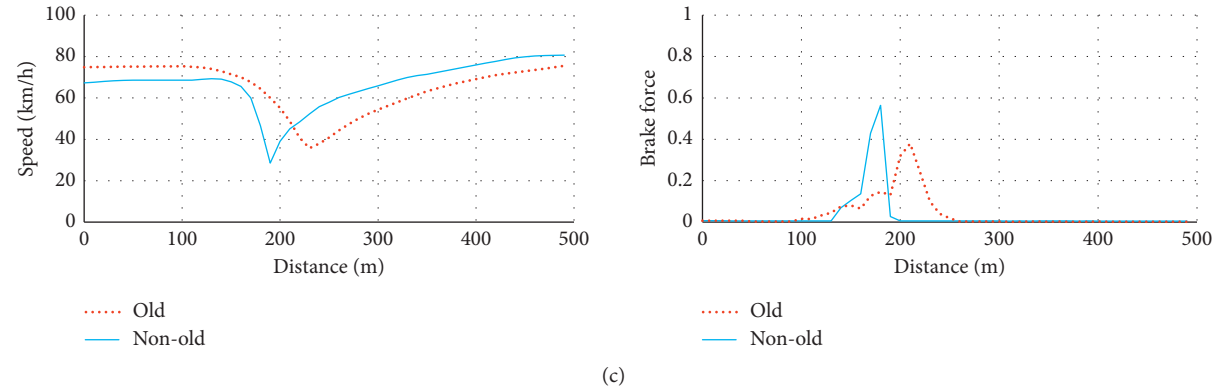

(c)

Figure 4: Comparison of driving behaviors according to age for incident #3 in the daytime experiment. (a) Group 1 (passed both static and dynamic vision tests). (b) Group 2 (passed the static vision test but failed the dynamic vision test). (c) Group 3 (failed both static and dynamic vision tests).

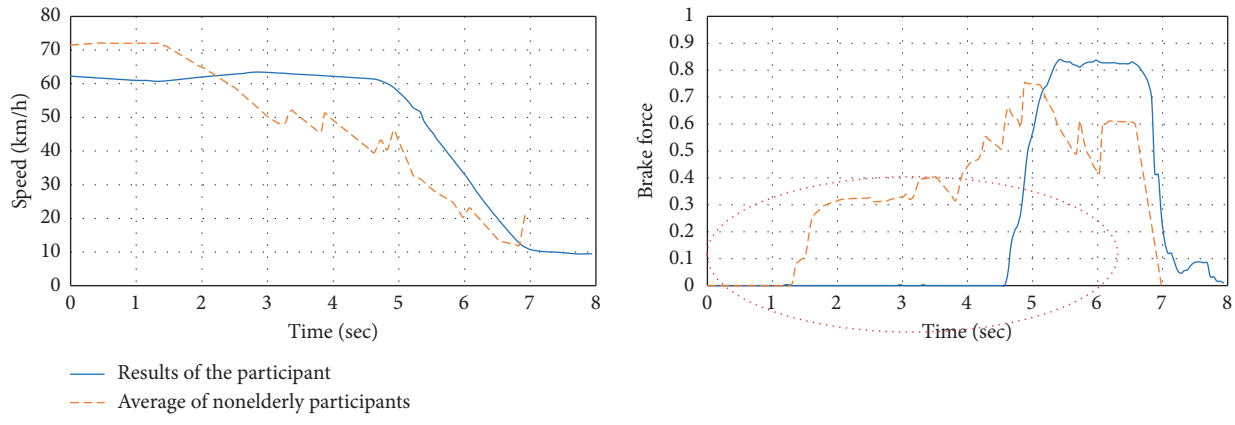

(a)

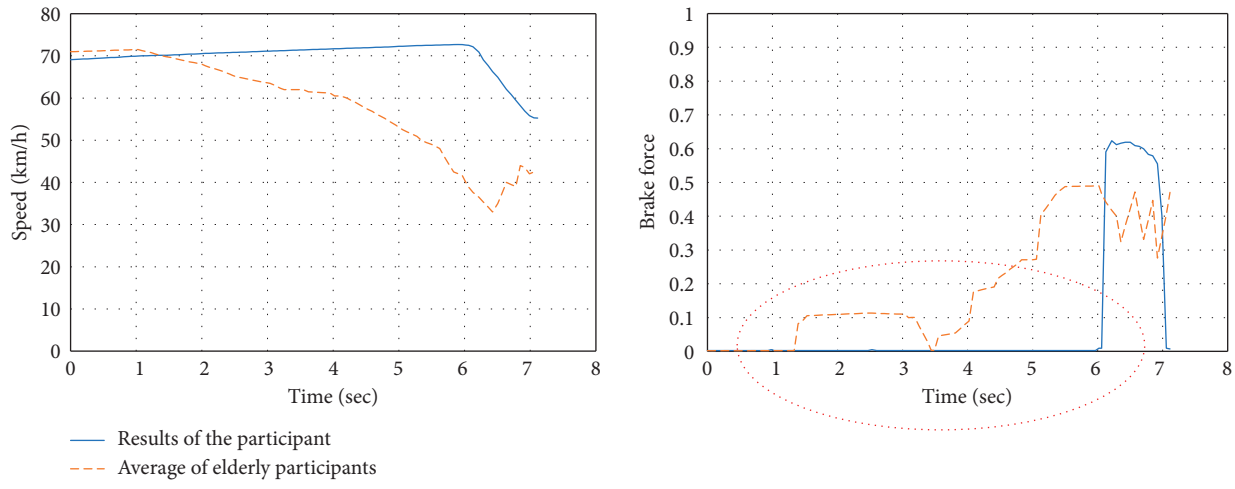

(b)

Figure 5: Cases of two problematic participants in the daytime experiment with incident #3. (a) The problematic female participant. (b) The problematic male participant.

identified a sudden event too late, she braked suddenly with great force, demonstrating how in real-life situations, severe crashes can be caused by low visual acuity. Figure 5 illustrates these participants' behaviors.

5. Conclusions

For the sake of traffic safety, it is of vital importance to determine whether drivers have adequate capabilities for

driving and to keep unqualified drivers off the roads. Therefore, driver performance evaluations are essential for identifying those not qualified to drive. However, there is currently much debate regarding the effectiveness of the driver license system in South Korea, due to the many traffic crashes caused by drivers with insufficient physical and mental abilities [34–39]. It is also quite difficult to assess driving performance indirectly through physical tests, such as visual acuity and muscle performance tests, because the correlation of those results with driving performance is to date unclear. Thus, we conducted a driving performance evaluation to improve traffic safety based on VR technology.

In the driving simulator experiments, many participants with lower visual acuity levels drove with greater variations in speed, failed to brake appropriately when confronted with sudden incidents, and failed to avoid crashes. Here, we produce statistically significant evidence that reduced visual acuity impairs driving performance, and through designed VR experiments, we demonstrate that the driving performance of participants with insufficient dynamic visual acuity can cause unsafe situations. We also found that dynamic acuity has a great deal of influence on driving performance in both the daytime and nighttime, and it can be an effective criterion for driver qualification. These findings suggest that the driver license system in South Korea should consider including dynamic visual acuity testing for better and safer driving.

However, there were some limitations to this study. The number of participants was only 65, not enough for analyzing the trends of declining visual acuity. Also, driving in virtual scenarios is different from driving on real roads. Nevertheless, this pioneering study shows how dynamic visual acuity can explain driving performance; more scientific studies are needed to prove that dynamic visual acuity is a reliable screening factor which does not change easily according to external circumstances or conditions. Also, further studies with larger sample sizes are needed to analyze more precisely the trends of visual acuity with aging, as well as more detailed physical and mental criteria for driving, such as hand-eye coordination, with the goal of finding clearer correlations between age and driving performance. It is necessary to test the driving performance of these same 65 participants on real roads to assess the similarity with the findings of this study. And finally, as noted earlier, this study applied the same threshold for both static and dynamic visual acuities, even though they can be different. To address this study limitation, more precise criteria and thresholds for dynamic visual acuity should be determined through more scientific driving performance studies.

Data Availability

The data used to support the findings of this study are available from the corresponding author upon request.

Conflicts of Interest

The authors declare that there are no conflicts of interest regarding the publication of this paper.

Acknowledgments

This work was partially supported by the 2019 Research Fund of the University of Seoul for Dongmin Lee. Also, this research was supported by the Basic Science Research Program through the National Research Foundation of Korea (NRF) funded by the Ministry of Education (2018R1D1A1B07049554) for Sooncheon Hwang.

References

[1] D. Shinar, *Traffic Safety and Human Behavior*, Emerald Publishing Limited, Bingley, UBingley, UK, 2nd edition, 2017.
[2] https://en.wikipedia.org/wiki/visual_acuity.
[3] C. Owsley, K. Ball, M. E. Sloane, D. L. Roenker, and J. R. Bruni, "Visual/cognitive correlates of vehicle accidents in older drivers," *Psychology and Aging*, vol. 6, no. 3, pp. 403–415, 1991.
[4] J. L. Keltner and C. A. Johnson, "Mass visual field screening in a driving population," *Ophthalmology*, vol. 87, no. 8, pp. 785–792, Aug. 1980.
[5] G. McGwin, V. Chapman, and C. Owsley, "Visual risk factors for driving difficulty among older drivers," *Accident Analysis and Prevention*, vol. 32, no. 6, pp. 735–744, 2000.
[6] C. Owsley, "Aging and vision," *Vision Research*, vol. 51, no. 13, pp. 1610–1622, 2011.
[7] D. R. Ragland, W. A. Satariano, and K. E. MacLeod, "Reasons given by older people for limitation or avoidance of driving," *The Gerontologist*, vol. 44, no. 2, pp. 237–244, 2004.
[8] C. A. Johnson and J. L. Keltner, "Incidence of visual field loss in 20,000 eyes and its relationship to driving performance," *Archives of Ophthalmology*, vol. 101, no. 3, pp. 371–375, 1983.
[9] A. Burg, "Vision and driving: a report on research," *Human Factors*, vol. 13, pp. 79–87, 1971.
[10] B. L. Hills and A. Burg, "A reanalysis of California driver vision data general findings," TRRL Report 768, U.K. Transport and Road Research Laboratory, Crowthorne, England, 1977.
[11] L. E. Decina, L. Staplin, and A. S. Spiegel, *Correcting Unaware Vision Impaired Drivers, No. 730009*, Pennsylvania Department of Transportation, Harrisburg, PA, USA, 1990.
[12] S. Subzwari and E. Desapriya, "Vision screening of older drivers for preventing road traffic injuries and fatalities," *Cochrane Database of Systematic Reviews*, 2006.
[13] A. Burg, "Lateral visual field as related to age and sex," *Journal of Applied Psychology*, vol. 52, no. 1, pp. 10–15, 1968.
[14] H. W. Hofstetter, "Visual acuity and highway crashes," *Journal of the American Optometric Association*, vol. 47, pp. 887–893, 1976.
[15] G. M. Long and D. F. Kearns, "Visibility of text and icon highway signs under dynamic viewing conditions," *Human Factors: The Journal of the Human Factors and Ergonomics Society*, vol. 38, no. 4, pp. 690–701, 1996.
[16] L. Wilkins, R. Gray, J. Gaska, and M. Winterbottom, "Motion perception and driving: predicting performance through testing and shortening braking reaction times through training," *Investigative Opthalmology and Visual Science*, vol. 54, no. 13, p. 8364, 2013.
[17] K. E. Higgins and J. M. Wood, "Predicting components of closed road driving performance from vision tests," *Optometry and Vision Science*, vol. 82, no. 8, pp. 647–656, 2005.
[18] H. Wang, X. Mo, Y. Wang, R. Liu, P. Qiu, and J. Dai, "Assessing Chinese coach drivers' fitness to drive: the

development of a toolkit based on cognition measurements," *Accident Analysis and Prevention*, vol. 95, pp. 395–404, 2016.

[19] T. Abe, K. Fujii, J. Seol et al., "Driving frequency associated with deficits in lower extremity function, dynamic vision, and physical activity in Japanese older adults," *Journal of Transport and Health*, vol. 9, pp. 282–287, 2018.

[20] D. Shinar and F. Schieber, "Visual requirements for safety and mobility of older drivers," *Human Factors: The Journal of the Human Factors and Ergonomics Society*, vol. 33, no. 5, pp. 507–519, 1991.

[21] C. Owsley and G. McGwin, "Vision impairment and driving," *Survey of Ophthalmology*, vol. 43, no. 6, pp. 535–550, 1999.

[22] A. K. Pradhan, K. R. Hammel, R. DeRamus, A. Pollatsek, D. A. Noyce, and D. L. Fisher, "Using eye movements to evaluate effects of driver age on risk perception in a driving simulator," *Human Factors: The Journal of the Human Factors and Ergonomics Society*, vol. 47, no. 4, pp. 840–852, 2005.

[23] H. L. Lew, J. H. Poole, E. H. Lee, D. L. Jaffe, H.-C. Huang, and E. Brodd, "Predictive validity of driving-simulator assessments following traumatic brain injury: a preliminary study," *Brain Injury*, vol. 19, no. 3, pp. 177–188, 2005.

[24] J. K. Muguro, M. Sasaki, and K. Matsushita, "Evaluating hazard response behavior of a driver using physiological signals and car-handling indicators in a simulated driving environment," *Journal of Transportation Technologies*, vol. 9, no. 4, pp. 439–449, 2019.

[25] J. Lengenfelder, M. T. Schultheis, T. Al-Shihabi, R. Mourant, and J. DeLuca, "Divided attention and driving," *Journal of Head Trauma Rehabilitation*, vol. 17, no. 1, pp. 26–37, 2002.

[26] D. Lee and J. Lim, "Driver behavior Analyses of 2+1 roads based on a driving simulation experiment," *KSCE Journal of Civil Engineering*, vol. 23, no. 3, pp. 1351–1359, 2019.

[27] S. C. Hwang, S. H. Kim, and D. M. Lee, "Driving behavior on hard-shoulder lanes in tunnels using a driving simulator," *International Journal of Highway Engineering*, vol. 21, no. 3, pp. 87–96, 2019.

[28] S. Krasniuk, S. Classen, and S. A. Morrow, "Relationships among vision, visual attention, and fitness to drive in adults with multiple sclerosis," *American Journal of Occupational Therapy*, vol. 71, no. 4, Article ID 7111500009p1, 2017.

[29] S. C. Kang and S. W. Lee, "an analysis of older drivers' riskiness using driving simulator and driving aptitude test," *Traffic Science Institute; Research of Traffic Safety*, vol. 32, pp. 5–14, 2013.

[30] D. C. Grabowski, "Elderly licensure laws and motor vehicle fatalities," *JAMA*, vol. 291, no. 23, p. 2840, 2004.

[31] Korea Agency for Infrastructure Technology Advancement, *Development of Driving Fitness Test Based on Virtual Reality*, Korea Agency for Infrastructure Technology Advancement, Anyang, Gyeonggi-do, Republic of Korea, 2017.

[32] J. Cohen, P. Cohen, S. G. West, and L. S. Aiken, *Applied Multiple Regression/Correlation Analysis for the Behavioral Sciences*, Erlbaum, Mahwah, NJ, USA, 3rd edition, 2003.

[33] D. Othayoth and K. V. Krishna Rao, "Factors influencing level of service for motorized vehicles at signalized intersection under mixed traffic condition," *Transportation in Developing Economies*, vol. 3, no. 2, 2017.

[34] S. J. Kang, S. H. Choi, B. H. Lee, J. C. Kwon, D. L. Na, and S. H. Han, "The reliability and validity of the Korean instrumental activities of daily living," *Journal of the Korean Neurological Association*, vol. 20, no. 1, pp. 8–14, 2002.

[35] Korea Centers for Disease Control and Prevention, *The Risk of Driving in Dementia Patients*, Korea Centers for Disease Control and Prevention, Cheongju-si, South Korea, 2009.

[36] S. J. Park, S. C. Lee, and H. R. Jang, "The influence of driving situational adaptability and chronic disease on driving behavior of elderly drivers," *Korean Journal of Psychological and Social Issues*, vol. 14, no. 2, pp. 1–19, 2008.

[37] S. Y. Park, Y. H. Kim, and H. C. Shin, "Selection framework of driving simulator scenarios for driver education based on traffic accident data analysis," *Journal of Transport Research*, vol. 23, no. 4, pp. 15–33, 2016.

[38] J. Charlton, S. Koppel, M. Odell et al., *Influence of Chronic Illness on Crash Involvement of Motor Vehicle Drivers, Report No. 300*, Monash University Accident Research Centre, Clayton, Victoria, Australia, 2nd edition, 2010.

[39] S. W. van Landingham, C. Hochberg, R. W. Massof, E. Chan, D. S. Friedman, and P. Y. Ramulu, "Driving patterns in older adults with glaucoma," *BMC Ophthalmology*, vol. 13, no. 1, 2013.

Hindawi
Journal of Advanced Transportation
Volume 2020, Article ID 7525721, 12 pages
https://doi.org/10.1155/2020/7525721

Research Article

Implementing Surrogate Safety Measures in Driving Simulator and Evaluating the Safety Effects of Simulator-Based Training on Risky Driving Behaviors

Eunhan Ka,[1] Do-Gyeong Kim,[2] Jooneui Hong,[3] and Chungwon Lee[4]

[1]*Institute of Engineering Research, Seoul National University, Seoul 08826, Republic of Korea*
[2]*Department of Transportation Engineering, University of Seoul, Seoul 02504, Republic of Korea*
[3]*Korea Development Institute, Sejong 30149, Republic of Korea*
[4]*Department of Civil and Environmental Engineering, Seoul National University, Seoul 08826, Republic of Korea*

Correspondence should be addressed to Chungwon Lee; chungwon@snu.ac.kr

Received 26 December 2019; Accepted 23 April 2020; Published 19 June 2020

Academic Editor: Inhi Kim

Human errors cause approximately 90 percent of traffic accidents, and drivers with risky driving behaviors are involved in about 52 percent of severe traffic crashes. Driver education using driving simulators has been used extensively to obtain a quantitative evaluation of driving behaviors without causing drivers to be at risk for physical injuries. However, since many driver education programs that use simulators have limits on realistic interactions with surrounding vehicles, they are limited in reducing risky driving behaviors associated with surrounding vehicles. This study introduces surrogate safety measures (SSMs) into simulator-based training in order to evaluate the potential for crashes and to reduce risky driving behaviors in driving situations that include surrounding vehicles. A preliminary experiment was conducted with 31 drivers to analyze whether the SSMs could identify risky driving behaviors. The results showed that 15 SSMs were statistically significant measures to capture risky driving behaviors. This study used simulator-based training with 21 novice drivers, 16 elderly drivers, and 21 commercial drivers to determine whether a simulator-based training program using the SSMs is effective in reducing risky driving behaviors. The risky driving behaviors by novice drivers were reduced significantly with the exception of erratic lane-changing. In the case of elderly drivers, speeding was the only risky driving behavior that was reduced; the others were not reduced because of their difficulty with manipulating the pedals in the driving simulator and their defensive driving. Risky driving behaviors by commercial drivers were reduced overall. The results of this study indicated that the SSMs can be used to enhance drivers' safety, to evaluate the safety of traffic management strategies as well as to reduce risky driving behaviors in simulator-based training.

1. Introduction

The worldwide number of annual fatalities in traffic crashes reached 1.35 million each year, and this number continues to increase steadily in the world [1]. Human errors cause about 90 percent of all road accidents [2], and the majority of human errors involve risky driving. Drivers with risky driving behaviors such as speeding, following other vehicles too closely (tailgating), erratic driving, and violation of traffic laws accounted for about 52% of severe traffic accidents [3]. Moderating risky driving behaviors have been achieved successfully using a variety of approaches that combine education, engineering, and enforcement; this approach to safety is known as the 3E principle [4]. Driver education has been used extensively to reduce risky driving behaviors. It has been reported to be an effective way to reduce traffic accidents by detecting risky driving behaviors and providing appropriate feedback to reduce these behaviors [5]. Risky driving behaviors should be measured and evaluated quantitatively to give appropriate feedback to drivers in order to reduce risky driving behaviors.

Current driver education programs have focused on educating drivers about the skills and attitudes necessary to become a safe driver. Videos and lectures about traffic

regulations and automobile-related knowledge, on-road training, and simulator-based training generally have been used in driver education programs. Videos and lectures help drivers acquire knowledge about driving safely by providing information about traffic regulations and the appropriate operation of automobiles. However, these approaches to teaching drivers have limitations in that they do not help improve the practical skills that are required in on-road driving [6]. On-road training with a driving instructor is an effective method to educate drivers to drive more safely on the road. However, even professional instruction and on-road training cannot address all of the potential crashes of driving because they cannot expose drivers to the various potential collision situations that can occur on the road.

Driving simulators are used extensively as a tool to instruct drivers to drive in a common driving environment as well as in collision situations that would be too dangerous to create in actual on-road driving [7]. The instructor can design various driving scenarios including myriads of road and traffic environments, movements of surrounding vehicles, and collision scenarios. Therefore, driving simulators can be used to give risky drivers repeated training with various collision situations. Driving simulators can be used to measure driving behaviors quantitatively as well as to acquire the trajectory data for surrounding vehicles [8]. However, there are issues concerning the validity of virtual simulations of real driving environments. Current studies have shown that they have similar patterns, but the driving behaviors in driving simulators and on-road driving may not be the same [7, 9]. In other words, driving simulators can be useful tools for educational purposes in driver education programs. In fact, the driving instructors involved in a previous study thought that one-hour simulator training was as effective as three hours of on-road training [10].

Most research on reducing risky driving behaviors based on driving simulators has been conducted with a focus on drivers' eye movements and the movements of the subject vehicle, i.e., movements such as erratic acceleration and deceleration, speed variation, and lane deviation [11–14]. Since risky driving behaviors cause severe road crashes, it is necessary to evaluate the crash potential in the interactions between the subject vehicle and surrounding vehicles, such as following leading vehicles (car-following) and changing lanes (lane-changing). However, few studies have evaluated the crash potential between the subject vehicle and surrounding vehicles, which would address the interactions between vehicles [15]. This study implemented realistic interactions between the subject vehicle and surrounding vehicles in a driving simulator by applying traffic flow models to the movements of surrounding vehicles. In addition, we examined surrogate safety measures (SSMs), which are used extensively in the field of road safety as useful measures for assessing crash potential or severity even on roads where no actual collisions have occurred. The SSMs can increase our understanding of the situations that cause collisions. In this study, the SSMs were used to evaluate risky driving behaviors in order to evaluate vehicles' crash potentials.

The aim of this study was to determine whether the SSMs can identify risky driving behaviors in driving simulators and whether the SSMs are effective in improving drivers' behaviors when the SSMs are used as evaluation measures in the simulator-based training.

2. Literature Review

Risky driving behaviors are defined differently by many organizations and in many studies. Since the motivation of a driver is difficult to determine, risky driving behaviors can only be judged and evaluated based on the motions of vehicles [16, 17]. Risky driving behaviors mean taking risks that endanger the safety of both the driver and other road users [18]. Generally, risky driving behaviors include speeding, noncompliance with traffic laws, tailgating, reckless changing speeds, erratic lane-changing, and threats to other drivers (yelling and horn honking) [3, 16, 19].

Driving simulators have been used increasingly for driver education because of the advantages they provide, including the freedom to present drivers with a wide variety of scenarios without any threat to their safety or the safety of other people [20]. Studies on reducing or evaluating risky driving behaviors using driving simulators have investigated mainly risky driving behaviors in terms of the drivers' reactions and the movements of vehicles. Studies of drivers' reactions have used the movements of the eyes, the focus of gazes, the duration of glances, and the number of fixations as measures to evaluate drivers' physical responses to collision situations [11, 14, 21]. These studies have shown that drivers' perceptions of conflict situations improve after they have had driver education in which eye-tracking systems to improve the ability of novice drivers and older drivers to recognize situations where collisions could occur. Various studies have used response time, pressure on the accelerator, and pressure on the brake pedal to measure drivers' responses to collision situations and red lights at intersections [12, 13, 22]. Measures related to drivers' reactions were used mainly to evaluate risk perception rather than to reduce risky driving behaviors.

Most of the studies related to the movements of vehicles have focused on the movements of the subject vehicle, and they evaluated primarily the risky behaviors of the drivers of the subject vehicle, e.g., erratic steering control, speeding, and tailgating. Erratic steering control involves the driver's sudden and unexpected changes in steering the vehicle or how far the driver allows the vehicle to deviate from the center of its lane. The steering angle, steering reversal rate, lane deviation, and mean lane position have been used in assessing erratic steering control [13, 14, 22–24]. Velocity, mean speed, speed variation, speeding, and acceleration are speeding-related measures that can be used to determine the driver's compliance with the speed limit and the reckless changing of speed [13, 14, 22, 25]. Evaluations of the gap distance between vehicles and time-to-collision (TTC) with a leading vehicle were made mainly in a car-following situation [15, 22]. However, the gap distance between vehicles and the TTC between the subject vehicle and the leading vehicle cannot take into consideration the accelerations and

decelerations of either vehicle. Also, few studies have considered the potential for crashes between vehicles when they are changing lanes [26].

Most studies have attempted to evaluate the effects of simulator-based training on risky driving behaviors. These studies focused principally on risky driving behaviors related to the movements of the subject vehicle. Since most risky driving behaviors require consideration of the subject vehicle's interactions with surrounding vehicles, it is essential to evaluate the crash potential with one or more of the surrounding vehicles. However, research considering the interactions between vehicles has rarely been conducted because the movements of surrounding vehicles would not be implemented realistically. This study attempted to introduce the SSMs into a simulator-based training program to evaluate the crash potential between vehicles and to reduce the risky driving behaviors associated with the surrounding vehicles.

3. Methodology

3.1. Framework. This study consisted of three parts: a survey of SSMs and scenario design, a preliminary experiment, and a simulator-based training program (see Figure 1). The SSMs can be classified into measures that consider only the subject vehicle and measures that consider both the subject vehicle and surrounding vehicles. Before the SSMs were used as measures of driving behaviors, it was necessary to test whether the SSMs could detect risky driving behaviors and conservative driving behaviors in a driving simulator. This study conducted a preliminary experiment for the sensitivity analysis of SSMs. The purpose of the sensitivity analysis of SSMs was to ensure that SSMs could detect extreme driving behaviors, i.e., normal, conservative, and risky driving. In a preliminary experiment, each driver was required to engage in one of the three types of driving behaviors (normal, conservative, and risky) in the driving simulator. Finally, this study used a quantitative evaluation based on the SSMs to analyze whether drivers reduced their risky driving behaviors after engaging in the simulator-based training program.

3.2. Survey of Surrogate Safety Measures. Since a simulator-based training requires immediate feedback concerning which driving behaviors are risky in the various driving scenarios, it is crucial to be able to calculate the SSMs used in the simulator-based training within a short time after driving in the driving simulators. This study reviewed numerous studies about road safety in order to investigate the SSMs that can be used in simulator-based training, and 31 SSMs were selected as alternatives. Since 11 of the SSMs were challenging to calculate instantaneously in driving simulators or unsuitable in evaluating driving behaviors, 20 out of the 31 SSMs were selected as implementable SSMs. For example, the Crash Index is a measure concerning the severity of a potential crash, and it is presented in the form of the kinetic energy of the crash [27]. It is challenging to translate kinetic energy values into an easily understandable account of the risk associated with a given participant's driving behaviors. Thus, this study excluded the Crash Index from the implementable SSMs and selected implementable SSMs as measures that can be explained easily to the drivers in simulator-based training.

The implementable SSMs were divided into "Relating to the subject vehicle" and "Relating to surrounding vehicles," depending on whether or not the SSMs related to interactions with surrounding vehicles. The SSMs relating to the subject vehicle can be calculated without any interactions with surrounding vehicles (nos. 1 to 9 in Table 1). The SSMs relating to surrounding vehicles consider interactions with surrounding vehicles, such as car-following situations and lane-changing situations (nos. 10 to 20 in Table 1). The gap distance in the car-following situation (no. 10) was used to confirm the validation of driving errors between the driving simulator and on-road driving [7]. The time-to-collision (TTC, no. 12) was used for studies in which driving behaviors in critical situations were compared [15, 22, 35]. However, the gap distance and the TTC between the subject vehicle and the leading vehicle have the limitation that the difference between the acceleration of the subject vehicle and the deceleration of the leading vehicle cannot be considered. This study used modified TTC (no. 13) and deceleration rate to avoid crash (no. 14) to evaluate the crash potential by considering the difference between the acceleration of the subject vehicle and the deceleration of the leading vehicle in situations where the subject vehicle is following the leading vehicle. The study in which the driving behaviors were analyzed in the lane-changing situation used the gap distance (no. 16 and no. 17) with the surrounding vehicles in a target lane [26]. This study adopted the SSMs (nos. 13, 14, 19, and 20) that had not been used to reduce risky driving behaviors in existing driving education programs to assess the crash potential between the subject vehicle and surrounding vehicles properly. The contribution of this study is to secure the effectiveness of driver education by capturing interactions between a subject vehicle and surrounding vehicles based on the simulator-based training using SSMs and then ultimately induce the prevention and reduction of road accidents.

The SSMs consist of measures with a single outcome for the dataset and measures with continuous outcomes calculated at every time step of the dataset. Accumulated speeding (AS), speed uniformity (SU), speed variation (SV), acceleration noise (AN), and lane deviation were measured with a single outcome and calculated after completing the driving scenarios. Measures with continuous outcomes should be transformed into a single representative value in order to evaluate how risky the drivers' driving behaviors were.

A single representative value of SSMs can be obtained either as the maximum (minimum) value of total outcomes, such as Max S, i.e., the maximum velocity in a conflict situation [33] or as the ratio of conflicts defined as exceeding the threshold value of each measure [27, 36]. This study adopted the minimum value as the representative value for SSMs related to lane-changing situations (see nos. 15 to 20 in Table 1). The method to define the threshold value for

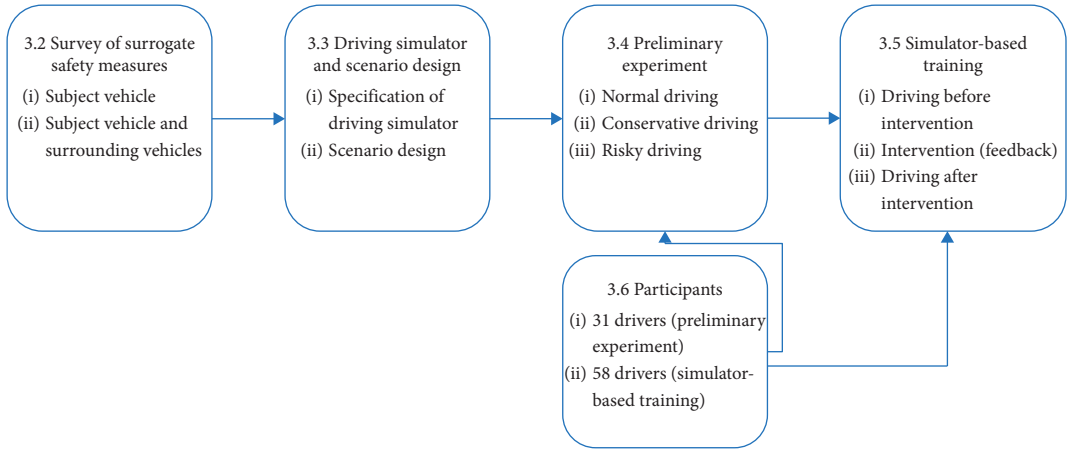

Figure 1: Framework of the study.

Table 1: Description of implementable surrogate safety measures.

Relation with surrounding vehicles	No.	Surrogate safety measure	Unit	Description
Relating to the subject vehicle	1	Accumulated speeding (AS)	kph	The normalized relative area (per unit length) bounded between the speed profile values higher than the speed limit and the speed limit line [28]
	2	Speed uniformity (SU)	kph	The normalized relative area (per unit length) bounded between the speed profile and the average speed line [28]
	3	Speed variation (SV)	kph	The standard deviation of the speed
	4	Acceleration (%)	m/s^2	The acceleration of the subject vehicle
	5	Deceleration (%)	m/s^2	The deceleration of the subject vehicle
	6	Acceleration noise (AN)	m/s^2	The root mean square deviation of the acceleration [29]
	7	Lane deviation	m	The standard deviation of lane position [30]
	8	Yaw rate (%)	°/s	The rotational velocity around the z-axis of the subject vehicle [31]
	9	Lane change (%)	—	The number of lane change manoeuvres completed
Relating to surrounding vehicles	10	Gap distance (%) (GD)	m	The longitudinal distance along a travelled way between one vehicle's leading surface and another vehicle's trailing surface [32]
	11	Proportion of stopping distance (%) (PSD)	—	The ratio of the distance available for manoeuvring to that of the necessary stopping distance to a projected point of collision [33]
	12	Time-to-collision (%) (TTC)	sec	The time interval required for one vehicle to strike another object if both objects continue on their current paths at their current speed [32]
	13	Modified TTC (%) (MTTC)	sec	The time interval required for one vehicle to strike another object if both objects continue on their current paths at their current speed and acceleration [32]
	14	Deceleration rate to avoid crash (%) (DRAC)	m/s^2	The deceleration required by the following vehicle to come to a timely stop or attain a matching lead vehicle speed to avoid a rear-end crash [34]
	15	Min_Front_GD	m	The minimum value of gap distance (GD) with leading vehicle of current lane in lane-changing situation
	16	Min_Lag_GD	m	The minimum value of gap distance (GD) with lag vehicle of target lane in lane-changing situation
	17	Min_Lead_GD	m	The minimum value of gap distance (GD) with leading vehicle of target lane in lane-changing situation
	18	Min_Front_TTC	sec	The minimum value of time-to-collision (TTC) with leading vehicle of current lane in lane-changing situation
	19	Min_Lag_TTC	sec	The minimum value of time-to-collision (TTC) with lag vehicle of target lane in lane-changing situation
	20	Min_Lead_TTC	sec	The minimum value of time-to-collision (TTC) with leading vehicle of target lane in lane-changing situation

counting the number of conflicts in each of the SSMs was derived from the existing literature [37]. The 85th percentile value of total participants' driving data distribution was used as the threshold for SSMs for which higher values indicated more risky driving behaviors (acceleration (%), yaw rate (%), lane change (%), gap distance (%), and proportion of stopping distance (%)). For SSMs for which lower values indicated more risky driving behaviors (deceleration (%), time-to-collision (%), modified TTC (%), and deceleration rate to avoid crash (%)), the 15th percentile value of total participants' driving data distribution was used as the threshold.

3.3. Driving Simulator and Scenario Design. The driving simulator used in this study was mounted on a six-degree-of-freedom motion system, with a size of $3500 \times 3500 \times 3500$ mm. The visual system for the driving simulator consisted of three 43-inch full HD LED monitors, providing a 150-degree field of view with a resolution of 5760×1080 pixels and a 60 Hz refresh rate. The virtual environment with various driving conditions was represented through the three monitors, with rear-view and side-view mirrors visible on the center monitor and side monitors, respectively (Figure 2(a)). The vehicle dynamics were validated based on the real motion of the Hyundai Sonata.

A part of the street grid in Seoul was implemented in a virtual environment in order to enhance the reality of the driving environment. The total length of the designed route in the scenario was 10.1 km, including freeway (2.3 km), urban roads (6.0 km), and rural roads (1.8 km) (Figure 2(b)). The freeway consisted of the main freeway segment with a posted speed limit of 110 kph and an off-ramp. The urban roads included ten signal intersections located every 200–400 m on a four-lane two-way road with a speed limit of 60 kph. The rural roads were either two- or four-lane, two-way roads with a speed limit of 80 kph.

The movements of surrounding vehicles significantly determine the mental load and ability to drive a vehicle. If the movements of the surrounding vehicles were not real enough, there is a possibility that drivers will drive a vehicle differently than they would in actual driving, meaning that the results and conclusions obtained from the simulation would not be applicable in actual driving. Many studies using driving simulators have been limited in expressing realistic movements because the movements of the vehicles were very strictly controlled to assess the drivers' abilities in certain crash situations [38]. Therefore, if the movements of the surrounding vehicle are unrealistic and strictly controlled irrespective of the movements of the subject vehicle, it would be difficult to expect the reduction of risky driving behaviors in actual driving on the road through simulator-based training. In order to implement the realistic interactions with surrounding vehicles, traffic flow models (i.e., a car-following model, a lane-changing model, and a gap-acceptance model) were modeled based on video data and vehicle trajectory data, and then, they were applied to the movements of the surrounding vehicles. Using the traffic flow models had the additional benefit of showing different movements in each trial, thereby increasing the sense of reality and preventing participants from adapting to the scenario [38]. The generalized model of car-following was estimated with data obtained from random vehicles on the West-Hanam IC and the West-Icheon IC of the Jungbu Highway [39]. The lane-changing model was implemented based on the vehicle trajectory data measured by nine video cameras in the upper 400 m section of the Middle East IC of the Seoul Ring Expressway for discretionary and mandatory lane-changing. The parameters of a logit model were estimated with the gap distance and the speed of the subject vehicle as independent variables. The logit model was estimated for the gap-acceptance model at the intersection. Data were collected using video cameras at six intersections in Seoul to estimate the parameters of the gap-acceptance model, and the data included the time gap, type of vehicle, and traffic volume. This study estimated the parameters of the logit models for an unprotected left turn, an unprotected right turn, and a roundabout using collected data.

3.4. Preliminary Experiment for Extreme Driving Behaviors with SSMs. This study conducted a preliminary experiment to analyze the sensitivity of SSMs for extreme driving behaviors. Before participating in the preliminary experiment, the participants were shown how to control a driving simulator and performed one to three minutes of practice driving to prevent simulator sickness and to adapt to the virtual environment of the driving simulator. To use the SSMs that could measure the crash potential of surrounding vehicles in a driving simulator, the sensitivity analysis of the SSMs was required to determine whether they could capture risky driving behaviors. In this study, the experimental methods that had been used in previous studies were used to analyze the sensitivity of the SSMs to extreme driving behaviors. Past participants were involved in a study of extreme driving behaviors that compared the difference in fuel consumption depending on driving behaviors and compared the difference in the performance of an urban network on driving behaviors [40, 41].

Participants in the preliminary experiment were asked to drive "normally," "conservatively," or "riskily." In normal driving, the participants drove the way they usually drive. In the conservative driving condition, the participants were asked to maintain a greater safe following distance, accelerate and decelerate as gently as possible, and keep their speed under the speed limit. In risky driving, the participants were required to complete their driving route within 10 minutes rather than the typical 15 minutes, to follow the leading vehicle more closely than the recommended safe distance, and to change lanes and the speed of the vehicle erratically.

3.5. Simulator-Based Training to Improve Driving Behaviors. This study used SSMs that statistically could capture risky and conservative driving within the simulator-based training conducted by the Korea Transportation Safety Authority (KOTSA). The simulator-based training consisted of three parts, i.e., driving before the intervention, intervention

Figure 2: Driving simulator and scenario in this study: (a) the driving simulator set-up; (b) the designed route in the scenario.

(feedback based on results of driving behaviors), and driving after the intervention.

Before the intervention, the participants drove an introduction drive for 1 to 3 minutes to become accustomed to the control of the driving simulator and the virtual environment. Subsequently, they drove the driving scenario as they usually would do, allowing the instructor to examine the extent of their risky driving behaviors.

The intervention consisted of two parts: feedback with a video replay of the driver's driving and a commentary video. The instructors provided feedback to the participants concerning how risky they drove in terms of six risky driving behaviors, i.e., speeding, reckless changing speed, rapid acceleration and deceleration, erratic steering control, tailgating, and erratic lane-changing. The speeding, reckless changing speeds, rapid acceleration and deceleration, and erratic steering control only assessed the movements of the subject vehicle. In contrast, the tailgating and erratic lane-changing assessed the crash potential with the surrounding vehicles in the normal driving environment. In typical drivers' education programs, the instructor evaluates the drivers' driving behaviors based on the movements of the subject vehicle and the crash potential with the surrounding vehicles in specific situations (i.e., speeding, reckless changing speeds, rapid acceleration and deceleration, and erratic steering control). In the simulator-based training using the SSMs of this study, the instructor informed the drivers the risky driving behaviors, including situations in which they were following a vehicle and changing lanes in a common driving environment and were riskier than other drivers. In other words, the contribution of this study is to evaluate the movements of the subject vehicle as well as the interactions between vehicles by identifying the risky driving behaviors such as tailgating in car-following situations and erratic lane-changing in lane-changing situations. Also, the instructor educated the drivers about safe methods for driving on the road to reduce the crash potential between the vehicles. In the commentary video, videos of actual crashes attributable to each of the six risky driving behaviors were shown to encourage safe driving.

After the feedback session at the end of the intervention, the drivers were asked to drive again so that their driving behaviors could be observed in order to determine whether their driving behaviors had been improved; i.e., whether their risky driving behaviors were reduced. The instructor showed the participants how much their driving had improved in terms of the frequency of six risky driving behaviors and to encourage safe driving.

3.6. Participants. For this study, we posted advertisements and recruited 43 participants for the preliminary study. Out of the 43 participants, 12 participants dropped out of the experiment due to simulator sickness, leaving 31 participants, i.e., 21 males and 10 females. The average age of the participants was about 36 years old, and the average driving experience of participants was almost 13 years.

Existing research on simulator-based training was mainly conducted with novice, elderly, and commercial drivers [13, 20, 23, 42, 43] because drivers in these three groups tend to have higher accident rates, making them the primary targets for improving risky driving [44–46]. Participants in the simulator-based training were recruited separately from the three driver groups by posted advertisements. Out of 69 participants, 11 participants dropped out of the experiment due to simulator sickness, leaving 58 participants, i.e., 21 novice drivers, 16 elderly drivers, and 21 commercial drivers. The average age of the participants was approximately 46 years old, and the average driving experience of participants was slightly more than 20 years. The demographic statistics of the participants are provided in Table 2.

4. Results

4.1. Results of the Sensitivity Analysis for Extreme Driving Behaviors with SSMs. In this study, we conducted a

Table 2: Demographics of the participants in this study.

Type	Preliminary experiment ($n = 31$)		Simulator-based training ($n = 58$)	
	N	Percent (%)	N	Percent (%)
Age				
20–29	13	41.94	20	34.48
30–39	7	22.58	2	3.44
40–49	6	19.35	4	6.90
50–59	2	6.45	16	27.59
≥60	3	9.68	16	27.59
Gender				
Male	21	67.74	43	74.14
Female	10	32.36	15	25.86
Driving years				
≤2 years	6	19.35	21	36.21
3–20 years	16	51.61	5	8.62
21–39 years	8	25.81	25	43.10
≥40 years	1	3.23	7	12.07
Crash experience				
None	26	83.87	42	72.41
1	2	6.45	4	6.90
2	3	9.68	11	18.97
≥3	0	0.00	1	1.72
Traffic violation				
None	24	77.41	37	63.79
1	5	16.13	13	22.41
2	1	3.23	4	6.90
≥3	1	3.23	4	6.90

sensitivity analysis for extreme driving behaviors to test whether SSMs could significantly distinguish between normal, conservative, and risky driving. Twenty SSMs were analyzed for extreme driving behaviors for 31 drivers. The SSMs were analyzed for the entire road section and the freeway section because the lane-changing in the urban road section was forced due to the direction of the designed travel route, in contrast to the discretionary lane changes in the freeway section. In this study, driving behaviors except lane-changing were evaluated over the entire road section, but lane-changing was evaluated only for the freeway section. Also, an ANOVA test and a post-hoc test (Tukey HSD) at the 95% significance level were performed to evaluate whether the SSMs could detect significant differences in extreme driving behaviors across the different conditions.

Differences were not statistically significant for five SSMs, i.e., lane deviation, DRAC, Min_Front_GD, Min_Lead_GD, and Min_Lag_TTC (Table 3). Lane deviation and DRAC, which evaluate driving behavior over the entire road section, did not exhibit significant differences. Few studies have compared lane deviations for different degrees of extreme driving behaviors. However, one previous study found that there was no significant difference in the mean of lane deviation before and after training [25]. In contrast to GD, TTC, and DRAC, the measure of minimum deceleration to avoid a collision has been known to be limited to reflect a conflict situation, and drivers may fail to adjust DRAC to avoid a conflict situation [47].

When a driver changes lanes on the freeway, the subject vehicle enters the target lane at a higher speed than the front vehicle in the current lane and the lead vehicle in the target lane. Min_Front_GD and Min_Lead_GD become shortened when changing lanes, and the driver changed lanes in a situation in which the driver maintained the distance between the surrounding vehicles necessary for changing lanes. Regardless of the driver's extreme driving behaviors, Min_Front_GD and Min_Lead_GD were not significantly different. However, Min_Front_TTC and Min_Lead_TTC, which reflect the relative speed differences between vehicles, showed statistically significant differences because the entry speed in risky driving is higher than that in conservative driving. Min_Lag_GD showed a statistically significant difference because drivers changed lanes at a shorter gap distance in risky driving and a longer gap distance in conservative driving than in normal driving. In the scenario of this study, the lag vehicle in the target lane decelerated when the subject vehicle entered the target lane because the car-following model was applied to the movements of surrounding vehicles. Therefore, there was no statistically significant difference between the extreme driving behaviors of Min_Lag_TTC due to the decrease in the speed of the lag vehicle even though the distance between the subject vehicle and the lag vehicle in the target lane was shorter in risky driving.

4.2. Results of Improvement for Risky Driving Behaviors with SSMs. In this study, we classified 15 SSMs into six types of risky driving behaviors to improve the driver's understanding of SSMs in an intervention of simulator-based

Table 3: Summary of statistics for surrogate safety measures in sensitivity analysis.

No.	SSMs	Entire road section			Freeway section		
		ANOVA		Post-hoc	ANOVA		Post-hoc
		F-value	p-value	p-value	F-value	p-value	p-value
1	AS	$F(2, 90) = 33.12$	0.00	0.00			
2	SU	$F(2, 90) = 35.73$	0.00	0.00			
3	SV	$F(2, 90) = 37.69$	0.00	0.00			
4	Acceleration	$F(2, 90) = 16.80$	0.00	0.00			
5	Deceleration	$F(2, 90) = 39.24$	0.00	0.00			
6	AN	$F(2, 90) = 28.41$	0.00	0.00			
7	Lane deviation	$F(2, 90) = 0.41$	0.66	—			
8	Yaw rate	$F(2, 90) = 30.77$	0.00	0.00			
9	Lane change	$F(2, 90) = 7.71$	0.00	0.00			
10	GD	$F(2, 90) = 29.05$	0.00	0.00			
11	PSD	$F(2, 90) = 29.58$	0.00	0.00			
12	TTC	$F(2, 90) = 16.22$	0.00	0.00			
13	MTTC	$F(2, 90) = 14.28$	0.00	0.00			
14	DRAC	$F(2, 90) = 2.91$	0.06	—			
15	Min_Front_GD				$F(2, 90) = 2.95$	0.06	—
16	Min_Lag_GD				$F(2, 90) = 11.74$	0.00	0.00
17	Min_Lead_GD				$F(2, 90) = 2.76$	0.07	—
18	Min_Front_TTC				$F(2, 90) = 6.33$	0.00	0.04
19	Min_Lag_TTC				$F(2, 90) = 0.16$	0.85	—
20	Min_Lead_TTC				$F(2, 90) = 8.87$	0.00	0.01

training. Fifty-eight drivers were provided with feedback on their driving behaviors based on 15 SSMs in simulator-based training, and they were taught how to reduce their risky driving behaviors.

4.2.1. Comparison among Novice, Elderly, Commercial, and Typical Drivers. Before analyzing the effect of simulator-based training using SSMs on the improvement of driving behaviors, it was necessary to identify how risky the drivers participating in the simulator-based training were. This is because drivers who had safe driving behaviors were less likely to improve their driving behaviors, even though they were trained. In this study, 31 drivers who participated in the sensitivity analysis experiment were selected as typical drivers to compare with the three driver groups, i.e., novice, elderly, and commercial drivers. Because the 31 drivers were recruited randomly irrespective of gender, age, and driving experience, the risky driving behaviors of the three driver groups before the intervention were analyzed and compared based on the normal driving of typical drivers. The larger the values of Min_Lag_GD, Min_Front_TTC, and Min_Lead_TTC were, the safer the drivers' driving behaviors drivers were. The smaller the values of the other SSMs were, the safer the driving behaviors of the drivers were (see Figure 3).

Novice drivers were found to be riskier than typical drivers except for Min_Lag_GD and Min_Lead_TTC (see Figure 3). Novice drivers have poor driving skills because of low driving experience [48]. Since novice drivers have difficulty in maintaining a safe distance from a leading vehicle because of their lack of driving experience, they were inclined to tailgate leading vehicles to a greater extent than typical drivers. Also, novice drivers had limited in-advance perception of dangerous situations, and therefore, it also was difficult for them to maintain a constant speed [43].

Elderly drivers were found to be riskier than typical drivers in the cases of deceleration, AN, and yaw rate. In contrast, other measures of elderly drivers were similar to or safer than that of typical drivers (see Figure 3). These results were consistent with the results that elderly drivers do not perceive the brake pedal pressure in the driving simulator as accurately as young drivers [43].

Commercial drivers were found to be riskier than typical drivers except for lane change and four SSMs related to tailgating (see Figure 3). This suggests that commercial drivers tend to be more risky drivers than typical drivers to save time, but maintaining a safe distance from a leading vehicle is essential for drivers of heavy trucks and buses [42].

4.2.2. Comparison of before and after Intervention by Driver Group. The SSMs used as evaluation measures were statistically tested at the 95% significance level with paired t-tests to determine whether drivers' behaviors improved before and after the training in simulator-based training (see Table 4). In the case of novice drivers, Min_Lag_GD and Min_Front_TTC in lane-changing situations showed that the improvement before and after the training was not statistically significant. With the exception of AS, acceleration, deceleration, and AN, elderly drivers did not show statistically significant improvements after the training. In the case of commercial drivers, there were statistically significant differences for all measures except for Min_Front_TTC in lane-changing situations. The improvement in driving behaviors after the training was the greatest in commercial drivers and the least in elderly drivers.

In the case of novice drivers, the improvements in speeding, rapid acceleration and deceleration, and tailgating

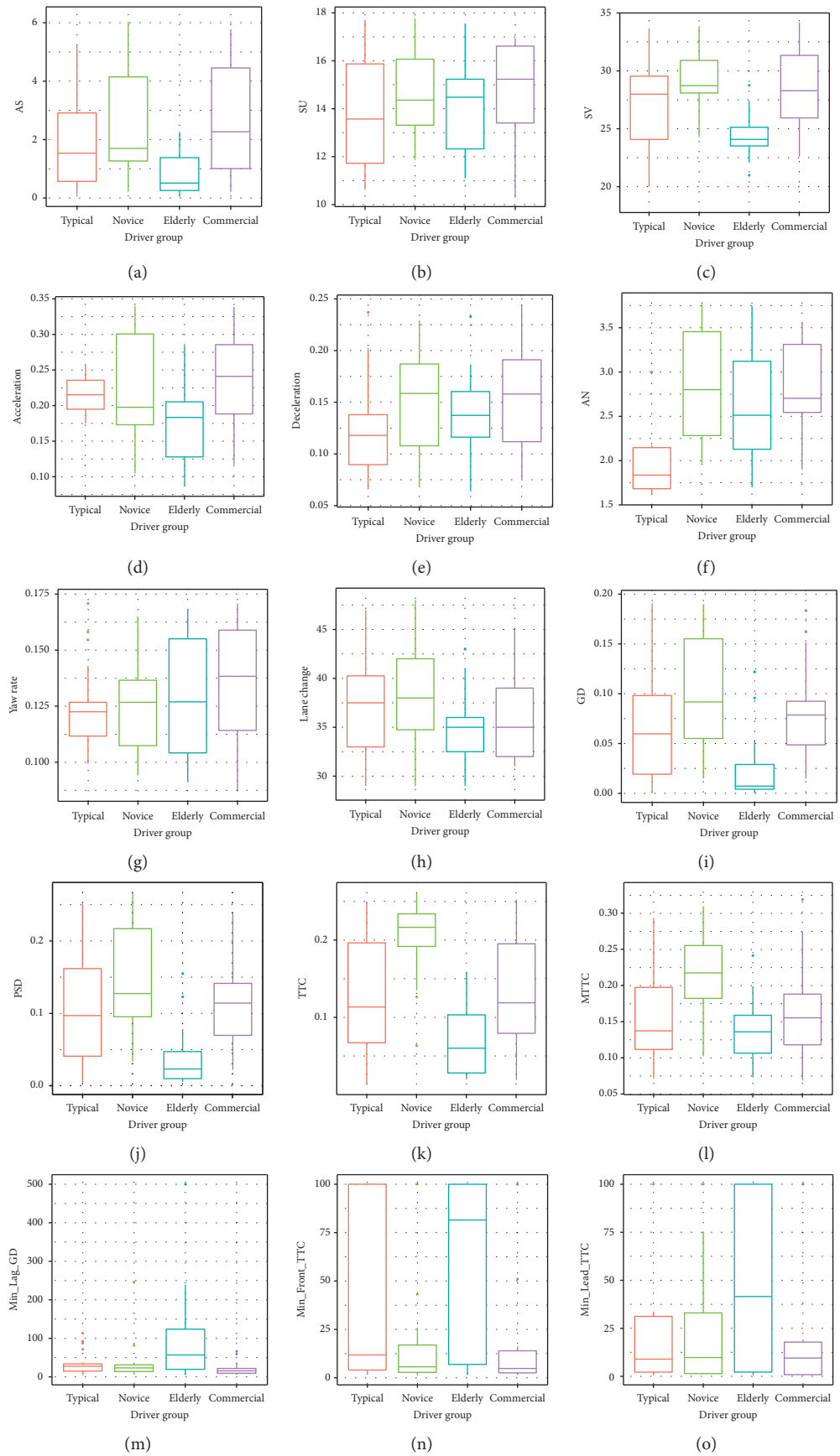

FIGURE 3: Comparison of surrogate safety measures by driver group: (a) AS (speeding); (b) SU (reckless changing speeds); (c) SV (reckless changing speeds); (d) acceleration (rapid acc. and dec.); (e) deceleration (rapid acc. and dec.); (f) AN (rapid acc. and dec.); (g) yaw rate (erratic steering control); (h) lane change (erratic steering control); (i) GD (tailgating); (j) PSD (tailgating); (k) TTC (tailgating); (l) MTTC (tailgating); (m) Min_Lag_GD (erratic lane-changing); (n) Min_Front_TTC (erratic lane-changing); (o) Min_Lead_TTC (erratic lane-changing).

Table 4: Summary of statistics for surrogate safety measures in before and after intervention.

Types of risky driving behaviors	SSMs	Novice ($n = 21$)			Elderly ($n = 16$)			Commercial ($n = 21$)		
		μ_{before}	μ_{after}	t-stat (p-value)	μ_{before}	μ_{after}	t-stat (p-value)	μ_{before}	μ_{after}	t-stat (p-value)
Speeding	AS	3.54	1.48	5.41 (0.00)	0.71	0.29	2.46 (0.03)	2.83	0.42	5.54 (0.00)
Reckless changing speeds	SU	15.03	12.97	4.10 (0.00)	13.51	12.73	1.29 (0.22)	15.50	13.37	5.20 (0.00)
	SV	30.62	25.53	6.34 (0.00)	23.00	21.86	1.92 (0.07)	28.70	23.50	9.19 (0.00)
Rapid acceleration and deceleration	Acceleration	0.24	0.15	6.94 (0.00)	0.21	0.17	2.28 (0.04)	0.24	0.14	8.70 (0.00)
	Deceleration	0.17	0.11	6.07 (0.00)	0.14	0.12	2.46 (0.03)	0.17	0.10	7.01 (0.00)
Erratic steering control	AN	2.97	2.27	6.20 (0.00)	2.80	2.49	3.19 (0.01)	2.95	2.04	8.54 (0.00)
	Yaw rate	0.14	0.12	2.85 (0.01)	0.13	0.12	1.95 (0.07)	0.14	0.12	3.57 (0.00)
	Lane change	39.38	36.43	1.89 (0.07)	35.94	33.69	1.35 (0.20)	37.10	33.90	3.36 (0.00)
Tailgating	GD	0.14	0.07	3.84 (0.00)	0.02	0.02	0.08 (0.94)	0.09	0.04	4.32 (0.00)
	PSD	0.19	0.10	4.42 (0.00)	0.04	0.03	0.56 (0.58)	0.12	0.06	5.07 (0.00)
	TTC	0.21	0.17	2.51 (0.02)	0.07	0.06	1.04 (0.31)	0.14	0.10	4.39 (0.00)
	MTTC	0.24	0.15	4.39 (0.00)	0.17	0.14	1.77 (0.10)	0.18	0.10	4.67 (0.00)
Erratic lane-changing	Min_Lag_GD	27.75	49.99	−0.88 (0.39)	79.01	90.95	−0.29 (0.78)	5.42	84.24	−2.45 (0.02)
	Min_Front_TTC	76.71	91.01	−0.30 (0.77)	117.18	76.87	0.89 (0.39)	27.97	127.39	−2.78 (0.05)
	Min_Lead_TTC	17.09	41.00	−2.66 (0.02)	58.17	60.47	−0.15 (0.88)	16.38	48.78	−2.78 (0.01)

were significant, but no significant improvements were observed in erratic lane-changing (see Table 4). Through the simulator-based training, most novice drivers improved their ability to maintain a safe distance from the leading vehicle. However, they did not show improvement in keeping a safe distance from adjacent vehicles in lane-changing situations. Therefore, although novice drivers improved following the simulator training in the car-following situation, additional training should be provided for maintaining a safe distance between vehicles when changing lanes.

Elderly drivers showed improvement in speeding, rapid acceleration, and deceleration (see Table 4). Since elderly drivers tend to be more defensive than other driver groups, they showed the least improvement in risky driving behaviors of the three driver groups. Compared to the younger drivers, elderly drivers were less aware of the brake pedal pressure in a driving simulator during deceleration. They showed a tendency to decrease speed rapidly in the driving simulator before the intervention. After the intervention, the deceleration behavior of elderly drivers was improved because the instructors requested that they begin their deceleration earlier to prevent erratic deceleration. However, there is a limit to the conclusions that the simulator-based training improved the erratic decelerating behavior of elderly drivers since their erratic deceleration behavior may have resulted from their use of the driving simulator.

After the intervention, the driving behaviors of commercial drivers were improved in all 15 SSMs. The improvements in speeding, rapid acceleration, rapid deceleration, and tailgating were more significant than the other risky driving behaviors (see Table 4). Since the commercial drivers had shown more risky driving behaviors than other groups of drivers, their driving behaviors were improved to a greater extent by the simulator-based training than driving behaviors of drivers for other groups. These results showed that the simulator-based training program is effective in reducing risky driving behaviors of various driver groups by providing feedback on how risky their driving behaviors are.

5. Conclusions

This study implemented SSMs in a simulator-based training program to evaluate the crash potential with surrounding vehicles. The movements of surrounding vehicles need to be realistic to consider the interactions with surrounding vehicles in driver education. Traffic flow models developed from data collected on real roads were implemented for the movements of surrounding vehicles (car-following, lane-changing, and gap-acceptance at intersection). Twenty SSMs were implemented in the driving simulator. The preliminary experiment that was conducted with 31 participants verified that 15 SSMs could be used to capture risky driving behaviors. The 15 selected SSMs were used as the measure for current simulator-based training in the Republic of Korea to evaluate the driving behaviors of novice, elderly, and commercial drivers.

After the intervention of the simulator-based training, the risky driving behaviors of novice drivers, elderly drivers, and commercial drivers were reduced in different ways. In the case of novice drivers, additional on-road training was required to reduce risky driving behaviors in lane-changing situations. For elderly drivers, the speeding and rapid acceleration behaviors were improved. However, other risky driving behaviors were not statistically reduced because elderly drivers already drive vehicles safely so that there was nothing to improve significantly except for speeding, rapid acceleration, and deceleration. The training using the driving simulator reduced the risky driving behaviors of commercial drivers. The reason that simulator-

based training was most effective for reducing the risky driving behaviors for commercial drivers was that their behaviors were risky compared to the behaviors of other groups of drivers.

The results of this study showed that SSMs could be used both for road safety and traffic management strategies and for the evaluation of individual drivers' driving behaviors in driver education. However, there were two limitations in this study that should be addressed in future research. First, the possibility that adaptation to manipulating a driving simulator after the intervention has a positive effect on reducing risky driving behaviors cannot be ruled out. This study did not compare drivers trained in simulator-based training using SSMs with drivers trained in the previous simulator-based training. In this study, there are improvements in various driving behaviors by giving the drivers feedback using SSMs, but it is possible that intervention without SSMs also could contribute to reducing risky driving behaviors. Therefore, future research should determine the extent to which the intervention based on feedback using SSMs contributes to reducing risky driving behavior compared to existing simulator-based training. Second, it is unclear whether simulator-based training using SSMs will result in the reduction of risky driving behaviors in actual driving. This study only analyzed instantaneous training effects in simulator driving. Future research should examine how simulator-based training using SSMs reduces risky driving behaviors in actual driving. Therefore, it is necessary to study whether the trends of SSMs are the same by comparing drivers in the existing simulator-based training with those in the simulator-based training proposed in this study by comparing actual driving data with data from the driving simulator.

Data Availability

The data used to support the findings of this study are available from the corresponding author upon request.

Conflicts of Interest

The authors declare that there are no conflicts of interest regarding the publication of this paper.

Acknowledgments

This research was supported by the Institute of Construction and Environmental Engineering and the Institute of Engineering Research at Seoul National University. The authors wish to express their gratitude for their support.

References

[1] World Health Organization, *Global Status Report on Road Safety 2018*, World Health Organization, Geneva, Switzerland, 2018.

[2] NHTSA, *National Motor Vehicle Crash Causation Survey: Report to Congress*, NHTSA, U.S. Department of Transportation, Washington, DC, USA, 2008.

[3] NHTSA, *Traffic Safety Facts Annual Report Tables*, NHTSA, Washington, DC, USA, 2019.

[4] T. R. Neuman, R. Pfefer, K. L. Slack et al., "NCHRP report 500," in *Guidance for Implementation of the AASHTO Strategic Highway Safety Plan: A Guide for Addressing Aggressive-Driving Collisions*, vol. 23, Transportation Research Board, Washington, DC, USA, 2003.

[5] T. Toledo, O. Musicant, and T. Lotan, "In-vehicle data recorders for monitoring and feedback on drivers' behavior," *Transportation Research Part C: Emerging Technologies*, vol. 16, no. 3, pp. 320–331, 2008.

[6] P. K. Alvaro, N. M. Burnett, G. A. Kennedy et al., "Driver education: enhancing knowledge of sleep, fatigue and risky behaviour to improve decision making in young drivers," *Accident Analysis & Prevention*, vol. 112, pp. 77–83, 2018.

[7] L. Meuleners and M. Fraser, "A validation study of driving errors using a driving simulator," *Transportation Research Part F: Traffic Psychology and Behaviour*, vol. 29, pp. 14–21, 2015.

[8] O. M. J. Carsten, J. A. Groeger, E. Blana, and A. H. Jamson, *Driver Performance in the EPSRC Driving Simulator: A Validation Study. Report No. GR/K56162*, University of Leeds, Leeds, UK, 1997.

[9] D. L. Fisher, M. Rizzo, J. Caird, and J. D. Lee, *Handbook of Driving Simulation for Engineering, Medicine, and Psychology*, CRC Press, Boca Raton, FL, USA, 2011.

[10] B. Kappé, M. van Emmerik, W. van Winsum, and A. Rozendom, *Virtual Instruction in Driving Simulators*, Presented at Driving Simulator Conference, Dearborn, MI, USA, 2003.

[11] D. L. Roenker, G. M. Cissell, K. K. Ball, V. G. Wadley, and J. D. Edwards, "Speed-of-Processing and driving simulator training result in improved driving performance," *Human Factors: The Journal of the Human Factors and Ergonomics Society*, vol. 45, no. 2, pp. 218–233, 2003.

[12] D. Crundall, B. Andrews, E. van Loon, and P. Chapman, "Commentary training improves responsiveness to hazards in a driving simulator," *Accident Analysis & Prevention*, vol. 42, no. 6, pp. 2117–2124, 2010.

[13] E. M. M. Jongen, K. Brijs, M. Komlos, T. Brijs, and G. Wets, "Inhibitory control and reward predict risky driving in young novice drivers - a simulator study," *Procedia—Social and Behavioral Sciences*, vol. 20, pp. 604–612, 2011.

[14] P. V. Leeuwen, R. Happee, and J. D. Winter, "Vertical field of view restriction in driver training: a simulator-based evaluation," *Transportation Research Part F: Traffic Psychology and Behaviour*, vol. 24, pp. 169–182, 2014.

[15] F. Bella and G. D'Agostini, "Combined effect of traffic and geometrics on rear-end collision risk," *Transportation Research Record: Journal of the Transportation Research Board*, vol. 2165, no. 1, pp. 96–103, 2010.

[16] AAA Foundation for Traffic Safety (AAAFTS), *Aggressive Driving: Research Update*, AAA Foundation for Traffic Safety, Washington, DC, USA, 2009.

[17] D. Wiesenthal, J. Roseborough, and C. Wickens, "Behavioral approaches for combating aggressive driving (Chap. 8)," in *Routledge Handbook of Transportation*, D. Teodorovic, Ed., Taylor & Francis, New York, NY, USA, 2015.

[18] I. Richer and J. Bergeron, "Differentiating risky and aggressive driving: further support of the internal validity of the Dula Dangerous Driving Index," *Accident Analysis & Prevention*, vol. 45, pp. 620–627, 2012.

[19] D. Lord and S. Washington, *Safe Mobility: Challenges, Methodology and Solutions*, Emerald Group Publishing, Bingley, UK, 2018.

[20] L. M. Martín-delosReyes, E. Jiménez-Mejías, V. Martínez-Ruiz, E. Moreno-Roldán, D. Molina-Soberanes, and P. Lardelli-Claret, "Efficacy of training with driving simulators in improving safety in young novice or learner drivers: a systematic review," *Transportation Research Part F: Traffic Psychology and Behaviour*, vol. 62, pp. 58–65, 2019.

[21] A. Pollatsek, V. Narayanaan, A. Pradhan, and D. L. Fisher, "Using eye movements to evaluate a PC-based risk awareness and perception training program on a driving simulator," *Human Factors: The Journal of the Human Factors and Ergonomics Society*, vol. 48, no. 3, pp. 447–464, 2006.

[22] Y. Ba, W. Zhang, G. Salvendy, A. S. K. Cheng, and P. Ventsislavova, "Assessments of risky driving: a Go/No-Go simulator driving task to evaluate risky decision-making and associated behavioral patterns," *Applied Ergonomics*, vol. 52, pp. 265–274, 2016.

[23] Y. Wang, W. Zhang, and G. Salvendy, "Effects of a simulation-based training intervention on novice drivers' hazard handling performance," *Traffic Injury Prevention*, vol. 11, no. 1, pp. 16–24, 2010.

[24] P. Freeman, D. M. Neyens, J. Wagner, F. Switzer, K. Alexander, and P. Pidgeon, "A video based run-off-road training program with practice and evaluation in a simulator," *Accident Analysis & Prevention*, vol. 82, pp. 1–9, 2015.

[25] L. Dorn and D. Barker, "The effects of driver training on simulated driving performance," *Accident Analysis & Prevention*, vol. 37, no. 1, pp. 63–69, 2005.

[26] Y. Ali, Z. Zheng, and M. M. Haque, "Connectivity's impact on mandatory lane-changing behaviour: evidences from a driving simulator study," *Transportation Research Part C: Emerging Technologies*, vol. 93, pp. 292–309, 2018.

[27] K. Ozbay, H. Yang, B. Bartin, and S. Mudigonda, "Derivation and validation of new simulation-based surrogate safety measure," *Transportation Research Record: Journal of the Transportation Research Board*, vol. 2083, no. 1, pp. 105–113, 2008.

[28] A. T. Moreno and A. García, "Use of speed profile as surrogate measure: effect of traffic calming devices on crosstown road safety performance," *Accident Analysis & Prevention*, vol. 61, pp. 23–32, 2013.

[29] R. Herman, E. W. Montroll, R. B. Potts, and R. W. Rothery, "Traffic dynamics: analysis of stability in car following," *Operations Research*, vol. 7, no. 1, pp. 86–106, 1959.

[30] M. R. Savino, "Standardized names and definitions for driving performance measures," MS. thesis, Tufts University, Medford, MA, USA, 2009.

[31] H. Hagelin, "Detection of critical events using limited sensors," MS. thesis, Linköping University, Linköping, Sweden, 2012.

[32] Society of Automotive Engineers, *SAE J2944 201506. Operational Definitions of Driving Performance Measures and Statistics*, Society of Automotive Engineers, Detroit, MI, USA, 2015.

[33] D. Gettman and L. Head, "Surrogate safety measures from traffic simulation models," *Transportation Research Record: Journal of the Transportation Research Board*, vol. 1840, no. 1, pp. 104–115, 2003.

[34] F. F. Saccomanno, F. Cunto, G. Guido, and A. Vitale, "Comparing safety at signalized intersections and roundabouts using simulated rear-end conflicts," *Transportation Research Record: Journal of the Transportation Research Board*, vol. 2078, no. 1, pp. 90–95, 2008.

[35] W. Wang, Q. Cheng, C. Li, D. André, and X. Jiang, "A cross-cultural analysis of driving behavior under critical situations: a driving simulator study," *Transportation Research Part F: Traffic Psychology and Behaviour*, vol. 62, pp. 483–493, 2019.

[36] D. Gettman, L. Pu, T. Sayed, S. Shelby, and I. T. S. Siemens, *Surrogate Safety Assessment Model and Validation*, Publication FHWA-HRT-08-05. FHWA, U.S. Department of Transportation, Washington, DC, USA, 2008.

[37] R. H. Wortman and J. S. Matthias, "An evaluation of driver behavior at signalized intersections," *Transportation Research Record*, vol. 904, pp. 10–20, 1983.

[38] J. Olstam, *Simulation of Surrounding Vehicles in Driving Simulators. PhD Thesis*, Linköping University, Linköping, Sweden, 2009.

[39] D. C. Gazis, R. Herman, and R. B. Potts, "Car-following theory of steady-state traffic flow," *Operations Research*, vol. 7, no. 4, pp. 499–505, 1959.

[40] M. F. Chang and R. Herman, "Driver response to different driving instructions: effect on speed, acceleration and fuel consumption," *Traffic Engineering and Control*, vol. 21, no. 11, pp. 545–550, 1980.

[41] R. Herman, L. A. Malakhoff, and S. A. Ardekani, "Trip time-stop time studies of extreme driver behaviors," *Transportation Research Part A: General*, vol. 22, no. 6, pp. 427–433, 1988.

[42] T. Rosenbloom and A. Shahar, "Differences between taxi and nonprofessional male drivers in attitudes towards traffic-violation penalties," *Transportation Research Part F: Traffic Psychology and Behaviour*, vol. 10, no. 5, pp. 428–435, 2007.

[43] B. Keshavarz, R. Ramkhalawansingh, B. Haycock, S. Shahab, and J. L. Campos, "Comparing simulator sickness in younger and older adults during simulated driving under different multisensory conditions," *Transportation Research Part F: Traffic Psychology and Behaviour*, vol. 54, pp. 47–62, 2018.

[44] B. Simons-Morton and J. Ehsani, "Learning to drive safely: reasonable expectations and future directions for the learner period," *Safety*, vol. 2, no. 4, p. 20, 2016.

[45] J. B. Cicchino and A. T. McCartt, "Critical older driver errors in a national sample of serious U.S. crashes," *Accident Analysis & Prevention*, vol. 80, pp. 211–219, 2015.

[46] X. Wang, Y. Xing, L. Luo, and R. Yu, "Evaluating the effectiveness of Behavior-Based Safety education methods for commercial vehicle drivers," *Accident Analysis & Prevention*, vol. 117, pp. 114–120, 2018.

[47] F. Cunto and F. F. Saccomanno, "Calibration and validation of simulated vehicle safety performance at signalized intersections," *Accident Analysis & Prevention*, vol. 40, no. 3, pp. 1171–1179, 2008.

[48] A. F. Williams, W. A. Leaf, B. G. Simons-Morton, and J. L. Hartos, "Vehicles driven by teenagers in their first year of licensure," *Traffic Injury Prevention*, vol. 7, no. 1, pp. 23–30, 2006.

Hindawi
Journal of Advanced Transportation
Volume 2020, Article ID 4629132, 10 pages
https://doi.org/10.1155/2020/4629132

Research Article

Driving Simulator Validity of Driving Behavior in Work Zones

Yanning Zhang,[1] Zhongyin Guo ,[1] and Zhi Sun[2,3]

[1]*Key Laboratory of Road and Traffic Engineering of the Ministry of Education, Tongji University, Shanghai 201804, China*
[2]*China State Construction Shandong Investment Corporation, Jinan 250101, China*
[3]*China State Construction Infrastructure Corporation, Beijing 100044, China*

Correspondence should be addressed to Zhongyin Guo; zhongyin@tongji.edu.cn

Received 15 February 2020; Accepted 25 May 2020; Published 9 June 2020

Academic Editor: Cheol Oh

Driving simulation is an efficient, safe, and data-collection-friendly method to examine driving behavior in a controlled environment. However, the validity of a driving simulator is inconsistent when the type of the driving simulator or the driving scenario is different. The purpose of this research is to verify driving simulator validity in driving behavior research in work zones. A field experiment and a corresponding simulation experiment were conducted to collect behavioral data. Indicators such as speed, car-following distance, and reaction delay time were chosen to examine the absolute and relative validity of the driving simulator. In particular, a survival analysis method was proposed in this research to examine the validity of reaction delay time. The result indicates the following: (1) most indicators are valid in driving behavior research in the work zone. For example, spot speed, car-following distance, headway, and reaction delay time show absolute validity. (2) Standard deviation of the car-following distance shows relative validity. Consistent with previous researches, some driving behaviors appear to be more aggressive in the simulation environment.

1. Introduction

Driving simulation has been increasingly popular in transportation research because of its efficiency, safety, and controllability. By using driving simulation, researchers can design a specific driving scenario, conduct experiments in a closed and safe environment, and collect precise and diverse data through sensors. These advantages are prominent when driving behavior occurs in a scenario that is dangerous or difficult to reproduce.

For simulation experiments, simulator validity is an unavoidable issue; it refers to the ability of a simulator to reproduce real-world driving accurately [1]. However, simulator validity is inconsistent when the type of the driving simulator or the driving scenario is different, and there is no standardized method for assessing simulator validity [1]. Therefore, it is appropriate to verify the validity of the apparatus before conducting a simulation experiment.

Many driving scenarios need to be verified; one of them is driving in work zones. Work zones are considered to have a negative impact on traffic safety and mobility because of lane closure and lower speed limits [2]. The vehicle speed at the beginning of the work zone always exceeds the speed limit, and the deceleration before the work zone is high [3]. At the same time, the risk of rear-end crash is higher than in nonwork zones [4–6]. It is dangerous to reproduce these driving scenarios in the real world, which makes the driving simulator a perfect tool for relevant researches.

The primary objective of this research is to verify the validity of behavioral research in the work zone. A field experiment and a corresponding simulation experiment were conducted here to collect behavioral data. Indicators were chosen to identify simulator validity. Moreover, a survival analysis method was proposed here to analyze the validity of reaction delay time.

The arrangement of this paper is presented as follows. Section 2 is an overview of the current literature. In the next section, the apparatus, participants, and experiment process are provided. Section 4 is the definition of indicators and the survival analysis method. The rest of the sections are the results, discussion, and conclusion.

2. Literature Review

Driving simulator validity is a prerequisite of simulation-based research. There are different classifications of simulator validity. One of the widely used simulator validity is absolute-relative validity. Absolute validity indicates that no significant differences between real-world driving and simulated driving. Relative validity indicates that simulated driving shows the same patterns as real-world driving. However, there are a limited number of research studies that validate a driving simulator by directly comparing simulated and real driving [1]. In these studies, statistical tests are a common method to verify absolute validity. In the meantime, direct comparison and regression models are methods to verify relative validity. Tornros [7] used the Tukey test to verify the absolute validity of speed behavior and lateral behavior in the tunnel driving. Helland et al. [8] and Meuleners and Fraser [9] used the paired sample *t*-test to verify the absolute validity in drunk driving and driving errors, respectively. ANOVA was used to identify the significant difference between real driving and simulated driving, too [10–12]. As for relative validity, Helland et al. [8] used the linear mixed model to verify the relative validity of drunk driving, while Riener [13] verified the relative validity of drivers' reaction delay time by direct comparison.

Data collected from real-world driving and simulated driving are the foundation of driving simulator validity verification. These data always presented in the form of behavioral indicators. Therefore, driving simulator validation research studies can be classified by the type of indicator. Common types of behavioral data are speed [11, 14], lateral position [10, 15], lane-changing behavior [16–18], driving errors [9], and others [19]. It is worth noting that validation research for car-following behavior is rarely mentioned in the review of simulator validation studies [1, 20]. In the above cases, indicators are related to the research topic. For example, Branzi [14] used the average speed for speed behavior research. Davenne [16] used inappropriate line crossing time, self-fatigue, and sleepiness for lane-changing behavior and driving fatigue research. Meuleners and Fraser [9] studied driving error with mirror checking, four-direction observations, the speed at interactions, obeying traffic lights, and obeying stop signs.

Speed behavior [21–23] and rear-end-crash-related behavior [6, 24–30] (merging behavior and car-following behavior) have been a primary concern of researchers because of the traffic feature of work zones. Besides naturalistic driving and field experiments, self-report and driving simulation are also used in the research studies for data collection. Debnath [21] compared self-nominated speeds and actual speeds in work zones, finding that participants generally underestimate the speed in work zones. Domenichini [22] conducted a simulation experiment and found that drivers always exceed the speed limit of work zones. These research studies used behavioral indicators to describe driving behaviors. Paolo and Sar [3] used spot speed and deceleration for speed behavior research in work zones. Lochrane et al. [27] used car-following distance and relative speed for car-following behavior research.

The existing studies show that driving simulators have been used in driving behavior research. Some validation research studies corresponding to the particular driving scenario have been proposed. However, there is a gap in simulator validity research for driving in work zones. In particular, simulator validity research for car-following behavior. The validity verification method is not standardized; the direct comparison is still a common method to verify relative validity. This research examines the simulator validity of driving in work zones, including the free-flow scenario and car-following scenario. Statistical methods and regression models are proposed here for validity verification. Especially, a survival analysis method is proposed here for time-event data like reaction delay time.

3. Experimental

3.1. Apparatus. A field experiment and a simulation experiment were conducted in this research. The field experiment data were collected by instrumented vehicles. The on-board data processing system integrated the data and output it at a frequency of 10 Hz. The driving simulator used in the simulation experiment consisted of an eight degree-of-freedom motion system, a fully instrumented vehicle, and a high-fidelity visual system. The motion system provided drivers with driving force feedback. Sensors of the instrumented vehicle collected data while driving. The visual system consisted of five simulation projectors; the projectors produced a view of horizontal 250 degrees and vertical 40 degrees. LCD monitors provided a view of rearview mirrors. SCANeR™ software was used to edit driving scenarios and integrate experiment data. Simulation data were also output at a frequency of 10 Hz. The apparatuses are shown in Figure 1.

3.2. Participants. The recruitment method of this research followed the method in Davenne et al.'s research [16]. 36 healthy men were recruited; all of them held a valid driving license and had daily-driving experience for at least one year. There were 20 drivers for the field experiment (mean age ± SD = 25.4 ± 3.5 years; mean driving age ± SD = 3.3 ± 1.5 years) and 16 matched drivers for the simulation experiment (mean age ± SD = 25.6 ± 2.4 years; mean driving age ± SD = 3.7 ± 1.1 years). A pretest was provided to ensure every participant is familiar with the requirement of experiments and the operation method of apparatus.

3.3. Experiment Tasks. The free-flow scenario and car-following scenario were chosen in this research. These scenarios were the same both in the field and simulation experiments. The field experiment was conducted on a two-way four-lane highway in Shandong Province, China. The length of the test section was 10 km, and the speed limit of the test section was 100 km/h. The road section in the driving simulator is shown in Figure 2. The speed limit sign and other essential preinformation signs were installed in the simulation experiment to reproduce the road section in the field experiment. To verify the relative validity, 2 × N design

(a) (b)

Figure 1: Experimental apparatuses: (a) the instrumented vehicle; (b) the driving simulator.

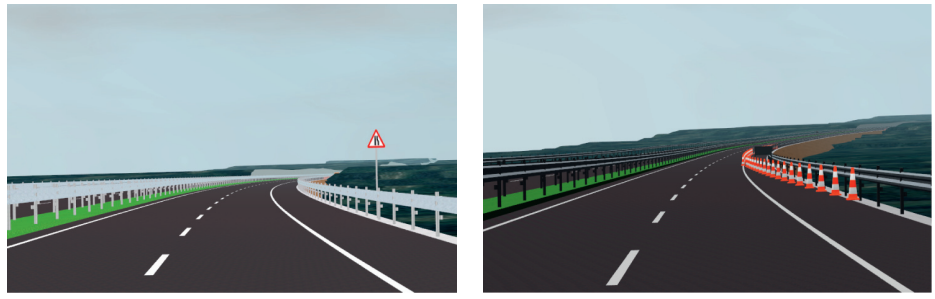

(a) (b)

Figure 2: Road section in the driving simulator.

with driving environments and other factors were employed in the study.

For the free-flow scenario, the factor was the lane closure type. Two tests were contained in the free-flow scenario; one of them closed the passing lane, and another closed the emergency lane. There were four work zones in each test.

For the car-following scenario, the factor was the leading vehicle's speed. The car-following scenario was designed as follows to reproduce the rapid deceleration at the beginning of work zones [3] and acceleration at the end of work zones. The driver of the following vehicle was required to follow the leading vehicle and keep it in the same lane for the whole test. The driver of the leading vehicle kept driving at a stable speed before accelerating or decelerating. The upper and lower bounds of the leading vehicle's speed were 40 km/h and 80 km/h; the gradient of speed changing was 20 km/h.

4. Indicators and Validation Methods

4.1. Driving Behavior Indicators. Free-flow indicators are spot speed, speed reduction, and speed reduction rate. The spots include the beginning of deceleration (BD) and the end of deceleration (ED). Speed reduction rate refers to the deceleration at the beginning of the work zone. The calculation method is shown in the following equation:

$$\mathrm{SRR} = \frac{v_{\mathrm{BD}} - v_{\mathrm{ED}}}{t_{\mathrm{D}}}, \tag{1}$$

where SRR is the speed reduction rate. v_{BD} is the speed at BD. v_{ED} is the speed at ED. t_{D} is the time for the vehicle to drive from BD to ED. The algorithm to identify the speed change point follows the method in Zhang's research [31].

Car-following indicators include car-following distance (average and standard deviations when speed is stable), headway (average and standard deviations when speed is stable), and reaction delay time. The standard deviation of the car-following distance represents the stability of car-following behavior. Define A as the acceleration/deceleration point of the leading vehicle and B as the acceleration/deceleration point of the following vehicle. The time interval between A and B is regarded as the reaction delay time.

4.2. Survival Analysis Method. The validation methods for nontime data are the Wilcoxon test and linear regression. In the meantime, a survival analysis method is proposed for time-event data such as reaction delay time. Survival analysis is a collection of statistical procedures for data analysis for which the outcome variable of interest is time until an event occurs [32]. According to the basic concept of survival analysis, the key elements of survival analysis include events, survival time t, the consequence of event (failure) δ, survivor functions of the event $S(t)$, and hazard function of the event $h(t)$.

In this study, an event refers to the following vehicle's response to the leading vehicle's speed change. Survival time is the reaction delay time. An event will be referred to as a failure if the following vehicle does not respond to the leading vehicle's speed change or the reaction delay time exceed the threshold. $S(t)$ represents the probability that the

survival time (reaction delay time) T exceeds the specified time t. Survivor function is a basic component of the survival analysis, and it obtains survival probabilities for different values of t, summarizing key information from survival data [32]. A nonparametric method called the Kaplan-Meier method is used in this study to estimate $S(t)$. The formula of the Kaplan–Meier method is shown in the following equations:

$$\widehat{S}\left(t_{(j)}\right) = \widehat{S}\left(t_{(j-1)}\right) \times \widehat{P}\left(T > t_{(j)} \,\middle|\, T \geq t_{(j)}\right). \tag{2}$$

Iterating equation (2), we have the following:

$$\widehat{S}\left(t_{(j)}\right) = \prod_{i=1}^{j} \widehat{P}\left(T > t_{(i)} \,\middle|\, T \geq t_{(j)}\right). \tag{3}$$

Data used for the Kaplan–Meier method is arranged in the ascending order of reaction delay time. $t_{(j)}$ is the j-th shortest reaction delay time. $\widehat{S}(t_{(j)})$ is the estimation of $S(t)$ at time $t_{(j)}$. $\widehat{P}(T > t_{(j)} \mid T \geq t_{(j)})$ is the probability that T is larger than $t_{(j)}$ when reaction delay T is larger or equal to $t_{(j)}$. $\widehat{S}(t_{(j)})$ is a step function.

Hazard function represents the instantaneous potential per unit time for the event to occur, under the premise that the following vehicle has not reacted to the change at time t. Instead of focusing on the continuity of the event, the hazard function focuses on the failure of the event. The hazard function is also called the conditional failure rate, and it is a regression model for survival analysis. The formula of hazard function $h(t)$ is shown in the following equation:

$$h(t) = \lim_{\Delta t \longrightarrow 0} \frac{P(t \leq T < t + \Delta t \mid T \geq t)}{\Delta t}. \tag{4}$$

The proportional hazards model (Cox model) is used to estimate $h(t)$. The formula of Cox model is shown in the following equation:

$$h\left(t_1\right) = h_0(t) \exp\left[\sum_{i=1}^{n} \beta_i X_i\right], \tag{5}$$

where X is the vector of independent variables. In most cases, X is a discrete variable. β_i is the coefficient of X_i. $h_0(t)$ is the nonparametric part of the Cox model, and it represents the baseline version of the hazard function.

For reaction delay time, the absolute validity is verified by comparing the difference of $S(t)$ between real-world driving and simulated driving. A chi-square test named Log-Rank test is used in this research. The relative validity is verified by comparing the coefficients of the Cox model.

5. Results

5.1. Free-Flow Validation

5.1.1. Spot Speed. The statistical result of spot speed is shown in Figures 3(a) and 3(b). For the beginning of deceleration, spot speeds in the simulation experiment are higher than in the field experiment (passing lane = 6.25 km/h, emergency lane = 3.63 km/h). Driving environments significantly affect spot speed when the passing lane is closed ($p = 0.0289$); driving environments do not affect spot speed when the emergency lane is closed ($p = 0.1397$). Regarding lane closure type as the independent variable (passing lane = 0, emergency lane = 1), linear regression results show that lane closure type has the same effect for real-world driving ($\beta = 5.91$, $p = 0.0164$) and simulated driving ($\beta = 3.29$, $p = 0.1370$). However, the coefficient for the simulation model is not significant.

For the end of deceleration, spot speeds in the simulation experiment are lower than in the field experiment (passing lane = 2.71 km/h, emergency lane = 2.79 km/h). However, driving environments have no significant effect on spot speed regardless of the lane closure type (passing lane: $p = 0.2209$; emergency lane: $p = 0.2290$). Linear regression results show that the lane closure type has the same effect for real-world driving ($\beta = -7.30$, $p = 0.0056$) and simulated driving ($\beta = -7.22$, $p = 0.0139$). Except for one spot (BD, passing lane), the result shows strong evidence of absolute validity.

5.1.2. Speed Reduction. The statistical result of speed reduction is shown in Figure 3(c). Speed reductions in the simulation experiment are higher than in the field experiment (passing lane = 8.96 km/h, emergency lane = 6.42 km/h). Driving environments have a significant effect on speed reduction (passing lane: $p = 0.0001$; emergency lane: $p = 0.0002$). Linear regression results show that the lane closure type has the same effect for real-world driving ($\beta = 1.39$, $p = 0.3270$) and simulated driving ($\beta = 3.93$, $p = 0.0807$). However, the coefficients of both driving environments are not significant. The result can be a sign of lacking simulator validity.

5.1.3. Speed Reduction Rate. The statistical result of the speed reduction rate is shown in Figure 3(d). Speed reduction rates in the simulation experiment are higher than in the field experiment (passing lane = 0.51 m/s^2, emergency lane = 0.29 m/s^2). Driving environments have a significant effect on the speed reduction rate (passing lane: $p < 0.0001$; emergency lane: $p < 0.0001$). Linear regression results show that the lane closure type has the same effect for real-world driving ($\beta = -0.0070$, $p = 0.8020$) and simulated driving ($\beta = -0.2298$, $p = 0.0196$). The coefficient for the real-world model is not significant. The result indicates that the speed reduction rate shows no simulator validity.

5.2. Car-Following Validation

5.2.1. Car-Following Distance. The statistical result of car-following distance is shown in Figures 4(a) and 4(b). For the average of the car-following distance, there is no significant difference between field experiment and simulation experiment (40 km/h: $p = 0.5318$; 60 km/h: $p = 0.6144$; 80 km/h: $p = 0.8845$). Leading vehicle's speed has the same effect for real-world driving ($\beta = 1.09$, $p < 0.0001$) and simulated driving ($\beta = 0.91$, $p < 0.0001$). The average of the car-following distance shows absolute validity.

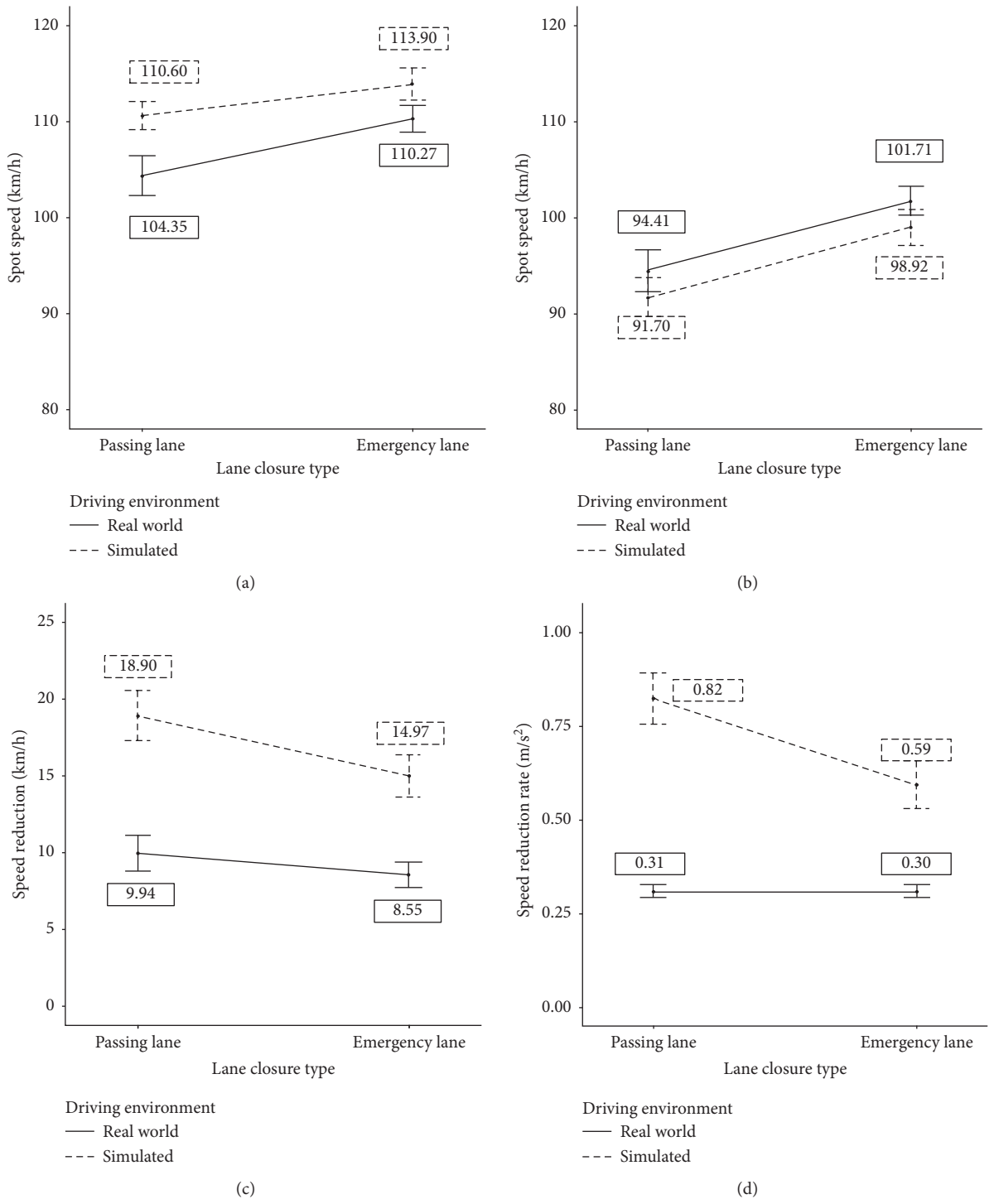

Figure 3: Statistic results of free-flow indicators: (a) spot speed at the beginning of deceleration; (b) spot speed at the end of deceleration; (c) speed reduction; (d) speed reduction rate. The error bars represent the standard deviation of indicators.

For the standard deviation of the car-following distance, the values in the simulation experiment are higher than in the field experiment (40 km/h: 0.39 m; 60 km/h: 1.79 m; 80 km/h: 3.93 m). Driving environments have a significant effect on the indicator (40 km/h: $p = 0.0009$; 60 km/h: $p = 0.0059$; 80 km/h: $p = 0.0136$). Leading vehicle's speed has the same effect for real-world driving ($\beta = 0.06$, $p = 0.0078$) and simulated driving ($\beta = 0.12$, $p < 0.0001$). The result shows the relative validity of the indicator.

5.2.2. Headway. The statistical result of the headway is shown in Figures 4(c) and 4(d). For the average of the headway, there is no significant difference between field

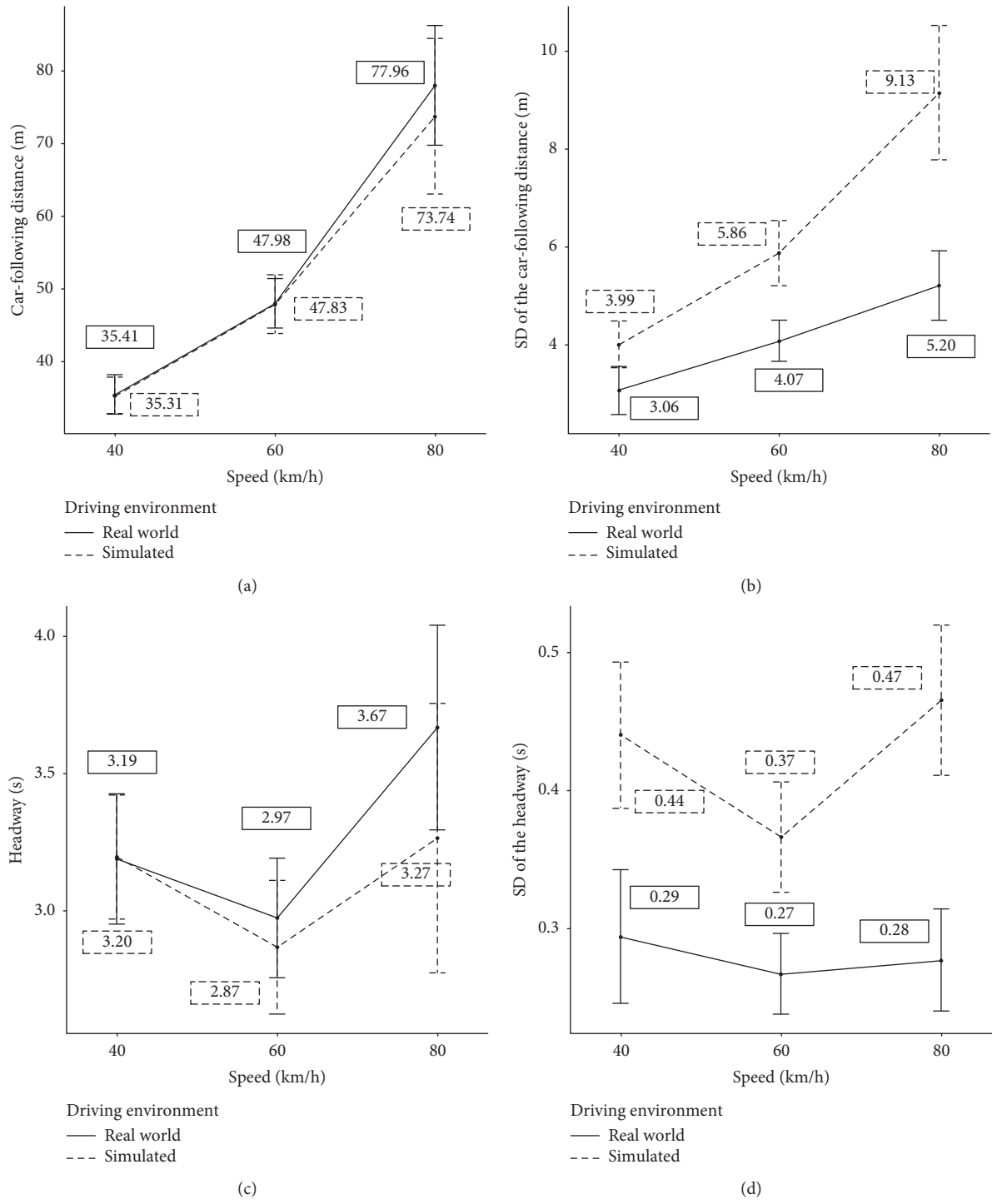

Figure 4: Statistic results of nontime car-following indicators: (a) car-following distance; (b) standard deviation of the car-following distance; (c) headway; (d) standard deviation of the headway. The error bars represent the standard deviation of indicators.

experiment and simulation experiment (40 km/h: $p = 0.8668$; 60 km/h: $p = 0.4406$; 80 km/h: $p = 0.7996$). Leading vehicle's speed affects headway in the same pattern. The average of the headway shows absolute validity.

For the standard deviation of the headway, the values in the simulation experiment are higher than in the field experiment (40 km/h: 0.15 s; 60 km/h: 0.10 s; 80 km/h: 0.19 s). Driving environments have a significant effect on the indicator (40 km/h: $p < 0.0001$; 60 km/h: $p = 0.0065$; 80 km/h: $p = 0.0049$). Figure 4(d) shows that the relationship between the leading vehicle's speed and the indicator is not linear. ANOVA result shows that the leading vehicle's speed ($p = 0.5987$) and the interaction ($p = 0.8927$) do not affect the indicator. Therefore the indicator shows no simulator validity.

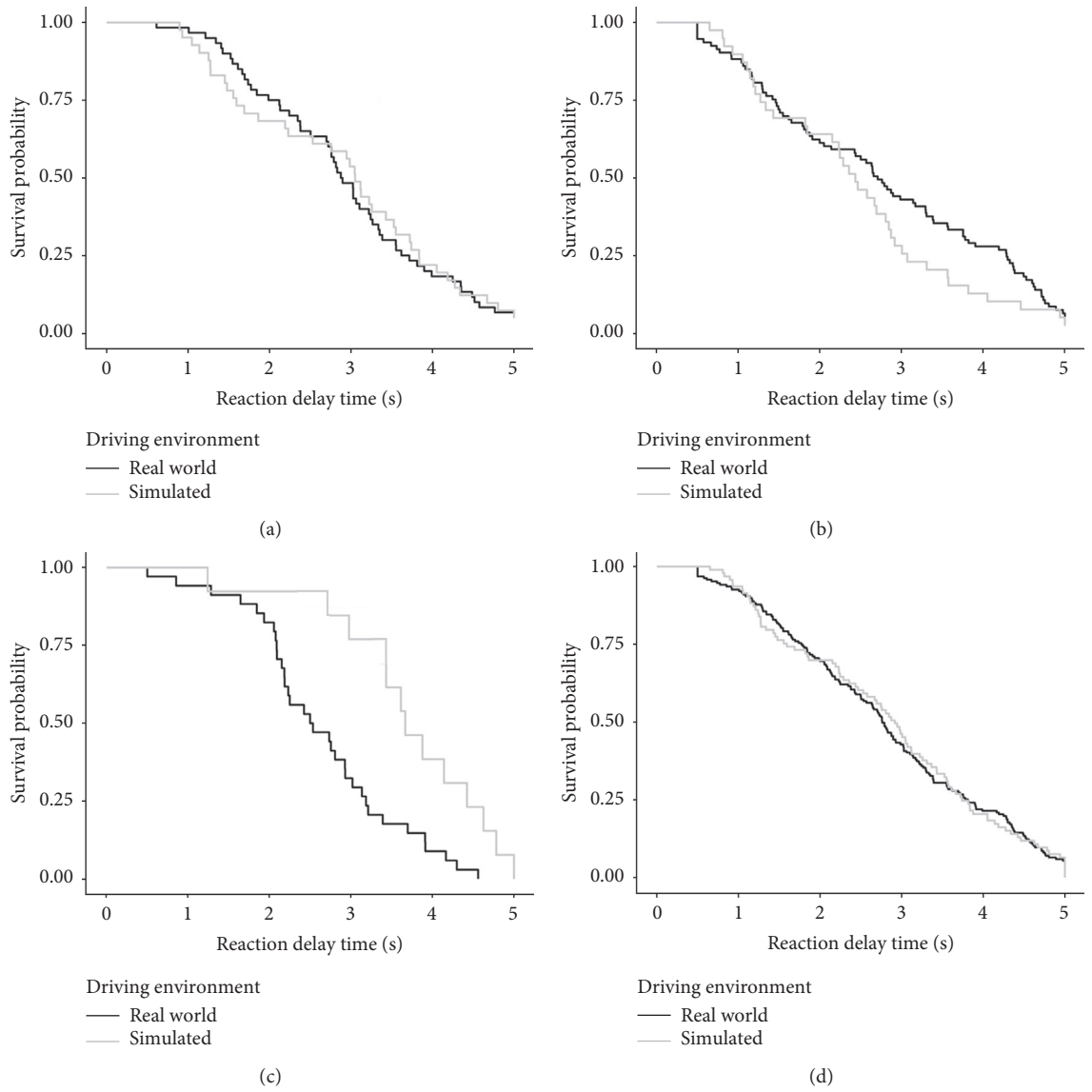

Figure 5: Results of reaction delay time. The leading vehicle's speed: (a) 40 km/h; (b) 60 km/h; (c) 80 km/h; (d) overall.

5.2.3. Reaction Delay Time. The statistical result of the reaction delay time is shown in Figure 5. The driving environment has no significant effect on the reaction delay time (overall: $p = 0.8000$; 40 km/h: $p = 0.9000$; 60 km/h: $p = 0.2000$; 80 km/h: $p = 0.0200$). Regarding leading vehicle's speed (1 for speed <50 km/h; 2 for speed <70 km/h; 3 for speed ≥70 km/h), leading vehicle's acceleration (0 for acceleration <0 m/s^2; 1 for acceleration ≥0 m/s^2), and car-following distance as the independent variable, the result of Cox model is shown in Table 1. The result shows that in the real-world model, the leading vehicle's acceleration and car-following distance affect reaction delay time significantly. The hazard ratio of the leading vehicle's acceleration is equal to 0.6014. It means when the leading vehicle is accelerating, the hazard function value of reaction delay decreases by 39.86% and the reaction delay time is longer. The hazard ratio of relative distance is equal to 0.9911. It means the hazard function value of reaction delay decreases by 8.55% for every 10 meters increase in the car-following distance. The reaction delay time is longer. In the simulation model, no independent variable affects the reaction delay time significantly. The survival analysis result shows that the reaction delay time has absolute validity.

6. Discussion and Conclusion

This research shows that for driving behavior in work zones, most of the indicators are valid. In the simulation experiment, the speed behavior in the free-flow scenario and the car-following behavior in the car-following scenario are consistent with which in the field experiment. For the speed behavior, vehicle dropping speed rapidly at the beginning of work zones, which is consistent with the study by Paolo and Sar [3]. Taylor et al. [33] pointed out that additional design features like temporary traffic barriers, reduced lane width, and crossover sections may influence vehicle speeds in work

Table 1: Result of the Cox model ($^{*}p < 0.05$).

Environment	Variable	Coefficient	Hazard ratio	p
Real-world	Leading vehicle's speed	0.1445	1.1554	0.2376
	Leading vehicle's acceleration	−0.5084	0.6014	$0.0014^{(*)}$
	Car-following distance	−0.0088	0.9911	$0.0046^{(*)}$
Simulation	Leading vehicle's speed	−0.0119	0.9881	0.9371
	Leading vehicle's acceleration	−0.0330	0.9674	0.8851
	Car-following distance	−0.0086	0.9913	0.1486

zones. For this research, lane closure is the main feature to affect vehicle speeds. In particular, the vehicle speed is lower and drops more rapidly when the passing lane is closed. As for the car-following behavior, car-following distance has a linear relationship with the leading vehicle's speed. Drivers prefer to keep a longer distance when the speed is higher. This behavior shows strong consistency between the field experiment and simulation experiment. The result of the Cox model indicates that reaction delay time is not a constant but an unfix value related to car-following distance and the leading vehicle's acceleration. This finding is proved by previous research studies [34–37]. Instead of treating the relationship between reaction delay time and independent variables as linear [34–36], this study uses a proportional hazards model to describe the probability distribution of reaction delay time. However, the model result for the simulation experiment is not significant. Perhaps further research is needed to find out the reason.

Past researches reported that driving simulators have relative validity, but do not exactly replicate the driving behavior of the real world [38]. Driving behaviors in the simulation experiment are more aggressive than in the field experiment. For example, vehicle speed in the simulation experiment is higher, and the deceleration at the beginning of the work zone is higher, too. These behaviors can conduct to a high probability of traffic crash [3]. Similar results were reported by previous researches [7, 14, 39–41]. The standard deviation of the car-following distance and standard deviation of the headway are higher in the simulation experiment, which means the car-following process is more stable in real-world driving. The safety of driving simulators may be an explanation of aggressive behaviors. Helland et al.[8, 15] reported that the aggressive driving behaviors in the simulation experiment can be explained by an enhanced perception of real danger in real-world driving compared to the simulator. Bella [41] conducted a similar conclusion.

Overall, the simulator validity of driving behaviors in work zones is verified. The speed behavior and car-following behavior in the simulation environment show a similar pattern as which in the real-world environment. A survival analysis method is proposed to replace the direct comparison method for simulator validity verification of the time-event data. Comparing to linear regression models, the proposed model can describe the probability distribution of reaction delay time. The result of this research can be theoretical support for simulation-based research, especially for driving behavior research in work zones. Consistent with previous researches, some behaviors are more aggressive in the simulation experiment, which needs further research to explain the mechanism.

This study deals with one critical issue of driving behavior research based on the driving simulator. The survival analysis method proposed in the study provides an effective way to verify time-event data. However, this study still has some limitations. First, in the free-flow validation study, the deceleration behavior is presented by spot speed. Although the spot speed can represent the deceleration behavior feature, it still should be noticed that this behavior is continuous. Thus in future research, the driving simulation validation based on speed profile should be discussed. Second, merging behavior or lane-changing behavior also is important in the work zone area [6, 28, 29]. The driving simulator validity of merging behavior will be an interesting topic. It should be mentioned that collecting merging behavior in real-world driving situations is a challenging job; advanced technology and method should be proposed to deal with it.

Data Availability

The data used to support the findings of this study are available upon request to Yanning Zhang, 1433932_zyn@tongji.edu.cn.

Conflicts of Interest

The authors declare that there are no conflicts of interest regarding the publication of this paper.

Acknowledgments

This research was financially supported by Technology Research and Development Plan of China State Construction Engineering Corporation (CSCEC-2017-Z-20) and the National Natural Science Foundation of China (71673201).

References

[1] R. A. Wynne, V. Beanland, and P. M. Salmon, "Systematic review of driving simulator validation studies," *Safety Science*, vol. 117, pp. 138–151, 2019.

[2] A. Z. Abdelmohsen and K. El-Rayes, "Optimizing the planning of highway work zones to maximize safety and mobility," *Journal of Management in Engineering*, vol. 34, no. 1, Article ID 04017048, 2018.

[3] P. Paolo and D. Sar, "Driving speed behaviour approaching road work zones on two-lane rural roads," *Procedia—Social and Behavioral Sciences*, vol. 53, pp. 672–681, 2012.

[4] Y. Qi, R. Srinivasan, H. Teng, and R. Baker, "Analysis of the frequency and severity of rear-end crashes in work zones," *Traffic Injury Prevention*, vol. 14, no. 1, pp. 61–72, 2013.

[5] C. Silverstein, J. Schorr, and S. H. Hamdar, "Work zones versus nonwork zones: risk factors leading to rear-end and sideswipe collisions," *Journal of Transportation Safety & Security*, vol. 8, no. 4, pp. 310–326, 2015.

[6] J. Weng and Q. Meng, "Rear-end crash potential estimation in the work zone merging areas," *Journal of Advanced Transportation*, vol. 48, no. 3, pp. 238–249, 2014.

[7] J. Törnros, "Driving behaviour in a real and a simulated road tunnel-a validation study," *Accident Analysis & Prevention*, vol. 30, no. 4, pp. 497–503, 1998.

[8] A. Helland, G. D. Jenssen, L.-E. Lervåg et al., "Evaluation of measures of impairment in real and simulated driving: results from a randomized, placebo-controlled study," *Traffic Injury Prevention*, vol. 17, no. 3, pp. 245–250, 2016.

[9] L. Meuleners and M. Fraser, "A validation study of driving errors using a driving simulator," *Transportation Research Part F: Traffic Psychology and Behaviour*, vol. 29, pp. 14–21, 2015.

[10] D. Hallvig, A. Anund, C. Fors et al., "Sleepy driving on the real road and in the simulator-a comparison," *Accident Analysis & Prevention*, vol. 50, pp. 44–50, 2013.

[11] S. T. Godley, T. J. Triggs, and B. N. Fildes, "Driving simulator validation for speed research," *Accident Analysis & Prevention*, vol. 34, no. 5, pp. 589–600, 2002.

[12] H. B. Ekanayake, P. Backlund, T. Ziemke, R. Ramberg, K. P. Hewagamage, and M. Lebram, "Comparing expert driving behavior in real world and simulator contexts," *International Journal of Computer Games Technology*, vol. 2013, pp. 1–14, 2013.

[13] A. Riener, "Simulating on-the-Road behavior using a driving simulator," in *Proceedings of Third International Conference on Advances in Computer-Human Interactions*, vol. 25–31, IEEE, Saint Maarten, Netherlands Antilles, March 2010.

[14] V. Branzi, L. Domenichini, and F. La Torre, "Drivers' speed behaviour in real and simulated urban roads—a validation study," *Transportation Research Part F: Traffic Psychology and Behaviour*, vol. 49, pp. 1–17, 2017.

[15] A. Helland, G. D. Jenssen, L. E. Lervag et al., "Comparison of driving simulator performance with real driving after alcohol intake: a randomised, single blind, placebo-controlled, cross-over trial," *Accident Analysis & Prevention*, vol. 53, pp. 9–16, 2013.

[16] D. Davenne, R. Lericollais, P. Sagaspe et al., "Reliability of simulator driving tool for evaluation of sleepiness, fatigue and driving performance," *Accident Analysis & Prevention*, vol. 45, pp. 677–682, 2012.

[17] A. Daurat, P. Sagaspe, L. Motak et al., "Lorazepam impairs highway driving performance more than heavy alcohol consumption," *Accident Analysis & Prevention*, vol. 60, pp. 31–34, 2013.

[18] M. Yun, J. Zhao, J. Zhao, X. Weng, and X. Yang, "Impact of in-vehicle navigation information on lane-change behavior in urban expressway diverge segments," *Accident Analysis & Prevention*, vol. 106, pp. 53–66, 2017.

[19] F. Galante, F. Bracco, C. Chiorri, L. Pariota, L. Biggiero, and G. N. Bifulco, "Erratum to "validity of mental workload measures in a driving simulation environment," *Journal of Advanced Transportation*, vol. 2018, Article ID 6713745, 1 pages, 2018.

[20] E. Blana, *Driving Simulator Validation Studies: A Literature Review*, Institute of Transport Studies University of Leeds, Leeds, UK, 1996.

[21] A. K. Debnath, R. Blackman, and N. Haworth, "A comparison of self-nominated and actual speeds in work zones," *Transportation Research Part F: Traffic Psychology and Behaviour*, vol. 35, pp. 213–222, 2015.

[22] L. Domenichini, F. La Torre, V. Branzi, and A. Nocentini, "Speed behaviour in work zone crossovers. A driving simulator study," *Accident Analysis & Prevention*, vol. 98, pp. 10–24, 2017.

[23] R. T. Steinbakk, P. Ulleberg, F. Sagberg, K. I. Fostervold, and K. I. Fostervold, "Analysing the influence of visible roadwork activity on drivers' speed choice at work zones using a video-based experiment," *Transportation Research Part F: Traffic Psychology and Behaviour*, vol. 44, pp. 53–62, 2017.

[24] H. Abdulsattar, A. Mostafizi, and H. Wang, "Surrogate safety assessment of work zone rear-end collisions in a connected vehicle environment: agent-based modeling framework," *Journal of Transportation Engineering, Part A: Systems*, vol. 144, no. 8, Article ID 04018038, 2018.

[25] Q. Meng and J. Weng, "Evaluation of rear-end crash risk at work zone using work zone traffic data," *Accident Analysis & Prevention*, vol. 43, no. 4, pp. 1291–1300, 2011.

[26] J. Weng, S. Xue, Y. Yang, X. Yan, and X. Qu, "In-depth analysis of drivers' merging behavior and rear-end crash risks in work zone merging areas," *Accident Analysis & Prevention*, vol. 77, pp. 51–61, 2015.

[27] T. W. P. Lochrane, H. Al-Deek, D. J. Dailey, and C. Krause, "Modeling driver behavior in work and nonwork zones," *Transportation Research Record: Journal of the Transportation Research Board*, vol. 2490, no. 1, pp. 116–126, 2015.

[28] J. Weng, G. Du, D. Li, and Y. Yu, "Time-varying mixed logit model for vehicle merging behavior in work zone merging areas," *Accident Analysis & Prevention*, vol. 117, pp. 328–339, 2018.

[29] J. Weng, G. Li, and Y. Yu, "Time-dependent drivers' merging behavior model in work zone merging areas," *Transportation Research Part C: Emerging Technologies*, vol. 80, pp. 409–422, 2017.

[30] K. Gao, H. Tu, L. Sun, N. N. Sze, Z. Song, and H. Shi, "Impacts of reduced visibility under hazy weather condition on collision risk and car-following behavior: implications for traffic control and management," *International Journal of Sustainable Transportation*, vol. 14, pp. 1–8, 2019.

[31] X. Zhang and H. B. Ghulam, "Estimation of driver reaction time from detailed vehicle trajectory data," in *Proceedings of the IASTED International Conference on Modelling, Simulation and Optimatization*, pp. 574–579, Montreal, Canada, January 2007.

[32] M. Carpenter, "Survival analysis: a self-learning text," *Technometrics*, vol. 39, no. 2, pp. 228-229, 1997.

[33] D. R. Taylor, S. Muthiah, B. T. Kulakowski, K. M. Kulakowski, and R. J. Mahoney, "Artificial neural network speed profile model for construction work zones on high-speed highways," *Journal of Transportation Engineering*, vol. 133, no. 3, pp. 198–204, 2007.

[34] A. Khodayari, A. Ghaffari, R. Kazemi, and R. Braunstingl, "A modified car-following model based on a neural network model of the human driver effects," *IEEE Transactions on Systems, Man, and Cybernetics—Part A: Systems and Humans*, vol. 42, no. 6, pp. 1440–1449, 2012.

[35] H. Ozaki, "Reaction and anticipation in the car-following behavior," in *Proceedings of the 13th International Symposium on Traffic and Transportation Theory*, vol. 49, no. 6, pp. 349–366, Lyon, France, July 1993.

[36] J. Zheng, K. Suzuki, and M. Fujita, "Car-following behavior with instantaneous driver-vehicle reaction delay: a neural-

network-based methodology," *Transportation Research Part C: Emerging Technologies*, vol. 36, pp. 339–351, 2013.

[37] R. Sipahi, F. M. Atay, and S.-I. Niculescu, "Stability of traffic flow behavior with distributed delays modeling the memory effects of the drivers," *SIAM Journal on Applied Mathematics*, vol. 68, no. 3, pp. 738–759, 2008.

[38] M. Matowicki and O. Přibyl, "Cross-study research on utility and validity of driving simulator for driver behavior analysis," *Acta Polytechnica CTU Proceedings*, vol. 12, p. 68, 2017.

[39] C. Llorca and H. Farah, "Passing behavior on two-lane roads in real and simulated environments," *Transportation Research Record: Journal of the Transportation Research Board*, vol. 2556, no. 1, pp. 29–38, 2016.

[40] D. Llopis-Castelló, F. J. Camacho-Torregrosa, J. Marín-Morales, A. M. Pérez-Zuriaga, A. García, and J. F. Dols, "Validation of a low-cost driving simulator based on continuous speed profiles," *Transportation Research Record: Journal of the Transportation Research Board*, vol. 2602, no. 1, pp. 104–114, 2016.

[41] F. Bella, "Driving simulator for speed research on two-lane rural roads," *Accident Analysis & Prevention*, vol. 40, no. 3, pp. 1078–1087, 2008.

Hindawi
Journal of Advanced Transportation
Volume 2020, Article ID 9461483, 11 pages
https://doi.org/10.1155/2020/9461483

Research Article

Evaluation of Section Speed Enforcement System Using Empirical Bayes Approach and Turning Point Analysis

Jisup Shim,[1] **Oh Hoon Kwon**,[2] **Shin Hyoung Park**,[2] **Sungbong Chung**,[3] **and Kitae Jang**[1]

[1]*Graduate School of Green Transportation, Korea Advanced Institute of Science and Technology, 291 Munji-ro, Yuseong-gu, Daejeon 34051, Republic of Korea*
[2]*Department of Transportation Engineering, Keimyung University, 1095 Dalgubeoldae-ro, Dalseo-gu, Daegu 42601, Republic of Korea*
[3]*Graduate School of Railroads, Seoul National University of Science and Technology, 138 Gongneung-gil, Nowon-gu, Seoul 01811, Republic of Korea*

Correspondence should be addressed to Kitae Jang; kitae.jang@kaist.ac.kr

Received 19 December 2019; Accepted 29 January 2020; Published 28 February 2020

Guest Editor: Inhi Kim

Speeding is a major risk factor for traffic-related injuries. As a countermeasure against speeding, automated speed enforcement systems (ASES) have been deployed in many countries. However, drivers' awareness of enforcement locations allows themselves to adjust vehicle speeds in the vicinity of the enforcement locations. This enforcement avoidance behavior leads to a criticism of the effectiveness of ASES, in which the system promotes abrupt changes in vehicle speed near enforcement locations, increasing crash risk as a side effect. To address this issue, the section speed enforcement system (SSES), which enforces overspeeding vehicles by their average travel speed over a section, has been devised. In this study, we evaluate traffic speed and safety data that were collected from sections with SSES on Korean expressways. The speed analysis showed that the vehicles reduced their speeds inside the enforcement section, and this reduction in speed variations across vehicles was also noticeable, signifying that the risk of traffic crash should be lower. In view of this, we have performed before and after comparative analysis using the empirical Bayes method with the comparison group. The outcomes estimate 43% reduction in crash occurrence after installation of SSES. Furthermore, turning point analysis confirmed that the reduction in crash occurrence ensued immediately after installation of SSES.

1. Introduction

Automated speed enforcement systems (ASES) have been introduced to mitigate speeding and are widely deployed in many countries. This type of enforcement system is installed to reduce traffic speed upstream of certain locations, especially where speeding-related crashes frequently occur. However, the local law often mandates informing drivers of enforcement locations, thereby drivers with that information naturally adjust their speeds to avoid enforcement: drivers tend to slow their speeds when approaching enforcement locations and return to their original speeds shortly after passing the locations [1–3]. This enforcement avoidance behavior leads to a criticism of the effectiveness of ASES, in which the system promotes abrupt changes in vehicle speed near enforcement locations, increasing crash risk as a side effect.

Hence, the section speed enforcement system (SSES) was devised to induce this enforcement avoidance behavior over elongated distance (i.e., make drivers maintain lower speeds over the section to avoid the enforcement) and to induce synchronicity of speed across vehicles over the roadway section. SSES employs a pair of cameras that are mounted at two ends of a section. The system records each vehicle's plate number and entry and exit times of the section and computes the vehicle's average travel speed over the section (Figure 1). If the average travel speed exceeds the speed limit of the section, the corresponding vehicle is automatically fined. This system was first adopted in the late 1990s, and many countries have implemented the system under various

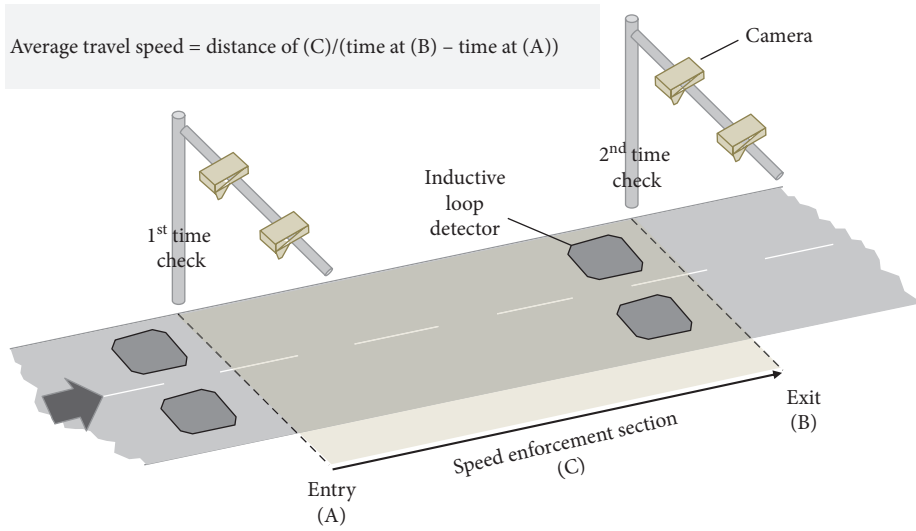

Figure 1: Illustration of section speed enforcement system.

names, including trajectory control in the Netherlands, average speed enforcement in the U.K., Tutor in Italy, point-to-point speed enforcement in Australia, and section control in the OECD [4].

Previous studies in various countries have reported that average speeds and crash occurrence diminished in roadway sections with SSES in operation [5–15]. Despite the consistency of outcomes across these studies, most of the studies were performed without comprehensive statistical analysis and, therefore, were unable to control for confounding factors and regression-to-the-mean [16]. Recently, some studies have employed the empirical Bayes (EB) approach to evaluate the safety benefits of SSES. Montella et al. [17] showed that total crashes after SSES installation diminished by 31.2%. Høye [2] performed meta-analysis based on outcomes across four different study sites and concluded with a summary effect of 20% reduction in crash occurrence. Using EB analysis, Høye [18] found 49% reduction in crashes with fatal and severe injuries after the installation of SSES. However, these studies did not investigate the specific effect of SSES on vehicle speed, the key antecedent for crash reduction as induced by SSES.

These studies evaluated crash occurrence using the EB method, which is widely used in controlling for confounding and regression-to-the-mean issues in the before-and-after study [19]. The EB method divides the entire period of evaluation into two separate time intervals, before and after the installation of the SSES. This is based on the assumption that the installation of SSES was the only intervention to reduce crash occurrence. However, if there were other unobserved factors, the inferences drawn from the EB could be invalid [20, 21]. Thus, it is necessary to evaluate the actual turning point in the trend of crash occurrence. An alternative method to validate or reinforce the causal inference from the EB method is turning point (TP) analysis, which can statistically identify changes in time-series data [22, 23].

In this context, we have collected vehicle speed and crash data from expressway sections where SSESs were in operation (Section 2). We examined speed profiles from loop detectors installed along three sections and compared outcomes with those from neighboring sections (Section 3). For all nine study sites, we performed EB and TP analyses to evaluate the effect of SSES on safety performance (Section 4). Finally, we explain the comprehensive effectiveness of SSES and discuss implications (Section 5).

2. Descriptions of Site and Data

2.1. Study Sites. In South Korea, ASES has since its inception in 1997 been deployed at more than 5,500 locations on roadways. In 2007, SSESs were first introduced on Korean expressways, and 48 SSESs were in operation over the network of Korean expressways as of 2018. Nine study sites, as listed in Table 1, were selected because SSESs were first installed at those sites such that sufficient observation of crash occurrence was possible.

2.2. Data for Speed Analysis. For cross-sectional speed analysis, three study sites out of nine were selected using the following criteria: (i) sites do not contain any attributes such as tunnels, bridges, or vertical and horizontal curves that may influence driving patterns compared to comparison sections and (ii) loop detector data were available. Only three study sites (ID 6, 8, and 9) were used for the speed analysis because we were unable to set up the comparison sections with the similar attributes and geometry in other six study sites. The selected sites comprise 36.6 lane-kilometers of 100 km/h zones and 28.2 lane-kilometers of 110 km/h zones. Loop detector data were obtained from all three study sites for all days (both weekdays and weekends). A year of speed data were obtained from each of the three study sites, while the SSESs were in effect.

2.3. Data for Safety Analysis. For the safety analysis, crash data and annual average daily traffic (AADT) were obtained

Table 1: Data for nine SSESs on Korean expressways.

Site ID	Route name (section ID)	Direction	Postkilometer		Distance	Speed limit	Attributes	Enforcement starting date	Analysis period*	AADT		No. of crashes	
			Start	End						Before	After	Before	After
1	Seohaean Expressway (I)	NB (to Seoul)	273.5	282.6	9.1 km	110 km/h	Bridge, rest area	01/15/2008	B/A 12-month	91,712	98,222	11	8
2	Seohaean Expressway (II)	SB (to Mokpo)	282.6	273.5	9.1 km	110 km/h	Bridge, rest area	01/15/2008	B/A 12-month	91,774	98,218	17	17
3	Pyeongtaek-Jecheon Expressway	WB (to Pyeongtaek)	11.2	5.5	5.7 km	100 km/h		12/24/2008	B/A 12-month	78,736	82,655	5	5
4	Yeongdong Expressway (I)	EB (to Kangnung)	168.5	176.0	7.5 km	100 km/h	Tunnel	12/26/2007	B/A 12-month	21,581	20,949	21	11
5	Yeongdong Expressway (II)	WB (to Incheon)	172.2	161.8	10.4 km	100 km/h	Tunnel	10/16/2009	B/A 33-month	58,263	59,429	54	25
6	Jungbunaeruk Expressway	(To Masan)	223.9	209.8	14.1 km	110 km/h		12/20/2008	B/A 24-month	19,051	19,612	16	17
7	Jungang Expressway	SB (to Busan)	242.8	237.2	5.6 km	100 km/h	Tunnel	02/21/2008	B/A 12-month	33,894	33,828	3	3
8	Daejeon–Tongyeong Expressway	SB (to Tongyeong)	85.5	78.0	7.5 km	100 km/h		01/01/2009	B/A 24-month	39,592	42,402	26	9
9	Yeongdong Expressway (III)	EB (to Kangnung)	215.2	226.0	10.8 km	100 km/h		12/07/2011	B/A 24-month	81,230	84,885	19	8

*B/A 12-month means 12-month analysis period before-and-after installation (total 24 months).

for the periods before and after SSES installation. The number of crashes is used in the EB method and TPA; the AADT data were used to construct a prediction model for the safety performance function (SPF), which is input to the EB method. In the safety analysis, we analyzed crash data for all nine study sites. A longitudinal before-and-after analysis was conducted in the safety analysis. SSESs for all nine study sites went into effect prior to 2011, and, therefore, long-duration observation of crash occurrence was possible. The study period is set from 2007 to 2013 because there were changes in geometry of some of our study sites after 2014, which may have affected crash occurrence. Details on each study site are furnished in Table 1.

3. Speed Profile Analysis

3.1. Cross-Sectional Analysis with Comparison Sections. Two groups were used for the comparative analysis. One group is the enforcement sections shown in Table 1, and the other group is a comparison section where the site attributes are almost identical to the enforcement sections except for the existence of enforcement. The comparison sections are selected as upstream and downstream sections surrounding the enforcement section because the same groups of drivers traveling in those sections and geometric and local characteristics are similar. Figure 2 illustrates the layouts of the enforcement and comparison sections in all three selected study sites. The sections are two-lanes along their length except auxiliary lanes in the vicinity of merging and diverging areas. To this end, only traffic data that were collected from mainline areas (i.e., lanes 1 and 2) are used in this study. In the case of the Yeongdong Expressway (ID 9), only one comparison section was used, unlike other sites. This is because the enforcement section is at the end of the Yeongdong Expressway, and, therefore, the downstream section was too short to be used as a comparison section.

3.2. Data Filtering. To enhance the comparability and to unveil changes in driving patterns along the sections, the collected loop detector data were filtered to include data only from unconstrained, free-flow travel conditions when drivers could travel at their desired speeds, and thus overspeeding could occur. In Figure 3, the fundamental diagram illustrates a relation between traffic flow and density. Although scatter plots of flow vs. density data could form various shapes such as reverse lambda, parabolic, and triangular, the diagram in any shape exhibits two distinguished regimes–free-flow and congested. On the left-side branch, the traffic is in the free-flow regime where speed remains at free-flow without any constraint, and the right-side branch presents congested regime where the flow is constrained.

Figure 3 displays scatter plots of flow versus density at one of the detectors among the study sites. Firstly, abnormal loop detector data were filtered out by using daily statistics algorithm by Chen [24]. To ensure that the values were from traffic that was not constrained, we secondly filtered out the data from periods when vehicular interactions occurred and thus obscured overspeeding patterns: data points associated with densities lower than 10 vehicles/km/lane, which correspond to approximately half of the density at capacity, were used in the present study [25]. The analysis of speed profile is intended to inspect changes in vehicle speeds solely due to the installation of SSES. If the data contain traffic conditions that constrained vehicle speeds (i.e., congestion), it is hard to distinguish whether the speed changes, if any, was due to the changes in drivers' speed-taking behavior that was induced by effect of SSES.

3.3. Effects of SSES on Vehicle Speed. To compare speed profiles between enforcement and comparison sections, descriptive summary statistics of each section were evaluated using a box-and-whisker plot (Figure 4). Bottom and top of box indicate first and third quartiles, respectively. Horizontal line in the middle of the box is the median. Top and bottom ends of the vertical line traversing the box are boundaries of data, excluding outliers. It is notable that boxes from the enforcement section are narrower and lower than those from the comparison sections. This means that vehicles traversed the enforcement section under more stable condition, as can be inferred from the lower mean and variance of speed in the enforcement section.

As shown in Figure 4, the three study sites showed the same speed analysis results that the average speed was lower than the speed limit throughout the enforcement section. One of the possible negative sides of SSES is the higher variance of speed at the beginning and the end of the enforcement section. Because SSES enforces vehicles by the average speed, there could be vehicles that move at high speeds in the beginning and lowered the speeds in the end or vice versa. However, this phenomenon was not observed in this study.

T-test and F-test were performed to statistically validate the differences of mean and variance between enforcement and comparison sections. The test results confirm that the differences are statistically significant at 5% significance level, and the speed variance is reduced not only along the enforcement section but also across vehicles.

4. Safety Analysis

In this section, we evaluate the effect of installing SSES on traffic safety. The EB method is applied to compare changes in crash occurrence before and after SSES installation (Section 4.1). Then, a comprehensive inference was drawn by applying meta-analysis to the outcome of the EB method at each site (Section 4.2). To validate that, if they exist, changes in crash occurrence happened prior to and near the installation of SSES, we performed TPA to statistically identify turning points in time-series crash occurrences (Section 4.3) and to compare turning points with the installation of SSES (Section 4.4).

4.1. EB Method with Comparison Group. In this study, the EB method with a comparison group was adapted to compare the safety performance before and after installation of SSESs. Because it employs a crash prediction model, the EB method can adjust regression-to-the-mean (RTM) bias [19] and can

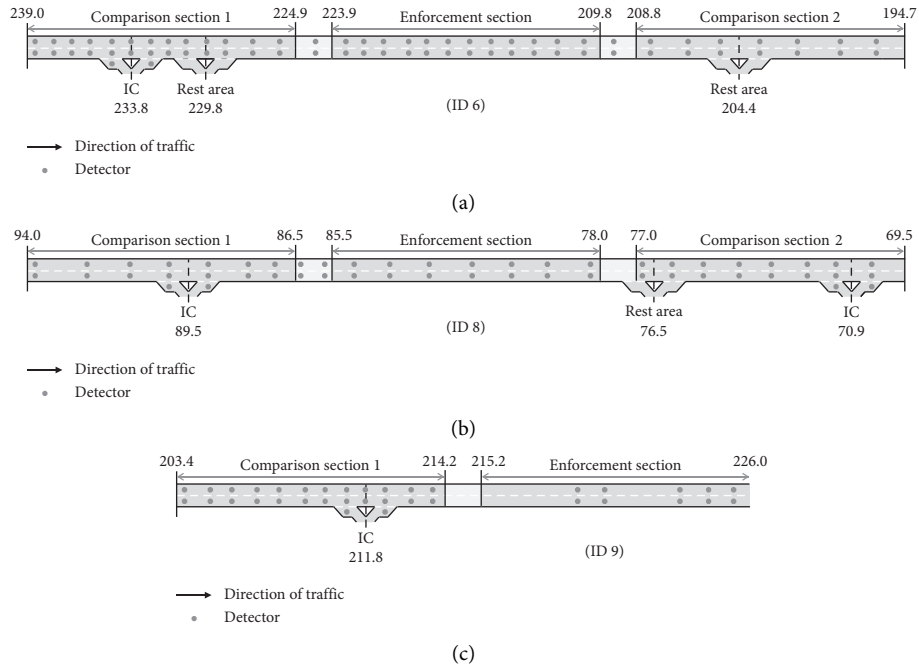

FIGURE 2: Illustrations of layouts of study and control sections: (a) Jungbunaeruk, (b) Daejeon-Tongyeong, and (c) Yeongdong III (not to scale).

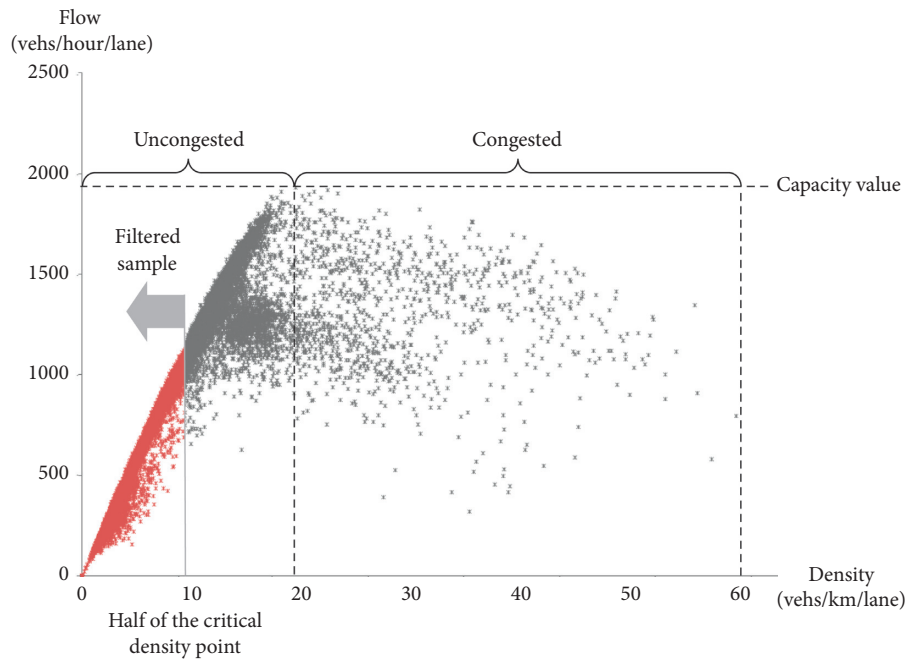

FIGURE 3: Fundamental diagram of a loop detector at a study site.

address changes in traffic volume. However, the effect of general changes (i.e., temporal trend) in traffic crashes from the before to after periods still exists. To adjust this issue, the comparison group method is combined for estimating the predicted number of crashes.

Generally, the treatment group is composed of the limited number of samples, and it can hardly incorporate the effect of temporal trend in crash occurrences. Meanwhile, the comparison group can affect the term, $\widehat{m}_i^b$, the predicted number of crashes that is estimated based on the information on the crash occurrences in the entire area as well as the SSES area. Hence, the EB method with the comparison group can account for the effect of temporal trend in crash occurrences in the area.

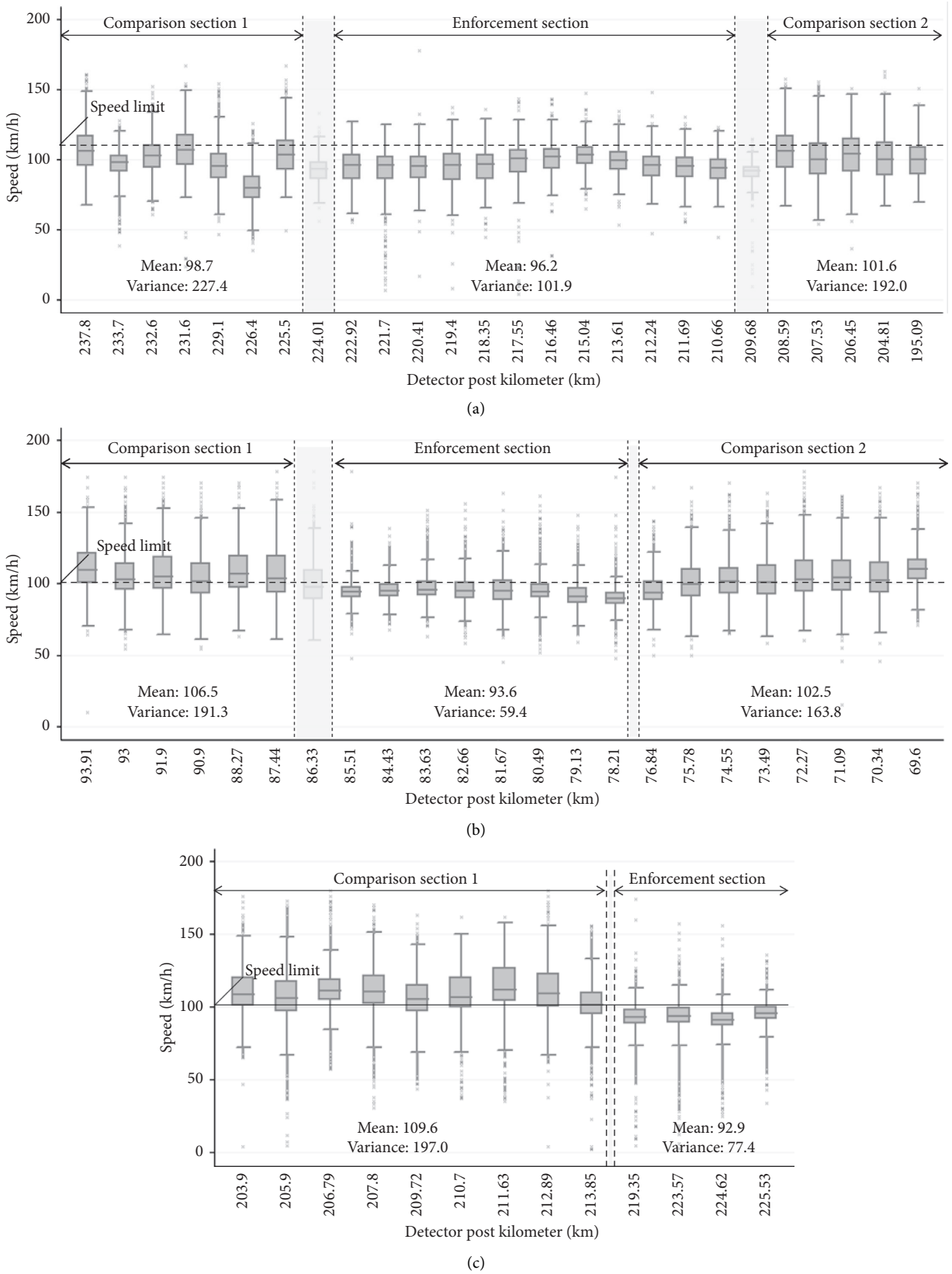

Figure 4: Speed distributions at loop detectors of three different study sites: (a) Jungbunaeruk Expressway (ID 6), (b) Daejeon–Tongyeong Expressway (ID 8), and (c) Yongdong Expressway (ID 9).

The effectiveness (e_i) is measured by comparing the numbers of crashes at a site i before and after the installation of SSES:

$$e_i = \frac{x_i^a}{\widehat{m}_i^b \cdot \left(C_i^a / C_i^b\right)}, \tag{1}$$

where x_i^a is the observed number of crash occurrences in the period after SSES went in effect and $\widehat{m}_i^b$ is the expected number of crashes that would have occurred in the same period if SSES had not been implemented. To consider the trend in crash occurrence that would have been expected regardless of SSES (i.e., changes that naturally occur), we adjusted $\widehat{m}_i^b$ by C^a/C^b. The numerator, C^a, is the observed number of crashes in the control group in the period after installing SSES, and C^b is the observed number of crashes in the control group in the period before installing SSES. All variables to compute e_i are observable, except for $\widehat{m}_i^b$.

$\widehat{m}_i^b$ is estimated as the weighted sum of the predicted number of crashes in the before-period (P_i^b) and the observed number of crashes in the before-period (x_i^b):

$$\widehat{m}_i^b = w^b \cdot P_i^b + \left(1 - w^b\right) \cdot x_i^b, \tag{2}$$

where the weight, w^b, is derived based on estimated outcomes of the prediction model:

$$w^b = \frac{1}{\left(1 + \alpha \cdot P_i^b\right)}. \tag{3}$$

In general, the prediction model is estimated using a negative binomial (NB) regression; the parameters in equation (3) are the estimated outcomes: α is the overdispersion parameter, and P_i^b is the expected number of crashes estimated from the prediction model. For the crash prediction model, we have used the crash data for four years (2007–2010) and the annual average daily traffic data from 1,128 roadway segments of Korean expressways. In this study, we adopted the prediction model that was previously specified for the same coverage of Korean expressways in Shim et al. [3]. The prediction model is crashes/year $= l \times \exp(0.225 + 1.45 * 10^{-5} * \text{AADT})$, where l is the length of the section and AADT is the average annual daily traffic for the section. The estimated overdispersion parameter k is 0.183.

4.2. Results: EB Method and Meta-Analysis. The descriptive statistics of crash data are summarized in Table 2. Also, the results of the EB analysis are summarized in Table 3 and show that crash occurrence diminished at eight out of the nine study sites. However, the reductions were statistically significant only at three sites (ID 5, 8, and 9) due to lack of crash occurrence, and the outcomes were found to vary widely across sites. This phenomenon often arises because crash occurrences are by nature rare events, and, therefore, only a few crashes were observed during the observation period. For more comprehensive evaluation of the overall effect of SSES, we performed meta-analysis with the outcomes from all nine study sites. Meta-analysis is a statistical approach that combines outcomes from multiple study sites. This study adapted a fixed-effect meta-analysis by Fleiss et al. [26] that combines the effectiveness (e_i) across the sites by assigning the inverse of variance as a weight factor. As a result, an overall index of effectiveness ($\widehat{E}$) and confidence interval were derived as follows:

$$\widehat{E} = \exp\left[\frac{\sum_{i=1}^n f_i * \ln(e_i)}{\sum_{i=1}^n f_i}\right],$$
$$95\%\ \text{C.I.} = \exp\left[\frac{\sum_{i=1}^n f_i * \ln(e_i)}{\sum_{i=1}^n f_i} \pm \frac{1.96}{\sqrt{\sum_{i=1}^n f_i}}\right], \tag{4}$$

where the weight factor (f_i) is estimated based on the variance of e_i and s_i^2 at each site.

$$f_i = \frac{1}{s_i^2}, \quad \text{where } s_i^2 = \frac{1}{m_i^a} + \frac{1}{\widehat{m}_i^b} + \frac{1}{C^a} + \frac{1}{C^b}. \tag{5}$$

As a result, $\widehat{E}$ is 0.57, meaning that the number of crashes decreased by 43% for all study sites. The confidence interval of $\widehat{E}$ ranges from 0.44 to 0.73—the upper level is well below one—implying that the overall effect of SSES reduces crash occurrences at 95% confidence level.

4.3. Turning Point Analysis. We employed statistical examination using TPA to determine whether turning points in crash occurrence were temporally consistent with the installation of SSESs [22]. TPA was performed based on the assumption that crash occurrences in n time intervals, $\{x_i : i = 1, \ldots, m, \ldots, n\}$, during our observation period were from two different distributions before and after an unknown turning point at m ($m < n$). The Poisson distribution was naturally the choice because crash occurrences are rare and discrete events over time. However, overdispersion (i.e., variance greater than the mean) often estimate plagues using the Poisson regression, which was also the case for our study.

This study generalized the application of TPA by using negative binomial (NB) distributions, which have two parameters in the probability mass function (PMF). Therefore, instead of computing Maximum a Posteriori, we used the Newton–Raphson method to search for the turning point, m, where two NB distributions are most likely to be different from a statistical perspective.

The two NB distributions (p_0 and p_1) with a conjugate prior distribution as a beta distribution have shaper parameters (α_0, α_1) and rater parameters (b_0, b_1), and turning point m is equally likely over time. Thus, $p_0 \sim \text{Beta}(\alpha_0, \beta_0)$, $p_1 \sim \text{Beta}(\alpha_1, \beta_1)$, and $m \sim \text{Uniform}(0, \text{n})$. We set $\alpha_0 = \alpha_1 = \overline{x}_i$ (mean of x_i) and $\beta_0 = \beta_1 = 1$. The posterior function, $f(m, p_0, p_1 \mid x_{1:n})$, the likelihood function, $L(x_{1:n} \mid m, p_0, p_1)$, and the prior function, $f(m, p_0, p_1)$, are as follows:

Table 2: Descriptive statistics for crashes in both the treated group and the comparison group.

Group	Period	Mean	Standard deviation	Min	Max
Treated group (SSES)	Before	19.1	15.03	3	54
	After	11.4	6.97	3	25
Comparison group	Before	22.0	14.66	10	47
	After	22.6	11.19	13	40

Table 3: Effectiveness of SSES at all study sites.

Site ID	Route name (section ID)	Index of effectiveness (e_i)	95% confidence interval	Standard error	Effectiveness ($1 - e_i$) (%)
1	Seohaean Expressway (I)	0.58	[0.24; 1.38]	0.10	42
2	Seohaean Expressway (II)	0.96	[0.50; 1.86]	0.06	4
3	Pyeongtaek–-Jecheon Expressway	0.93	[0.29; 3.00]	0.19	7
4	Yeongdong Expressway (I)	0.52	[0.24; 1.10]	0.07	48
5	Yeongdong Expressway (II)	**0.43**	**[0.26; 0.70]**	**0.03**	**57**
6	Jungbunaeruk Expressway	1.01	[0.51; 1.98]	0.06	−1
7	Jungang Expressway	0.54	[0.13; 2.18]	0.29	46
8	Daejeon–Tongyeong Expressway	**0.37**	**[0.17; 0.81]**	**0.07**	**63**
9	Yeongdong Expressway (III)	**0.35**	**[0.16; 0.73]**	**0.08**	**65**
Overall index of effectiveness ($\widehat{E}$)		**0.57** [0.44; 0.73]			**43**

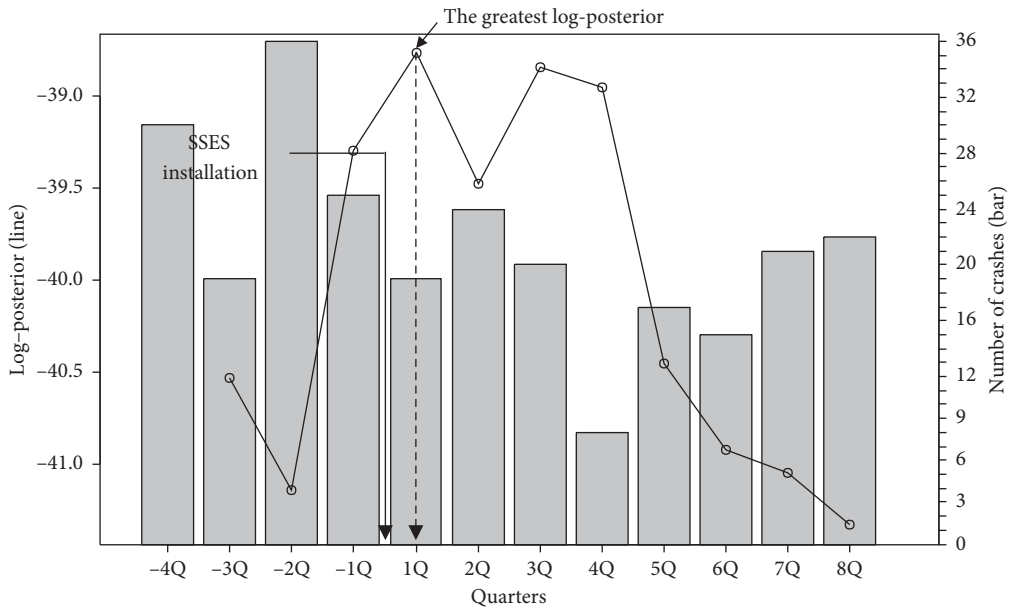

Figure 5: Comparison between time of SSES installation and greatest log-posterior values.

$$
\begin{aligned}
&f\left(m, p_0, p_1 \mid x_{1:\,n}\right) \propto L\left(x_{1:\,n} \mid m p_0, p_1\right) \cdot f\left(m,\ p_0, p_1\right) \\
&= L\left(m,\ p_0, p_1\right) \cdot f\left(m,\ p_0, p_1\right) \\
&\prod_{i=1}^{m} \binom{x_i + r_0 - 1}{x_i} p_0^{x_i} \left(1 - p_0\right)^{r_0} \cdot \prod_{i=m+1}^{n} \binom{x_i + r_1 - 1}{x_i} p_1^{x_i} \left(1 - p_1\right)^{r_1} \cdot \\
&\frac{\Gamma\left(\alpha_0 + \beta_0\right)}{\Gamma\left(\alpha_0\right) \cdot \Gamma\left(\beta_0\right)}\, p_0^{\alpha_0 - 1} \left(1 - p_0\right)^{\beta_0 - 1} \cdot \frac{\Gamma\left(\alpha_1 + \beta_1\right)}{\Gamma\left(\alpha_1\right) \cdot \Gamma\left(\beta_1\right)} p_1^{\alpha_1 - 1} \left(1 - p_1\right)^{\beta_1 - 1} \cdot \frac{1}{n}.
\end{aligned}
\tag{6}
$$

We have four unknown parameters r_0, r_1, p_0, and p_1. Starting from $m = 1$, we solve equations (8) and (9) using the Newton–Raphson method (for r_0 and r_1). Outcomes from these equations were then input to solve equations (10) and (11) (for p_0 and p_1). Using those four parameters, we updated $\ln(f)$. We iterate this procedure until $m = n$, and we search for m that will maximize $\ln(f)$.

$$\begin{aligned}\ln(f) = &\sum_{x=1}^{m} \ln\left(\Gamma\left(x_i + r_0\right)\right) - \sum_{i=1}^{m} \ln\left(\Gamma\left(x_i + 1\right)\right) - m \cdot \ln\left(\Gamma\left(r_0\right)\right) \\ &+ \sum_{i=m+1}^{n} \ln\left(\Gamma\left(x_i + r_1\right)\right) - \sum_{i=m+1}^{n} \ln\left(\Gamma\left(x_i + 1\right)\right) - (n-m) \cdot \ln\left(\Gamma\left(r_1\right)\right) \\ &+ \left(\alpha_0 - 1 + \sum_{i=1}^{m} x_1\right) \cdot \ln\left(p_0\right) + \left(m \cdot r_0 + \beta_0 - 1\right) \cdot \ln\left(1 - p_0\right) \\ &+ \left(\alpha_1 - 1 + \sum_{i=m+1}^{m} x_i\right) \cdot \ln\left(p_1\right) + \left((n-m) \cdot r_1 + \beta_{01} - 1\right) \cdot \ln\left(1 - p_1\right),\end{aligned} \tag{7}$$

$$\frac{\partial \ln(f)}{\partial r_0} = \sum_{i=1}^{m} \varphi\left(x_i + r_0\right) - m\varphi\left(r_0\right) + m \cdot \ln\left(1 - p_0\right) = 0, \tag{8}$$

$$\frac{\partial \ln(f)}{\partial r_1} = \sum_{i=m+1}^{n} \varphi\left(x_i + r_1\right) - (n-m) \cdot \varphi\left(r_1\right) + (n-m) \cdot \ln\left(1 - p_1\right) = 0, \tag{9}$$

$$\frac{\partial \ln(f)}{\partial p_0} = \frac{\alpha_0 + \sum_{i=1}^{m} x_i - 1}{\alpha_0 + \beta_0 + \sum_{i=1}^{m} x_i + r_0\, m - 2} = 0, \tag{10}$$

$$\frac{\partial \ln(f)}{\partial p_1} = \frac{\alpha_1 + \sum_{i=m+1}^{n} x_i - 1}{\alpha_1 + \beta_1 + \sum_{i=m+1}^{n} x_i + r_1\,(n-m) - 2} = 0. \tag{11}$$

4.4. Results: Turning Point Analysis. We have aggregated the outcomes from nine study sites to draw a more general inference about the temporal trend of crash occurrence as well as to compensate for the insufficient observation of crash occurrences. To this end, we counted crash occurrences in a quarter-year time interval and aggregated across sites with respect to the installation of SSESs. The x-axis in Figure 5 indicates the number of quarters relative to the time of SSES installation—the installation of SSESs is 0 and the month with SSES installed is not included in the analysis. Log-posteriori values are shown as a line along the primary y-axis, while the numbers of crashes are displayed as a bar graph along the secondary y-axis. Log-posteriori value continuously increases until 0 (i.e., installation of SSES) and gradually diminishes thereafter. Note how the maximum log-posteriori turning point temporally matches the installation of SSESs. This means that the most prominent statistical change in crash occurrence was observed after installation of SSES.

Figure 6 shows probability mass functions (PMF) of the two NB distributions—dividing the time period with respect to the turning point (i.e., before and after installation). The grey and black distributions are NB distributions before and after the turning point, respectively. The after-distribution is skewed to the left compared to the before-distribution, meaning that the probability of crash occurrence after the turning point is relatively low. In other words, the reduction in crash occurrence was statistically significant immediately after installation of SSES.

5. Conclusion

SSESs have been introduced to control speeding over roadway stretches and to remedy the enforcement avoidance behavior prevalent for ASES, including momentary slowing only at locations of enforcement [3]. In this study, based on data from nine Korean expressway sections where SSESs had been installed, we evaluate the effectiveness of SSES on reducing vehicle speed and crash occurrence. Speed distributions were constructed using vehicle speed data from loop detectors along the monitored expressway stretches. The distributions showed that both the mean and the variance of the speeds were lower inside the enforcement sections than in neighboring sections; especially, reductions in variances were pronounced. This implies that SSES can reduce vehicle speeds

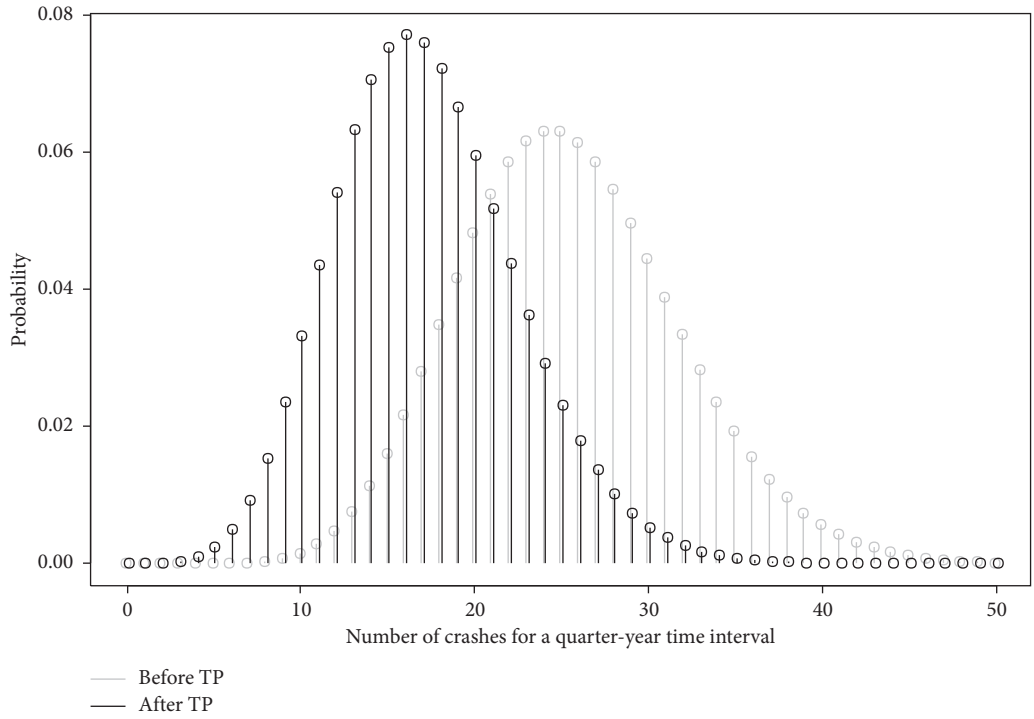

Figure 6: Probability mass functions of NB distributions before and after installation of SSES.

as well as speed variation across enforcement sections and, consequently, lowers the risk of crash occurrence.

To validate this conjecture, we performed in-depth analysis of crash data. First, we divided our observations into two time periods—before and after—and compared crash occurrences between the two time periods using the EB method. The outcomes indicated that crash occurrence decreased in eight of the nine study sites, and an overall 43% reduction was estimated when we combined the outcomes across sites using meta-analysis. TPA outcomes supplemented these findings and ensured that reductions in crash occurrence corresponded temporally to (i.e., happened shortly after) the installation of SSESs.

There are limitations when interpreting the results of safety analysis at each individual site because the effectiveness index may be affected by unobserved factors that reside in particular study sites. This becomes more pronounced at the sites with small samples. To compensate for this phenomenon, we performed meta-analysis, which allowed the evaluation of the comprehensive effect of SSES on the crash occurrences.

The findings from these analyses of traffic speed and safety suggest that SSES can stabilize traffic flow (reduce mean and variance of speeds) where it is installed and thereby have a positive effect on traffic safety. We reached this conclusion because averages and variations of vehicle speed are proportional to risk of crash [27–33], though observations of traffic flow and safety were performed separately. This separate observation was inevitable because observation of traffic crashes, which are rare as statistical events, generally requires substantial time. Because this study is based purely on observations, it is difficult to draw causal relationship between traffic conditions and safety effects. Furthermore, the period of data collection was limited. Studies based on long-term observations still remain a challenge for future research.

The present study demonstrated that SSES could stabilize vehicle speed over long distances because drivers tend naturally to avoid enforcement and, therefore, comply with the speed limit over monitored sections. It is evident from these observations that, unlike ASES, there were no momentary and abrupt speed reductions along sections with SSES. Furthermore, the 43% reduction in crash occurrence in the sections with SSES is 5.6 times greater than the reduction with ASES, which showed only a 7.6% reduction, as reported in a previous study also performed with data from Korean expressways [3]. It is manifested that SSES has more favorable effects on traffic safety and constant vehicle speed than does conventional ASES.

Data Availability

The speed and safety data of Korean Expressway used to support the findings of this study were supplied by Korea Expressway Corporation (http://www.ex.co.kr/). Requests for access to these data should be made to the data portal of Korea Expressway Corporation (http://data.ex.co.kr/).

Conflicts of Interest

The authors declare that they have no conflicts of interest.

Acknowledgments

This research was supported by a grant (19RDRP-B076268-06) from R&D Program funded by Ministry of Land, Infrastructure and Transport of Korean Government.

References

[1] E. De Pauw, S. Daniels, T. Brijs, E. Hermans, and G. Wets, "Automated section speed control on motorways: an evaluation of the effect on driving speed," *Accident Analysis & Prevention*, vol. 73, pp. 313–322, 2014.

[2] A. Høye, "Speed cameras, section control, and kangaroo jumps-a meta-analysis," *Accident Analysis and Prevention*, vol. 73, pp. 200–208, 2014.

[3] J. Shim, S. H. Park, S. Chung, and K. Jang, "Enforcement avoidance behavior near automated speed enforcement areas in Korean expressways," *Accident Analysis and Prevention*, vol. 80, 2015.

[4] ETSC, "Section control: towards a more efficient and better accepted enforcement of speed limits?," vol. 5ETSC Speed Fact Sheet, Etterbeek, Belgium, , 2009.

[5] M. H. Cameron, "Development of strategies for best practice in speed enforcement in western Australia," Supplementary Report, Monash University Accident Research Centre, Melbourne, Australia, 2008.

[6] K. Charlesworth, "The effect of average speed enforcement on driver behaviour," in *Proceedings of the Road Transport Information and Control-RTIC 2008 and ITS United Kingdom Members' Conference, IET*, Manchester, UK, May 2008.

[7] C. Stefan and M. Winkelbauer, *Section Control–Automatic Speed Enforcement in the Kaisermühlen Tunnel (Vienna, A22 Motorway)*, Kuratorium für Verkehrssicherheit, Vienna, Austria, 2006.

[8] H. Stoelhorst, "Reduced speed limits for local air quality and traffic efficiency," in *Proceedings of the European Congress and Exhibition on Intelligent Transport Systems and Services*, Geneva, Switzerland, June 2008.

[9] V. Punzo and E. Cascetta, "Impact on vehicle speeds and pollutant emissions of the fully automated section speed control scheme safety tutor on the naples urban motorway," in *Proceedings of the Paper Presented at the SIDT - Scientific Seminar - External Costs of Transport Systems: Theory and Applications*, Rome, Italy, 2010.

[10] E. Cascetta and V. Punzo, "Impact on vehicle speeds and pollutant emissions of an automated section speed enforcement system on the Naples urban motorway," in *Proceedings of the Transportation Research Board 2011 Annual Meeting*, vol. 17, Washington, DC, USA, January 2011.

[11] A. Montella, L. L. Imbriani, V. Marzano, and F. Mauriello, "Effects on speed and safety of point-to-point speed enforcement systems: evaluation on the urban motorway A56 Tangenziale di Napoli," *Accident Analysis & Prevention*, vol. 75, pp. 164–178, 2015.

[12] A. Montella, V. Punzo, S. Chiaradonna, F. Mauriello, and M. Montanino, "Point-to-point speed enforcement systems: speed limits design criteria and analysis of drivers' compliance," *Transportation Research Part C: Emerging Technologies*, vol. 53, pp. 1–18, 2015.

[13] H. Lahrmann, B. Brassøe, J. W. Johansen, and J. C. O. Madsen, "Safety impact of average speed control in the UK," *Journal of Transportation Technologies*, vol. 6, no. 5, pp. 312–326, 2016.

[14] M. Borsati, M. Cascarano, and F. Bazzana, "On the impact of average speed enforcement systems in reducing highway accidents: evidence from the Italian Safety Tutor," *Economics of Transportation*, vol. 20, p. 100123, 2019.

[15] D. Y. Kim, H. W. Lee, and K. S. Hong, "A study on effectiveness analysis and development of an accident prediction model of point-to-point speed enforcement system," *Journal of the Korean Society of Safety*, vol. 34, no. 5, pp. 144–152, 2019.

[16] D. W. Soole, B. C. Watson, and J. J. Watson, "Effects of average speed enforcement on speed compliance and crashes: a review of the literature," *Accident Analysis & Prevention*, vol. 54, pp. 46–56, 2013.

[17] A. Montella, B. Persaud, M. D'Apuzzo, and L. L. Imbriani, "Safety evaluation of automated section speed enforcement system," *Transportation Research Record: Journal of the Transportation Research Board*, vol. 2281, no. 1, pp. 16–25, 2012.

[18] A. Høye, "Safety effects of section control—an empirical Bayes evaluation," *Accident Analysis and Prevention*, vol. 74, pp. 169–178, 2015.

[19] E. Hauer, "Observational before/after studies in road safety," *Estimating the Effect of Highway and Traffic Engineering Measures on Road Safety*, Elsevier Science Ltd., Oxford, UK, 1997.

[20] J. Shim, K. Jang, S. H. Park, H.-S. Lee, H. Yeo, and O. H. Kwon, "Evaluating safety performance of climbing lane configurations on South Korean expressways," *Transportation Research Record*, vol. 2583, 2016.

[21] R. Elvik, "The predictive validity of empirical Bayes estimates of road safety," *Accident Analysis & Prevention*, vol. 40, no. 6, pp. 1964–1969, 2008.

[22] O. H. Kwon, Y. Yoon, and K. Jang, "Evaluating the effectiveness of the law banning handheld cellphone use while driving," *Safety Science*, vol. 70, pp. 50–57, 2014.

[23] U. Brüde and R. Elvik, "The turning point in the number of traffic fatalities: two hypotheses about changes in underlying trends," *Accident Analysis & Prevention*, vol. 74, pp. 60–68, 2015.

[24] C. Chen, *Freeway Performance Measurement System (PeMS). Research Reports, California Partners for Advanced Transit and Highways (PATH)*, Institute of Transportation Studies (UCB), Berkeley, CA, USA, 2003.

[25] C. F. Daganzo, *Fundamentals of Transportation and Traffic Operations*, Elsevier Science Inc., New York, NY, USA, 1997.

[26] J. L. Fleiss, B. Levin, and M. C. Paik, "The analysis of data from matched samples," *Statistical Methods for Rates and Proportions,* pp. 373–406, John Wiley & Sons, Inc., Hoboken, NJ, USA, 3rd edition, 1981.

[27] H. Yeo, K. Jang, A. Skabardonis, and S. Kang, "Impact of traffic states on freeway crash involvement rates," *Accident Analysis & Prevention*, vol. 50, pp. 713–723, 2013.

[28] C. Oh, S. Park, and S. G. Ritchie, "A method for identifying rear-end collision risks using inductive loop detectors," *Accident Analysis & Prevention*, vol. 38, no. 2, pp. 295–301, 2006.

[29] K. Chung, K. Jang, S. Oum, Y. Kim, and K. Song, "Investigation of attributes of kinematic waves preceding traffic collisions," in *Proceedings of the 17th ITS World Congress*, Busan, South Korea, October 2010.

[30] M. Abdel-Aty, J. Dilmore, and L. Hsia, "Applying variable speed limits and the potential for crash migration," *Transportation Research Record: Journal of the Transportation Research Board*, vol. 1953, no. 1, pp. 21–30, 2006.

[31] T. F. Golob, W. W. Recker, and V. M. Alvarez, "Freeway safety as a function of traffic flow," *Accident Analysis & Prevention*, vol. 36, no. 6, pp. 933–946, 2004.

[32] G. X. Liu and A. Popoff, "Provincial-wide travel speed and traffic safety study in saskatchewan," *Transportation Research Record: Journal of the Transportation Research Board*, vol. 1595, no. 1, pp. 8–13, 1997.

[33] S. Park, K. Jang, S. H. Park, D.-K. Kim, and K. S. Chon, "Analysis of injury severity in traffic crashes: a case study of Korean expressways," *KSCE Journal of Civil Engineering*, vol. 16, no. 7, pp. 1280–1288, 2012.

Hindawi
Journal of Advanced Transportation
Volume 2020, Article ID 3024101, 13 pages
https://doi.org/10.1155/2020/3024101

Research Article

Road Traffic Safety Risk Estimation Method Based on Vehicle Onboard Diagnostic Data

Xiaoyu Cai,[1,2] **Cailin Lei**,[1,2] **Bo Peng**,[1,2] **Xiaoyong Tang**,[3] **and Zhigang Gao**[3]

[1]*Chongqing Jiaotong University, College of Traffic and Transportation, Chongqing 400074, China*
[2]*Key Laboratory of Traffic System & Safety in Mountain Cities of Chongqing, Chongqing 400074, China*
[3]*Urban Transportation Big Data Engineering Technology Research Center of Chongqing, Chongqing 400020, China*

Correspondence should be addressed to Xiaoyu Cai; caixiaoyu@cqjtu.edu.cn

Received 7 September 2019; Revised 24 December 2019; Accepted 17 January 2020; Published 26 February 2020

Guest Editor: Bilal Farooq

Currently, research on road traffic safety is mostly focused on traffic safety evaluations based on statistical indices for accidents. There is still a need for in-depth investigation on preaccident identification of safety risks. In this study, the correlations between high-incidence locations for aberrant driving behaviors and locations of road traffic accidents are analyzed based on vehicle OBD data. A road traffic safety risk estimation index system with road traffic safety entropy (RTSE) as the primary index and rapid acceleration frequency, rapid deceleration frequency, rapid turning frequency, speeding frequency, and high-speed neutral coasting frequency as secondary indices is established. A calculation method of RTSE is proposed based on an improved entropy weight method. This method involves three aspects, namely, optimization of the base of the logarithm, processing of zero-value secondary indices, and piecewise calculation of the weight of each index. Additionally, a safety risk level determination method based on two-step clustering (density and k-means clustering) is also proposed, which prevents isolated data points from affecting safety risk classification. A risk classification threshold calculation method is formulated based on k-mean clustering. The results show that high-incidence locations for aberrant driving behaviors are consistent with the locations of traffic accidents. The proposed methods are validated through a case study on four roads in Chongqing with a total length of approximately 38 km. The results show that the road traffic safety trends characterized by road safety entropy and traffic accidents are consistent.

1. Introduction

With the rapid development of urban road traffic systems, traffic accidents have become a serious social problem that poses a grave threat to the safety of human lives and property. In the period from 2011 to 2017, the number of traffic accident casualties in China decreased each year but was still very high. On average, approximately 60,000 people died from traffic accidents each year. Research has shown that more than 95% of traffic accidents are caused by driver cognitive and behavior decision errors [1]. Therefore, studying road traffic accidents and safety risks from a driving behavior perspective can effectively support prevention and early warning for traffic accidents and improve road passing efficiencies and service levels.

Currently, road traffic safety risk is extensively studied. In general, the relevant research can be divided into three categories, including research that evaluates road traffic safety based on statistical indices for traffic accidents utilizing methods such as Bayesian networks (BNs) and accident rate methods; research that establishes an evaluation index system considering the different characteristics of people, vehicles, roads, and environment and evaluates road traffic safety using methods like analytic hierarchy processes (AHPs) and fuzzy evaluation; and research that evaluates road traffic safety based on driving behavior and traffic accident data.

Regarding the evaluation of road traffic safety based on statistical indices for traffic accidents, by analyzing methods for identifying accident-prone locations in China and elsewhere, Fang et al. proposed a level-based identification algorithm applicable to road traffic in China and a new

microevaluation method (the cumulative frequency curve method) for identifying accident-prone locations [2]. Xin comprehensively evaluated the road traffic safety state using the entropy weight-technique for order preference by similarity to ideal solution (TOPSIS) method based on five evaluation indices, namely, the number of traffic accident deaths, average number of deaths per accident, fatality rate, number of deaths per 10,000 vehicles, and number of deaths per 100,000 people [3]. Mbakwe et al. evaluated national highway traffic safety using the Delphi technique in conjunction with a BN model based on highway traffic accident data [4]. Mohan et al. and Wang et al. studied urban traffic safety evaluation methods based on accident rates [5, 6]. Sandhu et al. evaluated road traffic accident black spots using the kernel density estimation method based on road traffic accident data [7]. Dang et al. established a regional road traffic safety evaluation index system by multiple correlation analysis of traffic accident data [8]; similarly, these researchers evaluated urban road traffic safety based on accident rates. Wang et al. and Elvik et al. evaluated urban road traffic safety using BNs based on traffic accident data [9, 10]. From a traffic management perspective, Eusofe et al. and Gomes et al. evaluated road traffic safety based on traffic accident data [11, 12]. Zhang et al. established an equivalent accident frequency model based on the absolute accident frequency, accident consequences, and impact on traffic [13]; additionally, these researchers used this model in a combined location safety evaluation method for urban expressways.

Regarding establishment of road traffic safety evaluation indices based on the different characteristics of people, vehicles, road, and environment, Wang et al. used an eight-degree-of-freedom driving simulator to replicate the full range of combined alignments used on a mountainous freeway in China [14]; additionally, multiple linear regression models were developed to estimate the effects of the combined alignments on the lateral acceleration. Li et al. examined the effects of subjective and objective safety indices on road safety and analyzed the relationships between an objective safety index, which comprises road linearity, pavement, traffic facilities, and natural environment and road safety [15]. Sun et al. evaluated the traffic safety state of interwoven areas using indices such as the number of traffic conflicts, traffic count, and the length of the interwoven area [16]. Niu et al. evaluated the road traffic safety state using two indices, namely, the road conditions and traffic accidents [17]. Cheng et al. evaluated road traffic safety with road conditions as evaluation index [18]. Luo et al. established an urban traffic safety state evaluation model using a fuzzy algorithm with people, vehicles, roads, and environment as evaluation indices [19]. Li created a multilevel safety evaluation index system based on expressway linearity and established a comprehensive linear safety evaluation model for expressways based on the extension theory; additionally, Li determined the weights of indices using the entropy weight method and classified safety levels [20].

Regarding research on road traffic safety risks based on driving behavior, traffic flow, and traffic accident data, Gao et al. studied and analyzed a road traffic accident risk prediction model for the technical environment of continuous urban traffic observation and dynamic control (continuous data environment for short) based on logistic regression and random forests [21]. Chen et al. proposed a new hotspot identification method based on quantitative risk assessment and used this method to identify potential accident-prone locations on highways [22]. Yu et al. proposed a hybrid latent class analysis modeling approach to consider the heterogeneous effects of geometric features in accident risk analysis; additionally, these researchers established traffic accident risk analysis models using a Bayesian random parameter logistic regression algorithm [23]. Sun and Sun conducted modeling analysis on the real-time traffic flow parameters of expressways in Shanghai and the accident risk based on coil detector and accident data in combination with a BN model [24]. Xu and Shao established a dynamic whole-vehicle model for a certain microvehicle and a road model using the multibody dynamic software Automated Dynamic Analysis of Mechanical Systems (ADAMS); subsequently, these researchers used the models to conduct virtual simulations to quantitatively analyze the effects of driver behaviors on brake safety [25]. Based on driving behavior data, Min determined the road traffic safety state using an AHP and a comprehensive fuzzy evaluation method [26]. Li et al. and Qu et al. formulated road traffic safety evaluation methods based on traffic accident and driving behavior data [27, 28].

As mentioned above, the relevant research on road traffic safety evaluation has accumulated rich results but is still deficient to a certain extent due to the different evaluation methods and data involved. (1) The evaluation based on statistical indices for traffic accidents is performed after the occurrence of traffic accidents. It does not consider the fundamental causes of traffic accidents, including the aberrant driving behaviors, road, weather, and traffic conditions. Therefore, it is important to estimate road traffic safety risk in advance for accidents prevention; however, existing research is insufficient for preassessment of road traffic safety risk. (2) The research that establishes an evaluation index system considering the different characteristics of people, vehicles, roads, and environment is short of intermediate feature data for describing driving behaviors; thus, it is difficult to accurately predict road traffic safety risk. (3) Driving behavior data provides support for exploring the intrinsic causes of accidents; unfortunately, up to now most researches employ a small amount of driving behavior data which covers a few behavior patterns. As a result, it is difficult to depict traffic safety risk under various road conditions when driving behavior data is inadequate.

Hence, based mainly on onboard diagnostic (OBD) driving behavior data and the information entropy theory, this study establishes an urban road traffic safety risk evaluation index system and a relevant calculation method, investigates a traffic safety risk estimation method, and classifies road traffic safety risks.

2. Data Preprocessing

2.1. Brief Introduction to Vehicle OBD Data. In the main urban area of Chongqing, there are approximately 100,000

private vehicles with OBD devices installed. An OBD device updates and records 13 types of vehicle data (including global positioning system (GPS), driving behavior, and security alarm data) every 2–10 s. Based on a preliminary analysis of original data, two types of vehicle data, namely, GPS and driving behavior data, are primarily used in this study for analysis. Vehicle GPS data consist of 27 fields, including data type, vehicle identification number (ID), time, longitude, latitude, and speed. Driving behavior data consist of four fields, namely, data type, vehicle ID, time, and driving behavior type. Because an OBD device transmits data independently based on the type of data, it is necessary to match a vehicle's GPS and driving behavior data to obtain driving behavior and relevant information.

2.2. Driving Behavior and GPS Data Matching. Based on the vehicle ID and time fields in the GPS and driving behavior data collected by the OBD device onboard a vehicle, the vehicle's GPS and driving behavior data are matched to obtain aberrant driving behavior and relevant longitude and latitude information. Table 1 summarizes the driving behavior data obtained after data matching.

2.3. Classification of Road Sections. Vehicle driving behaviors are, to a relatively large extent, affected by road conditions. To accurately evaluate road traffic safety risk under different road conditions based on aberrant driving behaviors, road sections are classified into eight categories, according to three characteristic parameters (the slope gradient, radii of turns, and presence of openings). The classification standard of road sections is shown in Table 2.

3. Establishment of a Road Traffic Safety Risk Evaluation Index System Based on Aberrant Driving Behaviors

3.1. Correlation Analysis of Aberrant Driving Behaviors and Traffic Accidents. In actual traffic, aberrant vehicle driving behaviors, such as rapid acceleration, rapid deceleration, and rapid turning, can easily occur as a result of road, climate, and traffic conditions. When a vehicle exhibits an aberrant driving behavior, this behavior alone may result in an accident or may have a relatively significant impact on the surrounding vehicles, causing a multivehicle traffic accident. Therefore, there may be a relatively high probability of traffic accidents at high-incidence locations for aberrant driving behaviors.

To verify the above inference, a case study of Xuefu Avenue in Chongqing (sections between Si Gongli and Liu Gongli) was performed. Based on the aberrant driving behavior data of 8,486 vehicles in a 6-consecutive-day period (231 rapid acceleration data items, 416 rapid deceleration data items, 99 rapid turning data items, 12 speeding data items, and 87 high-speed neutral coasting data items), an aberrant driving behavior distribution heat map was produced using ArcGIS, as shown in Figure 1(a). Additionally, 1-month traffic accident data (23 accidents) for Xuefu Avenue were obtained from Chongqing municipal traffic management authorities. Figure 1(b) shows the location of each accident. As demonstrated in Figure 1, spatially, the locations of traffic accidents agreed well with the sections with high incidence of aberrant driving behaviors.

Additionally, 6-day aberrant driving behavior data (10,715 aberrant driving behavior data items for 42,558 vehicles) and traffic accident data in a month (302 traffic accidents) for two other roads, including Longteng Avenue and Shi Xiaolu Avenue, were gathered and processed. A matching analysis of these data, similar to that shown in Figure 1, was performed in Figures 2 and 3.

Accidents number and aberrant driving behavior frequency of each road section on the three avenues mentioned above were calculated, and their distribution curves were as shown in Figure 4.

Results show that, in most cases for the three avenues, when aberrant driving behavior frequency rises, accidents number increases, which infers that trends of aberrant driving behavior frequency and accident frequency are basically consistent with each other. There may be a few exceptions, where drivers can perceive a potential high safety risk and take corresponding precautions to avoid accidents as field survey implies. Nevertheless, aberrant driving behavior data can represent the risk of road traffic safety in general.

3.2. Selection of Road Traffic Safety Risk Evaluation Indices. For any road sections, the lower the aberrant driving behavior frequencies are, the more orderly the traffic flow is and the lower the probability of traffic accidents is, and vice versa. This phenomenon is very similar to the disorderliness of a system described by information entropy. In 1865, German physicist Rudolf Clausius proposed the concept of entropy. In 1948, Shannon quantified entropy to reflect the orderliness of a system [29]. The more orderly a system is, the lower the information entropy of the system is, and vice versa.

Therefore, a road traffic safety risk evaluation index system is established with the road traffic safety entropy (RTSE) as the primary index and the frequencies of various aberrant driving behaviors affecting the road traffic safety as the secondary indices (Table 3).

4. RTSE Calculation Method Based on an Improved Entropy Weight Method

4.1. Calculation Process for RTSE. Overall, the RTSE calculation method involves two steps, namely, calculating the values of the secondary evaluation indices and calculating the weights of the secondary indices and the value of RTSE.

The value of a secondary index (aberrant driving behavior frequency), P_{ij}^k, is calculated as follows:

$$P_{ij}^k = \frac{A_{ij}^k}{Z_{ij}^k}, \tag{1}$$

where i is the sections number, k is the time, j is the index number, A_{ij}^k is the aberrant driving behavior frequency for the road sections i corresponding to the index j within time

Table 1: Samples of driving behavior data.

Vehicle ID	Time	Direction angle	Speed	Altitude	Latitude	Longitude	Driving behavior type
fdc14ca4. . .bb4b130	2018/5/16 07:37:20	306	28	72	29.622507	106.522736	Rapid acceleration
fdc14ca4. . .bb4b130	2018/5/16 07:37:30	313	26	70	29.622723	106.52349	Rapid deceleration
fdc14ca4. . .bb4b130	2018/5/16 07:38:00	337	0	69	29.622875	106.52382	Rapid turning

Table 2: Classifications of example road sections.

Road condition	Bend		Straight line	
	With openings	Without openings	With openings	Without openings
Flat	Type I	Type II	Type III	Type IV
Sloped	Type V	Type VI	Type VII	Type VIII

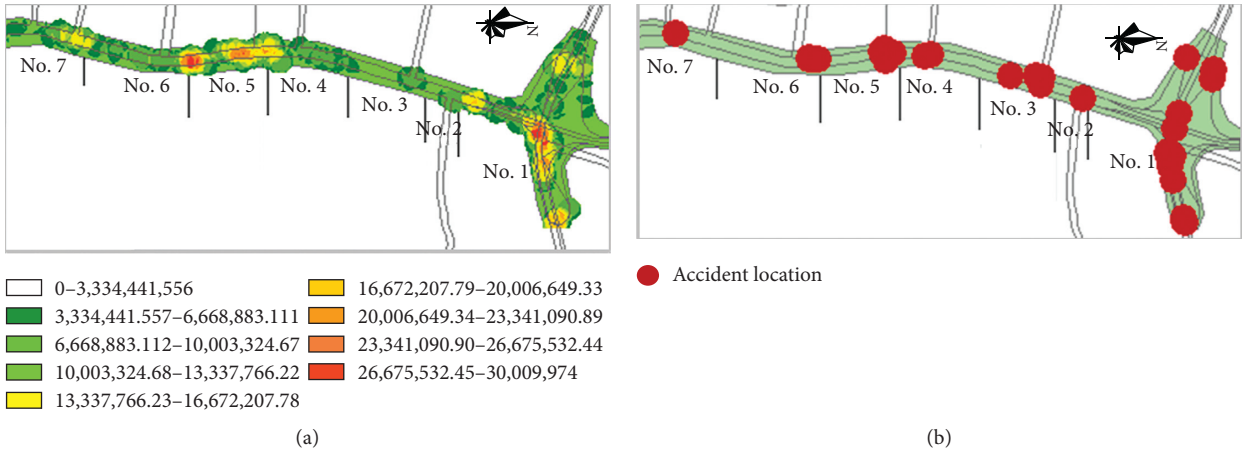

Figure 1: Aberrant driving behaviors and traffic accidents on Xuefu Avenue.

(a)

Figure 2: Continued.

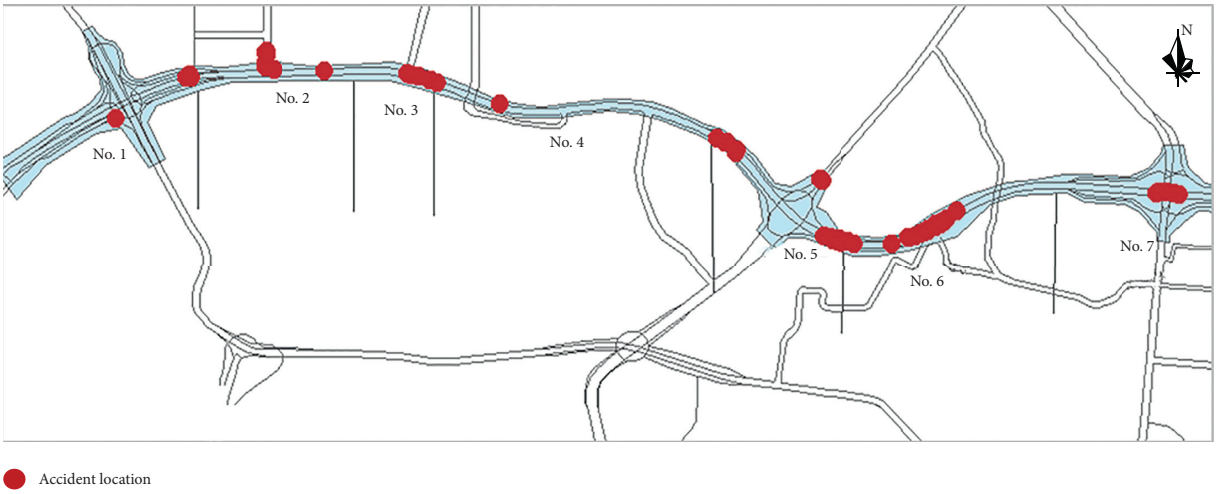

(b)

Figure 2: Aberrant driving behavior and traffic accidents on Longteng Avenue.

(a) (b)

Figure 3: Aberrant driving behavior and traffic accidents on Shi Xiaolu Avenue.

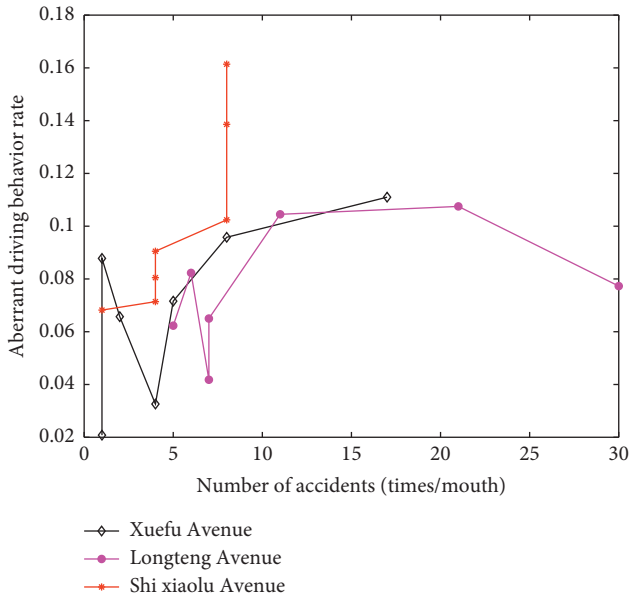

Figure 4: Distribution of frequencies of aberrant driving behaviors and traffic accidents.

Table 3: Evaluation index system.

Primary evaluation index	Secondary evaluation index
Road traffic safety entropy (RTSE)	Rapid acceleration frequency, rapid deceleration frequency, rapid turning frequency, speeding frequency, and high-speed neutral coasting frequency

k, and Z_{ij}^{k} is the number of OBD-equipped vehicles that travel through the road sections i within time k.

Several methods are available for calculating the weight of an index, including the entropy weight method, AHP, and principal component analysis. The entropy weight method determines the weight of an index based on the difference of the index from the other indices. The more significantly an index differs from other indices, the greater the weight of the index is. The entropy weight method is relatively applicable to description of the effects of aberrant driving behaviors on the road traffic safety risk level. For example, for several road sections differing in traffic accident frequency, if there is a relatively significant change in the frequency of a certain aberrant driving behavior and the frequencies of other aberrant driving behaviors remain basically unchanged, then the frequency of the aberrant driving behavior in question results in a difference in the accident frequency. Therefore, the aberrant driving behavior in question can be assigned a relatively large weight. The entropy weight method calculates the weight of an index in the following process:

(1) Data standardization:

$$\lambda_{ij}^{k} = \frac{P_{ij}^{k} - P_0}{P_1 - P_0}, \tag{2}$$

where $P_0 = \mathrm{Min}(P_{ij}^{1}, P_{ij}^{2}, \ldots, P_{ij}^{q})$ and $P_1 = \mathrm{Max}(P_{ij}^{1}, P_{ij}^{2}, \ldots, P_{ij}^{q})$.

(2) Calculation of the entropy value of the index h_j:

$$h_j = \sum_{i=1}^{n}\sum_{k=1}^{q}\left(-\lambda_{ij}^{k}\right)\log_a \lambda_{ij}^{k}, \tag{3}$$

where n is the total number of road sections, q is the number of time periods, and a, the base of the logarithm, is set to 2.

(3) Calculation of the weight of the index w_j:

$$w_j = \frac{1 - h_j}{\sum_{j=1}^{m}\left(1 - h_j\right)}, \tag{4}$$

where m is the total number of indices.

The entropy weight method can objectively calculate the weight of an index. However, when using this method in practice, optimization and demonstration are required. For example, setting the base a of the logarithm to an unsuitable value may result in a negative weight. It is impossible to calculate the entropy value of a zero-value index. Additionally, when the entropy values of all the indices are close to 1, the difference between the indices may be greater.

4.2. Improvement of the Entropy Weight Method

4.2.1. Optimization of the Base of the Logarithm a. When calculating the entropy value of an index, a used in the original entropy weight method is set to 2. In certain studies, a is set to 10 or the number of objects evaluated. This assignment may lead to an unreasonable weight for the index. Thus, it is proposed that a be set to the number of secondary evaluation indices. The reason is discussed below.

The information entropy proposed by Shannon primarily solves communication problems. There are only two basic computer storage units (binary), 0 and 1. When an event may have two consequences, each of which has a probability of 50%, the system results are the most random; that is, the level of disorderliness is the highest. Under this condition, the entropy value of the system is 1 when the logarithm of a is 2. Based on (4), when calculating the entropy values of indices, a needs to ensure that the maximum entropy is 1 and the weights of the indices are reasonably allocated when the indices have the same probability of occurrence.

Here, 2,000 groups of random numbers (including data groups in which each index has a value of 0.2) are generated under the following conditions: number of indices, 5; sum of indices, 1. A plot is created with the variance of each group of numbers as the x-axis and the product of each group of numbers as the y-axis, as shown in Figure 5. Evidently, the smaller the variance is, the greater the product is. The product reaches the maximum value of 3.2×10^{-4} at a variance of 0 (i.e., all the indices have a value of 0.2).

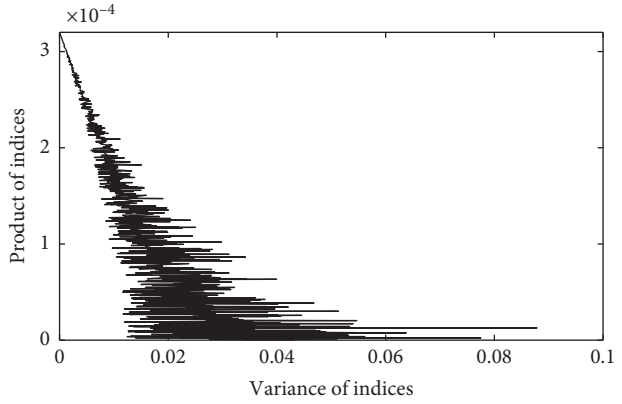

Figure 5: Relationship between the variance and product of data groups.

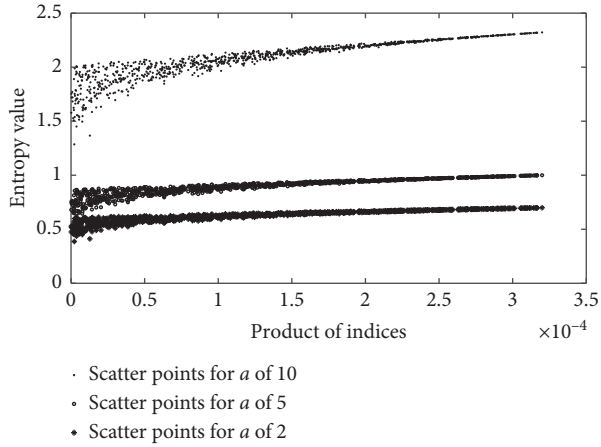

Figure 6: Relationship between a and the product of indices.

Then, the entropy value of the system is calculated with a of 2, 5, and 10 and the product of each group of data as the input. The relationship between the product of the indices and the entropy value of the system is shown in Figure 6.

The entropy value increases with the product of the indices. The entropy reaches the maximum value of 1 at a product of indices of 3.2×10^{-4} (i.e., all the indices have the same probability of occurrence) and a of 5. This result agrees with the information entropy theory. Therefore, when calculating the entropy value of an index, it is recommended that a be equal to the number of evaluation indices.

4.2.2. Zero-Value Processing of Secondary Indices. The original entropy weight method is unable to calculate the entropy value for zero-value data. The available studies mainly use two methods for processing zero-value data, namely, by directly discarding the group of zero-value data and adding an increment of 1 to the zero-value data. Here, an alternative method for processing zero-value data is proposed. When a certain evaluation index in a group has a zero value, 0.00001 is added to each index in the group. The reason is discussed below.

The aberrant driving behavior frequency varies relatively significantly between different road conditions. For upslope or long straight road sections, the probability of high-speed neutral coasting is almost 0. This result is an objectively existent phenomenon. Discarding the group of data in question leads to a deficient description of the objective phenomenon. Adding an increment of 1 to all the data accounts for this limitation. However, the slope of the logarithmic function for calculating the entropy value of an index continuously decreases as the value of the independent variable increases. If an increment of 1 is added to all the data, the difference in the entropy values between the other nonzero-value indices decreases, which relatively significantly affects the allocation of weights to the indices. Therefore, when a secondary index has a value of 0, it is recommended that a minor increment be added to all the index data and that the addition of this increment have a nonsignificant impact on the difference between indices.

Here, an example is given. There is a group of five indices with values of 0.23, 0.27, 0.21, 0.10, and 0.19. The weight of each index is calculated. Then, an increment ΔP ranging from 0.00000001 to 1 is added to each index. Subsequently, the change in the weight of each index is calculated. The relationship between the increment added to each index and the change in its weight is shown in Figure 7.

As demonstrated in Figure 4, when the increment ΔP is less than 0.00001, there is almost no change in the weight of each index. Therefore, when a secondary index has a value of 0, an increment of 0.00001 could be uniformly added to this group of data.

4.2.3. Weight Calculation Method. When the entropy values of all the indices are close to 1 and have a very slight difference, the weights calculated may differ multifold. Thus, a piecewise calculation method for the weights of the indices based on their entropy value distribution is proposed, as shown in

$$w_j'' = \begin{cases} \dfrac{\left(1 + \overline{h} - h_j\right)}{\left[\sum_{j=1, h_j \neq 1}^{m} \left(1 + \overline{h} - h_j\right)\right]}, & \text{Case1,} \\ \dfrac{\left(1 - h_j\right)}{\left[\sum_{j=1}^{m} \left(1 - h_j\right)\right]}, & \text{Case2,} \end{cases} \tag{5}$$

where case 1 describes a situation where there is a relatively small difference in the entropy values or indices and all entropy values are distributed in the range of (0.8, 0.91) or (0.95, 1); case 2 describes other situations.

When using (4) to calculate weights, if the entropy values of all the indices are close to 1 and differ nonsignificantly, then the weights calculated may differ multifold [30, 31]. Here, an example is given. Five indices are selected. Correspondingly, a group of data is selected as the entropy values for the indices. The maximum difference between the data in this group does not exceed 0.04. Additionally, the data in this group vary in the range close to [0.6, 1]. The weight of each index is calculated using (4). Moreover, the product of the weights of the indices is calculated. A plot is

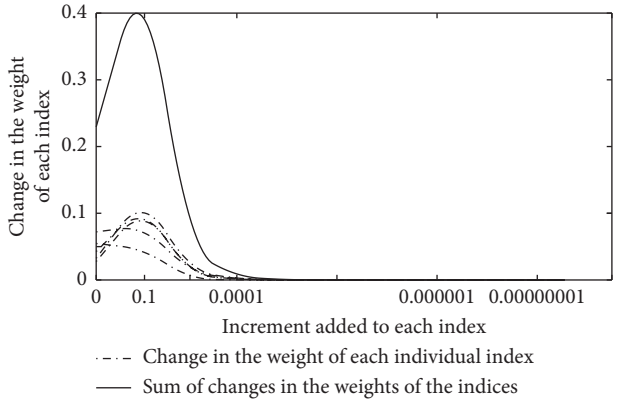

Figure 7: Relationship between the increment added to the indices and the changes in their weights.

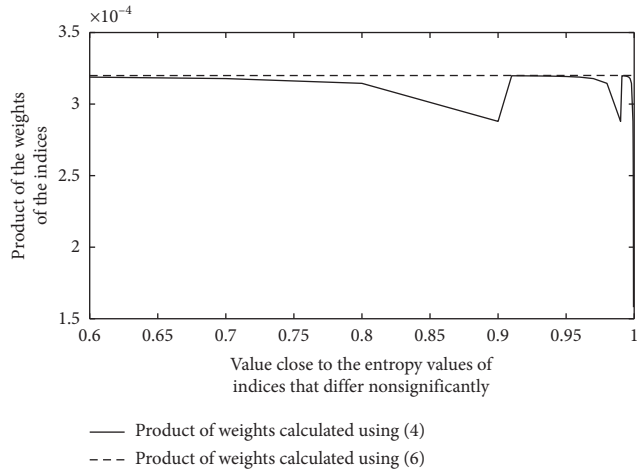

Figure 8: Product of the weights of the indices.

created with the values close to the entropy values of the indices as the x-axis and the product of the weights of the indices as the y-axis, as shown in Figure 8.

As mentioned previously, the product of a group of data increases as its variance decreases. As demonstrated in Figure 5, when the entropy values of all the indices are distributed in the range of (0.8, 0.91) or (0.95, 1), the variance of the weights of the indices is relatively large; that is, the difference between the weights of the indices is relatively large. Ouyang proposed an improved weight calculation method [32], as shown in

$$w_j' = \frac{1 + \overline{h} - h_j}{\sum_{j=1, h_j \neq 1}^{m} \left(1 + \overline{h} - h_j\right)}. \quad (6)$$

In this study, the weights of the indices are calculated using (6). The relationship between the values close to the entropy values of the indices and the product of the weights of the indices is shown in Figure 8. This method effectively addresses the problem of the entropy values of the indices differing nonsignificantly.

4.3. Calculation of RTSE. Based on the calculation of the weights of aberrant driving behavior frequencies on various types of road sections, the aberrant driving behavior frequencies p_{ij} for any road section and the RTSE value SH_i of the section i are calculated. One has

$$p_{ij} = \sum_{k=1}^{q} \frac{P_{ij}^k}{q}, \quad (7)$$

$$\mathrm{SH}_i = \sum_{j=1}^{m} w_j'' \times \left(-p_{ij}\right) \log_m\left(p_{ij}\right), \quad (8)$$

where the value of P_{ij} is set to 0.00001 when $P_{ij} = 0$.

4.4. Road Traffic Safety Risk Classification Based on Cluster Analysis

4.4.1. Road Traffic Safety Risk Level Determination Based on Two-Step Clustering. A high traffic safety risk does not necessarily translate to a large number of traffic accidents. The RTSE values of different type sections are not absolutely correlated with the number of traffic accidents.

Density-based spatial clustering of applications with noise (DBSCAN) is able to identify data points distributed in a relatively isolated manner based on the data distribution density, thereby preventing isolated data points from affecting classification. Then, k-means clustering is conducted based on various numbers of clusters to calculate the silhouette coefficients for various numbers of clusters (the higher the coefficient is, the better the cluster separation is). The optimum number of clusters is selected as the number of road safety risk classification levels.

4.4.2. Road Traffic Safety Risk Level Threshold Optimization Algorithm Based on k-Means Clustering. Level thresholds are calculated based on optimum k-means clustering results. It is assumed that there is a number of levels r. The number of classification level thresholds $(r-1)$ is calculated. The pseudocode of the algorithm (Algorithm 1) is as follows:

5. Validation Case Study

5.1. Selection of Example Roads. Chongqing, a typical mountainous city in China, has multiple centers and cluster-typed urban space. The clusters in Chongqing are connected only by expressways and arterial roads. In this study, the road traffic safety risks of Longteng Avenue (Road A, approximately 4.4 km long), Hongshi Avenue (Road B, approximately 2.5 km long), the Inner Ring Expressway and Airport Expressway (Road C, approximately 27 km long), and Xuefu Avenue (Road D, approximately 4.5 km long) in Chongqing are evaluated, as shown in Figure 9.

5.2. Data Preprocessing. By the OBD data processing method, the GPS and driving behavior data for 13,004

(1) int $r \longleftarrow k$-means number of clusters
(2) For int $t = 1$ to $r - 1$
(3) int $a_t \longleftarrow$ Safety entropy value of the center of the t^{th} cluster
(4) int $b_t \longleftarrow$ Safety entropy value of the center of the $(t+1)$th cluster
(5) int $s_t \longleftarrow$ Sum of the data in the tth and $(t+1)^{th}$ clusters
(6) int $f = 1$
(7) For float $e_{tf} = a_t$ to b_t
(8) int $c_{tf} \longleftarrow$ Volume of data in the tth cluster that is misclassified
(9) int $d_{tf} \longleftarrow$ Volume of data in the $(t+1)$th cluster that is misclassified
(10) $g_{tf} = 1 - ((c_{tf} + d_{tf})/s_t)$//Calculation of accuracy
(11) $e_{tf} = \text{etf} + 0.01$
(12) $B_t\ (f, 1{:}\ 2) = [e_{tf}, g_{tf}]$//The threshold and accuracy are stored in the matrix B_t
(13) $f = f + 1$
(14) End for
(15) $C_t \longleftarrow$ Generation of the threshold corresponding to the highest accuracy
(16) End for
(17) $C = [C_1, C_2, \ldots, C_{r-1}]$//A number of thresholds $(r-1)$ is successively stored in the vector C

Algorithm 1: Level threshold optimization algorithm ("⟵" represents value assignment).

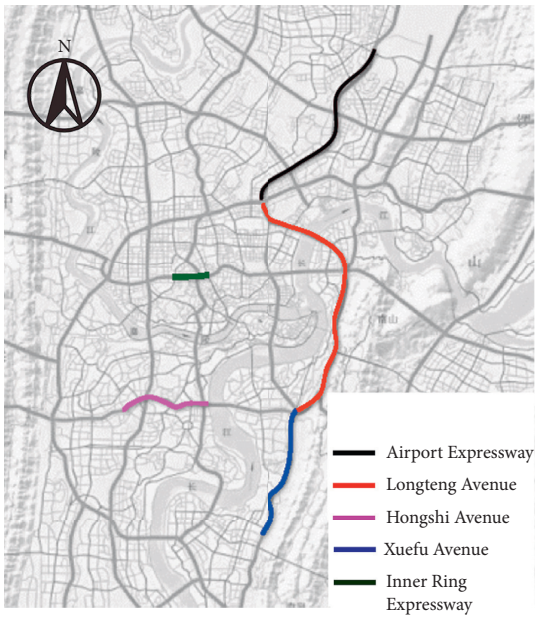

Figure 9: Example roads.

vehicles on Road A, 8,474 vehicles on Section B, 21,080 vehicles on Road C, and 8,486 vehicles on Road D, extracted from the OBD data, were matched each other.

By the classification standard of road section, the four road sections were divided into a total of 46 sections, each of which was 0.2–0.8 km long, as shown in Figure 10.

5.3. Calculation of RTSE Value

5.3.1. Calculation of the Weights of Secondary Indices for the Road Sections. By the improved entropy weight method, the weights of aberrant driving behavior frequencies for various types of road sections were calculated. Table 4 summarizes the results.

5.3.2. Calculation of the RTSE Values of the Road Sections. Based on the calculated weights for various types of road sections, the safety entropy values of the 46 road sections were calculated using (7) and (8). For example, the eight sections of road A have safety entropy values of 0.0436, 0.0278, 0.0318, 0.0385, 0.0439, 0.0358, 0.0277, and 0.0204.

5.3.3. Comparative Analysis of RTSE and Number of Traffic Accidents. There are obvious differences in traffic safety between signal-controlled urban arterial roads and expressways with and without openings. Twelve road sections of three types were selected from the example roads. The RTSE value of each road section was calculated and then compared with the number of traffic accidents during one month. Figure 11 shows the results.

As demonstrated in Figure 11, road safety entropy values are consistent with the change trend of traffic accidents, indicating that road safety entropy values can effectively represent road traffic safety risks.

5.4. Classification of Road Traffic Safety Risk

5.4.1. Determination of the Number of Risk Levels. The RTSE values and traffic accident data for 12 sections of signal-controlled arterial roads, 12 sections of expressways with openings, and 12 sections of expressways without openings (a total of 36 road sections) were selected. These data were then subjected to a DBSCAN analysis to remove the data points distributed in a relatively isolated manner. The remaining data points were subsequently subjected to k-means clustering analysis.

In MATLAB, the numbers of clusters obtained from 2-(Figure 12), 3-, and 4-means clustering were analyzed. Additionally, the silhouette coefficients for various numbers of clusters were calculated. The silhouette coefficients for k of 2, 3, and 4 were found to be 0.44, 0.37,

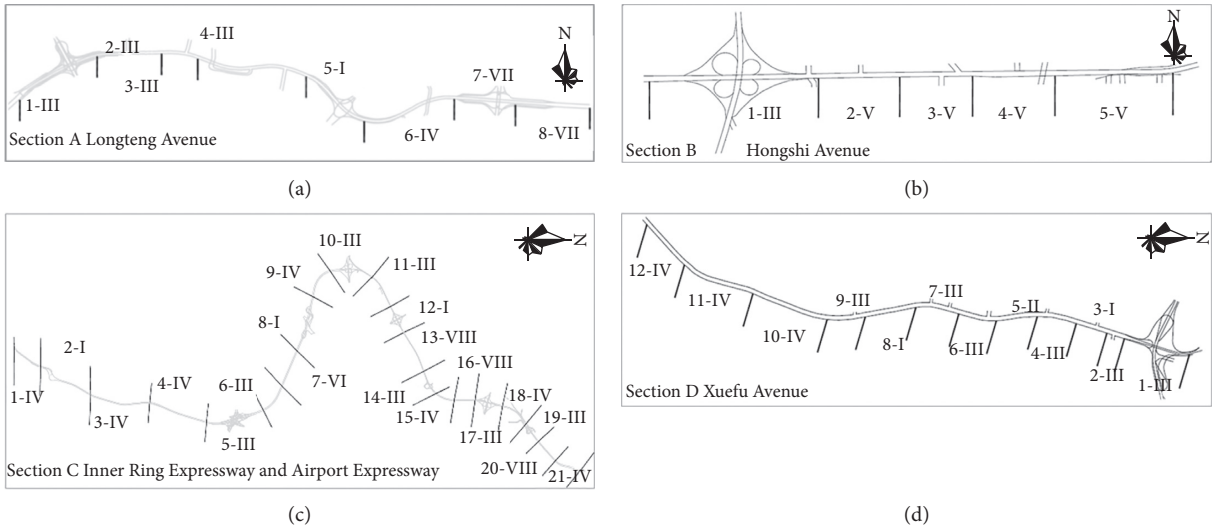

Figure 10: Classification of road section.

Table 4: Weights of aberrant driving behavior frequencies.

Road section types	Rapid acceleration frequency	Rapid deceleration frequency	Rapid turning frequency	Speeding frequency	High-speed neutral coasting frequency
I	0.19	0.19	0.16	0.30	0.18
II	0.18	0.23	0.18	0.26	0.21
III	0.16	0.21	0.18	0.33	0.16
IV	0.21	0.11	0.28	0.25	0.18
V	0.20	0.16	0.32	0.12	0.17
VI	0.25	0.14	0.27	0.24	0.14
VII	0.15	0.09	0.20	0.45	0.15
VIII	0.24	0.16	0.34	0.12	0.07

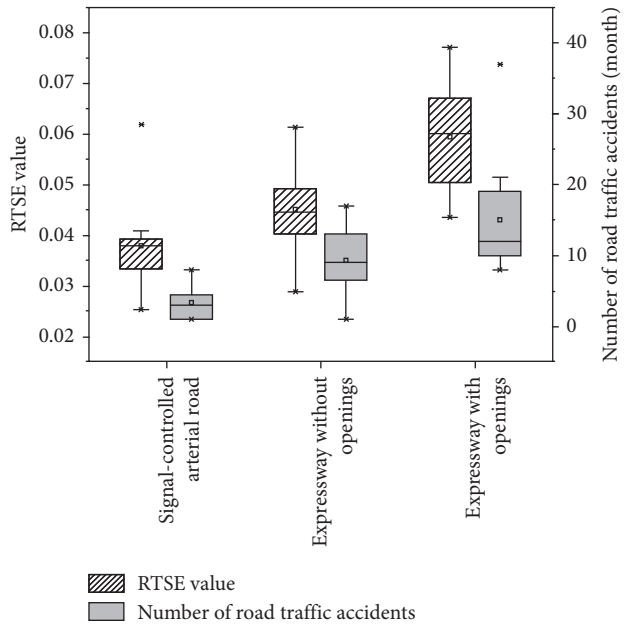

Figure 11: Comparative analysis of RTSE value and number of road traffic accidents.

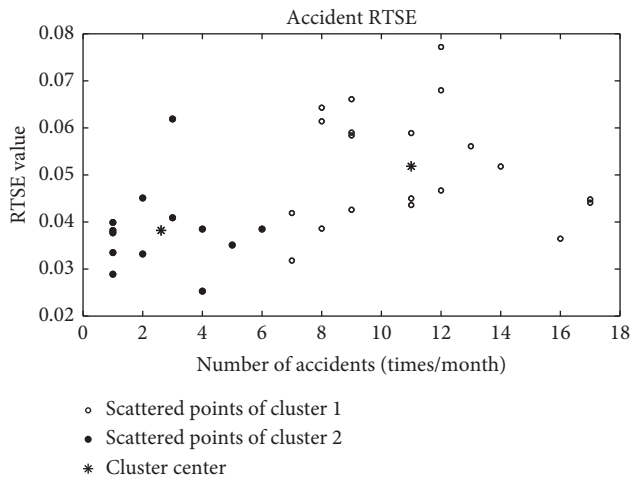

Figure 12: 2-means clustering results.

and 0.39, respectively. Evidently, 2-means clustering produced the best results. Thus, in this study, the road traffic safety risks are classified into two levels, namely, high and low risk.

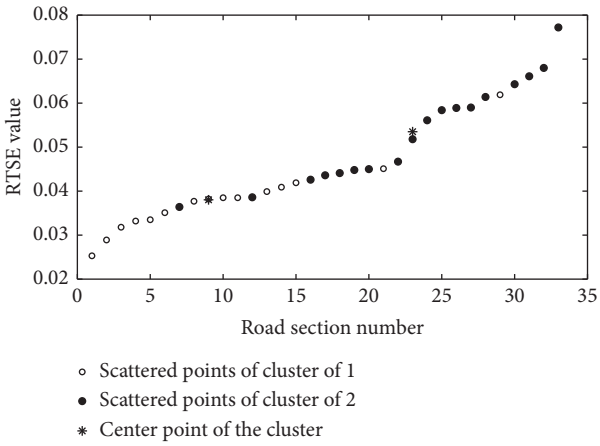

Figure 13: Sorted RTSE scatter points.

5.4.2. Calculation of Road Traffic Safety Risk Level Classification Threshold. In this part, *k*-means clustering, fuzzy clustering, and support vector machine were used to calculate risk classification thresholds and corresponding accuracies, on the basis of the 36 road sections' data as described in 4.4.1.

(1) k-Means Clustering. The RTSE values of all the road sections in class 1 and class 2 obtained from *k*-means clustering were sorted in an ascending order. Figure 13 shows the sorted data.

The classification accuracies of different RTSE threshold values for road traffic safety grading were calculated. The potential thresholds range from RTSE of clustering center of class 1 to that of clustering center in class 2. Figure 14 shows the threshold calculation result.

Evidently, the accuracy is the highest (87.88%) when the traffic safety risk level classification threshold for the road sections is 0.042.

(2) Fuzzy Clustering. Fuzzy clustering was conducted to separate data points of RTSE values and accident numbers into 2 classes, and the result was presented in Figure 15 and Table 5.

The RTSE values of all the road sections in class 1 and 2 obtained from Fuzzy clustering were sorted in an ascending order, and classification accuracies of different RTSE threshold values for road traffic safety grading were calculated. The potential thresholds range from RTSE of clustering center of class 1 to that of clustering center in class 2. The threshold calculation result was shown in Figure 16.

As the result of fuzzy clustering shows, traffic safety risk classification accuracy achieves the best (87.88%) when RTSE threshold is 0.041 or 0.042.

(3) Support Vector Machine. 15 road sections' RTSE values and accident numbers were selected for training support vector machine, and then it was used to classify traffic safety risk levels of all the road sections into two classes. The result shows that when the accuracy reaches the best (87.88%), the RTSE threshold is 0.041 or 0.042.

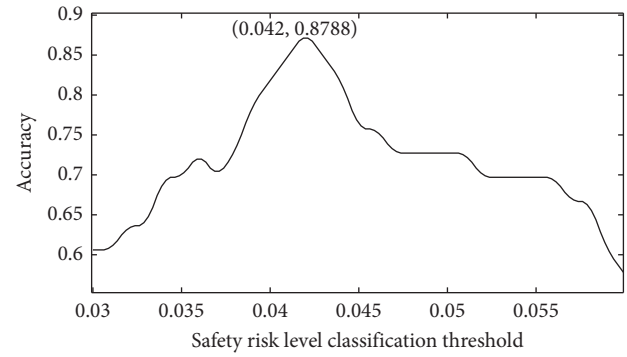

Figure 14: Road traffic safety risk level classification threshold and accuracy.

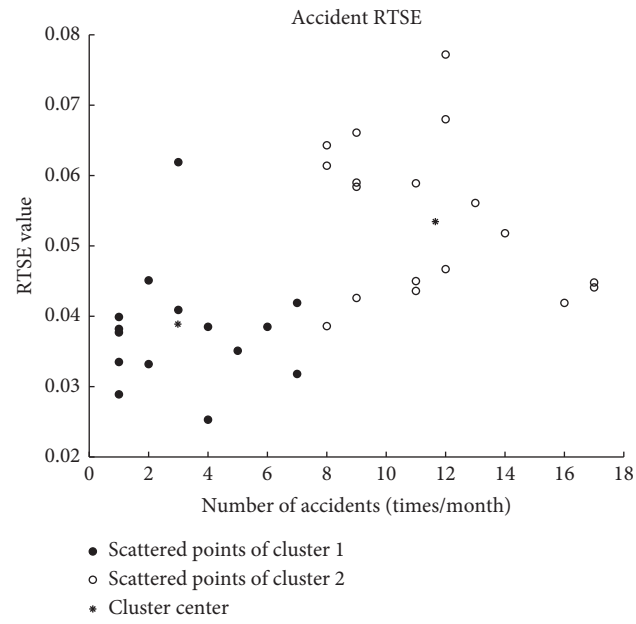

Figure 15: Fuzzy clustering result.

Table 5: Clustering centers of fuzzy clustering.

Class	Number of accidents (month)	RTSE values
Class 1	3.0	0.039
Class 2	11.6	0.053

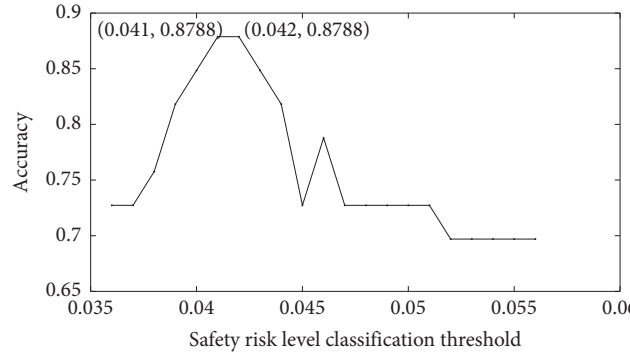

Figure 16: Fuzzy clustering calculation of road traffic safety entropy threshold and accuracy.

As we can see, classification accuracy achieves the highest as 87.88% when RTSE threshold is 0.042 for each of the three methods. Therefore, RTSE threshold is recommended to be 0.042 to identify road traffic safety risk level; that is to say, the road traffic safety is at a low level if RTSE is less than 0.042; otherwise, it is of high safety risk if RTSE is greater than 0.042.

6. Concluding Remarks

In this study, based on OBD vehicle driving behavior data, the correlation between aberrant driving behaviors and traffic accidents is analyzed. On this basis, a road traffic safety risk evaluation index system and an index calculation method are established based on information entropy theory. Additionally, based on traffic accident data, a road traffic safety risk estimation method is established through cluster analysis.

The validation case study demonstrates that the road traffic safety condition depicted by the RTSE value exhibits the same trend as that depicted by the number of traffic accidents. The road traffic safety risk prediction method established based on driving behavior data is able to effectively and objectively evaluate road traffic safety risk. The results derived from this study can effectively support identification of high road traffic safety risk locations, prevention, and early warning of traffic accidents. Additionally, these results can provide decision-making reference for traffic operation control in the collaborative vehicle-road environment.

Road traffic safety is affected by a multitude of factors, including the characteristics of road, driver, weather, and traffic conditions. This study is conducted primarily from the perspectives of driving behaviors and road conditions. As data continue to accumulate, it is necessary to conduct a classification study on the road traffic safety risk while considering more influencing factors.

Data Availability

The vehicle OBD data used to support the findings of this study were supplied by Chongqing Urban Transportation Big Data Engineering Technology Research Center under license and so cannot be made freely available. Requests for access to these data should be made to Zhigang Gao, 3585680376@qq.com.

Conflicts of Interest

The authors declare that there are no conflicts of interest regarding the publication of this paper.

Acknowledgments

This research is supported in part by Chongqing University Outstanding Talents Support Program, Chongqing Municipal Key Research and Development Project of Technology Innovation and Application Demonstration, Research Project of Chongqing Urban Traffic Big Data Engineering Technology Research Center, National Natural Science Foundation of China, Chongqing Research Program of Basic Research and Frontier Technology Innovation, and Scientific Research Project of Key Laboratory of Traffic System & Safety in Mountain Cities.

References

[1] L. Duan, *Study on the Model of Drivers' Cognitive Behavior Errors and Reliability Evaluation*, Central South University, Changsha, China, 2012.

[2] S.-E. Fang, Z.-Y. Guo, and W. Yang, "A new method for multiple location identification of highway traffic accidents," *Journal of Traffic and Transportation Engineering*, vol. 1, pp. 90–94, 2001.

[3] D.-Q. Xin, "Evaluation of road traffic safety in various urban areas of Shaanxi Province based on entropy weight-TOPSIS," *China Safety Science and Technology*, vol. 11, no. 10, pp. 118–122, 2015.

[4] A. C. Mbakwe, A. A. Saka, K. Choi, and Y.-J. Lee, "Alternative method of highway traffic safety analysis for developing countries using delphi technique and bayesian network," *Accident Analysis & Prevention*, vol. 93, pp. 135–146, 2016.

[5] D. Mohan, G. Tiwari, and S. Mukherjee, "Urban traffic safety assessment: a case study of six Indian cities," *IATSS Research*, vol. 39, no. 2, pp. 95–101, 2016.

[6] C. Wang, J.-X. Xia, Z.-B. Lu et al., "Safety evaluation method for urban intersection based on microscopic simulation and extreme value theory," *China Journal of Highway and Transport*, vol. 31, no. 176, pp. 292–299, 2018.

[7] H. A. S. Sandhu, G. Singh, M. S. Sisodia, and R. Chauhan, "Identification of black spots on highway with kernel density estimation method," *Journal of the Indian Society of Remote Sensing*, vol. 44, no. 3, pp. 457–464, 2016.

[8] X.-X. Dang, Y.-Q. Wang, Z.-H. Wu et al., "Improved generalized DEA evaluation model for regional road traffic safety," *Journal of Transportation Systems Engineering and Information Technology*, vol. 16, no. 4, pp. 11–16, 2016.

[9] J. Wang and H. Huang, "Road network safety evaluation using bayesian hierarchical joint model," *Accident Analysis & Prevention*, vol. 90, pp. 152–158, 2016.

[10] R. Elvik, H. Ulstein, K. Wifstad et al., "An empirical bayes before-after evaluation of road safety effects of a new motorway in Norway," *Accident Analysis & Prevention*, vol. 108, pp. 285–296, 2017.

[11] Z. Eusofe and H. Evdorides, "Assessment of road safety management at institutional level in Malaysia: a case study," *IATSS Research*, vol. 41, no. 4, pp. 172–181, 2017.

[12] S. V. Gomes, J. L. Cardoso, and C. L. Azevedo, "Portuguese mainland road network safety performance indicator," *Case Studies on Transport Policy*, vol. 6, no. 3, pp. 416–422, 2018.

[13] X.-Q. Zhang, X. Liu, Y. Zhu et al., "Location security analysis method for urban expressway based on internet data," *Journal of Transportation Systems Engineering and Information*, vol. 18, no. 5, pp. 57–63, 2018.

[14] X. Wang, T. Wang, A. Tarko, and P. J. Tremont, "The influence of combined alignments on lateral acceleration on mountainous freeways: a driving simulator study," *Accident Analysis & Prevention*, vol. 76, pp. 110–117, 2015.

[15] Z. Li, X. Zhou, X. Wang, and Z. Guo, "Study on subjective and objective safety and application of expressway," *Procedia—Social and Behavioral Sciences*, vol. 96, pp. 1622–1630, 2013.

[16] L. Sun, Y.-P. Li, J. Qian et al., "Traffic safety evaluation of interwoven area based on traffic conflict technology," *China Safety Science Journal*, vol. 23, no. 1, pp. 55–60, 2013.
[17] S.-F. Niu, Y.-X. Zheng, S.-D. Feng et al., "Traffic safety evaluation method for highway section based on accident tree," *Journal of Chongqing Jiaotong University*, vol. 32, no. 1, pp. 87–90, 2013.
[18] J.-Z. Cheng, Z.-F. Li, L.-C. Ren et al., "Research on fuzzy comprehensive evaluation of traffic safety based on road factors," *Journal of Taiyuan University of Science and Technology*, vol. 37, no. 4, pp. 296–301, 2016.
[19] Q. Luo, S.-G. Hu, H.-W. Gong et al., "Research and model construction of urban road traffic safety evaluation system," *Journal of Guangxi University (Natural Science)*, vol. 42, no. 2, pp. 587–592, 2017.
[20] B. Li, "Research on expressway linear safety evaluation based on extension theory," *Highway*, vol. 6, pp. 186–190, 2017.
[21] Z. Gao, W. Gao, R.-J. Yu et al., "Road traffic accident risk prediction model under continuous data environment," *China Journal of Highway and Transport*, vol. 31, no. 176, pp. 284–291, 2018.
[22] C. Chen, T.-N. Li, J. Sun et al., "Hotspot identification for Shanghai expressways using the quantitative risk assessment method," *International Journal of Environmental Research & Public Health*, vol. 14, no. 1, p. 20, 2017.
[23] R. Yu, X. Wang, and M. Abdel-Aty, "A hybrid latent class analysis modeling approach to analyze urban expressway crash risk," *Accident Analysis & Prevention*, vol. 101, pp. 37–43, 2017.
[24] J. Sun and J. Sun, "Active risk assessment of real-time traffic flow operation in urban expressway," *Journal of Tongji University (Natural Science)*, vol. 42, no. 6, pp. 0873–0879, 2013.
[25] J. Xu and Y.-M. Shao, "Quantitative analysis of the impact of driver driving behavior on brake safety," *Ergonomics*, vol. 4, pp. 29–32, 2007.
[26] Q. Min, *Road Traffic Safety Evaluation Method and Application Based on Simulated Driving*, University of Technology, Wuhan, China, 2014.
[27] X. Li, N. Zhao, and W. Zheng, "Evaluation of road traffic safety level based on cloud model," *Journal of Beijing University of Technology*, vol. 8, pp. 1219–1224, 2015.
[28] Z.-W. Qu, X. Qi, Y.-H. Chen et al., "Reverse variable lane release characteristics and its safety evaluation," *Journal of Transportation Systems Engineering and Engineering*, vol. 4, pp. 76–82, 2018.
[29] C. E. Shannon, "A mathematical theory of communication," *Bell Labs Technical Journal*, vol. 27, no. 4, pp. 379–423, 1948.
[30] H.-C. Zhou, G.-H. Zhang, and G.-L. Wang, "Multi-objective decision-making method for reservoir flood control operation based on entropy weight and its application," *Journal of Hydraulic Engineering*, vol. 38, no. 1, pp. 100–106, 2007.
[31] Y.-H. Li and J.-Z. Zhou, "Multi-objective flood control scheduling decision method based on improved entropy weight and vague set," *Hydroelectric Energy Science*, vol. 28, no. 6, pp. 38–41, 2010.
[32] S. Ouyang and Y.-L. Shi, "Improved entropy weight method and its application in power quality assessment," *Automation of Electric Power Systems*, vol. 37, no. 21, pp. 156–159, 2013.

Hindawi
Journal of Advanced Transportation
Volume 2020, Article ID 3867921, 11 pages
https://doi.org/10.1155/2020/3867921

Research Article

Automated Emergency Vehicle Control Strategy Based on Automated Driving Controls

Jaehyun (Jason) So,[1] **Jiwon Kang**,[2] **Sangmin Park**,[3] **Inseon Park**,[4] **and Jongdeok Lee**[5]

[1]*The Korea Transport Institute, Room 215, 370 Sicheong-daero, Sejong, Republic of Korea*
[2]*The Korea Transport Institute, Room G104, 370 Sicheong-daero, Sejong, Republic of Korea*
[3]*Smart Transportation Engineering Lab, Ajou University, 206, World Cup-ro, Yeongtong-gu, Suwon-si, Gyeonggi-do, Republic of Korea*
[4]*Dream ENG Co., 59, Oncheon-ro, Yuseong-gu, Daejeon, Republic of Korea*
[5]*The Korea Transport Institute, Room 425, 370 Sicheong-daero, Sejong, Republic of Korea*

Correspondence should be addressed to Jaehyun (Jason) So; jso@koti.re.kr

Received 31 October 2019; Accepted 26 December 2019; Published 1 February 2020

Guest Editor: Inhi Kim

This study proposes an integrated driving control strategy by taking advantage of the automated driving technology at the individual vehicle level and the traffic signal preemption strategy at the traffic infrastructure level. This aims to facilitate an automated driving-based emergency vehicle control and ultimately to achieve efficient and safe control of emergency vehicles. To this end, this study developed the integrated emergency vehicle control logic, implemented the logic in the microscopic traffic simulation environment using the simulation software's application programming interface capability, and evaluated the impacts of the proposed emergency vehicle control logic in the aspects of mobility and safety with different driving aggressiveness and preemption initiation settings. The study's results show that the proposed emergency vehicle control logic achieved benefits on mobility and safety and the benefits of emergency vehicle control strategy can be maximized when the signal preemption and the automated driving control operate in collaboration. Therefore, the proposed integrated approach of automated driving controls and signal preemption will be a great reference for enhancing automated driving technologies supporting a safe and fast mobility solution.

1. Introduction

Automated driving technologies have been spotlighted in recent years. Safety systems and applications are the core of the automated driving technology because safety is a critical value when a new transportation mode is deployed in reality. This emphasis on safety could reduce mobility on roadways due to frequent decelerations against projected dangers, indicating that there is a tradeoff between safety and mobility. To reduce this tradeoff and enhance the performance of automated driving technology in both safety and mobility, this study adopts an emergency vehicle (hereafter "EMV") as a representative traffic application that needs to achieve both mobility and safety at the same time. The emergency vehicles such as ambulances and police vehicles should reach the designated destinations fast and safe.

By focusing on the importance of EMVs, some previous studies developed traffic signal preemption strategies by manipulating traffic signal parameters in order to provide an exclusive passage to EMVs [1–4]. The recent studies took advantage of the wireless communications technology such as vehicle-to-vehicle (V2V) and vehicle-to-infrastructure (V2I) communications (hereinafter "V2X") in order to transmit the EMV's location information to traffic signal controllers in advance to reach the intersections. Based on these examples, it is expected that support from road infrastructure such as V2X communications and traffic signal controls can facilitate the operation of EMVs [5–8].

To sum up, this study takes advantage of the automated driving technology at the individual vehicle level and the traffic signal preemption strategy at the traffic infrastructure level in order to develop the automated EMV control strategy and ultimately to facilitate mobile and safe control of automated vehicles. Hence, this study develops the integrated EMV control algorithm and investigates the impacts of the EMV algorithm on mobility and safety using multiple driving aggressiveness scenarios. Furthermore, this study takes the optimum driving parameters set concerning mobility and safety performance measures into consideration.

2. Literature Review

2.1. Automated Vehicle Control Models. Vehicle automation has seen unprecedented development in the recent years. Levinson et al. [9] have shown the system structure and control algorithms of an automated vehicle. In order to simulate it in a microscopic traffic simulation context, the simulated vehicle has to imitate the automated vehicle's longitudinal and lateral movement behavior. In terms of longitudinal control or car-following behavior, unlike a human driver, who has a control variance, often modeled by Wiedemann74 model [10] or Gipps model [11], automated vehicles have almost zero latency and control variance. Kesting et al. [12] have presented the Enhanced Intelligent Driver Model (EIDM), which represents the car-following behavior of a vehicle with adaptive cruise control (ACC). Based on Kesting et al.'s EIDM, the following vehicle adjusts its acceleration based on the leading vehicle's speed, acceleration, distance, and its own speed, maintaining an acceptable following distance.

In terms of lateral control or lane change behavior, there are less intensive researches on this topic. Within traffic simulations, lane changes are modeled using a rule-based decision process [13], which looks into the necessity, possibility, and benefit of a proposed lane change action. Kesting et al. [14] proposed another gap based lane change model, which aims at minimizing breaking distance. This model, though, assumes that other vehicles in the vicinity follow the Intelligent Driver Model [15]; thus it is unsuitable for lane change decision-making, where nearby vehicles adopt a car-following behavior based on the Wiedemann model. Naranjo et al. [16] have presented a lane change mechanism based on fuzzy logic; it provides a smooth transition from one lane to another, whereas it assumes a relatively static nearby vehicle movement. Recent studies have moved to using neural networks to address this issue; Ulbrich and Maurer [17] propose a probabilistic decision network for the tactical lane change decision process. Two independent signal processing networks have been proposed to assess the nearby vehicles in different regions of interests (ROI). The output is the probability for whether a lane change is possible and the probability for whether a lane change is beneficial.

2.2. Traffic Signal Preemption. The first electric traffic signal was installed in 1914 in Cleveland and was equipped with a manual switch for firemen, which led to red signals in all approaches to facilitate the passage of the fire engine [18]. Beyond this manual signal preemption operation, three main technologies for automatic detection of emergency vehicles at signalized intersections have evolved and are used in practice. The first technology in use is based on the siren sound that is detected with directional microphones in order to determine the direction from which the emergency vehicle is approaching [3]. The second technology is based on emission of light or infrared strobes by the emergency vehicles that are detected by dedicated detectors located at the signal head. A third technology is based on radio transmission, which requires a separate technology for the positioning of the vehicle such as GPS or infrared beacons.

With Dedicated Short Range Communication (DSRC), a new technology is arising, which takes the radio based communication to a new level with higher bandwidths allowing an exchange of information with increasing volume. The evolving standards [19, 20] foresee data elements for Signal Request Messages (SRM) as well as a Signal Status Message (SSM) acknowledging the request. Furthermore, Emergency Vehicle Alerts (EVA) can be broadcasted by emergency vehicles to other road users in the vicinity in order to raise their awareness.

These novel functionalities are investigated in several research projects with different signal control algorithms including ImFlow [21] and Multi-Modal Intelligent Transportation Signal System (MMITSS) with its application Emergency Vehicle Priority (PRE-EMPT) [22].

3. Methodology

3.1. Study Assumption. This study develops the EMV control strategy by integrating automated driving technology and the existing traffic signal preemption strategy. While the EMV control strategy proposed in this study adopts state-of-the-art technologies, some technical assumptions are made in this study as follows:

(i) The EMV is equipped with a GPS device, capable of positioning the vehicle's location

(ii) The EMV is equipped with an on-board unit (OBU), capable of V2X communication

(iii) The EMV is equipped with vehicle sensors, capable of detecting adjacent vehicles

(iv) Traffic signal controllers in this road network are equipped with roadside units (RSU), capable of receiving the EMV's wireless transmission

In addition to the assumptions on technical requirements, further assumptions were made in terms of the EMV's driving maneuver as follows: the EMV has a desired speed of 100 km/h; the EMV drives within a normal driving concept, and no special right-of-way (ROW) is allowed to the EMV. For example, the EMV follows traffic signals, drives only within a lane, and is not allowed to drive on a contraflow lane; and adjacent vehicles respond to the EMV in a normal way based on the VISSIM's off-the-shelf car-following behaviors and do not take evasive maneuvers (e.g., stopping and evasive road

departure) against the EMV. This is because this study focuses on the utilization of automated driving controls for the purposes of both mobility and safety, rather than the specific driving maneuvers of EMV. In other words, this study removes other external impacts such as the EMV's special ROW and the normal vehicles' evasive maneuvers and only investigated the EMV's maneuver scenarios by different setting of automated driving control parameters.

3.2. Automated Driving Controls. An Enhanced Intelligent Driver Model (EIDM) is used for the vehicle's longitudinal control; for the vehicle's lateral control, a probabilistic lane change decision process is implemented. A set of aggressiveness levels are defined in order to evaluate the mobility and safety impact of driving strategies according to these levels.

3.2.1. Longitudinal Behavior Model. In order to model the car-following behavior of an automated vehicle, one needs to be aware of the significant differences from a human driver. Automated vehicles, compared to cars with human drivers, can be assumed to have zero reaction time, zero control variance, and no loss of attention.

The EIDM [17] is a time-continuous car-following model representing the ACC driving behavior; it also serves as the basis of an ACC implementation of real vehicles. The model extends the Intelligent Driver Model (IDM) presented by Treiber et al. [15] with a constant-acceleration heuristic (CAH). This avoids the formerly observed, sometimes unrealistic, behaviors in noncritical braking situations, for example, when a car changes lanes in front of another vehicle, causing the gap to be less than desired. The EIDM has inherited IDM's intuitive behavioral parameters: desired velocity, acceleration, comfortable deceleration, and desired minimum time headway.

The CAH and EIDM are given in the following equations:

$$a_{\mathrm{CAH}}(s, v, v_l, a_l) = \begin{cases} \dfrac{v^2 \tilde{a}_l}{v_l^2 - 2s\tilde{a}_l + \varepsilon}, & \text{if } v_l(v - v_l) \leq -2s\tilde{a}_l, \\ \tilde{a}_l - \dfrac{(v - v_l)^2 \Theta(v - v_l)}{2s}, & \text{otherwise,} \end{cases} \tag{1}$$

$$a_{\mathrm{EIDM}} = \begin{cases} a_{\mathrm{IDM}}, & \text{if } a_{\mathrm{IDM}} \geq a_{\mathrm{CAH}}, \\ (1 - c)a_{\mathrm{IDM}} + c\left[a_{\mathrm{CAH}} + b \tanh \dfrac{a_{\mathrm{IDM}} - a_{\mathrm{CAH}}}{b}\right], & \text{otherwise.} \end{cases} \tag{2}$$

The CAH determines the maximum acceleration a_{CAH} leading to no crashes. "The condition $v_l(v - v_l) \leq -2sv_l(v - v_l) \leq -2s\tilde{a}_l$ is true if the vehicles have stopped at the time the minimum gap $s = 0$ is reached" [12]. The Heaviside step function $\Theta(x)$ is used for eliminating negative approaching rates. The term $\tilde{a}$ is the minimum value of a and a_l, which are the accelerations of the subject vehicle and the leading vehicle, respectively, and ε is an extremely small number to prevent the denominator from being equal to zero. The acceleration of the ACC vehicle is expressed by a_{EIDM}. This again has two cases; only if the acceleration computed by the IDM is unrealistic is the second term in equation (2) used. The parameter c of this formula is a "coolness factor," which determines the weights placed on CAH and IDM.

Finally, the parameters are set as follows:

(i) Desired speed (v_0): 100 km/h
(ii) Free acceleration exponent (δ): 3
(iii) Desired time gap (T): 0.5 s
(iv) Minimum standing distance (s_0): 2.0 m
(v) Maximum acceleration (a): 4.2 m/s^2
(vi) Desired deceleration (b): 4.0 m/s^2
(vii) Coolness factor (c): 0.99

In order to demonstrate the difference between the EIDM and the Wiedemann model, which is the default car-following model in VISSIM, a testing scenario is created to reveal the responses given by the two models to a leading vehicle. The leading vehicle in this case uses the Wiedemann model and is placed 100 meters ahead of the subject vehicle to test the behavior in car following. The leading vehicle would undergo several changes of desired speeds. The reactions of the subject vehicle using different models are illustrated in Figure 1. The EIDM vehicle indicates higher maximum speeds and smoother accelerations/decelerations.

3.2.2. Lateral Behavior Model. As in Ulrich and Maurer [17], two signal processing networks are used to determine if a lane change is possible and beneficial with probabilistic outputs. These two signal processing networks were used as part of a neural network model; however, in this paper, the signal processing networks are implemented as the solo criteria for lane changing decisions with predefined thresholds.

The signal processing networks comprise two parts: a network for "lane change possible" decision process and a network for "lane change benefit" decision process. The lane

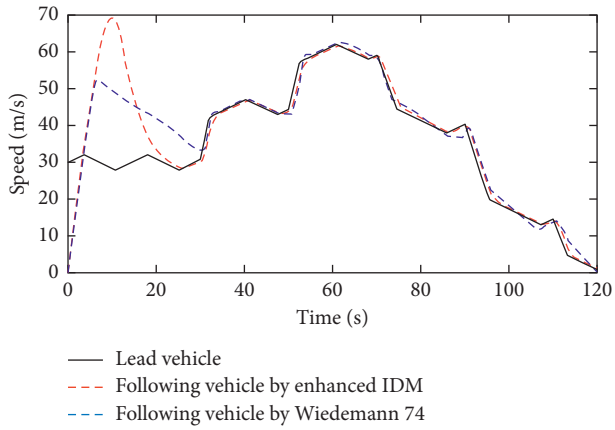

Figure 1: Comparison of car-following models.

change possibility is based on the dynamic vehicle in front of the subject vehicle on its own lane, the vehicle in front of the subject vehicle on its neighbor lane, and the vehicle behind the subject vehicle on its neighbor lane. The lane change benefit considers the direct front vehicle on the same lane and the front vehicle on the neighbor lane. If any front vehicle does not exist, then the benefit probability is set to zero directly. Note that only a 2-lane street is considered in the case study.

A threshold for each signal network is given based on aggressiveness levels, which dictates when a lane change action should be executed. This signal network considers relative distances, relative velocities, and time to collision with nearby vehicles around the subject vehicle.

The signal processing network for calculating an aggregated probability measurement to determine whether a lane change is possible is a mathematical calculation, aggregating each situation in the regions of interest (ROI). Each situation expresses its own possibility of performing a lane change on a scale from zero to one. The final result indicates the aggregated possibility. If no object exists in the ROI, the likeliness that a lane change is possible is directly set to 1. If an object does exist, then a series of cumulative Gaussian distributions translate the numeric values of the object attributes into a specific number value in the scale of zero and one, based on μ and σ given in each distribution. Object attributes include speed, distance, time gap (t = distance/v_{ego}), and time to collision (TTC = distance/($v_{\text{obj}} - v_{\text{ego}}$)). After calculating all the cumulative distribution functions, the intermediate results are aggregated into one measurement to represent a particular ROI, and finally a minimal value is selected from all ROI as the final probability for "lane change possible."

3.2.3. Driving Aggressiveness Settings. Driving aggressiveness can be defined with different parameter sets for the car-following and lane change models. The strategy in defining these driving aggressiveness levels was to make the EMV proactively take lane changes under maximum allowable maneuvering capacity. Therefore, the car-following parameters (i.e., desired time gap λ_T, maximum acceleration rate λ_a, and desired deceleration rate λ_b) were set at maximum as follows in order to allow a full driving capacity of the EMV:

(i) Desired time gap (λ_T): 0.5 seconds

(ii) Maximum acceleration rate (λ_a): 4.2 m/s^2

(iii) Desired deceleration rate (λ_b): 4.0 m/s^2

The aggressiveness levels were thus defined with different lane change criteria (i.e., lane change possibility and benefit probabilities), and the lane change possibility and benefit probabilities were assumed to be realistic in the range of 20% and 80%. The rationale of this boundary is based on the following assumptions: lane changes happen too frequently if the lane change criteria are set to happen when both the possibility and benefit probabilities are lower than 20%, and, in contrast, no lane changes would occur if the lane change criteria are set to happen when both the possibility and benefit probabilities are higher than 80%. Therefore, the driving aggressiveness levels were set with 16 different combinations of four different lane change possibility probability criteria (20%, 40%, 60%, and 80%) and four different lane change benefit possibility criteria (20%, 40%, 60%, and 80%). Figure 2 shows the selection concept of driving aggressiveness levels. The "20% of possibility probability and 20% of benefit probability" criteria scenario represents the most aggressive driving maneuver, while lane changes happen in the most conservative manner in the "80% of possibility probability and 80% of benefit probability" criteria scenario.

3.3. Signal Preemption. An emergency vehicle signal preemption (EVSP) strategy is designed to provide a signal priority to EMVs approaching a signalized intersection. The general logic of EVSP operates with the following processes: a request for preferential signal is transmitted to a traffic signal controller located at a specific intersection, when an EMV approaches the signalized intersection; once the signal controller receives the signal from the EMV including its location, the controller initiates the preset EVSP program; the EVSP program estimates the appropriate timing for green indication by estimating the queue discharge time and the arrival time of the EMV based on the EMV's location information; and the EVSP program provides green signal to the EMV's approach at the estimated timing in order for the EMV to pass through the intersection without delay.

This study adopted a coordinated dynamic traffic signal preemption strategy taking advantage of Intelligent Transportation Systems (ITS) technologies [2]. Basic criteria of EVSP are to make EMVs pass through a signalized intersection without delay and to minimize the side effect of EVSP on the other traffic. To meet these criteria, the green signal should be indicated at the effective timing after the queued vehicles and the moving vehicles are discharged. The EVSP in this study utilizes the dynamic notification time concept as shown in Figure 3 by estimating the remaining time for the EMV to arrive at the intersection.

To this end, the notification time is estimated based on switchover time, queue discharge time, and safety time

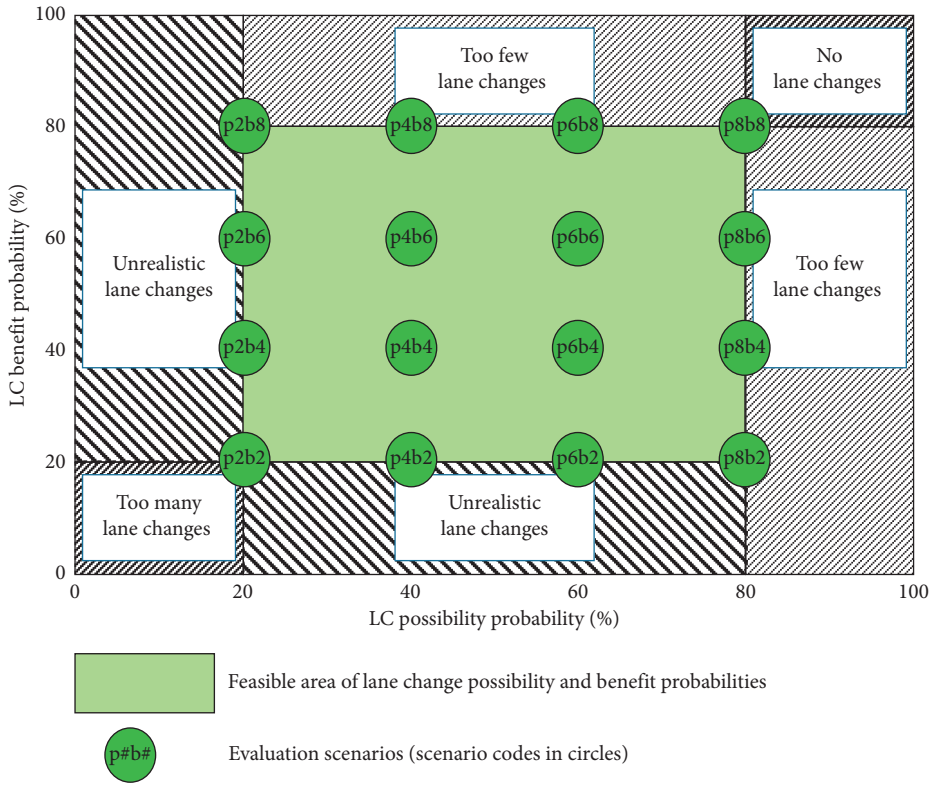

Figure 2: Descriptive concept of the evaluation scenarios.

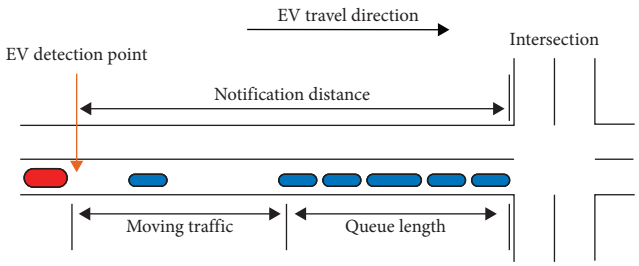

Figure 3: Dynamic notification distance based on queue length.

interval, as shown in equation (3). The switchover time is the sum of inter-green time and minimum green time; the discharge time is the amount of time required for queued traffic to be discharged; and the safety time interval is a time interval between the last queued vehicle and the EMV assuring a fluent passage and safety of the EMV. The safety time interval is assumed to be 3 seconds in this study.

$$\text{Notification time} = \text{switchover time} + \text{discharge time} + \text{safety time interval}. \quad (3)$$

3.4. Simulation Implementation

3.4.1. Traffic Simulation Model. To implement and evaluate the EMV control strategy proposed in this study, a microscopic traffic simulation approach is applied. VISSIM 10.0 [23] was selected due to its extensive capability of modeling traffic situations and implementing automated vehicle controls. VISSIM provides a component object model (COM) interface, which facilitates traffic controls based on the user's specific logic using programming languages. In addition, VISSIM also provides a driver model DLL file enabling users to interrupt off-the-shelf driver behavior logics in VISSIM and control vehicles as programmed and a vehicle actuated programming (VAP) module to manipulate traffic signal timings based on the detectors' information and the user's logic. Regarding the fact that the EMV control strategy in this study requires not only modeling of base traffic situations but also signal preemption and automated driving controls, VISSIM is an appropriate simulation software for the experiments in this study.

3.4.2. Network Modeling. The EMV control strategy proposed in this study was implemented and tested in a microscopic traffic simulation network representing the Frankfurter Ring road section, located in the city of Munich, Germany. The selected road section has three signalized intersections where Schleissheimer Str., Knorrstr., and Ingolstaedter Str. (from left) intersect. The stretch of this simulation network is 4.18 km from the west-most point to the east-most point, and the network was built using VISSIM as shown in Figure 4.

Data collection was made by Automatic Number Plate Recognition (ANPR) and manual measurements in order to build and calibrate a simulation network. The measurements took place from 8 AM to 9 AM on October 27, 2014, and each ANPR camera was located on the Frankfurter Ring road, while the other side roads were manually observed. In

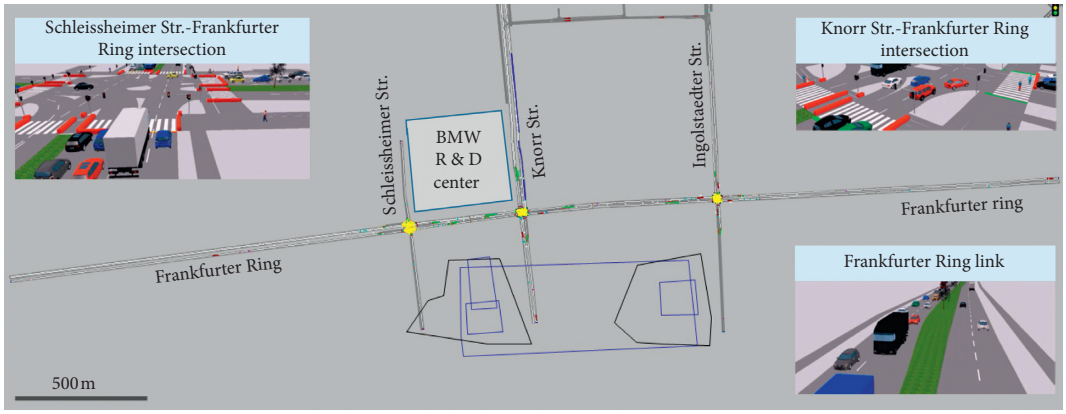

Figure 4: Frankfurter Ring VISSIM network.

addition, road geometry and traffic signal timing plan data were provided by the city of Munich. Finally, traffic volume, speed, travel time, and signal timing parameter data were collected, and these were used to build and calibrate the VISSIM network [24].

The model was calibrated and validated by adjusting car-following parameters in order to assure the model's reliability representing actual traffic situations in reality. For the calibrated parameters, standstill distance (CC0), headway time (CC1), following variation (CC2), negative following threshold (CC4), and positive following threshold (CC5) are used and adjusted based on turning counts, queue lengths, and travel times collected in the field [25]. The final model was satisfied with the calibration stopping criteria, since R^2 values were higher than 0.90 in the all measurements (i.e., turning volumes, queue lengths, and travel times) [24]. In addition, the model was fine-tuned using reduced speed areas and desired speed distributions in VISSIM in order to enhance the model's reliability.

3.4.3. Simulation Settings. Twelve simulation runs were made to capture variability in the simulation runs. The number of simulation runs was determined based on the computed sample size, and twelve simulation runs were statistically sufficient to cover the variability of this simulation at a 95% confidence level [26]. The entire simulation period was set to 1,800 seconds, while first 1,200 seconds of warm-up time were used to fill up the network with vehicles and the remaining 600 seconds of simulation period were used to evaluate the impact of the EMV.

3.4.4. Evaluation Settings. A total of 18 scenarios were set to assess the impact of the EMV control proposed in this study as shown in Table 1. Scenario 1 (base) does not implement any special treatment for EMVs, but the EMV is set to drive at 100 km/h by desire. Scenario 2 reflects a treatment at the infrastructure level and utilizes signal preemption for the EMV to pass through intersections without delay.

This scenario represents a conventional signal preemption strategy, which is the state-of-the-art treatment for EMVs in the past years. The other 16 scenarios utilize both signal preemption and automated controls and are set with different driving aggressiveness levels based on the lane change possibility and benefit probabilities, as defined in the previous section.

3.4.5. Driving Aggressiveness Settings. Scenario 3 reflects the most aggressive driving maneuver, which triggers lane changes if both the estimated lane change possibility and benefit probabilities are more than 20%. Scenario 18 represents the most conservative driving maneuver, which triggers lane changes only if the two probabilities are more than 80%. In addition, the EMV entered into the network at a different state of the traffic signal by increasing 10 seconds in each scenario in order to consider the influence of interruption timing in the signal cycle length. Since the intersections in the test-bed network operate with 90 seconds of cycle length, nine times of simulation run were implemented for each evaluation scenario.

3.4.6. Measures of Effectiveness. The impact of the EMV control proposed in this study was evaluated in terms of mobility and safety. The mobility impact was evaluated at both the network-wide level and the individual EMV level; the network-wide average delay was measured for the network-wide impact assessment; and travel time, average speed, and average delay were measured for the individual EMV. For the safety impact assessment, traffic conflicts, a probability of crashes, were estimated using vehicle trajectories extracted from VISSIM. A surrogate safety assessment model (SSAM) [27] is used to compute surrogate safety measures such as time-to-collision (TTC) and post-encroachment time (PET) and estimate traffic conflicts. A TTC value of less than or equal to 1.5 seconds and a PET value of less than or equal to 5.0 seconds were used as the thresholds for identifying traffic conflicts.

4. Analysis and Evaluation

4.1. Driving Maneuver. Average 0.5 lane change occurred in the base and 4 lane changes occurred in the signal preemption scenario. This shows that signal preemption was effective by providing green signal to EMV, while less than

Table 1: Evaluation scenarios.

Scenarios		Scenario code	Signal preemption	Automated driving	
				LC possibility criteria (%)	LC benefit criteria (%)
Scenario 1 (base)		Base	Not applied	—	—
Scenario 2 (signal preemption only)		SP	Applied	—	—
Signal preemption + automated control	Scenario 3	p2b2	Applied	20	20
	Scenario 4	p2b4	Applied	20	40
	Scenario 5	p2b6	Applied	20	60
	Scenario 6	p2b8	Applied	20	80
	Scenario 7	p4b2	Applied	40	20
	Scenario 8	p4b4	Applied	40	40
	Scenario 9	p4b6	Applied	40	60
	Scenario 10	p4b8	Applied	40	80
	Scenario 11	p6b2	Applied	60	20
	Scenario 12	p6b4	Applied	60	40
	Scenario 13	p6b6	Applied	60	60
	Scenario 14	p6b8	Applied	60	80
	Scenario 15	p8b2	Applied	80	20
	Scenario 16	p8b4	Applied	80	40
	Scenario 17	p8b6	Applied	80	60
	Scenario 18	p8b8	Applied	80	80

one lane change occurs if there is no interruption on traffic signal and driving behavior parameters (i.e., base scenario). For the automated control scenarios, 7 lane changes occurred when the lane change criteria were 20% of possibility and 20% of benefit; only 1 lane change occurred when either the lane change possibility criteria or the lane change benefit criteria were 80%; and the other automated control scenarios were between these two cases in the range from 1 time to 7 times, as shown in Figure 5(a). The results seem reasonable because lane changes would hardly occur if the lane change criteria are high (i.e., the most conservative behavior) and frequently occur if the lane change criteria are low (i.e., the most aggressive behavior).

The average speed of the EMV (Figure 5(b)) was the lowest in the base scenario because the EMV had to frequently stop due to red signals (no preemption). Average speed in the preemption scenario was higher than that of the base scenario because of the effective passage by the benefit of signal preemption. In the automated-control-integrated scenarios (i.e., integration of the automated control and the signal preemption), most scenarios showed higher average speed compared to the signal-preemption-only scenario, while the average speed in the conservative driving aggressiveness scenarios, in which the lane change criteria are higher than 60% in either possibility or benefit, was similar to the signal-preemption-only scenario in the range of 5%. This indicates that EMVs can drive faster with reasonable lane changes (i.e., neither too many nor too few lane changes).

The average acceleration rates (Figure 5(c)) were similar in all scenarios, but the ranges of acceleration rates in the base and signal preemption scenarios were a bit smaller than those in the other automated control scenarios. This is because the maximum acceleration rate and the desired deceleration rate were set at maximum in the automated control scenarios in order to allow a full driving capacity of EMV.

4.2. Mobility Impact. Based on delay and travel time measurements (Figures 6(a) and 6(b)), the EMV was faster than the other normal vehicles (i.e., black dots mean average delay of normal vehicles) in the range from 66.7% to 87.7%. Particularly, the "p2b4" scenario was the best and had 35.2% less delay compared to normal vehicles; the "p2b2," "p2b6," "p2b8," and "p4b2" scenarios followed (less delay in the range from 35.3% to 40.8% compared to normal vehicles); and the EMVs of the automated control scenarios that were set with 80% of lane change possibility or benefit criteria showed a better performance than the base scenario in terms of delay and travel time, but the performance was not significant compared to the other automated control scenarios. This is because EMV was relatively steady in the conservative scenarios and travelled with less lane changes in response to sluggish vehicles in forward.

4.3. Safety Impact. Traffic conflicts varied in the range from 1,184 to 1,438 in the network as shown in Figure 6(c), and the impact of automated vehicle control in the entire network appeared to be insignificant in terms of safety. Meanwhile, the automated vehicle control decreased traffic conflicts, since the numbers of conflicts involving EMV ranged from 4.4 to 7.6 in the automated control scenarios, while 8.9 conflicts were found in the base scenario.

4.4. Discussion. The findings based on the mobility and safety impact assessment results are discussed as follows:

(i) Increasing desired speed is effective to improve mobility of EMV by approximately 10% (i.e., base); signal preemption is effective for the mobility of EMV; and the integration of a signal preemption (treatment at road infrastructure) and an automated vehicle control (treatment at individual vehicle)

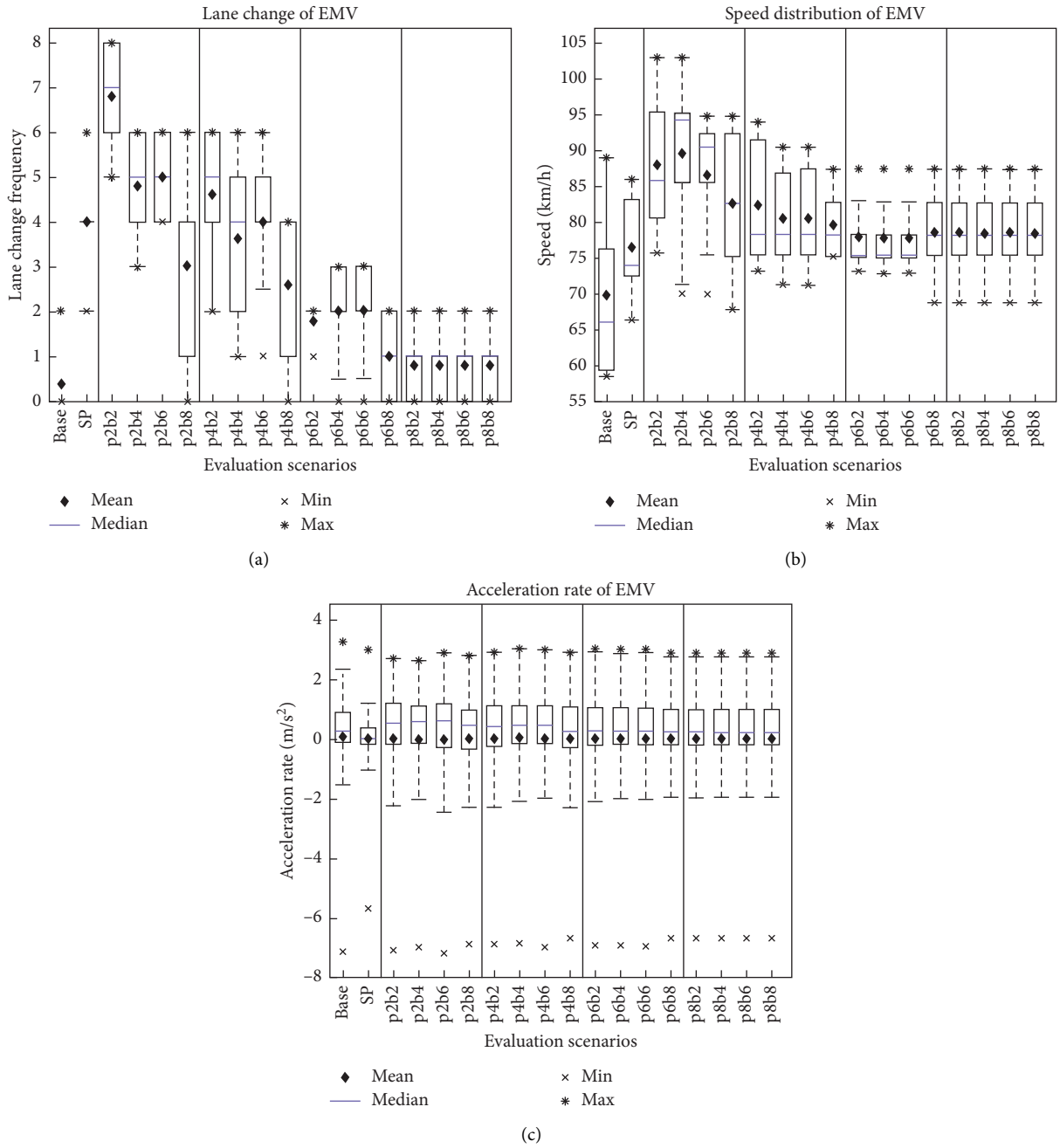

Figure 5: Driving maneuvers. (a) Lane change frequency. (b) Speed. (c) Acceleration rate (m/s^2).

significantly enhances the mobility of EMV by decreasing delay.

(ii) An integrated approach of an automated vehicle control and a signal preemption is beneficial for EMVs to reduce conflicts involving adjacent vehicles, while it does not provide significant side impact in the entire network.

(iii) A signal preemption is beneficial for EMV in terms of mobility and safety, but the impact can be maximized in integration with an automated vehicle control at the individual vehicle level.

(iv) The impact of automated vehicle control varies by different driving aggressiveness levels in terms of mobility and safety. For example, the most aggressive setting resulting in many lane changes performs well in terms of the mobility measures such as travel time and delay, while the most conservative setting resulting in few lane changes performs well in terms of safety. Therefore, the impact of automated vehicle control can be maximized with reasonable level of the driving aggressiveness setting (i.e., lane change criteria in this study) in consideration of both mobility and safety.

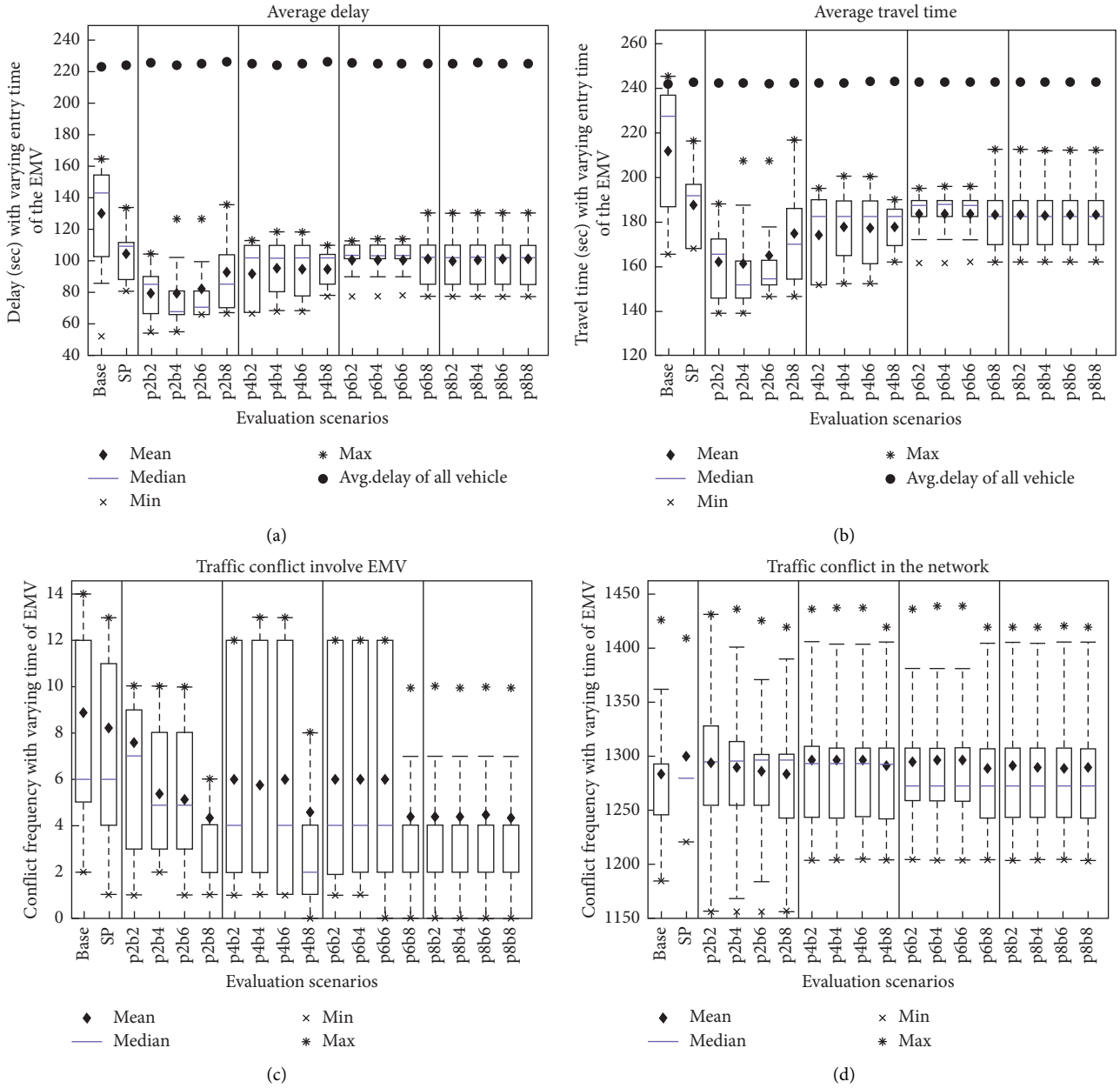

FIGURE 6: Safety and mobility assessment results. (a) Mobility measure, delay. (b) Mobility measure, travel time. (c) Safety measure, network-wide. (d) Safety measure, only EMV.

(v) The impacts on mobility and safety do not seem perfectly linear by the lane change parameter scenarios (16 parameter settings). This is because lane changes barely occurred when either the "benefit" parameter or the "possibility" parameter was set as 80%, which is conservative. On the other hand, lane changes frequently occurred when either the "benefit" parameter or the "possibility" parameter was set as 20%. This is the main reason behind the relationship between the parameter settings and the performance measures, but the other scenarios except the extreme settings appeared somewhat linear in the mobility and safety measures.

In order to find the reasonable level of the driving aggressiveness setting following the last finding in the above discussion, the optimum driving aggressiveness setting of EMV was captured in terms of mobility and safety. Figure 7 shows the performances of different EMV driving aggressiveness settings in two dimensions with the mobility and safety measures. Each data point represents the performance of each evaluation scenario including base, signal preemption, and 16 automated-control-integrated scenarios having different driving aggressiveness levels. In the most aggressive setting, the EMV can save approximately 20% of travel time compared to the p8b8 scenario (the most conservative setting), but 50% of traffic conflicts more occurred in the

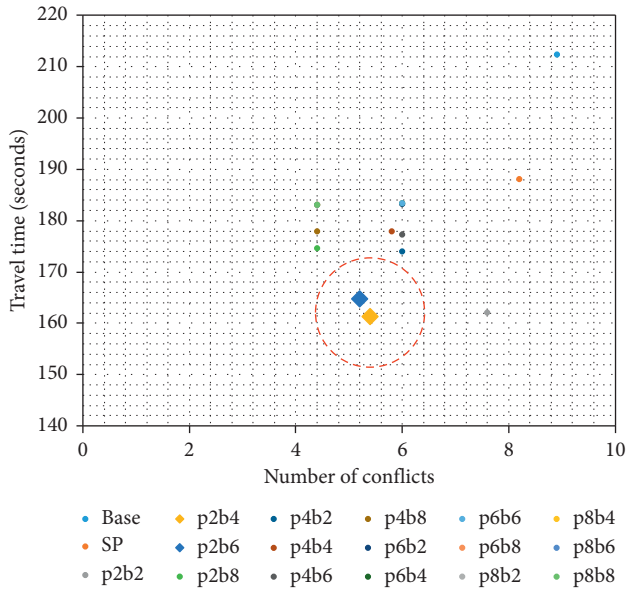

Figure 7: Multiobjective scatter plot.

p2b2 scenario (the most aggressive setting) compared to the most conservative setting. Although it could be still disputed what setting would be relevant for EMV, "p2b4" and "p2b6" settings (i.e., automated control in cooperation with signal preemption) appeared to be the most effective driving aggressiveness settings for EMV as the optimum driving aggressiveness setting in terms of both mobility and safety, which is the main objective of this study.

5. Conclusions

This study proposed an integrated approach of a signal preemption as the infrastructure-level traffic treatment and an automated driving control as the vehicle-level treatment in order to maximize the utilities of vehicle control including mobility and safety. Emergency vehicles (EMVs) such as ambulances and police vehicles were selected to implement this integrated vehicle control approach because the EMVs primarily need to reach their destinations fast and safe. Therefore, the integrated EMV control approach was developed based on the V2X wireless communications-based signal preemption strategy and the EIDM-based automated driving control, and the impacts of this automated EMV application were assessed with 16 different lane change aggressiveness levels (i.e., 16 different combinations of four lane change possibility criteria and four lane change benefit criteria) using a microscopic traffic simulation model. The measures of effectiveness included the driving maneuvers (lane change frequency, speed, and acceleration rate), the mobility measures (i.e., delay and travel time), and the safety measure (i.e., traffic conflicts).

The results showed that both the signal preemption and the automated driving control were beneficial to facilitate the EMV control in terms of mobility and safety, while they did not significantly provide negative impacts on adjacent normal vehicles. Importantly, the performance of the EMV was maximized when these two approaches were implemented at the same time. The results showed that the integrated approach was effective for the EMV to maintain its preset desired speed (i.e., 100 km/h) by providing a green passage at the signalized intersections and overtaking the lead vehicles driving in front of the EMV. In addition, the impact of automated vehicle control varies by different driving aggressiveness levels in terms of mobility and safety; aggressive settings having many lane changes performed well in terms of mobility, and the case was the opposite in terms of safety; and conservative settings having few lane changes were beneficial for safety, and the case was the opposite in terms of mobility. Therefore, these study results emphasize that the benefit of emergency vehicle control strategy can be maximized when the signal preemption and the reasonable levels of automated driving control settings operate in collaboration.

Nevertheless, this study should be enhanced with realistic behaviors of EMV and the other adjacent behaviors. Due to technical limitations on simulation modeling, this study was made with some assumptions that no special right-of-way (e.g., passing on red and driving on a contraflow lane) is allowed for EMV and adjacent vehicles do not take evasive maneuvers such as stopping and evasive road departure. Furthermore, the reasonable aggressiveness settings of automated driving control should be more investigated and validated through further studies. Besides, experimenting with additional scenarios including different traffic conditions and different penetration rates of other/adjacent vehicles would help to validate the results and findings of this study.

However, this study showed benefits of the integrated approach of the automated driving technology at the individual vehicle level and the traffic signal preemption strategy at the traffic infrastructure level. In addition, this study showed potentials of automated driving controls: not only the safety aspect but also the mobility aspect. Therefore, this study will be a great reference and a starting point of discussion toward advanced automated driving technologies supporting not only safe but also fast mobility solution.

Data Availability

All experimental data (i.e., vehicle trajectories including $x/y/z$, speed, and acceleration rate) used to support the findings of this study are available from the corresponding author upon request.

Conflicts of Interest

The authors declare that there are no conflicts of interest regarding the publication of this paper.

Acknowledgments

The authors thank researchers and colleagues of the Korea Transport Institute and the Chair of Traffic Engineering and Control at the Technical University of Munich for their sincere supports and advices. The first author especially thanks Mr. Liangyuan Tian (TED) for his sincere work in

developing source codes for the automated vehicles simulation. It should be also noted that this work was supported by the Institute for Information & Communications Technology Promotion (IITP) grant funded by the Korea Government (MSIT) (no. 2017-0-004000, development of 100 Mbps grade V2X and LTE communication system for cooperative driving).

References

[1] P. Koonce, *Traffic Signal Timing Manual*, Federal Highway Administration, Washington, DC, USA, 2008.

[2] X. Qin and A. M. Khan, "Control strategies of traffic signal timing transition for emergency vehicle preemption," *Transportation Research Part C: Emerging Technologies*, vol. 25, pp. 1–17, 2012.

[3] Federal Highway Administration, *Traffic Signal Preemption for Emergency Vehicle a Cross-Cutting Study*, US Federal Highway Administration, Washington, DC, USA, 2006.

[4] I. Yun, M. Best, and B. "Brian" Park, "Evaluation of transition methods of the 170E and 2070 ATC traffic controllers after emergency vehicle preemption," *Journal of Transportation Engineering*, vol. 134, no. 10, pp. 423–431, 2008.

[5] Y.-J. Lee, S. Dadvar, J. Hu, and B. B. Park, "Transit signal priority experiment in a connected vehicle technology environment," *Journal of Transportation Engineering, Part A: Systems*, vol. 143, no. 8, Article ID 05017005, 2017.

[6] Z. Li et al., "Intersection control optimization for automated vehicles using genetic algorithm," *Journal of Transportation Engineering, Part A: Systems*, vol. 144, no. 12, Article ID 04018074, 2018.

[7] Z. Lu, Q. Zhang, and X. Liu, "A formulation method of control protocol for intersection signal based on wireless communication technologies," in *Proceedings of the ICTIS 2013: Improving Multimodal Transportation Systems-Information, Safety, and Integration*, pp. 78–83, Wuhan, China, June 2013.

[8] K. Hou and J. Hu, "Vehicular networks communication analysis and speed guidance at signalized intersections," in *Proceedings of the International Conference on Transportation and Development*, Pittsburgh, PA, USA, July 2018.

[9] J. Levinson, J. Askeland, J. Becker et al., "Towards fully autonomous driving: systems and algorithms," in *Proceedings of the Intelligent Vehicles Symposium (IV)*, IEEE, Dearborn, MI, USA, June 2011.

[10] R. Wiedemann, *Simulation des Straßenverkehrsflusses*, Schriftenreihe des Instituts für Verkehrswesen der Universität Karlsruhe, Karlsruhe, Germany, 1974.

[11] P. G. Gipps, "A behavioural car-following model for computer simulation," *Transportation Research Part B: Methodological*, vol. 15, no. 2, pp. 105–111, 1981.

[12] A. Kesting, M. Treiber, and D. Helbing, "Enhanced intelligent driver model to access the impact of driving strategies on traffic capacity," *Philosophical Transactions of the Royal Society A: Mathematical, Physical and Engineering Sciences*, vol. 368, no. 1928, pp. 4585–4605, 2010.

[13] PTV, *PTV VISSIM 7 Introduction to the COM API*, PTV, Islamabad, Pakistan, 2015.

[14] A. Kesting, M. Treiber, and D. Helbing, "General lane-changing model MOBIL for car-following models," *Transportation Research Record: Journal of the Transportation Research Board*, vol. 1999, no. 1, pp. 86–94, 2007.

[15] M. Treiber, A. Hennecke, and D. Helbing, "Congested traffic states in empirical observations and microscopic simulations," *Physical Review E*, vol. 62, no. 2, pp. 1805–1824, 2000.

[16] J. E. Naranjo, C. Gonzalez, R. Garcia, and T. de Pedro, "Lane-change fuzzy control in autonomous vehicles for the overtaking maneuver," *IEEE Transactions on Intelligent Transportation Systems*, vol. 9, no. 3, pp. 438–450, 2008.

[17] S. Ulbrich and M. Maurer, "Probabilistic online POMDP decision making for lane changes in fully automated driving," in *Proceedings of the 16th International IEEE Conference on Intelligent Transportation Systems (ITSC 2013)*, IEEE, The Hague, The Netherlands, October 2013.

[18] E. A. Mueller, "Aspects of the history of traffic signals," *IEEE Transactions on Vehicular Technology*, vol. 19, no. 1, pp. 6–17, 1970.

[19] SAE, *J2735 Dedicated Short Range Communications (DSRC) Message Set Dictionary*, SAE, Warrendale, PA, USA, 2015.

[20] ETSI, *TS 103 301 Basic Set of Applications; Facilities Layer Protocols and Communication Requirements for Infrastructure Services*, ETSI, Sophia Antipolis, France, 2016.

[21] K. Van Vliet and S. Turksma, *ImFlow: Policy-Based Adaptive Urban Traffic Control*, ITS Europe, Dublin, Ireland, 2013.

[22] K. Ahn, H. A. Rakha, K. Kang, and G. Vadakpat, "MMITSS impacts assessment: field testing and simulation results," in *Proceedings of the Transportation Research Board 95th Annual Meeting Transportation Research Board*, Washington, DC, USA, 2016.

[23] PTV VISSIM/VISWALK 10, *PTV AG*, 2017, http://vision-traffic.ptvgroup.com/fileadmin/files_ptvvision/Downloads_N/0_General/2_Products/2_PTV_Vissim/Overview_PTVVissim10_EN.pdf.

[24] G. Grigoropoulos, "Managing the growth and the Transport integration of BMW FIZ future," in *Proceedings of the Transportation Systems Project Seminar*, Technical University of Munich, Munich, Germany, June 2015.

[25] A. A. Rrecaj and K. M. Bombol, "Calibration and validation of the VISSIM parameters-state of the art," *TEM Journal-Technology Education Management Informatics*, vol. 4, pp. 255–269, 2015.

[26] H. D. Robertson, *ITE Manual of Transportation Engineering Studies*, Prentice Hall, Englewood Cliffs, NJ, USA, 1994.

[27] D. Gettman, *Surrogate Safety Assessment Model and Validation: Final Report*, Federal Highway Administration (FHWA), Washington, DC, USA, 2008.

Hindawi
Journal of Advanced Transportation
Volume 2020, Article ID 2593410, 8 pages
https://doi.org/10.1155/2020/2593410

Research Article

Examining the Environmental, Vehicle, and Driver Factors Associated with Crossing Crashes of Elderly Drivers Using Association Rules Mining

Jia Yang,[1] **Keiichi Higuchi**,[2] **Ryosuke Ando**,[1] **and Yasuhide Nishihori**[1]

[1]*Research Department, Toyota Transportation Research Institute, 3-17 Motoshiro-cho, Toyota City, Aichi Prefecture 471-0024, Japan*
[2]*Civil Engineering and Environmental Design Course, Daido University, 40 Hakusui-cho, Minami-ku, Nagoya City, Aichi Prefecture 457-8532, Japan*

Correspondence should be addressed to Jia Yang; yang@ttri.or.jp

Received 10 October 2019; Accepted 7 January 2020; Published 1 February 2020

Guest Editor: Zhibin Li

In the aging society, reducing vehicle crashes caused by elderly drivers has become a crucial issue. To find effective methods to reduce these vehicle crashes, it is necessary to give some insights into the characteristics of vehicle crashes and those of traffic violations caused by elderly drivers. However, multiple significant factors associated with crossing crashes due to elderly drivers were not extensively observed in previous studies. To fill this research gap, this study identifies the crash pattern and examines the environmental, vehicle, and driver factors associated with crossing crashes due to elderly drivers. The 5-year crash data in Toyota City, Japan, are used for empirical analysis. The emerging data mining method called association rules mining is applied to discover various factors associated with crossing crashes of elderly and nonelderly drivers, respectively. The significant findings indicate that (1) elderly drivers are more likely to lead to crossing or right-turn crashes, compared with nonelderly drivers; (2) there are more factors including crash location (intersection without signal), lighting (daylight), road condition (dry and other), weather condition (clear and raining), vehicle type (light motor truck), and traffic violation (fail to confirm safety) associated with the large proportion of crossing crashes due to elderly drivers. The findings of this study can be used by traffic safety professionals to implement some countermeasures to reduce the crossing crashes due to elderly drivers.

1. Introduction

Vehicle crashes due to elderly drivers have been a significant concern for roadway traffic safety issues in Japan. The proportion of vehicle crashes due to elderly drivers has been increased by up to 20%, although the number of vehicle crashes has a trend to decrease from 2005 to 2015 [1]. Moreover, it is reported that population distribution in Japan is shifting toward a more significant representation of elderly people. It is estimated that the proportion of elderly people (≥65 years) is up to 31.6% in 2030, although this figure was 26.8% in 2013 [2]. It is expected that the number of elderly drivers will increase continuously over the next two decades.

Some incentive measures are implemented to ensure the driving safety of elderly drivers in Japan. For example, some local government distributes discount coupons for public facilities or free bus tickets to the elderly drivers who have returned their licenses voluntarily. However, it is reported that elderly drivers are unwilling to return licenses when there are not sufficient public transportation facilities near home, and private cars are indispensable for their daily life. As a result, the return rates of licenses in the metropolis, such as Tokyo and Osaka, are more significant than those in local cities in Japan, where the public transportation system is not sufficient, and many residents are living in suburban areas.

To reduce vehicle crashes due to elderly drivers, Japan National Police Agency has revised the Road Traffic Law and requires drivers older than 74 years who made some particular types of traffic violations to go to hospital for checking their cognitive ability to judge whether they are still

suitable for safety driving or not [3]. These particular types of traffic violations are related to the cognitive problem of elderly drivers. However, it is reported that the number of doctors cannot fulfill the massive demand for cognitive ability diagnosis for elderly drivers, and this demand will increase continuously in the next decade.

As one traditional measure for preventing and reducing vehicle crashes due to elderly drivers, an education program is considered as an ideal and effective way. To make the education program more effective, it is necessary to understand the distinctive crash pattern of elderly drivers compared with nonelderly drivers.

This study aimed to identify the distinctive crash pattern due to elderly drivers compared with nonelderly drivers and examine the environmental, vehicle, and driver factors associated with crossing crashes due to elderly drivers. Here, a crossing crash indicates a broadside collision where the side of one vehicle is impacted by the front or rear of another vehicle, which accounted for the most significant ratio of vehicle crashes due to elderly drivers. The 5-year vehicle crash data from 2009 to 2013 in Toyota City, Japan, are used for empirical analysis. One emerging data mining method called association rules mining is applied to discover various factors associated with crossing crashes of elderly and nonelderly drivers, respectively. Based on the findings of this study, knowledge of crash characteristics such as environmental, vehicle, and driver factors can be used to guide the design of countermeasures to improve the driving safety of elderly drivers.

The remainder of this article is organized as follows. Section 2 gives a brief literature review concerning the crash pattern analysis of elderly drivers and the data mining methodology, including classification trees and association rules mining. Section 3 introduces the association rules mining methodology implemented in this study. Section 4 describes the dataset used for empirical study and the results of fundamental statistical analysis of the different crash patterns between elderly and nonelderly drivers. Section 5 reports the results of association rules mining and discusses the different characteristics of association rules related to elderly and nonelderly drivers. Finally, this study is concluded in Section 6.

2. Literature Review

To propose effective countermeasures to reduce vehicle crashes due to elderly drivers, it is essential to understand the crash types in which they are involved and the circumstances that lead to their crashes. It is known that elderly drivers are overinvolved in angle, overtaking, merging, and intersection crashes, especially on the occasions when elderly drivers were turning left [4]. Meanwhile, elderly drivers are significantly overrepresented in intersection-related crashes. For example, it is reported that between 48% and 55% of fatal crashes involving drivers aged 80 years or older occurred in intersections, more than twice the driver aged 50 or less (23%) [5]. This might result from the fact that age-related cognitive, visual, and physical can impact their ability to perform driving tasks and navigate the types of complicated roadway situations where crashes due to elderly drivers often occur [6].

To propose an effective education program for elderly drivers to prevent vehicle crashes, it is crucial to understand the distinctive crash pattern of elderly drivers compared with nonelderly drivers. Previous studies have indicated that the crash pattern involving elderly drivers is different from that of nonelderly drivers [7, 8]. Elderly drivers are more likely to be involved in the crashes occurring in the intersections without signals, and crossing crashes take the most significant proportion among the crash types. It is well recognized that crossing crashes usually cause severe injury for drivers. To know the reasons for crossing crashes, previous studies have investigated the associated factors of crossing crashes [8–10]. These studies used the crash data to reveal the associated factors of crossing crashes. Based on these findings, we can give some countermeasures to prevent crossing crashes due to elderly drivers.

However, these previous studies were based on the traditional statistical methodology, which has a limited ability to reveal the associated relation between multiple factors and crash patterns. In this study, we are aiming to investigate various factors associated with crossing crashes due to elderly drivers rather than the frequency of crossing crashes. Literature reviews of previous studies using count data models, such as the poison regression or negative binomial regression model, were not illustrated because we are focusing on data mining methodologies used for crash pattern analysis in this study. One vehicle crash is defined as a rare, random, multifactor event always preceded by a state in which road users fail to cope with the current environment, and one crash results from a series of directly or indirectly associated events [11]. Therefore, the emerging data mining methodologies can help us find some valuable insights into the research field of vehicle crash pattern analysis by performing knowledge discovery from a large vehicle crash dataset compared with the traditional statistical methodology.

There are mainly two types of data mining methodologies used in previous studies for crash pattern analysis, namely the classification trees and association rules analysis. The research works using the classification trees can be found in some previous studies [12, 13]. One recent research work implemented by Montella et al. has indicated that from the methodological point of view, both the classification trees and association rules analysis were useful in providing nontrivial and unsuspected relations in vehicle crash analysis. That study concluded that classification trees structure allowed a straightforward understanding of the phenomenon under study. Meanwhile, association rules analysis provided new information hidden in the sample data [14]. Therefore, association rules mining is an ideal methodology because it might help us discover new dependence between various factors and crash patterns based on the vehicle crash data.

Research works applying the association rules mining method to roadway traffic safety problems can be found in some previous studies. For example, Pande and Abdel-Aty developed closely associated crash characteristics in the form of rules based on the association rules mining methodology [15]. Mirabadi and Sharifian applied this methodology to extend knowledge discovery and reveal association patterns of railway crashes in Iran [16]. Montella applied this

methodology to investigate the contributing factors to different crash patterns at urban roundabouts [11]. Based on the literature review, we found that this methodology is seldom applied in the field of crash pattern analysis of elderly drivers.

To find the countermeasures to reduce vehicle crashes due to elderly drivers, it is necessary to investigate the characteristics of the crash pattern of elderly drivers from various viewpoints by the association rules mining methodology, which can help us discover the knowledge behind the crash dataset. For this research motivation, this study applies the association rules mining method to investigate various factors related to crossing crashes of elderly drivers, which was not extensively investigated in most previous studies. The findings of this study can give some insights into significant factors associated with crossing crashes, which can be used in the education program for elderly drivers when they renew driver licenses.

3. Methodology

This study used association rules mining technology to perform the empirical analysis. Recently, this methodology is prevailed and is applied in the research field of traffic safety in previous studies [17, 18]. A brief introduction to this methodology is described here. A more detailed introduction to this methodology can be found in the study proposed by Hahsler et al. [19].

The data mining methodology on the transaction data using the association rules mining was proposed by Agrawal et al. [20]. This methodology is an association discovery approach used to discover the relative frequency of sets of items (i.e., crossing crash in this study) occurring alone and together in a given event (i.e., a crash observation in this study). The rules have the form "$X \longrightarrow Y$" in which X is the antecedent and Y is the consequent. In association rules, each rule can be expressed by three indexes: support, confidence, and lift. Support is the percentage of this rule existing in the dataset. Confidence is the ratio of support to the percentage of the antecedent in the dataset. Lift is a mathematical measurement to quantify the statistical dependence of a rule by the ratio of confidence to the percentage of the consequent. The computation methods of these indexes related to association rules are listed as follows:

$$
\begin{aligned}
S(X) &= \frac{\sigma(X)}{N}, \\
S(Y) &= \frac{\sigma(Y)}{N}, \\
S(X \longrightarrow Y) &= \frac{\sigma(X \cap Y)}{N}, \\
C(X \longrightarrow Y) &= \frac{\sigma(X \cap Y)}{S(X)}, \\
L(X \longrightarrow Y) &= \frac{\sigma(X \cap Y)}{S(Y)},
\end{aligned}
\tag{1}
$$

where $S(X)$ is the support of the antecedent X, $\sigma(X)$ is the number of observations with the antecedent X, $S(Y)$ is the support of the consequent Y, $\sigma(Y)$ is the number of observations with the consequent Y, $S(X \longrightarrow Y)$ is the support of the association rule $\{X \longrightarrow Y\}$, $\sigma(X \longrightarrow Y)$ is the number of observations with the antecedent X and consequent Y, N is the total number of observations in the dataset, $C(X \longrightarrow Y)$ is the confidence of the association rule $\{X \longrightarrow Y\}$, and $L(X \longrightarrow Y)$ is the lift of the association rule $\{X \longrightarrow Y\}$.

The lift of rule indicates the frequency of co-occurrence of the antecedent and the consequent to the expected co-occurrence under the assumption that they are independent. A value smaller than one indicates the contrary between them. A value equal to one indicates independence, and a value more significant than one indicates positive dependence. The higher value of lift indicates greater dependence [21]. The association rule in this study might involve multiple explanatory variables being set as antecedents. As a result, it can discover many valuable relations between single or multiple factors related to crossing crashes due to elderly drivers. A rule with one antecedent and one consequent is defined as a 2-product rule. Just like this, a rule with two antecedents and one consequent is defined as a 3-product rule.

For example, in a rule "violation = disobey stop sign $\longrightarrow$ crossing crash" (support = 2%, confidence = 70%, lift = 3.5), support indicates that percentage of observations, including both violation called disobey stop sign and crossing crash, is 2% in the whole dataset; confidence indicates that the percentage of observations, including both the violation called disobey stop sign and crossing crash, is 70% of the dataset; and lift indicates that violation called disobey stop sign is positively associated with crossing crash.

To implement this data mining technology, the apriori algorithm proposed by Agrawal and Srikant is applied in this study, which is a level-wise, breadth-first algorithm counting transactions [22]. Free statistical software R has a package called "arules" to make an analysis of association rules mining using this algorithm.

4. Data Preparation

This study used 5-year of vehicle crash records (2009–2013) obtained from the Traffic Safety and Crime Prevention Division, Social Affairs Department of Toyota City. The data were stored in a sorted format by occurring time in Microsoft Excel worksheet tables. Vehicle crash records in this study are the injured crash data, in which there was at least one person involved was injured. In the sample data, a vehicle crash is indicated in two rows in a table, in which each row records one actor in a vehicle crash. Here, the definition of one actor indicates a driver, a pedestrian, or an object. Meanwhile, two records are sorted by the severe level of fault: the order of the first actor and the second one. Each crash record had many attributes describing timestamp, environmental factors, traffic conditions, and driver characteristics. This study

only prepared a dataset, including the crash record of the driver who had higher faults, i.e., records of the first actor. Here, data of the second actor were excluded from the sample data because this study aimed to investigate the main contributor (the driver with a higher fault level) to a vehicle crash. Meanwhile, only crashes occurring in intersections or segments were used in this study because crossing crashes rarely occur in other locations such as the parking lot or square.

The total number of the sample data in this study is 9,706 (from 2009 to 2013), including 1,313 crashes due to elderly drivers (≥65 years old) and 8,393 crashed due to nonelderly drivers (<65 years old). Figure 1 illustrates the spatial distribution of vehicle crashes in Toyota City due to elderly and nonelderly drivers, respectively. It indicates that most crashes occurred in the urban area of Toyota City. This might indicate the trend that the level of social activities is higher in areas with a dense population, which leads to an increased risk of accidents [23].

The vehicle crash database contains many attributes related to the detail of crashes. We conducted a detailed literature review to investigate significant factors associated with the traffic violation and the crash type. Vehicle crashes of elderly and nonelderly drivers were examined in terms of frequency of the location, environmental, vehicle, and driver factors that were involved to know which factors were more likely to characterize the crash pattern of elderly drivers. Table 1 lists descriptive statistics of significant variables.

Location: Elderly drivers were not surprisingly, significantly more likely to crash in intersections without signal, consistent with the fact that they are the dangerous parts of the network because they present a driver with many points for possible conflict with other road users, often at high speeds and with minimal time to respond, and a lack of adequate in-vehicle crashworthiness opportunities [24]. By contrast, nonelderly drivers were significantly involved in crashes occurring in the segment. It might indicate that the driving region of nonelderly drivers is broader than that of elderly ones, and the risk of crashes occurring in the segment is increased.

Environmental factors: Elderly drivers were significantly more likely to crash in the lighting of daylight, whereas nonelderly drivers were more likely to crash in the lighting of night. Meanwhile, there were no significant differences between elderly and nonelderly drivers in the road condition or weather conditions being present when crashes occurred.

Vehicle factor: Elderly drivers were significantly more likely to cause crashes of light motor trucks, whereas nonelderly drivers were significantly more likely to cause crashes of ordinary motor trucks. This significant difference between elderly and nonelderly drivers might indicate that the primary purpose of driving ordinary motor trucks is transporting industrial commodities, which are seldom used by elderly drivers after retirement. By contrast, it is inferred that elderly drivers are more likely to drive light motor trucks for agricultural works in suburban areas of Toyota compared with nonelderly drivers.

Driver factor: For the traffic violation that was attributed to the cause of crashes, elderly drivers were significantly likely to fail to confirm safety, while nonelderly drivers were likely to be inattention. These differences might indicate that elderly drivers are paying attention to drive. However, they are likely to fail to confirm safety due to aging effects. For the type of crashes, elderly drivers were significantly likely to cause crossing or right-turn crashes, whereas nonelderly drivers were likely to cause rear-end crashes, consistent with the previous study [8].

To summarize, the crashes of elderly and nonelderly drivers differenced in location, lighting, vehicle type, traffic violation, and the type of crash. Elderly drivers are more likely to crash in intersections without signals and in the lighting level of daylight. They are also more likely to cause crashes of light motor trucks, make traffic violations in which they failed to confirm safety and be involved in crossing, and right-turn crashes.

5. Results and Discussion

This study used a package of "arules" in open-source statistical software R to conduct the association analysis [19]. To understand the difference between elderly and nonelderly drivers, we applied this methodology to sample data of them. The association rules of environmental, vehicle, and driver factors with crossing crashes are extracted from the generated rules using the apriori algorithm. Creating association rules for elderly and nonelderly drivers includes 5 steps: (1) generate rules with equal to or more than 2 items, (2) determine threshold values, (3) eliminate the rules with lift values outside the threshold, (4) eliminate the rules that have both support and confidence values lower than the thresholds, and (5) eliminate the redundant rules referring to the items of the antecedent. To find the association rules highly related to crossing crashes of elderly and nonelderly drivers, the threshold value for support is set to be 1% and that for confidence is set to be 70%.

The association rules of environmental, vehicle, and driver factors and crossing associated with crashes for elderly and nonelderly drivers are listed in Table 2. As the first rule related to elderly drivers, traffic violation of disobey stop sign was highly associated with crossing crashes (support = 0.023, confidence = 1.000, lift = 3.446). The explanation of the first rule is 2.3% of vehicle crashes were because of disobeying the stop sign and led to crossing crash; of traffic violation of disobey stop sign, 100% was crossing crashes; the proportion of crossing crashes with disobey stop sign was 3.446 times the proportion of crossing crashes in the complete dataset.

For elderly drivers, there were two rules having the highest lift value (3.446): "Violation = Disobey stop sign ⟶ Crossing crash" and "Violation = Disobey traffic lights, Location = Intersection with signal, Lighting = Daylight ⟶ Crossing crash." These two rules indicated the single factor or combination of factors that had the most significant proportion of crossing crash inside the crash type for elderly drivers. For

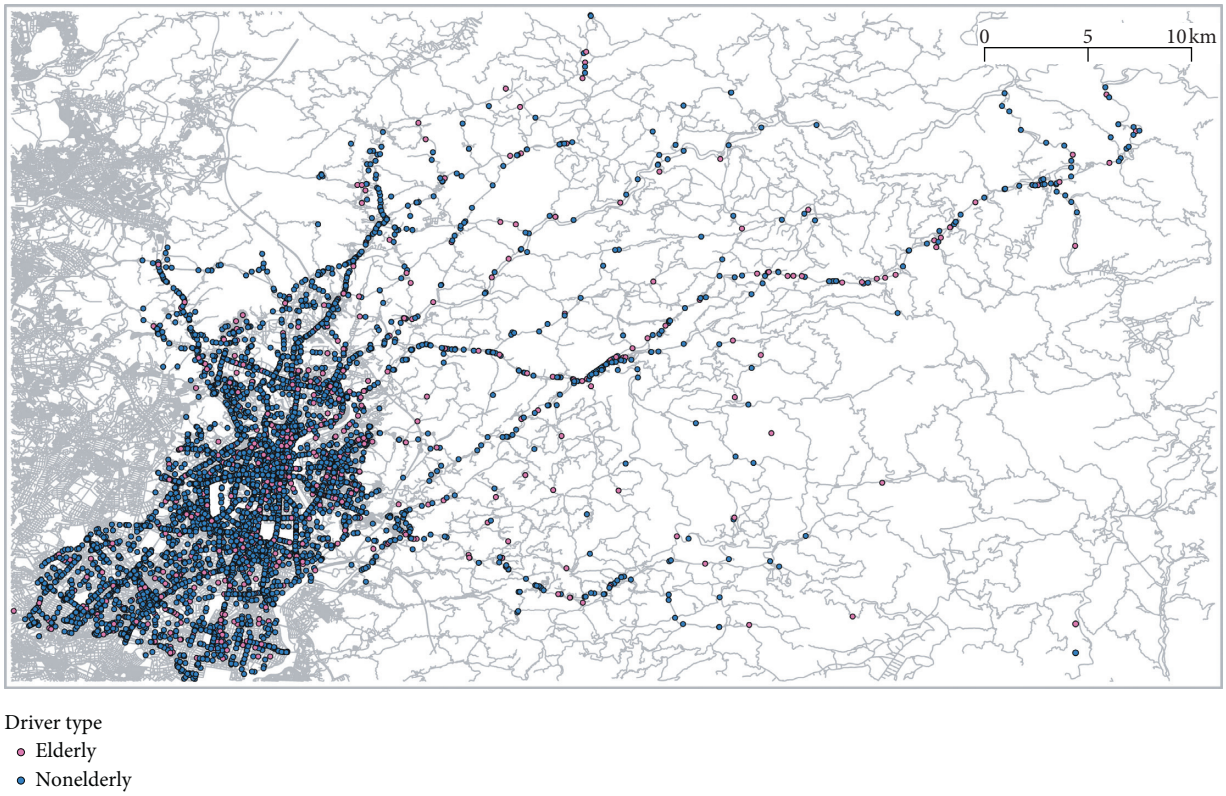

Figure 1: Vehicle crashes due to elderly and nonelderly drivers in Toyota City.

nonelderly drivers, the highest lift value (lift = 4.355) is found for a two-product rule: "Violation = Disobey stop sign ⟶ Crossing crash," indicating that the proportion of crossing crashes involving disobey stop sign is more than four times for proportion of crossing crash inside the crash type.

Compared with data mining results related to nonelderly drivers, different factors associated with relatively large proportion of crossing crashes included location (intersection without signal), lighting (daylight), road condition (dry or other), weather (clear or raining), vehicle type (light motor truck), and traffic violation (fail to confirm safety). These different factors might indicate different characteristics between elderly and nonelderly drivers, and elderly drivers might lead to crossing crashes associated with more factors compared with nonelderly drivers. Findings in this study can help us make some countermeasures to improve traffic safety by educating them. An interesting finding was that the traffic violation involving fail to confirm safety was highly associated with crossing crashes on some occasions, and these occasions should be set as the education targets for elderly drivers because elderly drivers were likely to make a traffic violation involving fail to confirm safety shown in Table 1.

The reasons for the different association rules extracted from vehicle crash data of elderly and nonelderly drivers are listed as follows:

(1) The proportion of crossing crashes concerning elderly drivers (29.0%) is significantly more than that of nonelderly drivers (23.0%) as shown in Table 1. The threshold value of confidence applied to association rules mining in this study is set as 70%. Therefore, the association rules concerning nonelderly drivers cannot be extracted from the dataset.

(2) Elderly drivers are likely to cause vehicle crashes in the daylight condition, which might indicate life and activity patterns of elderly people that they would like to go shopping or for leisure in the daytime reported in one previous study [25].

(3) Elderly drivers have a higher ratio of vehicle crashes caused by light motor trucks because households with elderly owners are more likely to own light motor trucks compared with that with nonelderly owners [26]. It might result from the fact that light motor trucks are helpful for farm or transportation works in Toyota City.

(4) Elderly drivers have a large proportion of traffic violations called fail to confirm safety. Here, the violation called fail to confirm safety is highly related to the crossing crashes, which is concluded in one previous study [8].

The strength of this study is that it can help us extend the knowledge to driving safety issues of elderly drivers. The crucial factors leading to crossing crashes of elderly drivers were indicated in this study, which was not observed in most previous studies. The findings from this study can give us some policy implications for elderly

Table 1: Descriptive statistics of significant variables.

		Elderly drivers		Nonelderly drivers	
		Percentage	99% CIs	Percentage	99% CIs
Crash location	Intersection with signal	22.2	19.2–25.1	19.0	17.9–20.2
	Intersection without signal	**39.2**	**35.7–42.7**	**34.1**	**32.8–35.4**
	Segment	**38.6**	**35.1–42.1**	**46.9**	**45.5–48.3**
	Total	100.0		100.0	
Lighting	Daylight	**61.5**	**58.0–64.9**	**50.0**	**48.6–51.4**
	Dawn	24.1	21.1–27.2	21.3	20.2–22.5
	Night	**14.4**	**11.9–16.9**	**28.7**	**27.4–29.9**
	Total	100.0		100.0	
Road condition	Dry	89.5	87.3–91.7	87.0	86.1–88.0
	Other	10.5	8.3–12.7	13.0	12.0–13.9
	Total	100.0		100.0	
Weather condition	Clear	77.1	74.2–80.1	74.5	73.3–75.7
	Raining	10.3	8.1–12.4	11.8	10.9–12.7
	Other	12.6	10.2–14.9	13.7	12.7–14.6
	Total	100.0		100.0	
Vehicle type	Light motor truck	**17.1**	**14.4–19.7**	**4.5**	**3.9–5.0**
	Light motor car	18.1	15.3–20.8	21.9	20.7–23.1
	Ordinary motor truck	**4.6**	**3.1–6.1**	**10.2**	**9.4–11.1**
	Ordinary motor car	60.2	56.8–63.7	63.4	62.0–64.8
	Total	100.0		100.0	
Traffic violation	Inattention	**22.0**	**19.1–25.0**	**30.8**	**29.5–32.1**
	Fail to confirm safety	**60.9**	**57.5–64.4**	**55.1**	**53.7–56.5**
	Incorrect operation	5.6	4.0–7.3	5.6	4.9–6.2
	Fail to observe objects	2.5	1.4–3.6	2.8	2.3–3.3
	Disobey traffic lights	3.0	1.8–4.2	2.2	1.8–2.6
	Disobey stop sign	2.3	1.2–3.3	1.3	1.0–1.6
	Other	3.7	2.3–5.0	2.2	1.8–2.6
	Total	100.0		100.0	
Crash type	With a pedestrian	8.1	6.1–10.0	5.5	4.8–6.1
	Single-vehicle	4.8	3.3–6.3	2.9	2.4–3.3
	Head-on	5.2	3.6–6.8	3.3	2.8–3.8
	Rear-end	**24.6**	**21.5–27.7**	**44.1**	**42.7–45.5**
	Crossing	**29.0**	**25.8–32.2**	**23.0**	**21.8–24.1**
	Right-turn	**10.4**	**8.3–12.6**	**7.0**	**6.3–7.7**
	Others	17.9	15.2–20.6	14.3	13.3–15.3
	Total	100.0		100.0	

Note. (1) Rows in bold indicates statistical significance (i.e., no overlap in the 99% confidence level). (2) Two-vehicle crashes are classified to head-on, rear-end, crossing, right-turn, and others in this study.

drivers' safety issues. To reduce the crossing crashes due to elderly drivers, an adequate education program for elderly drivers can be proposed to indicate risk factors such as the location, time period, and traffic violation. Meanwhile, the development of an advanced driving assistant system is crucial to supplement the traffic violation called fail to confirm safety, which is highly related to crossing crashes. In addition, it might be more necessary for the drivers of light motor trucks because this type of vehicle is related to crossing crashes, indicated by the results of the association rules applying to elderly drivers.

The limitations of this study are listed as follows:

First, vehicle crash data used in this study were the vehicle crashes in which at least one person (a passenger or a driver) was injured. Therefore, property-only crash data were not included in the sample, which might indicate different results of crash analysis studies, including both property-only and injured crashes. We have interviewed the researcher in the National Research Institute of Police Science, Japan, to understand the reason why property-only crashes are not included in the electrical data. The answer to this question is that the number of property-only crashes is vast, and policemen did not record this type of vehicle crashes in the Microsoft Office Excel worksheet.

Second, this study did not consider the factor of regional characteristics, such as the difference in urban and suburban areas. This factor might be related to crossing crashes in the sample data because this type of crashes usually occurs in an intersection without signal control. In this study, the association rules mining method was applied in the vehicle crash data collected in the region of Toyota. Here, Figure 1 illustrates that the east part of Toyota with a sparse road network and the west part of Toyota with a

Table 2: Association rules of crossing crashes for elderly and nonelderly drivers.

Antecedent	Types	Support	Confidence	Lift
Elderly drivers				
Violation = disobey stop sign	2-product	0.023	1.000	3.446
Violation = disobey traffic lights	2-product	0.027	0.897	3.093
Location = intersection with signal	3-product	0.027	0.972	3.350
Lighting = daylight	4-product	0.023	1.000	3.446
Lighting = daylight	3-product	0.023	0.938	3.231
Weather = clear	4-product	0.018	0.958	3.303
Vehicle = ordinary motor car	3-product	0.014	0.900	3.102
Weather = clear	4-product	0.011	0.933	3.216
Lighting = daylight and location = intersection without signal				
Type = light motor truck	4-product	0.037	0.738	2.545
Violation = fail to confirm safety	5-product	0.033	0.754	2.600
Road = dry	5-product	0.033	0.741	2.555
Road = other	4-product	0.017	0.710	2.446
Violation = fail to confirm safety	5-product	0.014	0.731	2.518
Weather = raining	4-product	0.024	0.705	2.428
Violation = fail to confirm safety	5-product	0.021	0.730	2.515
Nonelderly drivers				
Violation = disobey stop sign	2-product	0.013	1.000	4.355
Violation = disobey traffic lights	2-product	0.020	0.904	3.936
Vehicle = ordinary motor car	3-product	0.011	0.914	3.982
Location = intersection with signal	3-product	0.020	0.908	3.955

Note. One 6-product rule related to elderly drivers was not shown in Table 2.

dense road network. Therefore, results based on vehicle crash data, in general, cannot reflect the impact of regional characteristics on vehicle crash types.

6. Conclusions and Future Tasks

The current study used the crash data due to elderly and nonelderly drivers for five years (2009–2013) in Toyota City to identify the crash pattern and investigate the significant environmental, vehicle, and driver factors associated with crossing crashes of elderly drivers. A data mining technology called association rules mining is applied in this study, which can identify the valid and understandable pattern underlying in a massive crash dataset. The association rules mining is implemented using a package "arules" included in statistical software R.

Results of fundamental statistical analysis have indicated that elderly drivers are more likely to crash in the intersections without signals and in the lighting of daylight. They are also more likely to cause crashes of the light motor truck, make traffic violations in which they failed to confirm safety, and be involved in crossing, and right-turn crashes. Results of association rules mining have indicated that there are more factors associated with crossing crashes of elderly drivers than nonelderly drivers. These factors include the crash location (intersection without signal), lighting (daylight), road condition (dry and other), weather condition (clear and raining), vehicle type (light motor truck), and traffic violation (fail to confirm safety). These results might reveal the different characteristics of the crash pattern of elderly drivers due to their aging effects.

For one future task of this study, we will incorporate the factor of regional characteristics, i.e., the difference in urban and suburban areas indicated in the limitation of this study. Therefore, we will divide the sample data into two categories, namely, the category in urban areas and that in suburban areas. The association rules mining method will be applied to two data categories, respectively. Meanwhile, it is expected that extracted association rules are different for these two categories because the occurrence of crossing crashes have a higher probability in urban areas with a high density of intersections, compared to suburban areas.

Data Availability

The vehicle crash data were provided by the Traffic Safety and Crime Prevention Division, Social Affairs Department of Toyota City. Meanwhile, these data in Toyota City are collected and recorded by the Aichi Prefectural Police in Japan.

Disclosure

Two earlier versions of this study have been presented at the 12th International Conference of the Eastern Asia Society for Transportation Studies in Ho Chi Minh City, Vietnam, and the 98th Annual Meeting of the Transportation Research Board in Washington, D.C., USA, respectively.

Conflicts of Interest

The authors declare that there are no conflicts of interest regarding the publication of this article.

Acknowledgments

This study was supported in part by the Mitsui Sumitomo Insurance Welfare Foundation 2016.

References

[1] The Tokio Marine Research Institute, "Elderly drivers and vehicle crashes," 2015, http://www.tmresearch.co.jp/sensor/wp-content/uploads/sites/2/2015/05/SENSOR_No.17.pdf in Japanese.

[2] Statistics Bureau, Ministry of Internal Affairs and Communications, "Population of elderly people in Japan," 2013, http://www.stat.go.jp/data/topics/topi721.htm in Japanese.

[3] Japan National Policy Agency, "Development of the provisions of the traffic safety measures for elderly drivers," 2017, http://www.keishicho.metro.tokyo.jp/menkyo/koshu/koureisha_anzen.html in Japanese.

[4] D. R. Mayhew, H. M. Simpson, and S. A. Ferguson, "Collisions involving senior drivers: high-risk conditions and locations," *Traffic Injury Prevention*, vol. 7, no. 2, pp. 117–124, 2006.

[5] L. Staplin, K. Lococo, S. Byington, and D. Harkey, "Highway design handbook for older drivers and pedestrian," Report No. FHWA-RD-01-103, Federal Highway Administration, Washington, DC, USA, 2001.

[6] K. Anstey, J. Wood, S. Lord, and J. Walker, "Cognitive, sensory and physical factors enabling driving safety in older adults," *Clinical Psychology Review*, vol. 25, no. 1, pp. 45–65, 2005.

[7] Institute for Traffic Accident Research and Data Analysis, "Vehicle crashes of elderly drivers: trend and characteristic," 2007, in Japanese, http://www.itarda.or.jp/itardainfomation/info68.pdf.

[8] T. Matsuura, "Series of crashes pattern of elderly drivers: crossing crashes," *Traffic Safety Education*, vol. 51, no. 6, pp. 18–26, 2016, in Japanese.

[9] D. F. Preusser, A. F. Williams, S. A. Ferguson, R. G. Ulmer, and H. B. Weinstein, "Fatal crash risk for older drivers at intersections," *Accident Analysis & Prevention*, vol. 30, no. 2, pp. 151–159, 1998.

[10] X. S. Wang and M. Abdel-Aty, "Right-angle crash occurrence at signalized intersections," *Transportation Research Record: Journal of the Transportation Research Board*, vol. 2019, no. 1, pp. 156–168, 2007.

[11] A. Montella, "Identifying crash contributory factors at urban roundabouts and using association rules to explore their relationships to different crash types," *Accident Analysis and Prevention*, vol. 43, no. 4, pp. 1451–1463, 2011.

[12] G. López and J. De Oña, "Extracting crash patterns involving vulnerable users on two-lane rural highways," *Securitas Vialis*, vol. 9, no. 1–3, pp. 1–13, 2017.

[13] S. Moral-García, J. Castellano, C. Mantas, A. Montella, and J. Abellán, "Decision tree ensemble method for analyzing traffic accidents of novice drivers in urban areas," *Entropy*, vol. 21, no. 4, 360 pages, 2019.

[14] A. Montella, R. De Oña, F. Mauriello, M. Rella Riccardi, and G. Silvestro, "A data mining approach to investigate patterns of powered two-wheeler crashes in Spain," *Accident Analysis & Prevention*, vol. 134, Article ID 105251, 2020.

[15] A. Pande and M. Abdel-Aty, "Market basket analysis of crash data from large jurisdictions and its potential as a decision support tool," *Safety Science*, vol. 47, no. 1, pp. 145–154, 2009.

[16] A. Mirabadi and S. Sharifian, "Application of association rules in Iranian Railways (RAI) accident data analysis," *Safety Science*, vol. 48, no. 10, pp. 1427–1435, 2010.

[17] K. Wang and X. Qin, "Exploring driver error at intersections," *Transportation Research Record: Journal of the Transportation Research Board*, vol. 2514, no. 1, pp. 1–9, 2015.

[18] S. Das, R. E. Avelar, K. Dixon, and X. D. Sun, "Pedestrian crash analysis using association rules mining," in *Proceedings of the Transportation Research Board 96th Annual Meeting*, vol. 17, Washington, DC, USA, January 2017.

[19] M. Hahsler, B. Grün, and K. Hornik, "Arules—a computational environment for mining association rules and frequent item sets," *Journal of Statistical Software*, vol. 14, no. 15, pp. 1–25, 2005.

[20] R. Agrawal, T. Imieliński, and A. Swami, "Mining association rules between sets of items in large databases," *ACM SIGMOD Record*, vol. 22, no. 2, pp. 207–216, 1993.

[21] K. J. Cios, W. Pedrycz, R. W. Swiniarski, and L. Kurgan, *Data Mining: A Knowledge Discovery Approach*, Springer Press, New York, NY, USA, 2007.

[22] R. Agrawal and R. Srikant, "Fast algorithms for mining association rules in large databases," in *Proceedings of the 20th International Conference on Very Large Data Bases*, pp. 487–499, Santiago, Chile, September 1994.

[23] S. Nieminen, O.-P. Lehtonen, and M. Linna, "Population density and occurrence of accidents in Finland," *Prehospital and Disaster Medicine*, vol. 17, no. 4, pp. 206–208, 2002.

[24] J. Oxley, B. Fildes, B. Corben, and J. Langford, "Intersection design for older drivers," *Transportation Research Part F: Traffic Psychology and Behaviour*, vol. 9, no. 5, pp. 335–346, 2006.

[25] Ministry of Land, Infrastructure, Transport and Tourism, "Life and Activity Patterns of Elderly People," 2017, http://www.mlit.go.jp/common/001176318.pdf, in Japanese.

[26] J. Yang, H. Kato, R. Ando, and Y. Nishihori, "Analysing household vehicle ownership in the Japanese local city: case study in Toyota City," in *Proceedings of the Inaugural World Transport Convention 2018*, Beijing, China, 2018.

Hindawi
Journal of Advanced Transportation
Volume 2019, Article ID 2497459, 20 pages
https://doi.org/10.1155/2019/2497459

Research Article

Exploring the Effects of Signs' Design and In-Vehicle Audio Warning on Driver Behavior at Flashing-Light-Controlled Grade Crossings: A Driving Simulator-Based Study

Jingsi Yang,[1] Xuedong Yan,[1] Qingwan Xue,[2] Xiaomeng Li,[3] Ke Duan,[1] Junyu Hang,[1] and Wanjun Li[1]

[1]*MOT Key Laboratory of Transport Industry of Big Data Application Technologies for Comprehensive Transport, School of Traffic and Transportation, Beijing Jiaotong University, Beijing 100044, China*
[2]*Beijing Key Laboratory of Urban Intelligent Traffic Control Technology, North China University of Technology, Beijing 100144, China*
[3]*Centre for Accident Research and Road Safety-Queensland (CARRS-Q), Institute of Health and Biomedical Innovation (IHBI), Queensland University of Technology (QUT), Kelvin Grove 4059, Queensland, Australia*

Correspondence should be addressed to Xuedong Yan; xyan1@utk.edu

Received 16 September 2019; Revised 25 November 2019; Accepted 5 December 2019; Published 31 December 2019

Guest Editor: Cheol Oh

The complex environment at grade crossings and the severe collision consequences give rise to the concern of safety condition at crossings among traffic control authorities. Optimizing conventional devices and applying emerging technologies are worthwhile measures to improve the safety conditions at grade crossings. In this study, a flashing-light running (FLR) warning system was proposed to reduce crossing violation and improve performances of drivers at flashing-light-controlled grade crossings (FLCGCs). Forty-four fully licensed drivers aged between 30 and 48 years participated in a driving simulator study to investigate the efficacy of two countermeasures of the system: proposed design of signs and pavement markings (PSM) for grade crossing, and two-stage in-vehicle audio warning (IVAW) technology. A range of flashing light trigger timing and two foggy conditions were designed in this experiment to test the system applicability. Drivers' gender and vocation were considered as well to examine drivers' adaptation to the new proposed system. Five variables were collected and analyzed in this study to investigate the effectiveness of the system, i.e., drivers' compliance, approaching mean speed, brake reaction time, deceleration, and red-to-crossing time. Results showed that drivers' driving performances were improved in both PSM only condition and PSM + W condition. The FLR warning system could eliminate the negative effects of foggy weather and reduce gender differences in driver behaviors to some extent. These findings suggested that the FLR warning system has a potential to reduce the probability of grade crossing collisions.

1. Introduction

Grade crossings where the roadway and railroad tracks intersect have created serious conflicts between trains and vehicles. In 2004, 729 accidents involving grade crossings occurred in China, with a total of 513 casualties and 2292 hours of interruption on the main line operation, resulting in direct economic losses of up to ¥12 million (around 1.68 million USD) [1]. Similar figures have been observed in other countries as well. In Europe, grade crossing crashes led to 604 fatalities and casualties in 2011, which accounted for more than one quarter of all railway crashes [2]. In the US, collisions at grade crossings are frequent, with 267 fatalities and 826 injuries related to grade crossings in 2018 [3]. Therefore, grade crossing safety has been one of the top worldwide issues that attracts the attention of relevant transport authorities and the public [4, 5]. Among all the causes of grade crossing collisions, driver behavior on approaching to grade crossings is one of the main contributors [6], indicating the need for countermeasures targeting at drivers to improve the safety condition at grade crossings.

In China, the grade crossings could be divided into guarded crossings and nonguarded crossings, and about 62% of them are nonguarded crossings [7], where more driver errors and violations could be observed. Regarding the nonguarded crossings, two kinds of crossings can be defined according to the warning devices provided, e.g., passive crossings and active crossings. Passive crossings provide static warning devices only, e.g., STOP signs, pavement markings, and advanced warning signs. Drivers are required to observe the crossing and check if there are trains approaching before they cross. Different from passive crossings, active crossings provide active warning devices that can be real-time adjusted, e.g., flashing light or a gate with flashing light. Drivers are not allowed to enter the crossing if the gate is dropped down and/or the red lights are flashing. Compared with passive control, lower crash rates and greater compliance at grade crossings with active control devices have been reported in both historical crash data analyses and driving simulator studies [5, 8, 9]. However, drivers may fail to comply with active grade crossing control for a variety of reasons. For flashing-light-controlled crossings, driver errors and violations have been frequently observed due to the absence of physical obstructions [10]. However, little attention has been paid to such kind of grade crossings. Ideally, grade separation is the most effective solution for avoiding grade crossing conflicts, but it cannot be widely applied due to the high cost involved [11]. Therefore, there is a large demand to develop lower-cost technologies or devices to improve drivers' compliance and behavior at flashing-light-controlled grade crossings (FLCGCs).

When developing effective FLCGCs, a thorough understanding of drivers' crossing behavior is of great importance. Due to the overestimated remaining time and misunderstanding of the warning information, at least 55% of drivers still chose to cross the tracks even when the red lights were flashing [10, 12]. Though without yellow signal, there is a region of roadway existing upstream of crossings at the onset of flashing light, which is similar to the "dilemma zone" of roadway intersections. When the driver encounters a signal change, he or she may neither stop nor cross successfully due to a high approaching speed, underestimating the required braking distance or exercising an aggressive behavior [13]. Drivers' incorrect decisions at the onset of flashing light may lead to flashing-light running (FLR) violations, and drivers' sudden stop action in front of the crossings may result in rear-end collisions with the vehicles behind them. Furthermore, instead of waiting for the end of the flashing lights, some drivers tended to cross the track once the train left the crossing while the red lights were still flashing. This kind of behavior may put the drivers in great risk if a second train was approaching [14].

Many safety approaches to decrease FLR violations at grade crossings have focused on countermeasures applied either on the intersecting road or the grade crossing itself (e.g. signs, pavement markings, and flashing lights' warning time). It can be inferred that drivers can perceive hazards associated with a grade crossing by signs and markings, and thus change their travel speeds to achieve a safe and smooth driving process [15–18]. However, static signs and markings provide limited help in assisting drivers to make stop/go decisions. Meanwhile, the role of signs and markings is degraded under adverse weather conditions, such as foggy weather. In-vehicle audio warning (IVAW) countermeasure based on intelligent vehicle infrastructure cooperative (IVIC) technology can make up for the defects of static signs and markings [19]. Many studies have confirmed that IVAW can improve driver behavior. However, the lack of the ability to inform drivers about failures of the IVAW could counterbalance the safety benefits. There is no doubt that the reliability of traditional signs and markings is irreplaceable in comparison to the IVAW. Nevertheless, few research studies to date have considered the mutual assistance of these two countermeasures to improve the safety condition of grade crossings.

2. Literature Review

This paper proposed two novel low-cost grade crossing treatments. Traffic signs and pavement markings are the basis of traditional traffic management. IVAW is an emerging and popular intelligent management technique. This paper aims to propose a more reasonable design and placement of signs and markings and, on this basis, propose a matched IVAW program. It is assumed that the mutual assistance of these two countermeasures can improve the reliability and effectiveness of the flashing-light running (FLR) warning system.

2.1. A Series of Signs and Pavement Marking Countermeasures. In China, there is a lack of grade crossings design standards to match the information requirement of drivers. The shortcomings of signs and markings practice have not been adequately addressed. The Manual on Uniform Traffic Control Devices (MUTCD, USA) [20] suggests that all grade crossings (unless a four-quadrant gate system) should install the dynamic envelope markings (DEMs) to indicate the clearance requirement of the train. The DEMs are used to depict dangerous areas where the vehicles and the train may collide. Moreover, if automatic gates are not presented and if there are two or more tracks at one grade crossing, a supplemental number of tracks plaque should be mounted below the crossbuck sign to indicate the possibility of multiple trains crossing. However, no similar requirements were applied in Chinese relevant standards.

In general, grade crossing warning sign is placed near the grade crossings to remind drivers of a potential stop. Drivers may understand that the sign is associated with a crossing, but they might not understand its behavioral implications [21]. The information required by the driver depends on the nature of the crossing. In the case of FLCGCs, drivers do not need to recognize the hazard, but they do need to prepare to slow down and pay attention to the change of flashing light. Therefore, it is necessary to provide drivers with the information about the type of crossing ahead. The 'Signal Ahead' sign and pavement marking (see Figures 1(a) and 1(b)) have been listed in the MUTCD to alert drivers of a

(a) (b) (c)

Figure 1: Signal ahead sign and marking at a signalized intersection, flashing-light ahead sign at a grade crossing. (a) Signal ahead sign (MUTCD); (b) signal ahead marking (MUTCD); and (c) flashing-light ahead sign (New Zealand, Australia).

signalized intersection in front. Previous studies have shown that these could help drivers make proper stop/go decision and reduce the dilemma zone effect [22]. Flashing-light ahead sign has been widely adopted in New Zealand and Australia (see Figure 1(c)). However, it is not yet very clear where the sign should be positioned at grade crossings and how the sign can impact drivers' crossing behavior.

The advance placement distance of grade crossing warning signs can be calculated based on the design speed. In China, signal ahead and grade crossing warning sign are typical signs that warn drivers of the potential stop situation. The advance placement distance is based on the 2011 AASHTO Policy with the stopping sight distance (as shown in the following equation (1)) subtracting the sign legibility distance of 55 m.

$$\mathrm{SSD} = 0.278Vt + 0.039\frac{V^2}{a}, \quad (1)$$

where SSD is the stopping sight distance (m); V is the design speed (km/h); t is the brake reaction time (2.5 s); and a is the deceleration rate (3.4 m/s^2).

Another typical condition in MUTCD is absent in the Chinese standard. The condition considers locations where the road user must spend some time to adjust speed and change lanes in heavy traffic because of a complex driving situation. The distances are determined by providing the driver with a premaneuver time of 14.0 to 14.5 seconds for vehicle maneuvers (2011 AASHTO Policy, decision sight distance as shown in equation (2)). Similarly, a sign legibility distance of 55 m is considered.

$$\mathrm{DSD} = 0.278Vt + 0.039\frac{V^2}{a}, \quad (2)$$

where DSD is the decision sight distance (m); V is the design speed (km/h); t is the premaneuver time (between 14.0 s and 14.5 s); and a is the deceleration rate (3.4 m/s^2).

It should be noted that MUTCD does not specify how to optimize the warning sign placement in terms of traffic safety and operation. This paper proposed the application of a series of signs and pavement markings for FLCGCs.

2.2. In-Vehicle Audio Warning Countermeasure. Considerable research and innovation has occurred on IVAW countermeasure for crossing safety. Larue et al. [23] found that IVAW resulted in higher compliance rates when a train was approaching the passive crossing. The IVAW also resulted in lower speeds closer to the crossing, faster brake response times, and larger safety margins at passive crossings [24, 25]. However, the IVAW had limited effect at active crossings, and an important reason is that the verbal warning was provided when the flashing lights were activated and it was hard for drivers to collect sufficient information and make a quick response [23]. Therefore, the delivery time of warning messages could seriously influence the effectiveness of the warning system [26, 27]. In fact, drivers could avoid most violations if the warning messages were delivered in advance of the flashing light activation, especially in the case of short time to stop line when the flashing light was activated. In terms of the warning systems proposed in prior studies, auditory warning messages are usually used to remind drivers of train approaching and require drivers to take appropriate actions immediately. The system that only provides an emergency warning message is called single-stage advance warning systems (SSAWS). The SSAWS only published the warning once, but it left drivers with little time to identify and respond to the possible hazardous situation. Nevertheless, the two-stage advance warning system can help drivers maintain safer driving conditions by providing a piece of forecast information that draws drivers' attention at the first stage [28, 29]. The considerable lower cost of IVAW application compared to conventional active devices provides extra motivation for their use [30, 31], and their effectiveness will be examined in this study.

2.3. Impacts of Foggy Conditions on Driver Behavior. The effects of different weather conditions on traffic crashes have been paid much attention in the field of transportation research [32, 33]. Among the adverse weather conditions, fog is the most hazardous one, which is more likely to result in high crash frequency (19.54%) and severe crash outcome [34, 35]. Driving in fog can be risky for drivers of all levels of abilities as the fog leads to a substantial reduction in visibility [36]. Among all the adaptions of driving behaviors in fog, changing speed is the most typical one. Drivers tended to approach a grade crossing at speeds that were too high for them to stop and, therefore, high speed has become a major contributing factor in many of the crashes that occurred in foggy conditions [37]. Although driving behaviors in fog weather have been investigated in many studies, few of them have addressed how drivers' behaviors at highway-rail grade crossings were affected by fog. Additionally, it is expected that the proposed countermeasures at grade crossings could offset the negative impacts of fog weather and provide more

safety benefits for drivers. The common negative impact of various adverse weather conditions mainly comes from the impairment on drivers' visibility and the increased mental workload while driving. Therefore, the investigation of the effectiveness and reliability of the proposed countermeasures in fog could also indicate their applicability potential in other adverse weather conditions.

2.4. Impacts of Driver Characteristics on Driver Behavior. Driver characteristics have been found to be related to unintended human errors, intentional actions, and risk-seeking behaviors on road [38–40]. Among driver characteristics, gender [5, 41] and vocation [42, 43] were acknowledged to differentiate drivers' performances with a great variance. Several studies reported that female drivers committed fewer violations than male drivers [41, 44, 45]. The violation behaviors were strongly related to collision likelihood and consequently, male drivers were more likely to be involved in injuries and fatalities crashes compared to females [46, 47]. Besides, drivers' vocation was another factor related to traffic violations and road crashes [48]. Professional drivers (such as taxi, bus, or truck drivers) had a high probability of traffic crashes due to a high exposure on road and the high possibility of fatigue driving [49]. Moreover, professional drivers may perform differently from nonprofessional drivers because of different levels of driving skills. Generally, taxi drivers were more experienced, more sensitive to the impending changes in the road geometry, and behaved more skillfully in both longitudinal and lateral vehicle control than private car drivers [50]. Although many previous studies analyzed drivers' gender and vocation characteristics in traffic violations and crash-involvement risk, it is still not clear whether there are gender and vocation differences on driving behaviors in the process of approaching a grade crossing.

2.5. Objectives of This Study. In summary, the current traffic signs and pavement markings for FLCGCs of China provide insufficient information to drivers, and the design of the United States and Australia is worth learning. For IVAW, the existing literature rarely referred to two-stage IVAW, especially when it is used with traffic signs. Additionally, drivers' characteristics and foggy conditions contribute to different driving behavior patterns. However, their effects on driver behavior in the process of approaching a grade crossing remain unclear. Toward this end, this paper presents a driving simulator experiment study that aims at investigating the effectiveness of the lower-cost FLR warning system at the flashing-lights-controlled grade crossings. The research framework of the study is presented in Figure 2. Compared with previous studies, this paper improves current knowledge in four aspects: (1) this paper proposes a flashing-light running (FLR) warning system that includes improved signs and markings (PSM) design and a two-stage IVAW; (2) instead of designing some flashing light trigger timing (FLTT), this study focuses on drivers' stop/go decisions under a set of continuously scattering points within the predefined range of FLTT; (3) a range of FLTT is designed in combination with a binary choice of heavy fog conditions to test the applicability of FLR warning system in adverse visibility condition; and (4) driver characteristics, e.g., gender and vocation, are considered in this study to examine different drivers' adaptation to the new proposed PSM and IVAW.

3. Method

3.1. Participants. Forty-seven full-licensed participants were recruited to participate in this driving simulator study. Three participants experienced simulator discomfort and were not able to complete the experiment. Therefore, a total of 44 participants aging from 30 to 48 years (Mean = 37.2, S.D. = 26.1) were included in the experiment. They comprised 21 professional drivers (14 male and 7 female) and 23 nonprofessional drivers (10 male and 13 female). The professional drivers were full-time taxi drivers with an average driving experience of 17.7 years and an average annual driving distance of 94.7 thousand kilometers. The nonprofessional drivers were from different occupations and drove for daily purposes only. Their average driving experience was 9.7 years, with an average annual driving distance of 19.2 thousand kilometers.

3.2. Apparatus. In this study, driving simulation experiment and data collection were carried out using the Beijing Jiaotong University (BJTU) driving simulator (as shown in Figure 3). The high-fidelity driving simulator consists of a one degree-of-freedom motion base platform, an environmental noise simulation system, a digital video replay system, and a curved projection screen providing a 300 degrees front/peripheral field of view at a resolution of 1400×1050 pixels. The full-size vehicle cockpit (Ford Focus) in the simulator is designed in full accordance with a real vehicle and the inside components include the steering wheel, dashboard, brake pedal, throttle, and seats, etc. Meanwhile, it also provides a set of software programs for driving scenario design, virtual traffic environment simulation, virtual road design, and scenario presentation. The sampling frequency of the driving data was 60 Hz.

3.3. Scenario Design. The experiment was a 3 (crossing type) $\times$ 5 (FLTT) $\times$ 2 (foggy condition) within-subjects repeated-measures design. The three crossing types considered the design of the signs and pavement markings for grade crossings and the presence or absence of two-stage warning. Detailed explanations of the three crossing types are:

(i) Baseline: conventional design of signs and pavement markings for grade crossing in China;

(ii) PSM: the proposed design of signs and pavement markings for grade crossing without warning:

(iii) PSM + W: the proposed design of signs and pavement markings for grade crossing with warning.

FLTT depended on the time of the vehicle arriving at the stop line. Five kinds of FLTT that varied from 2 s to 6 s with 1 s

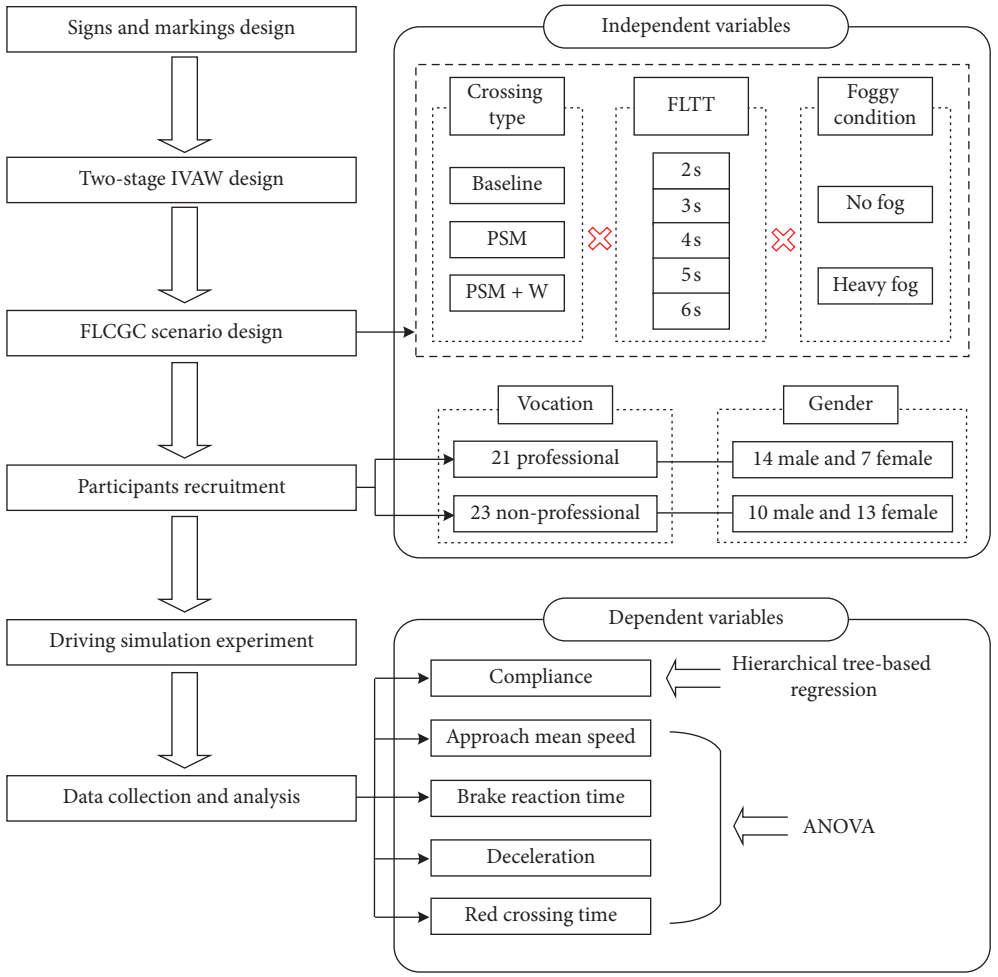

Figure 2: Research framework.

(a) (b)

Figure 3: Illustration of BJTU driving simulator system. (a) Driving simulator; (b) monitoring and controlling systems.

interval were designed in this study. In addition, two foggy conditions including clear and heavy fog were considered to test the effect of PSM and IVAW on drivers' crossing behavior under different foggy conditions. The visibility in heavy fog scenario was 50 m. Thus, a total of 30 different types of experimental scenarios were performed in this study.

The road designed in this experiment was a two-lane, two-way road with lane width of 3.5 m per lane and the speed limit was 70 km/h. All grade crossings were evenly distributed on the road, with each two of them connected by an 800 m straight road segment. The flashing-light signal was activated when the time for the vehicle to arrive at the stop line met the FLTT. Once activated, the red light started flashing at a rate of 60 Hz, accompanied by an audible warning beep (60 dB) ringing at a rate of 60 Hz. The signal duration was 15 s.

The baseline grade crossing followed Chinese design standards and required signage are displayed in Figure 4(a).

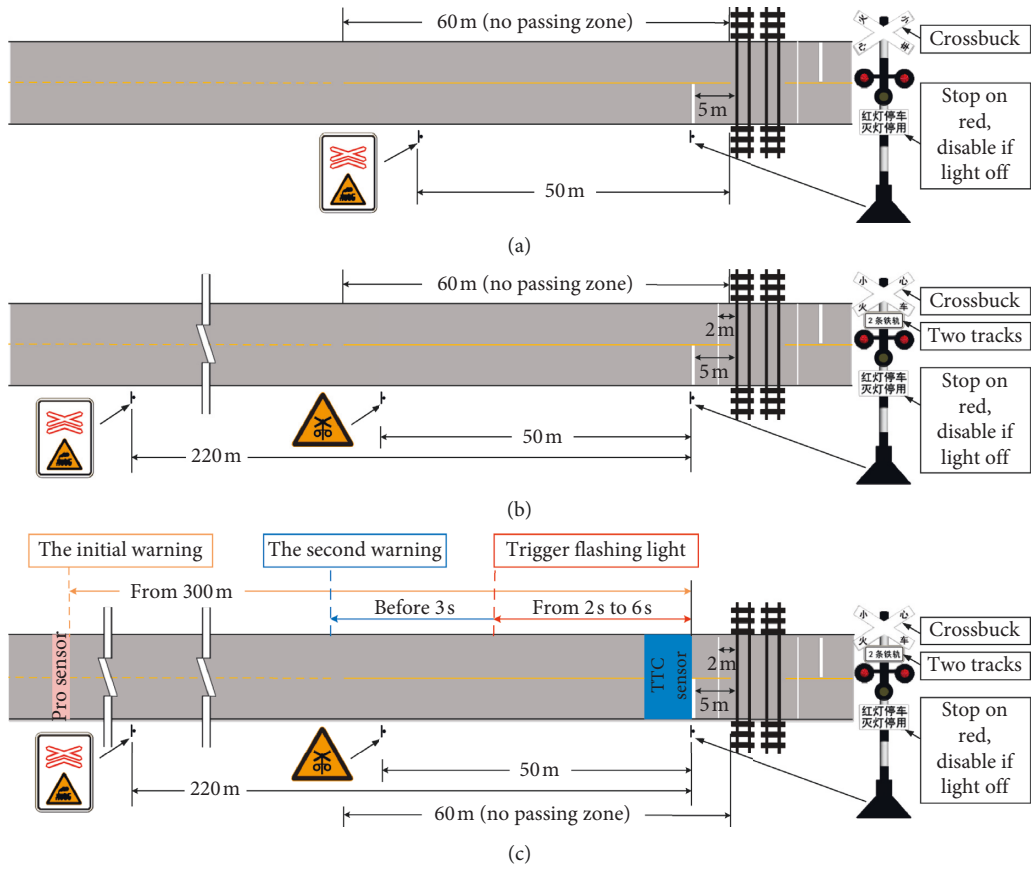

Figure 4: Standard and proposed design of signs and pavement markings for grade crossing of China. (a) Standard design of signs and pavement markings for grade crossing of China; (b) proposed design of signs and pavement markings for grade crossing; (c) diagram of the grade crossing with warning.

The stop line and flashing-light signal were placed 5 m in advance of the crossing railway. The flashing-light signal was assembled on the side of the road together with a crossbuck sign and a "STOP ON RED, DISABLE IF LIGHTS OFF" sign. Meanwhile, a nonguarded grade crossing with multiple tracks sign was positioned on the right side of the road 50 m prior to the railway. The proposed design of traffic control devices for grade crossing was adjusted based on the baseline design (Figure 4(b)). For the flashing lights, a supplemental number of tracks plaque was mounted below the crossbuck sign. DEMs (dynamic envelope markings) were recommended to place on the road 2 m in advance and parallel to the railway. Nonguarded grade crossing with multiple tracks signs were moved to 220 m away from the stop line. In addition, a flashing-light ahead sign was installed 50 m in front of the crossing to provide information to drivers regarding whether they should prepare to stop or go through.

The IVAW triggered verbal cautions: "Flashing lights controlled grade crossing at 300 meters ahead, please be careful!" and "The flashing lights are about to turn red, please slow down!." The initial warning was released when the vehicle was 300 m away from the stop line, and the second was released at 3 s prior to the flashing lights activation, as shown in Figure 4(c).

In this study, two sets of experimental driving routes were designed to test participants' driving performances during the process of approaching grade crossings. One route composed of eight baseline grade crossings and it was 6.4 km in length. In order to minimize drivers' adaptability, memorability, and predictive probability to the repeated tests, five grade crossings with different FLTT were randomly selected as the test grade crossings. The other two grade crossing types were grouped together. The route consisted of fourteen grade crossings designed according to the recommended signs and pavement markings, and the length was 11.2 km. Ten test grade crossings (2 (PSM and PSM + W) × 5 FLTT) were randomly selected from the route. Then, the test crossings of each route were randomly sorted to form three sequences of FLTT. The route of each driver for each driving was randomly selected, so that each driver experienced thirty test grade crossings in different orders.

3.4. Procedure. All participants were briefed about the experiment upon their arrivals. Before formal experiment, all participants were given at least 5 min of training so that they could familiarize with the virtual driving environment and the simulated driving operation. Participants were instructed to practice accelerating and braking gently and to practice maintaining the speed and steering wheel.

Before the experiment, each participant was asked to sign an informed consent form and fill out demographics and general driving questionnaires. In the formal test, they were required to drive and behave as they normally would. The participants were also notified that they could quit the experiment at any time in case of motion sickness or any kind of discomfort. Then, participants drove each scenario under two foggy conditions (clear and heavy fog) in a random sequence to counterbalance the order effect. Each of them was given a break between the tests. One session lasted approximately 1 h for each participant and a compensation of 200 Chinese RMB (about 30 U.S. dollars) was provided for their successful completion.

3.5. Data Analysis. As Figure 5 shows, the factors considered in this study included foggy conditions, gender, vocation, crossing type, and FLTT. Five dependent variables were collected and used to test the effect of PSM and IVAW on drivers' crossing behavior, e.g., compliance or not, approaching mean speed, brake reaction time, red crossing time, and deceleration. Detailed definitions of the above dependent measures were explained as follows:

Compliance or not (Yes = 1; No = 0): the variable represents whether the driver complied with the traffic rules at the grade crossing.

Approaching mean speed: mean speed on approach to the crossing was measured at five distances in front of the crossing: 300 m, 220 m, 100 m, 50 m, and 20 m.

Brake response time (BRT): the time was determined by measuring the time at which the subject vehicle triggered a train crossing "event" (a "warning" or 3 s prior to a "flashing red light") to the time at which the participant first depressed the brake pedal. It was for those approaches where participants did not violate the grade crossing controls.

Deceleration: the change rate of velocity during the period from the time of brake to the time when a maximum brake was reached. It was for those approaches where participants did not violate the grade crossing controls.

Red crossing time (RCT): the time was measured from the time at which the flashing light was activated to the time at which the subject vehicle arrived at the stop line. It reflects the severity of the driver's violation. It was for those approaches where participants violated the grade crossing controls.

The compliance variable was analyzed using hierarchical tree-based regression. The specifications for tree construction include: CHAID algorithm was applied; the maximum tree depth was set as 3 levels; and the significance values for splitting nodes and merging categories were set as 0.05. The minimum number of cases for parent nodes was set as 100 and the minimum number of cases for child nodes was set as 50. Other measures of driving performance were analyzed using ANOVA and used an α-level of 0.05 to determine statistical significance. All analyses were carried out using IBM SPSS Statistics 22.

4. Results

4.1. Compliance. Table 1 lists compliance rates with different factors, including foggy condition, gender, vocation, crossing type, and FLTT. Results of hierarchical tree-based regression are shown in Figure 6. The final tree structure for compliance involved three splitting variables, including gender, crossing type, and FLTT. It means that the aforementioned three variables significantly influenced drivers' compliance, among which FLTT was the most important factor, followed by gender and crossing type. No statistically significant effect of vocation and foggy conditions was found on drivers' compliance.

As shown in Figure 6, the tree contains three levels. In the first level, the compliance (Node 0) was divided into three child nodes (Node 1–3) according to FLTT. In the second level, Node 1 was divided into two child nodes (Node 4-5) by gender, whereas Node 2 and Node 3 were both divided into two child nodes (Nodes 6-7 and Nodes 8-9, respectively) by crossing type. In the third level, Node 4 and Node 5 were divided into two child nodes (Nodes 10-11 and Nodes 12-13) by crossing type. The detailed characteristics could be identified as follows:

In the first level: it was found that FLTT was the most important influencing factor on compliance. For earlier FLTT (4 s, 90.2%; 5 s, 93.6%; 6 s, 93.9%), 92.6% of drivers complied with the rules, which was much higher than the proportion of drivers under the 2 s (34.5%) and 3 s (75.0%) conditions.

In the second level: in the condition of earlier FLTT (4–6 s), gender was the most influencing factor for compliance. 96.7% of female drivers chose to comply with the rules, which was 7.6% higher than the proportion of male drivers. However, for the later FLTTs, e.g., 2 s and 3 s, crossing type was the significant factor among all the factors and no statistically significant effect of gender was found on drivers' compliance. The baseline and PSM were classified into the same subgroup, which means that drivers tended to make the same choice of whether to comply with the rules. The interaction effect of crossing type and FLTT can be more intuitively observed in Figure 7. When the FLTT was 2 s, the compliance rate of PSM + W crossings (65.9%) was found to be significantly higher than that of PSM crossings and baseline (12.5%). When the FLTT was 3 s, 94.3% of drivers who drove in PSM + W scenarios chose to comply with the rules, which was much higher than drivers in baseline and PSM scenarios (65.3%).

In the third level: when the FLTT varied from 4 s to 6 s, both male and female drivers' compliance rates were significantly influenced by crossing type. For female drivers, the baseline and PSM were classified into the same subgroup which means that female drivers tended to make the same choice of whether to comply with the rules. 95% of female drivers tended to comply with the rules in the condition of baseline and PSM, whereas the compliance rate of female drivers in the condition of

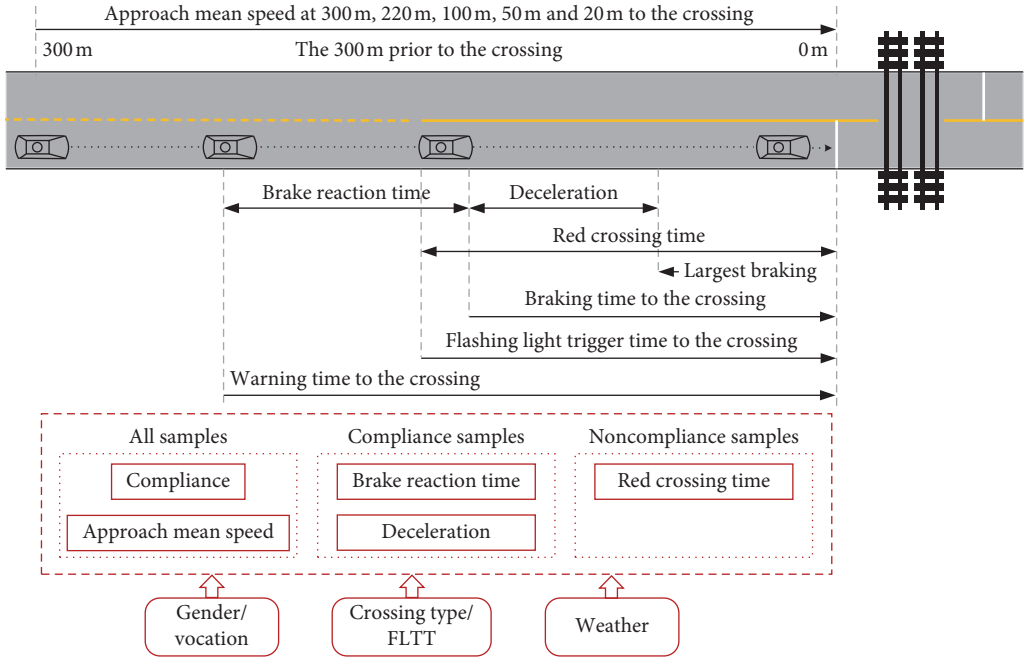

Figure 5: Dependent and independent variables in this study.

Table 1: Basic description for compliance rates.

Effect	Classification	Yes		No		Total
		Count	*N*%	Count	*N*%	Count
Foggy condition	Clear	502	76.1	158	23.9	660
	Fog	520	78.8	140	21.2	660
Gender	Male	538	74.7	182	25.3	720
	Female	484	80.7	116	19.3	600
Vocation	P	478	75.9	152	24.1	630
	NP	544	78.8	146	21.2	690
Crossing type	Baseline	307	69.8	133	30.2	440
	PSM	309	70.2	131	29.8	440
	PSM + W	406	92.3	34	7.7	440
FLTT (s)	2	91	34.5	173	65.5	264
	3	198	75.0	66	25.0	264
	4	238	90.2	26	9.8	264
	5	247	93.6	17	6.4	264
	6	248	93.9	16	6.1	264
Total		1022	77.4	298	22.6	1320

PSM + W reached 100%. For male drivers, 91.7% of drivers under the PSM and PSM + W conditions complied with the rules, which was 7.7% higher than those under baseline condition.

4.2. Approaching Mean Speed. For drivers who complied with the rules, their speed profiles while approaching different types of grade crossings were calculated. Figure 8 presents the approaching mean speed (AMS) profiles for different FLTTs. Each subfigure provides the mean speed of subject vehicle from 400 m in front of a crossing to 10 m behind it (the stop line is considered as 0 m from the grade crossing). It can be found that for all three types of crossings, drivers almost kept a constant approaching speed. In baseline, drivers approached the crossing at a higher speed until they observed the warning sign at 45 m distance and then started to slow down. However, drivers started to slow down earlier at PSM crossings than baseline. As the warning signs were 220 m ahead of crossings, drivers approached the crossing at a lower speed. At PSM + W crossings, drivers received a voice message when they were 300 m in front of the crossing, which prompted them to slow down earlier and approach at lower speeds compared with the other conditions.

Effects of foggy condition, gender, vocation, crossing type, and FLTT on drivers' approaching speed were further analyzed at five distances of interest: 300 m to the crossing

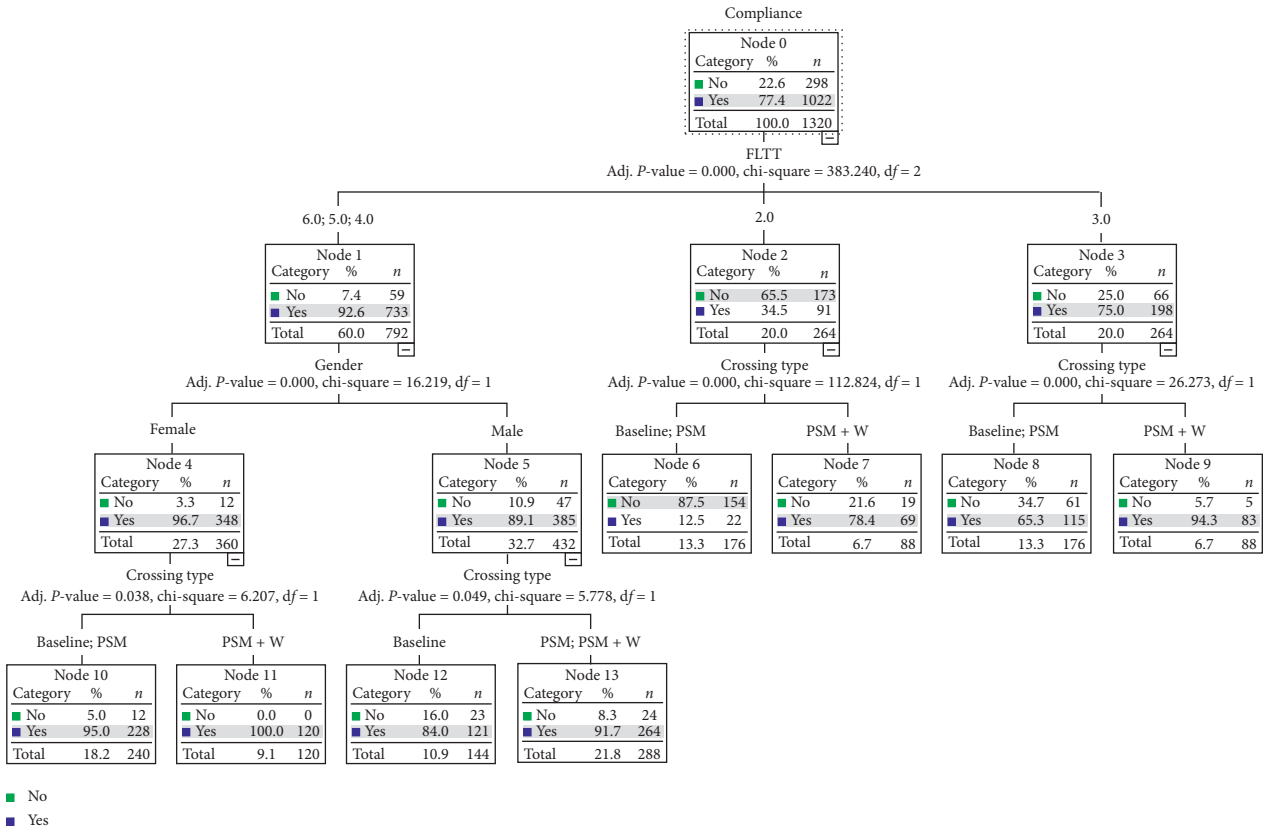

Figure 6: Hierarchical tree-based regression (HTBR) model: predicting drivers' compliance within different categories of factors.

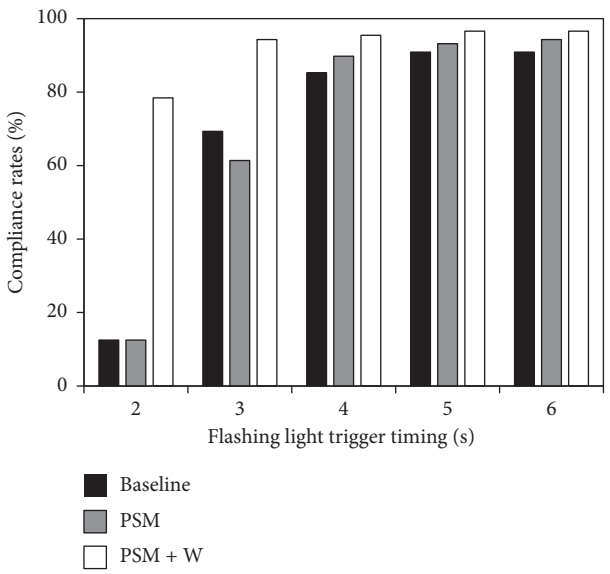

Figure 7: Proportions of drivers who compliant after the flashing light triggered.

(the initial warning occurred at this position under PSM + W condition), 220 m to the crossings (a nonguarded grade crossing with multiple tracks sign was adopted under PSM and PSM + W conditions), 100 m to the crossing, 50 m to the crossing (a flashing-light ahead sign was adopted under PSM and PSM + W conditions), and 20 m to the crossing. Table 2 shows the mean speed within different categories under different factors conditions, and Table 3 summarizes the ANOVA results for these measures.

At 300 m to the grade crossing, mean speed was significantly affected by foggy conditions ($F = 187.055$, $P < 0.001$) and gender ($F = 5.583$, $P = 0.018$). The mean speed in no fog was significantly higher than that in heavy fog and male drivers' mean speed was higher than that of female drivers. However, no significant effect was found for all the other factors on speed at 300 m to the crossing.

ANOVA analysis (as shown in Table 3) showed that drivers' approaching speed at 220 m to the crossing was significantly affected by foggy conditions ($F = 179.128$, $P < 0.001$) and crossing type ($F = 35.005$, $P < 0.001$). Similar to the mean speed at 300 m to the crossing, the mean speed at 220 m in no fog was also significantly higher than that in heavy fog. As for three kinds of crossing types, smallest speed could be found at PSM + W crossings, while no obvious difference between PSM crossings and baseline was observed.

At 100 m to the grade crossing, crossing type ($F = 85.097$, $P < 0.001$), foggy conditions ($F = 11.610$, $P = 0.001$), and their interaction effect ($F = 3.238$, $P = 0.040$) had significant influence on the mean speed. As Figure 9 illustrated, drivers tended to keep a lower speed at 100 m to PSM crossings than in baseline. The mean speed at PSM + W crossings was lowest among all the three crossing types. Moreover, the mean speed in no fog was larger than that in heavy fog

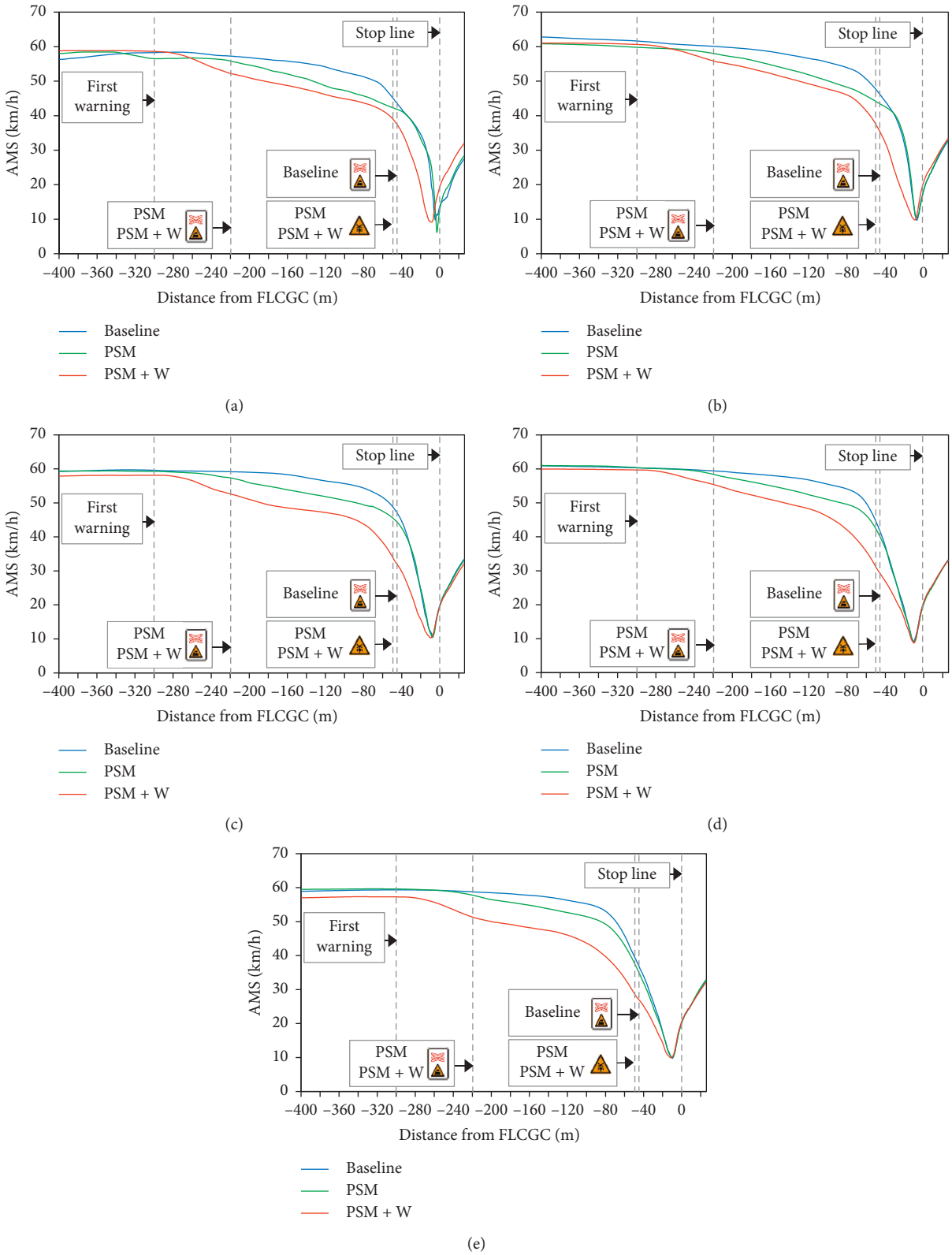

Figure 8: Approaching mean speed profiles for different flashing light trigger timings. (a) The FLTT was 2 s; (b) the FLTT was 3 s; (c) the FLTT was 4 s; (d) the FLTT was 5 s; (e) the FLTT was 6 s.

under both PSM and PSM + W conditions, whereas for baseline, no difference was found between clear and heavy fog conditions.

At 50 m to the grade crossing, foggy conditions exhibited a significant impact on mean speed ($F = 5.080$, $P = 0.024$) and drivers maintained a higher speed in heavy fog than that

Table 2: Mean speed within different categories of factors.

Effect	Classification	Parameter	Speed 300	Speed 220	Speed 100	Speed 50	Speed 20
Foggy condition	Clear	Mean	63.41	60.95	52.00	41.00	25.04
		S.D.	67.35	77.72	116.85	165.93	262.75
	Fog	Mean	55.94	53.36	50.07	42.44	25.53
		S.D.	130.66	147.83	139.57	153.25	208.01
Gender	Male	Mean	60.19	57.55	51.34	41.28	24.07
		S.D.	124.19	139.93	145.29	178.89	261.02
	Female	Mean	59.00	56.62	50.66	42.25	26.75
		S.D.	99.22	112.07	109.71	136.93	200.35
Vocation	P	Mean	59.57	56.88	51.19	41.65	24.86
		S.D.	121.40	138.89	129.91	177.84	276.51
	NP	Mean	59.71	57.35	50.88	41.79	25.68
		S.D.	105.69	116.96	128.57	143.81	197.23
Crossing type	Baseline	Mean	59.86	59.14	55.30	46.18	28.82
		S.D.	114.47	108.86	113.43	149.87	250.92
	PSM	Mean	60.08	58.43	51.78	46.18	29.56
		S.D.	108.58	118.27	128.76	155.25	273.12
	PSM + W	Mean	58.99	53.81	46.01	34.62	17.48
		S.D.	116.13	138.87	101.77	97.94	90.29
FLTT (s)	2	Mean	59.34	56.98	50.92	45.40	36.98
		S.D.	129.46	136.37	137.35	161.25	292.17
	3	Mean	60.64	58.03	51.48	44.23	30.54
		S.D.	105.66	118.53	123.11	156.10	235.84
	4	Mean	59.02	56.39	51.02	43.15	23.09
		S.D.	111.92	128.76	134.80	175.54	166.92
	5	Mean	60.16	57.83	51.12	39.77	18.43
		S.D.	100.65	111.68	120.38	129.66	100.78
	6	Mean	59.07	56.40	50.61	36.08	17.40
		S.D.	117.49	141.11	131.59	121.83	103.77

Table 3: ANOVA summary table of the effect of factors on approaching mean speed.

Source	d.f.	*F*-ratio				
		Speed 300	Speed 220	Speed 100	Speed 50	Speed 20
Foggy condition	1	187.055*	179.128*	11.610*	5.080*	0.458
Gender	1	5.583*	3.768	1.141	2.537	14.530*
Vocation	1	0.485	1.340	0.090	0.020	0.094
Crossing type	2	1.578	35.005*	85.097*	138.235*	136.307*
FLTT	4	1.385	1.483	0.231	30.888*	124.173*
Crossing type × foggy condition	2	1.382	0.749	3.238*	1.520	0.171
Crossing type × gender	2	0.540	0.569	0.058	0.681	0.237
Crossing type × vocation	2	0.576	1.036	0.043	0.180	1.698
FLTT × crossing type	8	0.304	0.739	0.578	1.754	14.872*
FLTT × foggy condition	4	0.842	1.196	0.546	2.262	7.451*
FLTT × gender	4	0.179	0.213	0.095	0.521	0.874
FLTT × vocation	4	0.043	0.207	0.332	0.573	0.196

*Significant at the 0.05 level.

in no fog (42.44 km/h vs. 41.00 km/h). FLTT ($F = 30.888$, $P < 0.001$) and crossing type ($F = 138.235$, $P < 0.001$) were also significant factors of mean speed. Drivers' mean speed gradually decreased with the increase of FLTT. For three crossings, significant speed reduction could be found at PSM + W crossings, whereas no obvious difference between PSM crossings and baseline was found.

Finally, ANOVA analysis showed that at 20 m to the crossing, gender had a significant impact on mean speed ($F = 14.530$, $P < 0.001$) and male drivers kept a smaller mean speed than female drivers. Furthermore, the mean speed was also significantly affected by crossing type ($F = 136.307$, $P < 0.001$), FLTT ($F = 124.173$, $P < 0.001$), and their interaction ($F = 14.872$, $P < 0.001$). Figure 10 shows drivers' mean speed under different crossing types and foggy conditions in each FLTT condition. Generally, drivers' approaching speed decreased with the increase of FLTT for all crossings. The mean approaching speed at PSM + W crossing was significantly lower than that of PSM crossing and baseline. With the increase of FLTT, the difference of speed between

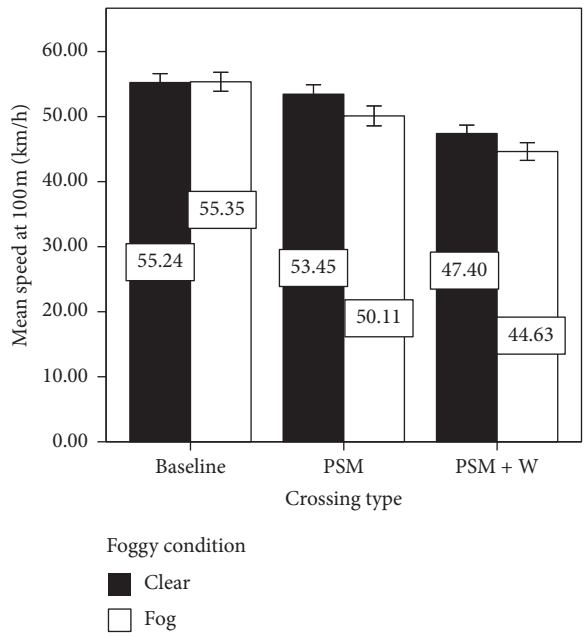

Figure 9: Mean speed at 100 m to the crossing for the interaction between crossing type and foggy condition.

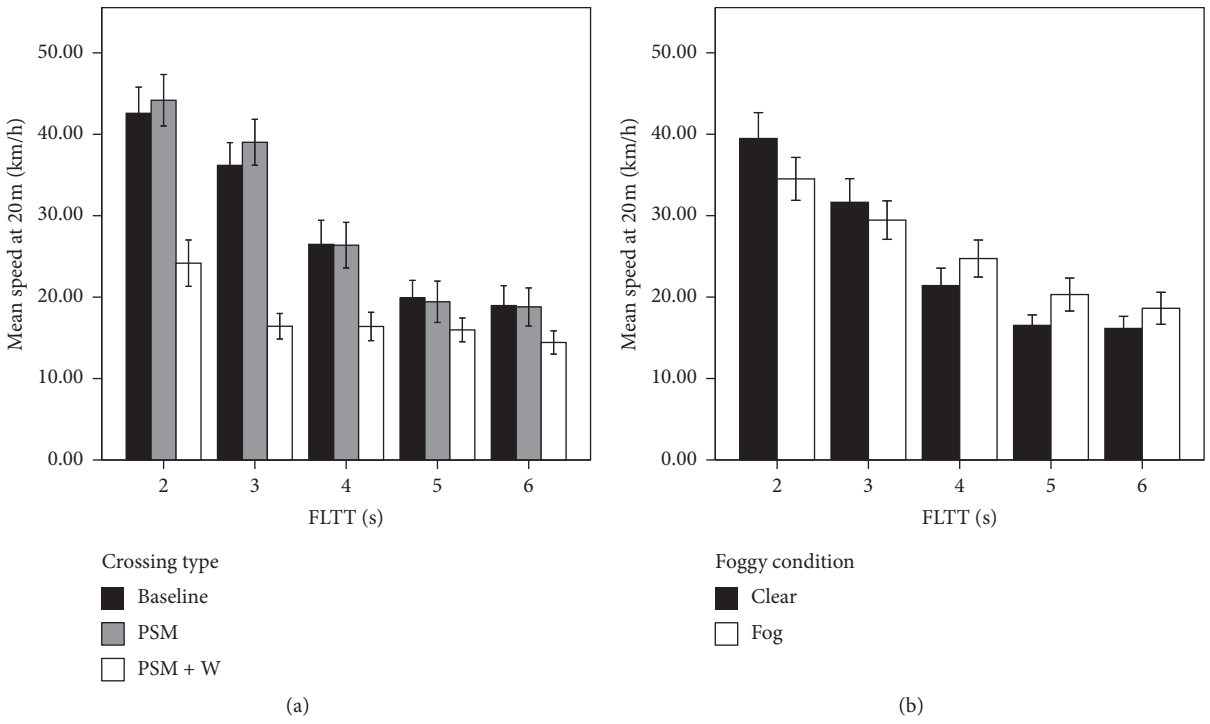

Figure 10: Mean speed at 20 m to the crossing under different FLTTs. (a) The interaction effect between FLTT and crossing type; (b) the interaction effect between FLTT and foggy condition.

PSM + W crossing and the other two crossing types became smaller. For foggy conditions (as shown in Figure 10(b)), different patterns could be found for different FLTTs. Generally, when FLTT was late, e.g., 2 s and 3 s, drivers maintained a larger speed in clear weather than in heavy fog. However, for early FLTTs, the results were quite opposite as drivers' mean speed was larger in heavy fog than in clear weather.

4.3. Brake Response Time. Table 4 lists driving performance with different factors, including foggy condition, gender, vocation, crossing types, and FLTTs. According to the ANOVA results (Table 5), foggy conditions ($F = 35.269$, $P < 0.001$), gender ($F = 6.625$, $P = 0.001$), crossing type ($F = 305.019$, $P < 0.001$), and FLTT ($F = 25.587$, $P < 0.001$) all had significant impacts on BRT. Regardless of the crossings

types, drivers' BRTs in clear weather were smaller than that in heavy fog and male drivers tended to brake earlier than female drivers. However, no statistically significant difference was found between professional and nonprofessional drivers. For crossing types, drivers braked earlier at PSM crossing and PSM + W crossing compared to baseline, especially at PSM + W crossing. For different FLTTs, drivers' BRTs were larger in the condition of earlier FLTTs.

Moreover, three significant interaction effects were found, e.g., crossing type × foggy conditions ($F = 7.037$, $P = 0.001$), crossing type × gender ($F = 4.533$, $P = 0.011$), and FLTT × foggy conditions ($F = 4.554$, $P = 0.001$). Figure 11 presents the mean BRT for different combinations of crossing types and gender. It could be noted that male and female drivers had significant differences in BRT at baseline crossings. However, the gender difference in BRT was degraded when PSM was applied, especially for the PSM + W condition. Figure 12 presents drivers' BRT for different combinations of FLTT and foggy conditions. It could be found that the difference of BRTs between clear and heavy fog became larger as the FLTT increased.

4.4. Deceleration. The ANOVA results for deceleration indicate the significant impacts of foggy condition ($F = 3.924$, $P = 0.048$) and vocation ($F = 8.673$, $P = 0.003$). Drivers' decelerations in clear weather were smaller than that in heavy fog, and professional drivers tended to brake with larger deceleration than nonprofessional drivers. Similar to the BRT, deceleration was also influenced by crossing type ($F = 84.017$, $P < 0.001$), FLTT ($F = 22.208$, $P < 0.001$), and their interaction ($F = 2.341$, $P = 0.017$). According to Table 4, drivers' deceleration in the PSM conditions was slightly reduced compared with the baseline. In the PSM + W condition, the deceleration was further reduced, which demonstrates that warning messages enabled drivers to brake with a more comfortable deceleration with least fluctuations. Figure 13 presents the mean deceleration for different FLTTs. The FLTT varied from 3 s to 6 s and, for the earlier FLTTs, the deceleration gradually reduced as well as the standard deviation. However, the deceleration of the latest FLTT (2 s) was not the largest, because drivers were more likely to go through the crossings and less likely to brake in such situation. When the PSM was used, the deceleration rate was largest for the latest FLTT (2 s), especially for the PSM + W condition, which implies that drivers relying on the IVAW may take an emergent brake.

Moreover, the interaction of crossing type × foggy condition ($F = 5.733$, $P = 0.003$) also illustrated a significant impact on deceleration. Figure 14(a) presents the mean deceleration for different combinations of crossing types and foggy conditions. In no fog, the deceleration for PSM showed no significant differences in comparison to the group of baseline, whereas the deceleration under the PSM + W condition reduced significantly. Differently in heavy fog, the deceleration significantly reduced under both PSM and PSM + W conditions. Moreover, for baseline, drivers' deceleration in fog was much greater than that in clear weather. However, in PSM and PSM + W conditions, the difference of deceleration between fog and clear weather was reduced.

Although gender ($F = 0.215$, $P = 0.643$) did not show significant impact on deceleration, the interaction effect between crossing type and gender ($F = 2.998$, $P = 0.050$) was significant. As illustrated in Figure 14(b), female drivers were more likely to exhibit a larger deceleration than male drivers under the baseline condition. On the contrary, female drivers' deceleration was smaller than that of male drivers at PSM and PSM + W crossings, indicating that male drivers could control the vehicles more smoothly whereas female drivers were more sensitive to the changes in signs and warning messages.

4.5. Red Crossing Time. According to the ANOVA results (Table 5), both gender ($F = 8.918$, $P = 0.003$) and vocation ($F = 4.523$, $P = 0.034$) exhibited significant impacts on RCT. Male drivers' RCTs were significantly longer than female drivers' (5.81 s vs 3.64 s). Similarly, nonprofessional drivers also spent more time during approaching than professional drivers. The main effect of FLTT ($F = 11.706$, $P < 0.001$) and its interaction effect with vocation ($F = 3.912$, $P = 0.004$) on RCTs were also significant. As illustrated in Figure 15, as the FLTT increased, nonprofessional drivers' RCTs increased rapidly, whereas professional drivers' RCTs increased relatively slowly with fewer fluctuations. In this experiment, no clear impact of crossing types ($F = 0.304$, $P = 0.738$) and foggy conditions ($F = 0.352$, $P = 0.553$) on RCTs was found.

5. Discussion

5.1. Influencing Mechanism of PSM and IVAW on Driving Behavior. The study conducted a simulator-based experiment to examine the effects of PSM and IVAW on drivers' driving performances during the process of approaching grade crossings controlled by flashing light. In addition, whether the effects of PSM and IVAW varied with drivers' gender, vocation, and foggy conditions was tested in this study as well.

Generally, users' compliance rate can be used to evaluate system effectiveness in varying safety countermeasures [5, 23]. The hypothesis that PSM is associated with safer driver behavior compared with current signs and markings is not supported by the compliance data. 70.2% of participants successfully stopped at the PSM grade crossing, whereas 69.8% of participants successfully stopped at the baseline grade crossing. The similar proportion of participants who made compliances at both crossings may be due to the similarity in perceptual cues provided by passive traffic control devices. Both signs and marking designs provided drivers with a "soundless" warning of the nonguarded grade crossings in front. For crossing with flashing light but without IVAW, drivers are not informed whether the flashing light is about to turn red. If the flashing light is activated when the vehicle is close to the crossing, drivers may make hasty and incorrect stop/go decisions. At both "soundless" crossings, over one-third of drivers made a violation when the FLTT was 3 s, and the violation rate

Table 4: Mean driving performance within different categories of factors.

Effect	Classification	BRT (s)	Decelerate (m/s/s)	RCT (s)
Foggy condition	Clear	2.17 ± 2.48	2.09 ± 1.49	4.67 ± 20.49
	Fog	2.69 ± 2.53	2.25 ± 1.35	5.28 ± 29.02
Gender	Male	2.33 ± 2.40	2.18 ± 1.43	5.81 ± 27.39
	Female	2.57 ± 2.72	2.17 ± 1.42	3.64 ± 17.67
Vocation	P	2.41 ± 2.54	2.27 ± 1.45	4.73 ± 21.57
	NP	2.47 ± 2.60	2.09 ± 1.39	5.21 ± 27.90
Crossing type	Baseline	3.50 ± 1.80	2.62 ± 1.69	4.88 ± 22.63
	PSM	3.32 ± 1.82	2.37 ± 1.80	4.74 ± 26.29
	PSM + W	1.29 ± 1.01	1.69 ± 0.53	6.16 ± 26.05
FLTT (s)	2	0.97 ± 0.68	2.33 ± 1.10	3.70 ± 22.42
	3	1.87 ± 1.95	2.51 ± 2.05	4.99 ± 18.75
	4	2.48 ± 2.30	2.40 ± 1.92	7.35 ± 18.09
	5	2.70 ± 2.55	1.99 ± 1.00	10.09 ± 31.98
	6	3.10 ± 2.48	1.82 ± 0.71	9.22 ± 8.17
Total		2.44 ± 2.57	2.17 ± 1.42	4.96 ± 24.65

Table 5: Results of ANOVA for dependent measures.

Source	d.f.	*F*-ratio		
		BRT	Deceleration	RCT
Foggy condition	1	35.269*	3.924*	0.352
Gender	1	6.625*	0.215	8.918*
Vocation	1	0.020	8.673*	4.523*
Crossing type	2	305.019*	84.017*	0.304
FLTT	4	25.587*	22.208*	11.706*
Crossing type × foggy condition	2	7.037*	5.733*	0.184
Crossing type × gender	2	4.533*	2.998*	0.388
Crossing type × vocation	2	0.783	0.811	2.977
FLTT × crossing type	8	1.640	2.341*	0.358
FLTT × foggy condition	4	4.554*	1.178	0.632
FLTT × gender	4	1.158	0.490	1.087
FLTT × vocation	4	0.243	0.184	3.912*

*significant at the 0.05 level.

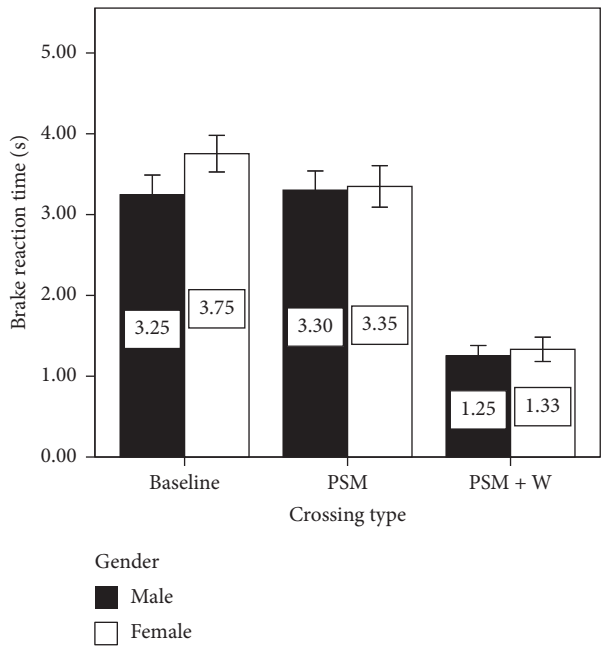

Figure 11: Mean BRT for the interaction between crossing type and gender.

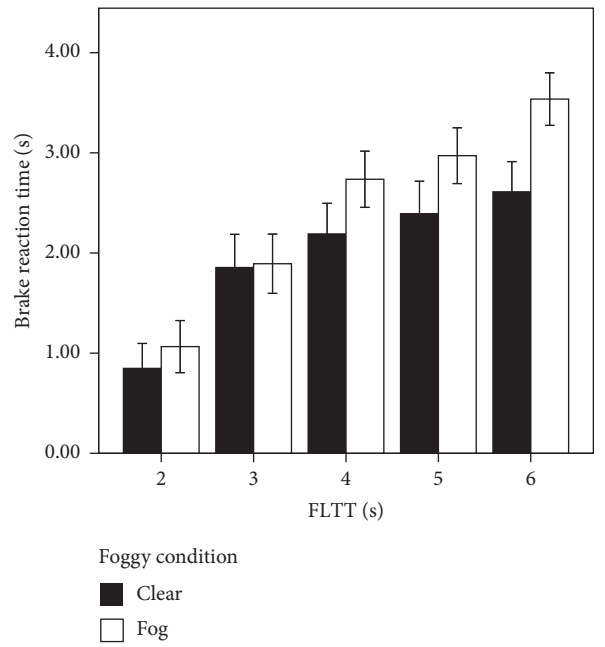

Figure 12: Mean BRT for the interaction between flashing light trigger timings and foggy condition.

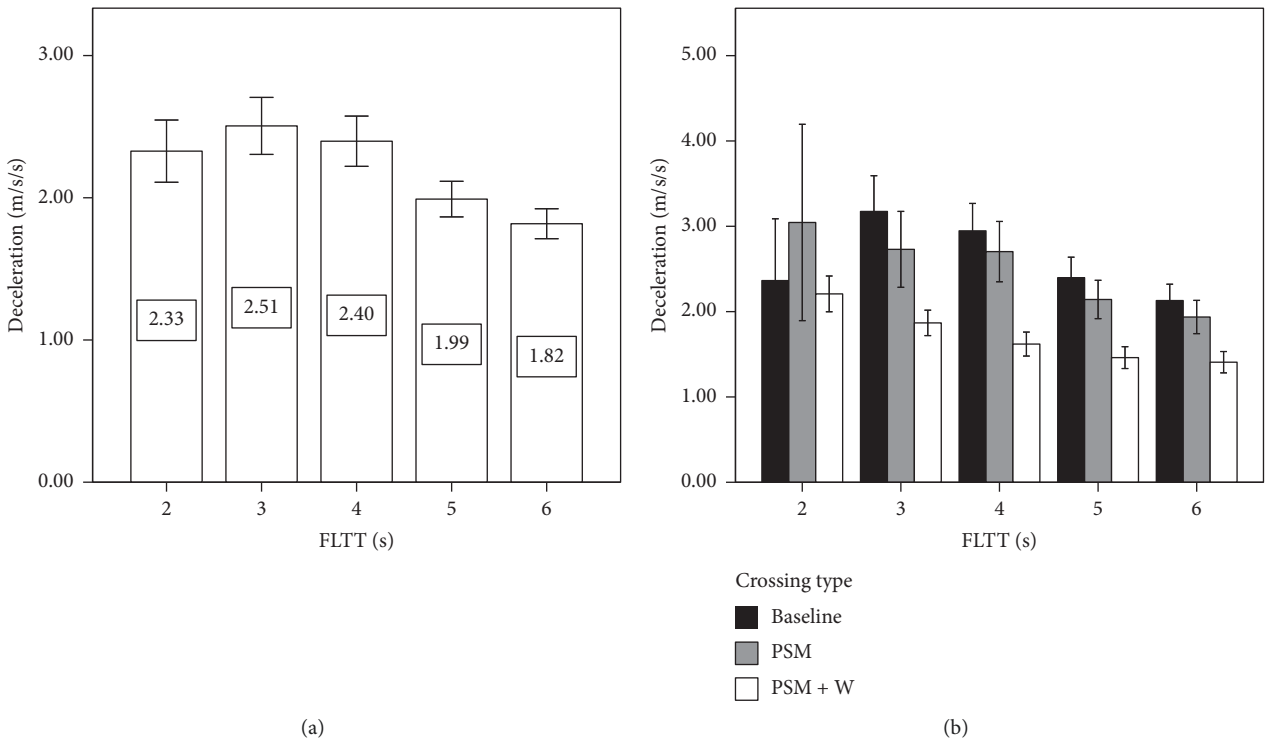

Figure 13: Mean decelerations under different flashing light trigger timing. (a) The main effect of FLTT; (b) the interaction effect between FLTT and crossing type.

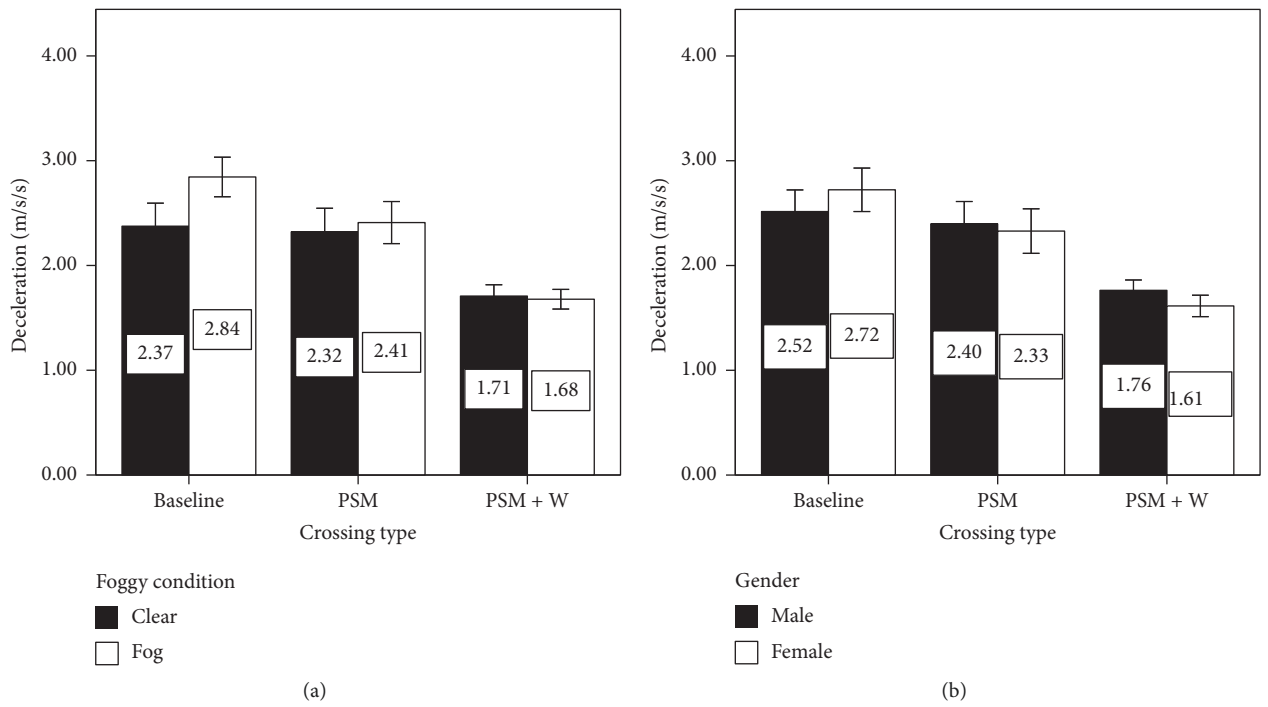

Figure 14: Mean decelerations under different crossing types. (a) The interaction effect between crossing type and foggy condition; (b) the interaction effect between crossing type and gender.

reached 87.5% when the FLTT was 2 s. This result is also supported by the approaching mean speed (AMS) profile of those drivers who chose to violate the flashing lights. Figure 16 illustrates an example and shows a tendency for drivers to reduce speed before subsequently accelerating to pass through the grade crossing. It is possible that some

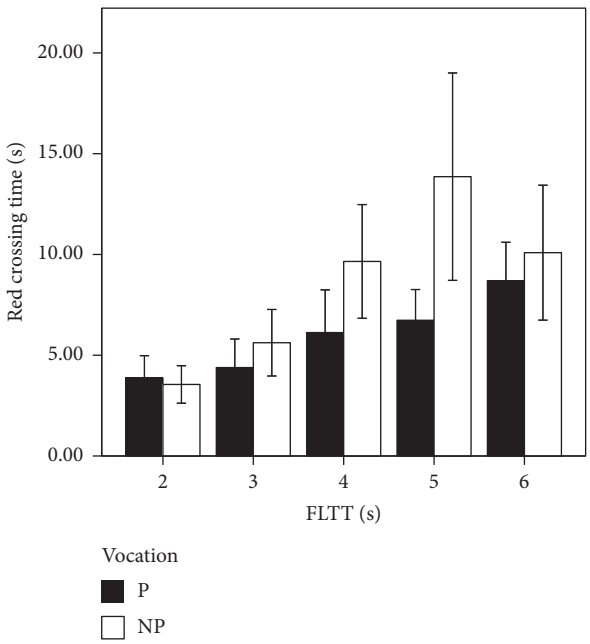

Figure 15: Mean RCT for the interaction between FLTT and vocation.

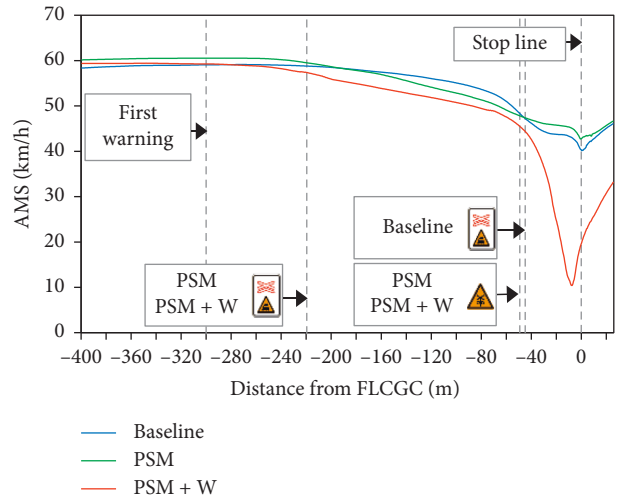

Figure 16: Approaching mean speed profiles of violation when the FLTT was 2 s.

drivers crossed the grade crossings because they felt it hard to stop, or they did not see a train coming [4, 51]. As expected, the additional IVAW resulted in a higher compliance rate (92.3%) as compared to the conventional signage intervention. In particular, the IVAW sharply reduced the number of participants deciding to go through the crossing at late FLTTs.

Although the system seems to affect the compliance rate, drivers' speed change patterns should also be investigated to better understand the performance of the system. The mean speed reduction on approach to a crossing can highlight the safety benefit and it has been investigated in various studies [5, 52, 53]. In this study, it is found that the speed patterns at different types of crossings were significantly different. Compared to baseline crossings, PSM led to an earlier slowing down before 220 meters to the crossings. The speed reduction from 220 meters to 50 meters can possibly be explained by the placement of nonguarded grade crossing signs and grade crossing signal ahead signs. The finding confirms that drivers would pay attention to signs and take corresponding action when approaching the grade crossings. However, the speed profiles of both PSM crossings and baseline were highly coincident as drivers got closer to the crossings. It is likely that the presence of advance warning signs merely affected the perception of crossing, instead of drivers' stop-go decisions. After receiving the first-stage warning information at PSM + W crossings, drivers had obvious deceleration behavior. Meanwhile, compared with the other two types of grade crossings, the brake for stop appeared earlier at PSM + W crossings and the whole deceleration process was smoother owing to the second-stage warning.

In addition, the safety improvement of PSM and PSM + W is supported by shorter BRT and smaller deceleration (see Figure 17). Overall, the BRT and deceleration at PSM crossings were slightly smaller than that of baseline. Specifically, drivers under the PSM + W condition responded to the events earlier with least fluctuations. Drivers' BRT was longer and their deceleration was smaller in the condition of earlier FLTTs. This indicates that drivers would slow down in advance to deal with the change of flashing light when they were closer to the grade crossing and then make well-prepared actions. Thus, they had sufficient time to move to the brake pedal and pressed slowly and continuously until stopping in front of the stop line. Moreover, the deceleration of the latest FLTT (2 s) was not the largest, because drivers were more likely to go through the crossings. Thus, the mean speed at 20 m to the PSM crossings was higher than that of baseline.

5.2. Applicability of the System in Foggy Weather. Reduced visibility in fog increases the risk of collision to some extent, and most drivers are likely to perform safety-related adaptations [54, 55]. In this study, the heavy fog resulted in a late response to the change of flashing light at baseline crossings. Especially at earlier FLTTs, the BRT in heavy fog condition was obviously longer than that in no fog condition. It was hard for drivers to detect and respond to the flashing light in fog until the vehicle was 50 m to the crossing. In such case, drivers had to take a greater deceleration, which may increase their involvement in rear-end crash. Moving the warnings upstream in foggy weather could enhance drivers' situation awareness in advance, and this is supported by a lower approaching speed and deceleration and a shorter reaction time. In no fog, the PSM did not show benefit in improving reaction time as drivers can easily detect the crossings. When the IVAW was applied, the reaction time and deceleration in both foggy conditions were greatly reduced, suggesting the advantages of IVAW over PSM and baseline. The finding shows that the system can compensate for the insufficient visibility in fog. Additionally, the study shows that foggy conditions have no significant

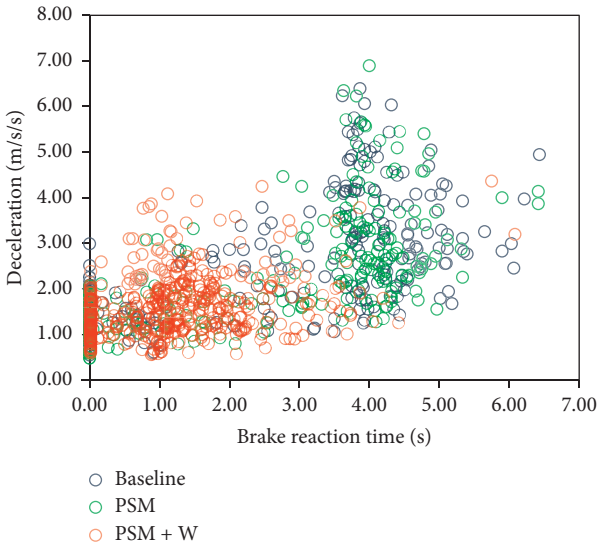

Figure 17: Brake reaction time and deceleration under different crossing types.

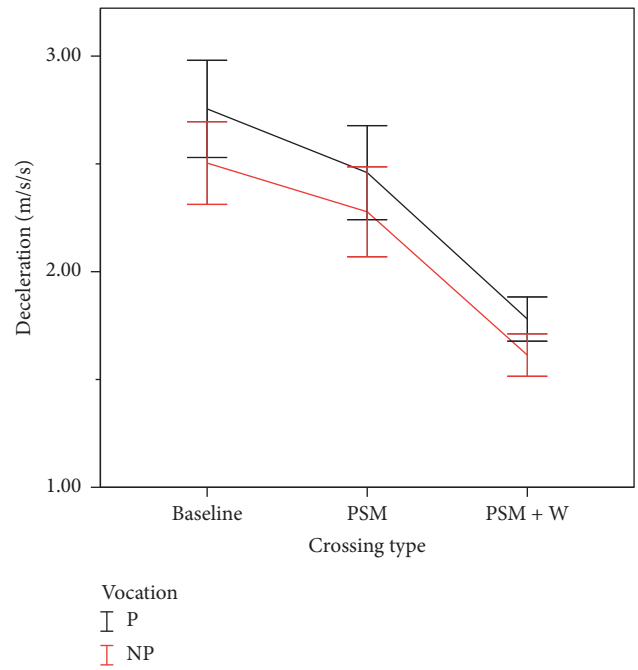

Figure 18: Deceleration under different crossing types × vocation.

impact on the compliance rate. The result implies that the possibility for intentional violation should be higher than the unintentional violation in the study, as the visibility condition in fog is more likely to increase unintentional violation rate.

5.3. Adaptability of Drivers with Different Characteristics to the System. Drivers' characteristics played an important role in perception, decision-making, and reaction during the process of approaching grade crossings. For example, compared with female drivers, male drivers were more likely to violate the flashing light, which is consistent with the previous observations [45, 56]. Especially in the case of earlier FLTTs, gender was a key demographic variable influencing compliance rate, and thus it was preferentially used to examine the effectiveness of the system. Female drivers were not sensitive to the change of signs and markings design, but the additional IVAW could increase the compliance rate to 100%. Furthermore, our findings indicated that compared with female drivers, male drivers tended to brake earlier, but the application of two countermeasures narrowed the gap of BRTs between different genders. On the other hand, the RCT of male drivers was 2.2 s (59.6%) longer than that of female drivers, which implies that male drivers tended to be more cautious and conservative in dealing with dangerous situations. However, no gender effect was observed on the approaching speed and deceleration in this study, and this is consistent with previous studies [57]. It is speculated that male drivers and female drivers are similar in vehicle control abilities when approaching a grade crossing.

As for vocation, professional drivers were more likely to cross the crossing with short RCTs than nonprofessional drivers. Especially when the FLTT increased, professional drivers tended to act faster and thus had a smaller risk of vehicle-train crash. It is confirmed that professional drivers have more driving experience and are more skillful in crash avoidance [58, 59]. However, for those professional drivers who made stop decisions, they had more abrupt deceleration than nonprofessional drivers (as illustrated in Figure 18). A possible explanation is that those drivers had actually prepared to accelerate to pass through the crossings before light flashing. The two countermeasures investigated in the study did not discriminate the effect on deceleration of professional and nonprofessional drivers. Although vocation did not have significant impacts on the compliance rate and approaching speed, it was found that nonprofessional drivers drove slightly higher speeds than professional drivers when approaching the grade crossings. A similar finding has been reported in the prior study, with nonprofessional drivers driving faster than professional drivers when approaching the intersections [42]. In the baseline condition, professional drivers (35.24%) have a larger violation rate than nonprofessional drivers (25.65%). Similarly, previous studies have reported that professional drivers were more inclined to cross the intersection during the yellow indication period because they had a higher economic pressure and need to save time while driving [57, 60]. Many professional drivers have formed the habit of accelerating during the yellow light interval [61]. Thus, when they encountered a flashing light change at grade crossings, they were less willing to wait for the train. The phenomenon was most evident when the FLTT was 4 s. In this case, the compliance rate of professional drivers (86.51%) was 6.97% lower than that of nonprofessional drivers (93.48%). The PSM and PSM + W narrowed the difference in compliance rates between different vocations. Furthermore, there was no difference between professional drivers and nonprofessional drivers on BRT. It implied that drivers' perceptual

response largely depend on the drivers' physiological character, instead of the drivers' skill and personal habit.

6. Conclusion

The driving simulator experiment illustrates the effects of crossing types on driver behavior in a range of FLTTs. The study contributes to a better understanding of the effectiveness of conventional devices and advanced warning technology used at grade crossings. The results suggest that PSM could offer limited safety benefits. To some extent, the PSM resulted in lower AMS, shorter BRT, smaller deceleration, and shorter RCT, whereas no evident difference in compliance rate was observed compared with baseline. When the IVAW was in use, the compliance rate was improved remarkably, especially under late FLTTs (i.e., 2 s, 3 s). In addition, the ASM, BRT, and deceleration were substantially reduced with small fluctuations. In general, the positive effect of PSM was most obvious when the FLTT was 3 s, whereas the IVAW enhanced driving performances under various conditions. The study reveals that the countermeasure combining PSM and IVAW can be developed as a safety tool for assisting in drivers' stop/go decision and safe driving at grade crossings.

The study also demonstrates the negative impact of foggy weather on driving behavior, though the impact could be remedied by both PSM and IVAW. It could be expected that the intervention system should have comparable effectives in other adverse conditions with impaired visibility, such as rainy weather or night condition.

The analysis of driver characteristics suggests that gender should be considered as an important factor for predicting the grade-crossing-crash risk. Overall, male drivers showed better performance than female drivers, but the gender difference was reduced by using PSM and IVAW. The system seems to be more effective for professional drivers, whereas nonprofessional drivers who made a go decision showed more hesitation and increased the likelihood of vehicle-train crash.

In summary, the study explored how foggy condition, gender, vocation, and FLTT affected drivers' performance at flashing-light-controlled grade crossings. The results prove the effectiveness of traffic signs design and IVAW, and suggest the combination use of countermeasures to maximize the safety benefits. The FLR warning system designed in the study was effective in enhancing drivers' performances and assisting drivers to safely pass through the grade crossings. It implies that the two-stage IVAW matched with PSM not only provides real-time and higher security, but also enhances the reliability of the system by PSM. Moreover, the system was capable to mitigate the negative effects of foggy weather and reduce drivers' individual difference during the crossing process, which indicates that the system has good applicability and adaptability. Findings of the study provide important guidance for the traffic control, infrastructure design, and driver assistance system development regarding grade crossings in China.

7. Limitations and Future Research

The study provided a pioneer research toward the understanding of grade-crossing-approaching behaviors under different factors' effect. A main limitation of the current study is that the BRT and RCT are relative values, which cannot be directly used as a reference for engineering standards. The limitation could be compromised by using supplementary measures, e.g., eye movement to detect the time when drivers actually perceive the traffic signs and flashing lights. Although the IVAW provides a positive impact on driver behavior over conventional flashing lights, the detailed design features need further modification/establishment before more concrete conclusions can be drawn. Examples of design features include the choice of words and delivery time of audio warning messages. Additionally, we did not consider the effect of age on driving performance in the experiment design. Previous studies sufficiently proved that aging affects the injury severity rate and driving performance [46, 62, 63]. Thus, it is suggested to explore the effects of age on grade-crossing-approaching behaviors in future research.

Data Availability

The behavioral data used to support the findings of this study are restricted by the independent ethics committee (IRB) in order to protect the privacy of participants.

Conflicts of Interest

The authors declare that there are no conflicts of interest regarding the publication of this paper.

Acknowledgments

This work is financially supported by National Natural Science Foundation of China (71771014, 71621001).

References

[1] Publishing House of Yearbook of China Transportation & Communications, *Yearbook of China Transportation & Communications*, Publishing House of Year Book of China Transportation & Communications, Beijing, China, 2005.

[2] European Railway Agency, *Intermediate Report on the Development of Railway Safety in the European Union*, European Railway Agency Safety Unit, Valenciennes, France, 2013.

[3] FRA, *Total Highway-Rail Crossing Incidents Casualties by State*, FRA, Mumbai, India, 2019, http://safetydata.fra.dot.gov/officeofsafety/publicsite/summary.aspx.

[4] C. M. Rudin-Brown, M. G. Lenné, J. Edquist, and J. Navarro, "Effectiveness of traffic light vs. boom barrier controls at road-rail level crossings: a simulator study," *Accident Analysis & Prevention*, vol. 45, pp. 187–194, 2012.

[5] L.-S. Tey, L. Ferreira, and A. Wallace, "Measuring driver responses at railway level crossings," *Accident Analysis & Prevention*, vol. 43, no. 6, pp. 2134–2141, 2011.

[6] J. Lee, D. Nam, and D. Dark, "Analyzing the relationship between grade crossing elements and accidents," *Journal of the Eastern Asia Society for Transportation Studies*, vol. 6, pp. 3658–3668, 2005.

[7] M. Zhao, "Analysis of the safety status of railway level crossings in China and countermeasures," *Professional Circle*, vol. 2, pp. 144-145, 2007.

[8] R. A. Raub, "Examination of highway-rail grade crossing collisions nationally from 1998 to 2007," *Transportation Research Record: Journal of the Transportation Research Board*, vol. 2122, no. 1, pp. 63–71, 2009.

[9] F. F. Saccomanno, P. Y.-J. Park, and L. Fu, "Estimating countermeasure effects for reducing collisions at highway-railway grade crossings," *Accident Analysis & Prevention*, vol. 39, no. 2, pp. 406–416, 2007.

[10] F. L. Meeker and R. A. Barr, "An observational study of driver behavior at a protected railroad grade crossing as trains approach," *Accident Analysis & Prevention*, vol. 21, no. 3, pp. 255–262, 1989.

[11] P. Cairney, T. Gunatillake, and E. Wigglesworth, *Reducing Collisions at Passive Railway Level Crossings in Australia*, Austroads, Sydney, Australia, 2002.

[12] Australian Transport Council, *National Railway Level Crossing Safety Strategy*, Australian Transport Council, Canberra, Australia, 2003.

[13] P. Papaioannou, "Driver behaviour, dilemma zone and safety effects at urban signalised intersections in Greece," *Accident Analysis & Prevention*, vol. 39, no. 1, pp. 147–158, 2007.

[14] E. Tenkink and R. Van der Horst, "Car driver behavior at flashing light railroad grade crossings," *Accident Analysis & Prevention*, vol. 22, no. 3, pp. 229–239, 1990.

[15] V. Beanland, E. Grant, G. J. M. Read et al., "Challenging conventional rural rail level crossing design: evaluating three new systems thinking-based designs in a driving simulator," *Safety Science*, vol. 110, pp. 100–114, 2018.

[16] M. H. Cale, A. Gellert, N. Katz, and W. Sommer, "Can minor changes in the environment lower accident risk at level crossings? Results from a driving simulator-based paradigm," *Journal of Transportation Safety & Security*, vol. 5, no. 4, pp. 344–360, 2013.

[17] E. Hauer, "Speed and safety," *Transportation Research Record: Journal of the Transportation Research Board*, vol. 2103, no. 1, pp. 10–17, 2009.

[18] T. Radalj and B. Kidd, "A trial with rumble strips as a means of alerting drivers to hazards at approaches to passively protected railway level crossings on high speed western Australian rural roads," in *Proceedings of the Road Safety Research, Policing and Education Conference*, Wellington, New Zealand, November 2005.

[19] X. Fu, S. He, J. Du, and T. Ge, "Effects of in-vehicle navigation on perceptual responses and driving behaviours of drivers at tunnel entrances: a naturalistic driving study," *Journal of Advanced Transportation*, vol. 2019, Article ID 9468451, 13 pages, 2019.

[20] Federal Highway Administration, *MUTCD (Manual of Uniform Traffic Control Devices)*, Federal Highway Administration, Washington, DC, USA, 2009.

[21] N. J. Lerner, D. J. Ratte, and J. Walker, "Driver behavior at rail-highway grade crossings," FHWA Project No. DTFH61-88-Z-00145 Federal Highway Administration, U.S. Department of Transportation, Washington, DC, USA, 1989.

[22] X. Yan, E. Radwan, D. Guo, and S. Richards, "Impact of "Signal Ahead" pavement marking on driver behavior at signalized intersections," *Transportation Research Part F: Traffic Psychology and Behaviour*, vol. 12, no. 1, pp. 50–67, 2009.

[23] G. S. Larue, I. Kim, A. Rakotonirainy, N. L. Haworth, and L. Ferreira, "Driver's behavioural changes with new intelligent transport system interventions at railway level crossings—a driving simulator study," *Accident Analysis and Prevention*, vol. 81, pp. 74–85, 2015.

[24] L.-S. Tey, G. Wallis, S. Cloete, L. Ferreira, and S. Zhu, "Evaluating driver behavior toward innovative warning devices at railway level crossings using a driving simulator," *Journal of Transportation Safety & Security*, vol. 5, no. 2, pp. 118–130, 2013.

[25] M. M. Porter, P. Irani, and T. A. Mondor, "Effect of auditory road safety alerts on brake response times of younger and older male drivers," *Transportation Research Record: Journal of the Transportation Research Board*, vol. 2069, no. 1, pp. 41–47, 2008.

[26] C. Ho and C. Spence, "Using peripersonal warning signals to orient a driver's gaze," *Human Factors: The Journal of the Human Factors and Ergonomics Society*, vol. 51, no. 4, pp. 539–556, 2009.

[27] A. Tang and A. Yip, "Collision avoidance timing analysis of DSRC-based vehicles," *Accident Analysis & Prevention*, vol. 42, no. 1, pp. 182–195, 2010.

[28] GM and Delphi-Delco Electronic Systems, *Automotive Collision Avoidance System Field Operational Test: Warning Cue Implementation Summary Report*, GM, Detroit, MI, USA, 2002.

[29] S. Talmadge, R. Chu, C. Eberhard, K. Jordan, and P. Moffa, "Development of performance specifications for collisions avoidance systems for lane change crashes," No. HS-809 414 Transportation Research Board, Alexandria, VA, USA, 2000.

[30] B. Graham and C. Hogan, *Low Cost Level Crossing Warning Device*, Sinclair Knight Merz and VicTrack Access, Victoria, Canada, 2008.

[31] S. S. Roop, C. E. Roco, L. E. Olson, and R. A. Zimmer, *An Analysis of Low-Cost Active Warning Devices for Highway-Rail Grade Crossings*, Texas Transportation Institute, College Station, TX, USA, 2005.

[32] N. Eluru, M. Bagheri, L. F. Miranda-Moreno, and L. Fu, "A latent class modeling approach for identifying vehicle driver injury severity factors at highway-railway crossings," *Accident Analysis & Prevention*, vol. 47, pp. 119–127, 2012.

[33] R. Harb, E. Radwan, X. Yan, and M. Abdel-Aty, "Light truck vehicles (LTVs) contribution to rear-end collisions," *Accident Analysis & Prevention*, vol. 39, no. 5, pp. 1026–1036, 2007.

[34] K. Haleem and A. Gan, "Contributing factors of crash injury severity at public highway-railroad grade crossings in the U.S," *Journal of Safety Research*, vol. 53, pp. 23–29, 2015.

[35] W. Hao and J. R. Daniel, "Severity of injuries to motor vehicle drivers at highway-rail grade crossings in the United States," *Transportation Research Record: Journal of the Transportation Research Board*, vol. 2384, no. 1, pp. 102–108, 2013.

[36] X. Yan, X. Li, Y. Liu, and J. Zhao, "Effects of foggy conditions on drivers' speed control behaviors at different risk levels," *Safety Science*, vol. 68, pp. 275–287, 2014.

[37] J. B. Edwards, "The relationship between road accident severity and recorded weather," *Journal of Safety Research*, vol. 29, no. 4, pp. 249–262, 1998.

[38] K. Peltzer and W. Renner, "Superstition, risk-taking and risk perception of accidents among South African taxi drivers," *Accident Analysis & Prevention*, vol. 35, no. 4, pp. 619–623, 2003.

[39] W. Y. Mergia, D. Eustace, D. Chimba, and M. Qumsiyeh, "Exploring factors contributing to injury severity at freeway merging and diverging locations in Ohio," *Accident Analysis & Prevention*, vol. 55, pp. 202–210, 2013.

[40] K. Obeng, "Gender differences in injury severity risks in crashes at signalized intersections," *Accident Analysis & Prevention*, vol. 43, no. 4, pp. 1521–1531, 2011.

[41] J. Abraham, T. K. Datta, and S. Datta, "Driver behavior at rail-highway crossings," *Transportation Research Record: Journal of the Transportation Research Board*, vol. 1648, no. 1, pp. 28–34, 1998.

[42] J. Wu, X. Yan, and E. Radwan, "Discrepancy analysis of driving performance of taxi drivers and non-professional drivers for red-light running violation and crash avoidance at intersections," *Accident Analysis & Prevention*, vol. 91, pp. 1–9, 2016.

[43] X. Yan, E. Radwan, and D. Guo, "Effects of major-road vehicle speed and driver age and gender on left-turn gap acceptance," *Accident Analysis & Prevention*, vol. 39, no. 4, pp. 843–852, 2007.

[44] J. Davey, N. Ibrahim, and A. Wallace, "Human factors at railway level crossings: key issues and target road user groups," in *Proceedings of the Swinburne University Multi-modal Symposium on Safety Management and Human Factors*, Melbourne, Australia, February 2006.

[45] D. Parker, A. S. R. Manstead, S. G. Stradling, and J. T. Reason, "Determinants of intention to commit driving violations," *Accident Analysis & Prevention*, vol. 24, no. 2, pp. 117–131, 1992.

[46] W. Hao, C. Kamga, and J. Daniel, "The effect of age and gender on motor vehicle driver injury severity at highway-rail grade crossings in the United States," *Journal of Safety Research*, vol. 55, pp. 105–113, 2015.

[47] L.-S. Tey, S. Zhu, L. Ferreira, and G. Wallis, "Microsimulation modelling of driver behaviour towards alternative warning devices at railway level crossings," *Accident Analysis & Prevention*, vol. 71, pp. 177–182, 2014.

[48] G. Botes, "A systemic study of the attitudes of minibus taxi drivers towards traffic law enforcement as a basis for the formulation of a management system for the South African minibus taxi industry," *Dissertation Abstracts International*, vol. 58, p. 1575, 1997.

[49] F. Meng, S. Li, L. Cao et al., "Driving fatigue in professional drivers: a survey of truck and taxi drivers," *Traffic Injury Prevention*, vol. 16, no. 5, pp. 474–483, 2015.

[50] X. Li, X. Yan, and S. C. Wong, "Effects of fog, driver experience and gender on driving behavior on S-curved road segments," *Accident Analysis & Prevention*, vol. 77, pp. 91–104, 2015.

[51] M. W. Pickett and G. B. Grayson, *Vehicle Driver Behaviour at Level Crossings*, Transport Research Laboratory, Crowthorne, UK, 1996.

[52] O. K. Ng and F. F. Saccomanno, "Speed reduction profiles affecting vehicle interactions at level crossings with no trains," *Transportation Research Record: Journal of the Transportation Research Board*, vol. 2149, no. 1, pp. 108–114, 2010.

[53] N. J. Ward and G. J. S. Wilde, "A comparison of vehicular approach speed and braking between day and nighttime periods at an automated railway crossing," *Safety Science*, vol. 19, no. 1, pp. 31–44, 1995.

[54] R. Ni, J. J. Kang, and G. J. Andersen, "Age-related declines in car following performance under simulated fog conditions," *Accident Analysis & Prevention*, vol. 42, no. 3, pp. 818–826, 2010.

[55] K. L. M. Broughton, F. Switzer, and D. Scott, "Car following decisions under three visibility conditions and two speeds tested with a driving simulator," *Accident Analysis & Prevention*, vol. 39, no. 1, pp. 106–116, 2007.

[56] D. Yagil, "Gender and age-related differences in attitudes toward traffic laws and traffic violations," *Transportation Research Part F: Traffic Psychology and Behaviour*, vol. 1, no. 2, pp. 123–135, 1998.

[57] X. Yan, Y. Zhang, and L. Ma, "The influence of in-vehicle speech warning timing on drivers' collision avoidance performance at signalized intersections," *Transportation Research Part C: Emerging Technologies*, vol. 51, pp. 231–242, 2015.

[58] J. R. Dalziel and R. F. S. Job, "Motor vehicle accidents, fatigue and optimism bias in taxi drivers," *Accident Analysis & Prevention*, vol. 29, no. 4, pp. 489–494, 1997.

[59] C.-M. Tseng, "Operating styles, working time and daily driving distance in relation to a taxi driver's speeding offenses in Taiwan," *Accident Analysis & Prevention*, vol. 52, pp. 1–8, 2013.

[60] S. Jing, T. Li, L. Xiaoyue, X. Yao, and A. Paul, "A survey of taxi drivers' aberrant driving behavior in Beijing," *Journal of Transportation Safety & Security*, vol. 6, no. 1, pp. 34–43, 2014.

[61] B. Verplanken and S. Orbell, "Reflections on past behavior: a self-report index of habit strength," *Journal of Applied Social Psychology*, vol. 33, no. 6, pp. 1313–1330, 2006.

[62] S. Islam and F. Mannering, "Driver aging and its effect on male and female single-vehicle accident injuries: some additional evidence," *Journal of Safety Research*, vol. 37, no. 3, pp. 267–276, 2006.

[63] S. Boufous, C. Finch, A. Hayen, and A. Williamson, "The impact of environmental, vehicle and driver characteristics on injury severity in older drivers hospitalized as a result of a traffic crash," *Journal of Safety Research*, vol. 39, no. 1, pp. 65–72, 2008.